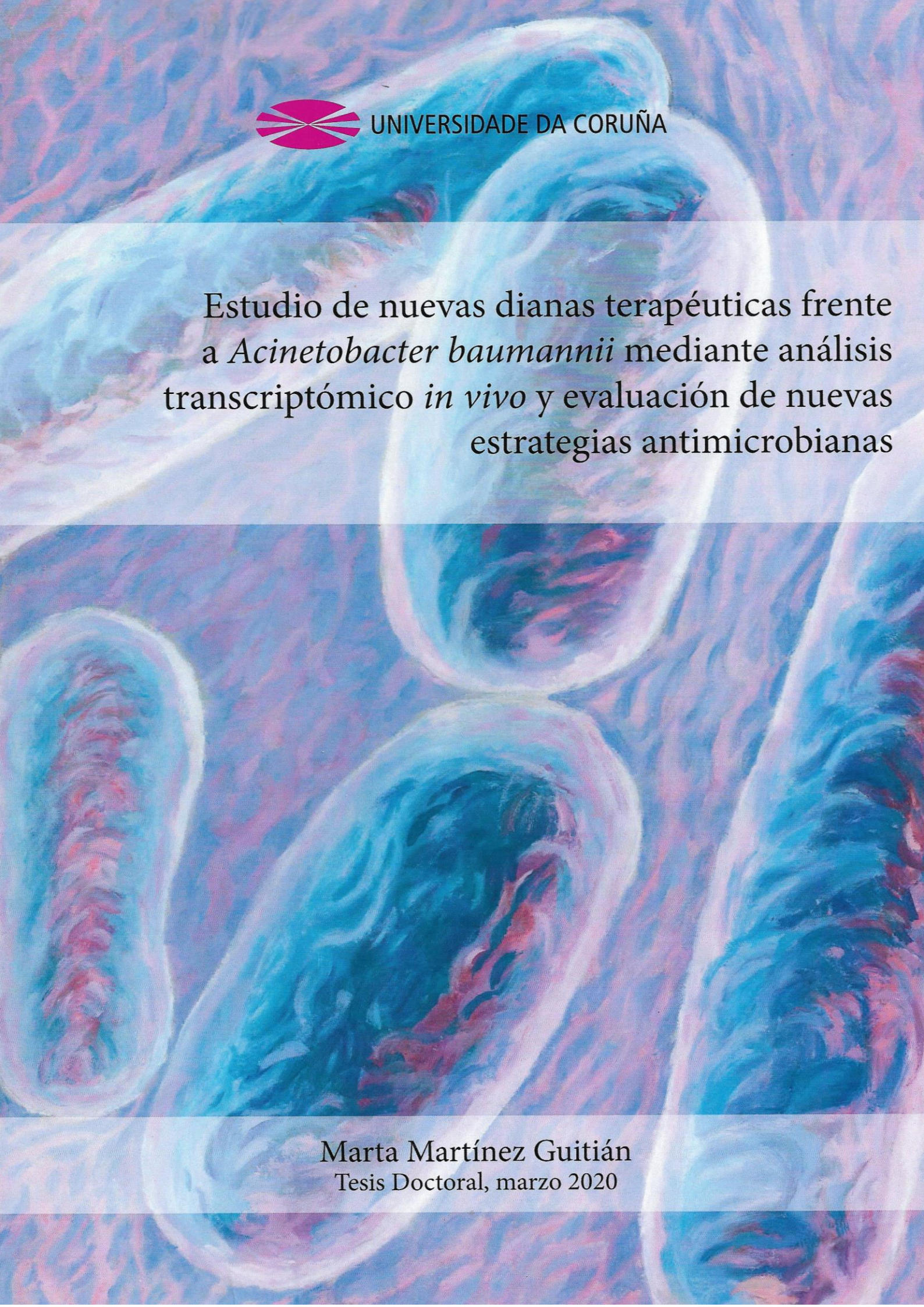

UNIVERSIDADE DA CORUÑA

Estudio de nuevas dianas terapéuticas frente a *Acinetobacter baumannii* mediante análisis transcriptómico *in vivo* y evaluación de nuevas estrategias antimicrobianas

Marta Martínez Guitián

Tesis Doctoral, marzo 2020

Estudio de nuevas dianas terapéuticas frente a *Acinetobacter baumannii* mediante análisis transcriptómico *in vivo* y evaluación de nuevas estrategias antimicrobianas.

Marta Martínez Guitián

Tesis doctoral

Marzo 2020

Directores: Dr. Alejandro Beceiro Casas y Dr. Germán Bou Arévalo

Tutor: Dr. Alejandro Beceiro Casas

Programa de doctorado en Ciencias de la Salud (RD99/2011)

Instituto de Investigación Biomédica de A Coruña (INIBIC)
Complexo Hospitalario Universitario de A Coruña (CHUAC)
Universidade da Coruña (UDC)

UNIVERSIDADE DA CORUÑA

Los directores de esta Tesis Doctoral, el **Dr. Alejandro Beceiro Casas**, Doctor en Ciencias Biológicas por la Universidad de A Coruña e investigador Miguel Servet II del Instituto de Investigación Biomédica de A Coruña y el **Dr. Germán Bou Arévalo**, Doctor en Ciencias Biológicas por la Universidad Autónoma de Madrid, Jefe de Servicio de Microbiología del Complexo Hospitalario Universitario de A Coruña (CHUAC) y profesor asociado de la Universidad de Santiago de Compostela

CERTIFICAN:

Que Dña. Marta Martínez Guitián, Licenciada en Farmacia por la Universidad de Santiago de Compostela, ha realizado en el Servicio de Microbiología y en el Instituto de Investigación Biomédica (INIBIC) del Complexo Hospitalario Universitario de A Coruña, bajo su dirección y tutela, el trabajo **"Estudio de nuevas dianas terapéuticas frente a *Acinetobacter baumannii* mediante análisis transcriptómico *in vivo* y evaluación de nuevas estrategias antimicrobianas"**, el cual, reúne todas las condiciones para ser presentado como Tesis Doctoral.

Y para que así conste, y surta los efectos oportunos, firmamos el presente certificado en A Coruña, marzo de 2020.

Dr. Alejandro Beceiro Casas
Director/Tutor

Dr. Germán Bou Arévalo
Director

Agradecimientos.

Cuando entré en el laboratorio, la realización de la Tesis Doctoral me parecía un camino muy largo… ¡y qué rápido ha pasado! A lo largo de este camino, tuve la gran suerte de cruzarme con personas que pusieron su granito o, más bien, montañas de arena para que hoy esté cerrando esta etapa. Mis compañeros se convirtieron en una gran familia con la que viví momentos de mucho esfuerzo y trabajo, pero también de satisfacción, alegría y diversión. Son ellos los que me hicieron seguir adelante en los momentos de frustración y por los que no cuesta nada, o casi nada, levantarse para ir a trabajar cada mañana. Por eso me gustaría dedicarles estas líneas.

En primer lugar, me gustaría agradecer a mis directores de Tesis. Germán, gracias por brindarme la oportunidad de formar parte de tu gran equipo de investigación. Álex, gracias por la confianza que depositaste en mí, por tu paciencia y dedicación; por ser exigente porque sabías que podía dar más de mí misma y por tus “que te pires” y “búscate la vida” con gran sentido del humor. Sin duda, eres la clave de que haya llegado hasta aquí.

Marga, aunque en el papel no esté reflejado, has sido una codi más durante estos años. Esta Tesis Doctoral también es parte de tu esfuerzo y trabajo.

Juanca, mi gran compañero de batalla en primera línea de fuego. Sin ti no estaría terminando de escribir esta Tesis. Este trabajo es tan tuyo como mío, desde la parte experimental hasta redactar este documento. Tienes mi más profunda admiración tanto científicamente como personalmente. Gracias por tu apoyo incondicional, por tu lealtad, por tu nobleza y por hacerme feliz cada día. Sin duda, eres lo mejor que me llevo de esta etapa. Te quiero mucho, mi amor.

Laura, hemos trabajado codo con codo las horas que hiciera falta para sacar adelante el trabajo. Gran parte de esta Tesis Doctoral también es tuya. Gracias por estar siempre dispuesta a ayudar y a explicar un millón de veces cómo se hacen los *knock-out*, aunque en mi caso no surgió efecto... Se te echa mucho de menos.

Kelly, mi *little princess*, gracias por echar siempre una mano, la mayoría de las veces sin que te dijese nada. Gracias por esa serenidad en momentos de estrés y por tu

implicación máxima, aunque nos quedemos en el labo hasta las mil. Tienes ese don de empatizar mucho y de anteponer siempre a los demás a ti misma, lo que te hace muy especial.

Cris, qué gran fichaje. No podía haber una incorporación mejor que tú. Estos meses que llevas en el laboratorio sólo viste mi estrés pre-Tesis; hubo una época que no era así, te lo prometo. Gracias por tu paciencia infinita porque últimamente te estoy cambiando mucho tu organización de los ensayos, por poner siempre buena cara a todo, y a todos, y por ser la mejor traductora que podría tener.

Patri, mi asturiana betanceira favorita. Cuando llegué al labo me convertí en tu sombra; gracias por esa paciencia infinita a mis torpezas de principiante, y de no tan principiante, y por esos "ratitos" que me esperabas para ir a comer. Gracias por escucharme siempre y por dar soluciones a todo con esa sensatez tuya tan característica. Eres pura bondad, gran compañera y mejor amiga. Si el mundo estuviese lleno de Patris, sería infinitamente mejor.

Mariló, gracias por la gran acogida que me diste cuando llegué al INIBIC y por acelerar mis protocolos para que terminase antes para ir a la cafetería. Si hay una persona con la que me reí mucho estos años, esa eres tú; a pesar de que hablas muy poco. Fue genial trabajar a tu lado. El labo, desde luego, no es lo mismo sin ti.

Eva, no sabes lo que te eché de menos cuando te mandaron para el CHUAC. Tu alegría y naturalidad llenan cada rincón del labo y el INIBIC se quedó medio vacío. Gracias por aguantar todas mis histerias con las celulillas y ayudarme siempre, ya sea limpiando la campana o en el nitrógeno, trabajos que no son muy gratificantes.

Astrid, estuve en tu casa antes de conocerte y eso ya dice mucho del gran corazón que tienes. Eres una gran anfitriona de Chantada y haces que todos nos sintamos en familia; de ahí que vayamos tantas veces. Gracias por estar siempre dispuesta a ayudar, ya sea en trabajo de poyata, en el animalario, con las celulillas o en dar ideas y soluciones. Siempre generas muy buen ambiente a tu alrededor y dejas huella en la gente que te conocemos. Es un lujo tenerte de compañera.

Sori, gracias por esas dosis de realidad, que vienen muy bien de vez en cuando, y por tu retranca que tantos buenos momentos nos dio. Eres una persona sincera, sensata y

cabal. Me gustaría agradecerte en especial la cantidad de veces que te di la lata con temas administrativos, burocráticos y de redacción para el depósito de esta Tesis, que me han facilitado muchísimo las cosas. Gracias por tu paciencia por mis torpezas informáticas y no informáticas, mis torpezas en general. Un millón de besitos y abracitos.

Juan, gracias por ser tan didáctico y siempre estar dispuesto a enseñar y a ayudar. Cuando llegué al labo estaba muy perdida y es de agradecer el hecho de tener un compañero que te dedicase su tiempo. Gracias también por luchar por mejorar nuestras condiciones laborales.

Bruno es admirable la sencillez que tienes. Gracias por tus consejos, por escuchar siempre los problemas en nuestros experimentos en el día a día, por tu ayuda en temas informáticos, aunque te suponga salir dos horas más tarde, por ir feliz al labo y contagiar esa felicidad.

Jorge, aunque odie que hables de β-lactamasas en momentos de descanso, he de reconocer que he aprendido mucho. Gracias por brindarte a ayudar siempre, por dar un punto más de locura al labo y por tu buen humor, excepto cuando te llamamos desordenado.

Miriam, es un lujo poder trabajar a tu lado ya que aprendí muchísimo de ti. Gracias por tus consejos cuando los experimentos no salían, por preocuparte siempre, por tus ánimos y por tu paciencia infinita en cuanto a nuestros horarios poco rigurosos en el animalario.

Laura F., gracias por dejarme elegir siempre la música en la radio y por aceptar, a veces resignada, mis bromas y tonterías. También es de agradecer tu paciencia en mis días malos y que siempre guardaste en tu casa nuestros regalos del amigo invisible en las cenas de Navidad.

Inés eres la dulzura personificada. Gracias por crear buen ambiente, por dejarme siempre el ordenador de mesa del sitio en el que te sientas y porque siempre te parece bien todo. Es una pena que no vaya al próximo ECCMID porque tendría una guía estupenda de París.

Víctor, es una lástima que no coincidiésemos más tiempo trabajando. Gracias por tu amabilidad cuando necesitamos algo del INIBIC.

Maricuchi, gracias por ese trabajo que no siempre se ve, como son la preparación del material y la realización de los pedidos. Me ahorraste muchas horas, sobre todo, en la preparación de las placas de microdilución para las cepas del multicéntrico de enterobacterias.

Gracias a Mariki, Lucía, Antón y Mohammed, es entrañable la ilusión con la que pronuncias "buenos días" cada mañana.

Gracias también a los que estuvisteis en el labo y ahora ya no estáis. Charlie, gracias por tu paciencia infinita enseñándome a hacer geles de acrilamida y Western-blot y por iniciarme con las celulillas. Detrás de esa ceja levantada y una respuesta un tanto gruñona, hay todo un buenazo con un corazón tan grande que no le cabe en el pecho.

Meri, tu sentido de humor es infinito. Cuando te fuiste del labo se te echó mucho en falta. Gracias por ayudarme con las celulillas en mis inicios y por preocuparte en este tiempo qué tal llevaba la escritura de la Tesis.

Silvia, gracias por nunca perder tu sonrisa, porque siempre ayudabas en lo que fuese, a pesar de tus jornadas maratonianas, y por ser la mejor guía de la Praia das Catedrais que se pueda tener.

Clara, gracias por tus consejos con los ratoncitos, por estar interesada siempre en nuestros trabajos en los congresos y por llevar hasta el exprimidor de naranjas cuando vamos a pasar una noche fuera de casa.

Gracias a mis compañeros de la Clínica, Bego, Anita, María José e Inma. Gracias por facilitarme material y por preguntarme siempre por la Tesis. Gracias también por esos postres que compartíais con nosotros en la cocina del Materno.

También quería agradecer a mis compañeros del INIBIC, ya que viví 4 años de esta Tesis con ellos. En primer lugar, María Moreno gracias por solucionar todos y cada uno de los problemas que me fueron surgiendo en el día a día, me facilitaste muchísimo el trabajo. Siempre es un placer bajar al INIBIC a hacerte una visita, aunque te ponga la excusa de tomar el café en el Materno que, además, es muy creíble.

Gracias a Isa y a Mariajo… ¡qué sería de mis celulillas sin vuestros consejos! A mis compañeros de Proteómica, Jesús y Valentina, gracias por el tiempo que dedicasteis a la identificación de proteínas inmunogénicas en el MALDI. Gracias a mis compañeras de Histomorfología, Noa y Bea, por vuestra paciencia con mis problemas en el miscroscopio y por enseñarme técnicas de tinción. Bea Caramés y Uxía, muchas gracias por ayudarme con el citómetro; sin vosotras no sabría ni por dónde empezar.

Gracias a todos los compañeros que estabais en la misma situación que yo, compartimos plazos de entrega, dudas y preocupaciones.

También me gustaría acordarme de todas aquellas personas que no están vinculadas con el laboratorio y que, sin embargo, me ayudasteis mucho durante este proceso.

Mi Lauriña, una comida o un café en Santiago siempre es una recarga de energía. Gracias por estar siempre ahí. Rosa y Fernando, aunque nos separen más de 300km de distancia, seguimos hablando como si nos viésemos el día anterior y eso es lo que más valoro de las buenas amistades. Los tres sabéis lo importantes que sois para mí, os quiero mucho.

Fary, gracias por cambiar mi rutina del día a día; tus planes de fin de semana siempre son una desconexión. Gracias por tu apoyo, aunque me digas que voy a ser una Doctora de “mentirijilla”.

Iria, muchas gracias por esas tardes de verano en la playa y por tu apoyo durante este tiempo.

Ana, Pilar y Juan Carlos, gracias por abrirme las puertas de vuestra casa y por tratarme como una más.

Pedro, no podía tener un compañero de vida mejor. Siempre estás ahí apoyándome en todos los retos que me propongo y bajándome a la realidad de vez en cuando. Tenemos esa complicidad, que uno ya sabe lo que está pensando el otro con sólo una mirada. Te quiero mucho, hermanito.

Madrina, gracias por ser una segunda madre. Te implicaste al máximo en nuestra infancia y educación. Siempre estás cuando te necesitamos. Te quiero mucho.

Papi y mami soy todo lo que soy gracias a vosotros. Gracias por vuestro esfuerzo, por anteponer mis sueños a todo, por quitarme todas las piedras que me he ido encontrando a lo largo del camino y por levantarme cada vez que me he caído. Siempre habéis luchado porque persiguiera mis objetivos. Sois mi admiración y mi ejemplo a seguir. Os quiero mucho.

Mami gracias por esa portada de Tesis, eres toda una artista.

Gracias a todos de corazón y perdón por si me he olvidado de alguien.

Índice.

Resumo.

Acinetobacter baumannii é un patóxeno nosocomial que presenta unha gran plasticidade xenética e resistencia antimicrobiana frecuentemente implicado en brotes hospitalarios difíciles de controlar. O estudo do xenoma deste patóxeno permítenos seleccionar aqueles xenes máis interesantes como posibles dianas terapéuticas.

Nesta Tese preséntase unha análise transcriptómica global do ARN bacteriano illado directamente dos pulmóns de ratos infectados con *A. baumannii*, coa finalidade de identifica-los xenes implicados no desenvolvemento da infección.

Os xenes *hisF* e *lpxB* atopáronse sobreexpresados durante a infección. HisF atópase implicado na persistencia en pulmón pola inhibición do reclutamento de macrófagos e da producción de IL-6 por parte do hospedador. A traducción de LpxB, proteína esencial implicada na síntese de LPS, foi inhibida empregando tecnoloxía antisentido

A colistina, antibiótico cunha elevada toxicidade, emprégase principalmente no tratamento de cepas multirresistentes e é considerado de última opción terapéutica. O MD3 é un inhibidor de SPasas que presenta sinerxia coa colistina, sendo así un candidato prometedor no tratamento de infeccións causadas por *A. baumannii*, incluindo cepas resistentes a colistina.

A análise transcriptómica *in vivo* permitiunos identificar unha serie de xenes como dianas terapéuticas potenciais e avaliáronse novas estratexias e compostos antimicrobianos para o tratamento de *A. baumannii*.

Resumen.

Acinetobacter baumannii es un patógeno nosocomial con gran plasticidad genética y resistencia antimicrobiana, implicado en brotes hospitalarios difíciles de controlar. El estudio del genoma de este patógeno nos permite seleccionar aquellos genes más interesantes como posibles dianas terapéuticas.

En esta Tesis se presenta un análisis transcriptómico global del ARN bacteriano aislado de los pulmones de ratones infectados con *A. baumannii*, con la finalidad de identificar aquellos genes implicados en el desarrollo de la infección por neumonía.

Los genes *hisF* y *lpxB* se encontraron sobreexpresados durante la infección. HisF está implicado en la persistencia en pulmón debido a la inhibición del reclutamiento de macrófagos y la producción de IL-6 por parte del huésped. La traducción de LpxB, proteína esencial implicada en la síntesis de LPS, ha sido inhibida empleando tecnología antisentido.

La colistina, antibiótico con elevada toxicidad, se utiliza en el tratamiento de cepas multirresistentes y es considerado de última opción terapéutica. El inhibidor de SPasas MD3 presenta sinergia con la colistina, siendo así un candidato prometedor en el tratamiento de infecciones causadas por *A. baumannii*, incluyendo cepas resistentes a colistina.

El análisis transcriptómico *in vivo* nos permitió identificar una serie de genes como dianas terapéuticas potenciales y se evaluaron nuevas estrategias y compuestos antimicrobianos para el tratamiento de *A. baumannii*.

Abstract.

Acinetobacter baumannii is a nosocomial pathogen that presents great genetic plasticity and antimicrobial resistance frequently implied hospital outbreaks difficult to control. The study of the genome of this pathogen allows us to select the most interesting genes as possible therapeutic targets.

This Thesis presents a global transcriptomic analysis of bacterial RNA isolated directly from the lungs of mice infected with *A. baumannii*, in order to identify those genes involved in the development of pneumonia infection.

hisF and *lpxB* genes were found to be overexpressed during infection. HisF is involved in lung persistence due to inhibition of macrophage recruitment and IL-6 production by the host. The translation of LpxB, the essential protein involved in the synthesis of LPS, has been inhibited using antisense technology.

Colistin, an antibiotic with a high toxicity, is mainly used in the treatment of multi-resistant strains and is considered the last therapeutic option. MD3 is a SPasas inhibitor that presents synergy with colistin, thus being a promising candidate in the treatment of infections caused by *A. baumannii*, including colistin-resistant strains.

In vivo transcriptomic analysis allowed us to identify several genes as potential therapeutic targets and evaluated new strategies and antimicrobial compounds for the treatment of *A. baumannii*.

Abreviaturas.

AAC Aminoglucósido acetiltransferasa

ACB *Acinetobacter calcoaceitus-Acinetobacter baumannii*

ADN Ácido desoxirribonucleico

AICAR 5'-(5-aminoimidazol-4-carboxamida) ribonucleótido

AMP Monofosfato de adenosina

AMPK Monofosfato de adenosina cinasa

ARN Ácido ribonucleico

ARNm Ácido ribonucleico mensajero

ASOs Oligómeros antisentido

ATP Trifosfato de adenosina

BAL Lavado broncoalveolar (*bronchoalveolar lavage*)

BIP 2,2'-bipiridil

BLEA Betalactamasa de espectro ampliado

BNA Puente de ácido nucleico (*bridged nucleic acid*)

CHDL β-lactamasa de clase D que hidroliza carbapenem (*carbapenem-hydrolyzing class D β-lactamases*)

CLSI Instituto de Estándares Clínicos y de Laboratorio (*Clinical and Laboratory Standards Institute*)

CME Complejos de membrana externa

CMI Concentración mínima inhibitoria

COL Colistina

col. Colaboradores

CO_2 Dióxido de carbono

CPPs Péptidos permeabilizantes de células (*cell permeabilizing peptides*)

CRAB *Acinetobacter baumannii* resistente a carbapenems

DBO Diazabiciclooctanones

DHP-I Dehidropeptidasa renal de tipo I

DMEM Medio de Dulbecco Eagle modificado (*Dulbecco's Modified Eagle Medium*)

DNAsa I Desoxirribonucleasa I

DO_{600} Densidad óptica a 600 nanómetros

EC Comisión enzimática (*Enzyme Comission*)

ECDC Centro Europeo de Prevención y Control de Enfermedades (*European Centre for Disease Prevention and Control*)

EDTA Ácido etilendiaminotetraacético

ELISA Ensayo por inmunoabsorción ligado a enzimas (*enzyme-linked immunosorbent assay*)

FDA Administración americana de Medicamentos y Alimentos (*U.S. Food and Drug Administration)*

Fe^{2+} Estado ferroso del hierro

Fe^{3+} Estado férrico del hierro

HBSS Solución de sal equilibrada de Hank (*Hank's Balanced Salt Solution*)

IDSA Sociedad Americana de Enfermedades Infecciosas (*Infectious Diseases Society of America)*

IgG Inmunoglobulina G

IgM Inmunoglobulina M

IGP Imidazol glicerol fosfato sintasa

IL-6 Interleuquina 6

ImGP Imidazol glicerol fosfato

INSeq Secuenciación de inserción

KPC Carbapenemasa de *Klebsiella pneumoniae* (*K. pneumoniae* carbapenemase)

L-Ara4N Arabinosa

LB Medio Luria-Bertani

LNA Ácido nucleico bloqueado (*locked nucleic acid*)

LPS Lipopolisacárido

MDR Cepa multirresistente (*multidrug-resistant*)

mHBSS Solución de sal equilibrada modificada de Hank (*modified Hank's Balanced Salt Solution*)

min. Minutos

mL Mililitro

µL Microlitro

mM Milimolar

NPs Nanopartículas

OMS Organización Mundial de la Salud

OMV Vesículas de membrana externa (*outer membrane vesicles*)

OXA Oxacilinasa

PBP Proteína de anclaje a penicilina (*penicillin binding protein*)

PCR Reacción en cadena de la polimerasa (*polymerase chain reaction*)

PEG Polietilenglicol

pEtn Fosfoetanolamina

PG Peptidoglicano

PMO Oligómeros morfolinos fosforodiamidatos (*phosphorodiamidate morpholino oligomers*)

PNA Ácido peptídico nucleico (*peptide nucleic acid*)

PNAG Polisacárido β-(1-6)-N-acetilglucosamina

pPNA Ácido peptídico nucleico conjugado al péptido permeabilizante de células (*cell permeabilizing peptide – peptide nucleic acid*)

PRFAR N'-(5'-fosforibosil)-formimino-5-aminoimidazol-4-carboxamida ribonucleótido

PS Fosforotionato (*phosphorothioate*)

PTK Proteína tirosina quinasa (*protein tirosin kinase*)

qRT-PCR Retrotranscripción y reacción en cadena de la polimerasa cuantitativa

RND División resistencia-nodulación-célula (*resistance-nodulation-cell*)

rpm Revoluciones por minuto

SB Medio Super Broth

SIDA Síndrome de inmunodeficiencia adquirida

SPasa Proteasa de péptido señal de tipo I (*type I signal peptidase*)

spp Especies

Thr-172 Treonina-172

TNF-α Factor de necrosis tumoral-alpha

T2SS Sistema de secreción tipo II (*type 2 secretion system*)

T6SS Sistema de secreción tipo VI (*type 6 secretion system*)

UCI Unidad de Cuidados Intensivos

UFC Unidades formadoras de colonias

VIH Virus de inmunodeficiencia humana

XDR Cepa extensamente resistente (*extensively drug-resistant*)

Figuras y tablas.

Índice de figuras.

Figuras de la introducción.

Índice de tablas.

Figuras de la introducción.

I. INTRODUCCIÓN

Introducción.

Las enfermedades infecciosas han sido una de las principales causas de mortalidad a lo largo de la historia. El descubrimiento de la penicilina G por Alexander Fleming en 1928 supuso un antes y un después en la historia de la medicina. La primera purificación del antibiótico se produjo en 1939, pero hasta mediados de los años 40 no se lograron mejorar las condiciones de producción y distribución [1]. Desde entonces, se han descrito una gran cantidad de moléculas antimicrobianas relacionadas o no con la molécula inicial de la penicilina. Sin embargo, de forma paralela a este desarrollo terapéutico, las bacterias han ido evolucionando y desarrollando nuevos mecanismos de resistencia a los antibióticos utilizados.

La resistencia a los antibióticos es un proceso natural en la evolución de las bacterias. Consecuentemente, el uso de compuestos antimicrobianos impulsa la selección de mutantes resistentes, la adquisición de genes de resistencia y el sobrecrecimiento de bacterias con una resistencia intrínseca [2]. Actualmente, el aumento de las tasas de resistencia a antibióticos es un problema global de enorme relevancia. Cada año mueren 700.000 personas por causas relacionadas con la resistencia antimicrobiana en todo el mundo. Si se permite que el problema persista, se calcula que para el año 2050 la resistencia antimicrobiana habrá causado la muerte de más de diez millones de personas/año, lo que representa un número mayor que aquellas personas fallecidas debido a cáncer, diabetes, accidentes de carretera, enfermedades diarreicas y VIH/SIDA. Las pérdidas económicas también podrían ser devastadoras; se prevé que los costes de salud a nivel mundial podrían variar entre 300.000 millones y más de 1 billón de dólares al año [3].

Recientemente, la OMS publicó una lista de “patógenos prioritarios” resistentes a antibióticos, en la que se incluyen las 12 especies bacterianas más peligrosas para la salud. Esta lista se divide en tres categorías en función de la urgencia en la obtención de nuevos agentes antimicrobianos: prioridad crítica, alta o media. *Acinetobacter baumannii* y *Pseudomonas aeruginosa* resistentes a carbapenems y enterobacterias resistentes a carbapenems y a cefalosporinas de tercera generación constituyen la categoría de **prioridad crítica** [4].

Las infecciones causadas por el género *Acinetobacter* spp. obtuvieron una mayor relevancia durante los años 60 y 70, en paralelo a la utilización creciente de las unidades de cuidados intensivos (UCI). *Acinetobacter* spp. fue considerado inicialmente un oportunista comensal, un patógeno de baja virulencia. En cambio, en décadas posteriores, la creciente ubicuidad, la intensidad de la ventilación mecánica, la cateterización central y urinaria, junto con el uso inadecuado de terapias antimicrobianas ha causado un aumento en la frecuencia y severidad de las infecciones causadas por *Acinetobacter* spp. [5].

La resistencia a los antimicrobianos en *A. baumannii* ha aumentado drásticamente durante las dos últimas décadas, con una mayoría de aislamientos clínicos multirresistentes (***multidrug-resistant***, **MDR**, resistentes a al menos un antibiótico en tres o más familias de antibióticos) o extremadamente resistentes a los antibióticos (***extensive drug-resistant***, **XDR**, resistente a al menos un agente de todas las categorías de antimicrobianos, salvo dos o menos) [6].

La Sociedad Americana de Enfermedades Infecciosas (*Infectious Diseases Society of America*, IDSA) ha destacado, bajo el acrónimo "ESKAPE", los 6 patógenos bacterianos resistentes a antibióticos más complicados y relevantes. En estas siglas se incluyen *Enterococcus faecium*, *Staphylococcus aureus*, *Klebsiella pneumoniae*, *Acinetobacter baumannii*, *Pseudomonas aeruginosa* y *Enterobacter* spp., los cuales son capaces de "escapar" a la acción bactericida de los antibióticos y representan un paradigma en la patogénesis y transmisión de resistencias [7].

El mal uso de los antibióticos y la poca inversión en el desarrollo de nuevos fármacos dentro de este campo han hecho que en las últimas décadas apenas se hayan comercializado alternativas reales para estos patógenos multirresistentes, lo que origina la imperiosa necesidad de diseñar y evaluar nuevas terapias antimicrobianas. Esta Tesis Doctoral aborda la búsqueda de nuevas dianas terapéuticas y el desarrollo de nuevos compuestos antimicrobianos frente al patógeno nosocomial ***Acinetobacter baumannii***.

1. Relevancia de las infecciones nosocomiales.

Las infecciones nosocomiales, también conocidas como infecciones adquiridas en el hospital, son aquellas que se contraen del entorno o a través del personal y pacientes de un establecimiento sanitario. Las unidades de cuidados intensivos (UCI) y de reanimación de los hospitales albergan pacientes enfermos extremadamente vulnerables a estas infecciones, proporcionando un nicho para patógenos oportunistas. Éstos se adaptan al entorno con gran facilidad, ya que sobreviven en ambientes hostiles y desfavorables para su desarrollo, como son las estancias hospitalarias. Esto se debe a que adquieren mecanismos de resistencia, los cuales, facilitan la persistencia en superficies bióticas y abióticas. Por consiguiente, estos patógenos pueden diseminarse con facilidad entre pacientes.

Un estudio epidemiológico realizado por la OMS reveló que alrededor del 8,7% de los pacientes hospitalizados presentaron una infección nosocomial y que más de 1,4 millones de personas en todo el mundo la sufren cada año. Además, las infecciones nosocomiales son una de las principales causas de mortalidad [8].

2. El género *Acinetobacter.*

El género *Acinetobacter* spp. está formado por un grupo heterogéneo de bacilos o cocobacilos Gram negativos. No fermentan la glucosa y son aerobios estrictos, inmóviles, catalasa positivo, oxidasa negativo y con un alto contenido de guanina y citosina en su ADN de entre el 39% y el 47% [9]. Crecen bien en todos los medios de cultivo de rutina, siendo su temperatura óptima de crecimiento de 33 a 35º C.

El primer aislamiento se remonta a 1911, cuando el microbiólogo holandés Beijerinick describió un microorganismo denominado *Micrococcus calcoaceticus,* el cual, fue aislado a partir de una muestra de tierra y cultivado en un medio mínimo que contenía calcio-acetato. En 1954 Brisou y Prevot propusieron el género *Acinetobacter* (proveniente del griego *akinetos*, "inmóvil") para diferenciarlo de los organismos móviles dentro del género *Achromobacter* [9]. El género *Acinetobacter* fue

ampliamente aceptado en 1968 después de que Baumann y col. publicasen un estudio, en el cual concluyeron que *Acinetobacter* pertenecía a un solo género y no podía ser subclasificado en diferentes especies según las características fenotípicas [10]. En 1971, el Subcomité sobre la taxonomía de *Moraxella* y bacterias relacionadas reconoció oficialmente el género *Acinetobacter* basándose en dicha publicación de Baumann [9]. La taxonomía más reciente, ha incluido el género *Acinetobacter* en la familia *Moraxellaceae*, dentro del orden *Gammaproteobacteria*, el cual incluye los géneros *Moraxella*, *Acinetobacter*, *Psychrobacter* y otros organismos relacionados.

A día de hoy, el género *Acinetobacter* engloba 63 especies y la última incorporada fue *Acinetobacter wuhouensis* en agosto de 2018 [11]. Dentro de este género, se incluye un conjunto de seis especies denominado complejo ***A. calcoaceticus – A. baumannii*** (**ACB**). Estas especies son muy similares fenotípicamente y se encuentran estrechamente relacionadas entre sí; son las siguientes: *A. calcoaceticus*, *A. baumannii*, *A. pitti* (antiguamente nombrada como *Acinetobacter* especie genómica 3), *A. nosocomialis* (antiguamente nombrada como *Acinetobacter* especie genómica 13 TU), *A. seifertii* y *A. dijkshoorniae* [12].

El complejo ACB es el más importante desde el punto de vista clínico. La mayoría de las enfermedades nosocomiales y brotes son causados por cepas pertenecientes a este grupo y, dentro del mismo, destaca *Acinetobacter baumannii*, responsable del 2 al 8% de las infecciones totales causadas por Gram negativos en hospitales [13].

2.1. El patógeno *Acinetobacter baumannii*.

A. baumannii es un patógeno causante de un amplio abanico de infecciones nosocomiales graves. La **neumonía** adquirida en el hospital representa la manifestación clínica más común de la infección por *A. baumannii*. Estas infecciones ocurren con más frecuencia en pacientes que reciben ventilación mecánica en el entorno de cuidados intensivos. La neumonía asociada a ventilación mecánica resulta de la colonización de *A. baumannii* de las vías aéreas a través de exposición ambiental, seguida por el desarrollo de la infección [14].

Las **bacteriemias** en las UCI son otra manifestación clínica frecuente de *A. baumannii.* El origen de estas infecciones suele ser infecciones del tracto respiratorio inferior o de dispositivos intravasculares. Los factores de riesgo asociados con la adquisición de estas infecciones incluyen la inmunosupresión, el uso de respiradores asociados, el fracaso de la terapia antibiótica, la colonización previa de *A. baumannii* y la utilización de procedimientos invasivos [14].

La tasa bruta de mortalidad para neumonías producidas por *A. baumannii* se sitúa entre el 40% y el 70%, mientras que para bacteriemias se encuentran en torno al 28% y el 43%. No obstante, la mortalidad atribuible a este patógeno es objeto de controversia debido a que la infección nosocomial producida por *A. baumannii* en realidad está asociada con un aumento de la mortalidad, siempre y cuando existan otros factores subyacentes [14].

Otras infecciones nosocomiales producidas por este patógeno oportunista son infecciones de la piel y de tejidos blandos, infecciones de heridas, infecciones del tracto urinario y meningitis secundaria.

Con menos frecuencia, *A. baumannii* también puede causar infecciones adquiridas en la comunidad, incluyendo neumonía y bacteriemia [13]. Éstas suelen estar relacionadas con problemas previos del paciente como el alcoholismo, tabaquismo, enfermedad pulmonar crónica y diabetes mellitus. La neumonía adquirida en la comunidad es más grave que la neumonía nosocomial, generalmente es fulminante. Las tasas de mortalidad también son altas, entre el 48% y el 60%, y la muerte del paciente se produce dentro de los 8 días tras el diagnóstico. No obstante, es difícil aclarar si las causas de esta infección grave son los propios factores del huésped o los factores de virulencia específicos de la bacteria. La neumonía adquirida en la comunidad por *A. baumannii* se han observado casi exclusivamente en climas tropicales, concretamente, en el sudeste asiático y Australia tropical [15].

A. baumannii se caracteriza también por poseer una excelente persistencia, lo que le permite adaptarse con facilidad a condiciones ambientales muy desfavorables como es el ambiente hospitalario. Esto explica el éxito de su capacidad infectiva, la facilidad de adquisición de mecanismos de resistencia y de producir brotes nosocomiales.

3. Patogénesis en *Acinetobacter baumannii*.

La patogenicidad se define como la capacidad que presenta un agente para causar o favorecer el desarrollo de enfermedades. Cabe destacar que la patogénesis de *A. baumannii* sigue siendo muy desconocida, a pesar de la importancia clínica de sus infecciones [16,17].

Las bacterias patógenas, como en el caso de *A. baumannii*, poseen varios factores que les permiten incrementar su **virulencia.** Clínicamente, la predicción de los factores de virulencia en un patógeno bacteriano es muy deseable, ya que un diagnóstico rápido y estandarizado puede mejorar y/o especificar el tratamiento [17]. En *A. baumannii* existen fenotipos asociados a factores de virulencia, los cuales, varían de forma notable en función de las distintas cepas. Estos fenotipos son movilidad, adhesión e invasión a células eucariotas, formación de biopelículas o *biofilm*, absorción de hierro o desarrollo de la cápsula celular, entre otros [18,19].

3.1. Movilidad.

Se han descrito tres tipos de movilidad en bacterias Gram negativas: *swarming*, *swimming* y *twitching*. Inicialmente, *Acinetobacter* se ha descrito como un microorganismo inmóvil, debido a la carencia de genes que codifican flagelos [20]. Esto conlleva a que no presenta movilidad *swarming*, ya que está mediada por los mismos. Sin embargo, el hecho de que no presente flagelos no significa que no pueda propagarse por la superficie mediante un movimiento que no requiera de estos orgánulos, como es el caso de la movilidad *twitching* [21].

La movilidad ***twitching***, a diferencia de la movilidad *swarming* y *swimming*, se caracteriza por un movimiento lento con apariencia espasmódica y sobre superficie. Este tipo de movilidad no está mediada por flagelos, sino que se encuentra impulsada por la extensión y retracción del pili tipo IV, el cual, es regulado por diferentes genes implicados en el ensamblaje, la movilidad y el desarrollo de filamentos. El pili tipo IV es

un conjunto de apéndices proteicos que están asociados a procesos de transformación bacteriana, adhesión a superficies bióticas y abióticas y a movilidad *twitching* [21,22].

3.2. Formación de *biofilm* y *quorum sensing*.

La adhesión a las células huésped es el primer paso de la colonización o infección. Las bacterias, al adherirse a las superficies, se agregan en una matriz polimérica hidratada denominada **biopelícula** o ***biofilm***. Ésta constituye una comunidad de microcolonias bacterianas altamente estructurada [21,23]. La formación de *biofilm* es un proceso progresivo, que consta de varios pasos entre los que se incluyen i) la adhesión inicial de las bacterias a una superficie; ii) la maduración del *biofilm*, durante la cual, se forman canales que permiten la entrada de nutrientes a las capas más profundas y, iii) finalmente, el desprendimiento del mismo gracias a la acción de nucleasas y proteasas [24].

La formación de *biofilm* está relacionada con la señalización/comunicación bacteriana (***quorum sensing***). Existen diferentes sistemas de señalización empleados por bacterias, a través de los cuales, ésta produce una pequeña molécula que puede ser secretada por difusión o mediante transporte activo hacia el exterior celular. Al aumentar la concentración bacteriana, estas moléculas secretadas se unen a proteínas receptoras. Este receptor constituye un inductor que permite la transcripción de genes. Hay autores que defienden la necesidad de esta comunicación para el inicio de la formación de *biofilm*, la formación de canales y el desprendimiento mediado por la expresión regulada de un número de genes [24].

A. baumannii presenta gran capacidad para adherirse a superficies abióticas por largos periodos de tiempo, por ejemplo, a catéteres. Del mismo modo, es capaz de adherirse fácilmente a las células epiteliales bronquiales humanas, lo que explica la colonización y persistencia en el organismo [25]. Esta facilidad de adhesión a superficies es debido a la producción de *biofilm*; por lo que suponen una gran preocupación debido a sus efectos perjudiciales en muchos sistemas médicos mecanizados, lo que los convierte en un reservorio de contaminación bacteriana [24].

3.3. Sistemas de captación de hierro y sideróforos.

El hierro es uno de los elementos más abundantes en la corteza terrestre y puede existir en dos estados oxidativos: ferroso (Fe^{2+}) y férrico (Fe^{3+}). Todos los organismos vivos presentan sistemas de solubilización, transporte y almacenamiento de hierro, ya sea ferroso o férrico, para satisfacer sus necesidades [26].

Este elemento es esencial para el crecimiento bacteriano debido a su actividad redox y su implicación en procesos metabólicos vitales para la bacteria, actuando como cofactor. Por tanto, el hierro juega un papel muy importante a la hora de infectar, colonizar tejidos y en la patogénesis de la bacteria [27].

Uno de los sistemas de captación de hierro más importantes en procariotas es el **sistema Feo**, con afinidad por el **Fe^{2+}**. Aunque inicialmente fue descubierto en *E. coli*, también se ha descrito en *A. baumannii*. Este sistema de captación de hierro está codificado por el operón *feoABC*. FeoB es la única proteína cuya función es conocida. Se trata de una proteína de alto peso molecular que presenta una región N-terminal con un dominio GTPasa en el citoplasma, a través del cual regula el transporte, y una región C-terminal embebida en la membrana citoplasmática. Por la contra, las funciones de FeoA y FeoC son desconocidas. Ambas son proteínas de pequeño tamaño y FeoC es la región menos conservada del sistema Feo, ya que en muchos organismos el operón *feo* carece del gen *feoC* [28,29].

Nuestro grupo ha demostrado la importancia del gen *feoA* de *A. baumannii* en su virulencia y su implicación en la absorción de hierro, la adhesión a células eucariotas, la formación de *biofilm* y la resistencia al estrés oxidativo [19] (ver *anexo II*).

En condiciones *in vivo*, el hierro no se encuentra fácilmente disponible debido a la captación por parte de células eucariotas a través de proteínas, tales como la transferrina o la lactoferrina, que son componentes del sistema inmune innato [26,30]. Por lo tanto, las bacterias responden produciendo quelantes específicos de hierro, como son los **sideróforos**. Éstos son productos biosintéticos con gran afinidad por el **Fe^{3+}** [26]. *A. baumannii* presenta tres sideróforos: acinetobactina, baumanoferrina y fimsbactina. La acinetobactina es un factor de virulencia firmemente establecido en modelos murinos de infección y está altamente conservado [31].

La amplia distribución de estos sistemas de captación de hierro en *A. baumannii* implica que la absorción de hierro contribuye favorablemente a la patogenicidad de esta especie.

3.4. Polisacáridos de superficie.

El polisacárido de superficie de mayor relevancia en *A. baumannii* es el **lipopolisacárido (LPS)** y es el componente principal de la membrana externa de las bacterias Gram negativas. El LPS está formado por un dominio hidrofóbico denominado lípido A, un núcleo de oligosacárido no repetido (*core*) y un polisacárido distal compuesto de estructuras repetidas con longitudes variables denominadas antígeno O. Algunas de sus funciones son la evasión bacteriana del sistema inmune y su localización superficial contribuye a la interacción de la bacteria con el ambiente [32]. También se ha descrito que el lípido A es la región más tóxica e inflamatoria, la cual, es un factor importante responsable de la gravedad de las sepsis causadas por *A. baumannii* [32,33]. El LPS también es antigénico debido a su capacidad para inducir la respuesta inmune innata, lo que lo convierte en un candidato prometedor para el diseño de vacunas [34].

El **polisacárido capsular K1** es considerado un factor de virulencia importante en bacilos Gram negativos, pero no representa un papel tan importante en la patogenicidad de *A. baumannii*. Russo y col. identificaron dos genes necesarios para la polimerización y el ensamblaje de la cápsula. El primero, *ptk*, codifica una supuesta proteína tirosina quinasa (PTK) y el segundo, *epsA*, codifica una supuesta proteína de exportación de polisacáridos de la membrana externa (EpsA). Estos dos genes son esenciales para la supervivencia de la bacteria *in vivo* [35].

Otro polisacárido de superficie importante en *A. baumannii* es el **β-(1-6)-N-acetilglucosamina (PNAG)**, el cual, es esencial para la integridad del *biofilm* producido por este patógeno [21].

3.5. Sistemas de secreción.

Los sistemas de secreción son canales proteicos dependientes de ATP que se localizan en la membrana de las bacterias y cuya función es expulsar proteínas y otras moléculas biológicas al exterior celular, favoreciendo la interacción de la bacteria con el entorno.

En *A. baumannii* existen diferentes tipos de sistemas de secreción. Uno de ellos es el **sistema de secreción tipo II (T2SS)**, el cual, está formado por un complejo proteico constituido por 12-15 proteínas distintas que generalmente están codificadas en un solo operón [36]. El T2SS media la secreción de toxinas y enzimas hidrolíticas, incluyendo proteasas, lipasas, lipoproteínas y enzimas que descomponen carbohidratos complejos. También es necesario para la supervivencia *in vivo* y la virulencia de este patógeno. Los sustratos de T2SS se unen al mismo para su transporte a través de la membrana externa mediante las vías *Sec* o TAT [37].

Recientemente, se ha demostrado la presencia del **sistema de secreción tipo VI (T6SS)** en diferentes especies de *Acinetobacter*. El T6SS, además de introducir proteínas a través de las membranas celulares procariotas y eucariotas, proporciona una ventaja de colonización en el medio ambiente o durante la infección de muchos patógenos [38].

- Vesículas de membrana externa.

Las vesículas de membrana forman parte de un sistema de secreción utilizado por muchas bacterias Gram negativas. Este sistema permite la diseminación de productos bacterianos al entorno y promueve la interacción con otras células, evitando el contacto entre las mismas. Las vesículas de membrana están involucradas en la adquisición de nutrientes, el mantenimiento de la estructura del *biofilm* y en la transferencia horizontal de genes, entre otros procesos [39].

Las **vesículas de membrana externa** son un tipo de vesículas de membrana y son producidas por células procariotas en crecimiento, no durante la lisis o muerte celular. Su estructura es esférica con una bicapa y de un tamaño medio entre 50 y 200 nm de diámetro [40]. Se producen cuando una pequeña porción de la membrana externa se abulta llevando consigo el contenido periplásmico; por lo que están formadas

principalmente por lipopolisacárido, proteínas periplásmicas, proteínas de la membrana externa, fosfolípidos, ARN y ADN [39,40].

En el año 2011, nuestro grupo demostró que *A. baumannii* libera vesículas de membrana externa capaces de transportar el gen $bla_{\text{OXA-24/40}}$, el cual confiere resistencia a carbapenems, sin pérdida de viabilidad; constituyendo así una posible forma de diseminación de plásmidos con genes de resistencia a antibióticos de impacto clínico [40].

3.6. Bombas de expulsión.

Las bacterias han desarrollado sistemas de expulsión de compuestos tóxicos para prevenir su acumulación intracelular. Estas **bombas de expulsión** son canales proteicos que se extienden a lo largo de la membrana externa y son dependientes de energía, por lo que no implican la alteración o degradación de fármacos [41]. Las bombas de expulsión juegan un papel importante en el establecimiento de la resistencia de las bacterias a una amplia gama de compuestos tóxicos, incluyendo antibióticos [42], y constituyen entre el 6 y el 18% de todos los sistemas de transporte presentes en cualquier especie bacteriana [41].

En bacterias Gram negativas puede existir una sinergia entre las bombas de expulsión y una baja permeabilidad de la membrana externa, lo que supone un incremento de la resistencia a antibióticos [41].

A. baumannii presenta diferentes tipos de sistemas de expulsión, de los cuales, los de mayor relevancia son **AdeABC** y **AdeIJK**. El operón *adeABC* se encuentra en el 80% de los aislamientos clínicos y está regulado por el sistema de dos componentes AdeRS. Por otra parte, el operón *adeIJK* se expresa en niveles bajos, lo que lleva a una disminución débil de la actividad de algunos antibióticos; pero un incremento en su expresión contribuye a la resistencia a múltiples fármacos. En *A. baumannii* se han descrito otros sistemas adicionales de expulsión: a) CraA, que confiere resistencia a cloranfenicol; b) AbeS, implicado en resistencia a detergentes; y c) AbeM, una familia de expulsión de compuestos tóxicos y antibióticos [43].

3.7. Porinas.

La membrana externa de las bacterias Gram negativas constituye una barrera selectiva de permeabilidad. Las **porinas** son canales proteicos en forma de barril-β que permiten la captación de nutrientes y moléculas hidrofílicas mediante transporte pasivo. La única exclusión de este tipo de transporte es por límite de tamaño y el diámetro de las porinas varía en función de las distintas especies bacterianas. Las porinas fueron caracterizadas por primera vez en un aislamiento de *E. coli* en 1976 [41].

La principal porina de *A baumannii* y la más abundante en su membrana externa se denomina **OmpA**. Ésta se encuentra altamente conservada entre diferentes especies bacterianas [44]. En *A. baumannii* juega un papel muy importante en el mantenimiento de la estructura de la membrana externa y en la patogénesis, ya que facilita la unión de células eucariotas, la invasión y su apoptosis [45]. Smani y col. demostraron que la pérdida del gen *ompA* en *A. baumannii* está implicada en un aumento en la sensibilidad a ácido nalidíxico, aztreonam y cloranfenicol [44]. Este aumento de la sensibilidad podría deberse a cambios inespecíficos en la permeabilidad de la membrana externa como resultado de la pérdida de este componente estructural [45].

A. baumannii presenta otras porinas en su membrana externa implicadas en su virulencia, como son **CarO**, **OprD-like** y **Omp33-36**. Éstas se encuentran estrechamente relacionadas también con la resistencia de *A. baumannii* a carbapenems, debido a que facilitan la difusión del antibiótico a lo largo de su membrana externa. Se ha demostrado que la expresión de estas porinas se encuentra reducida en cepas de *A. baumannii* resistentes a dicho antibiótico β-lactámico [46].

La porina Omp33-36 ha sido ampliamente estudiada por nuestro grupo y se concluyó su implicación en la inducción de la apoptosis celular mediante la activación de la caspasa y en la posterior modulación de la autofagia. También se observó una mayor persistencia de las cepas de *A. baumannii* portadoras de esta proteína en el interior de macrófagos, causando citotoxicidad [47].

4. Terapias antimicrobianas frente a *A. baumannii* y sus principales mecanismos de resistencia.

El tratamiento de elección frente a *A. baumannii* todavía no se ha establecido. De forma rutinaria se utiliza un carbapenem en monoterapia o combinado a un aminoglucósido, como para otros bacilos Gram negativos. *A. baumannii* presenta una gran plasticidad genética para adquirir resistencias, lo que explica que una gran proporción de los aislamientos de esta especie son resistentes a carbapenems **(CRAB)** [48]. Los antimicrobianos actuales para el tratamiento de infecciones causadas por CRAB, por ejemplo polimixinas, tigeciclina y aminoglucósidos, están lejos de ser opciones terapéuticas perfectas debido a sus propiedades farmacocinéticas y tasas de resistencia crecientes (tablas 1 y 2).

Tabla 1: Comparación de las tasas de resistencia a antimicrobianos en *A. baumannii* entre los años 2000 y 2010. Éstas se evaluaron en dos periodos durante el estudio. Tabla modificada de Fernández-Cuenca F., *et al.* Enferm. Infecc. Microbiol. Clin. 2013. doi: 10.1016/j.eimc.2012.06.010.

Antimicrobiano	Tasas de resistencia en %, 2001 (n = 221 Ab)	Tasas de resistencia en %, 2010 (n = 446 Ab)	Diferencia entre ambos periodos	*p* valor
Piperacilina	93	94	+ 1	0,74
Ceftazidima	83	99	+ 16	0,000
Sulbactam	53	65	+ 12	0,0042
Imipenem	48	82	+ 34	0,000
Meropenem	43	83	+ 40	0,000
Doripenem	NT	86	ND	ND
Gentamicina	96	70	− 27	0,000
Tobramicina	79	60	− 19	0,0001
Amikacina	65	49	− 17	0,0001
Tetraciclina	91	83	− 8	0,0096
Doxiciclina	68	70	+ 2	0,53
Minociclina	34	30	− 4	0,30
Tigeciclina	NT	23,9	ND	ND
Ciprofloxacino	98	94	− 5	0,0074
Rifampicina	51	30	− 21	0,000
Colistina	0,0 (polimixina B)	3	+ 3	0,0068

ND: no disponible; NT: no testado.

Tabla 2: Principales mecanismos de resistencia a antibióticos en *A. baumannii*. Tabla modificada de McConnell MJ., *et al.* FEMS Microbiol. Rev. 2013; 37:130–55. doi:10.1111/j.1574-6976.2012.00344.

Antibiótico	Mecanismos de resistencia más relevantes	Ejemplos
β-lactámicos	Inactivación enzimática	β-lactamasas (AmpC, TEM, VEB*, PER, CTX-M, SHV) Carbapenemasas (OXA-23, -24/40, -51, -58, 143, VIM, IMP, NDM-1, -2)
	Alteración de las PBPs	PBP2
	Disminución de la expresión de porinas	OmpA, CarO, Omp 33–36, OprD-like
	Bombas de expulsión	AdeABC
Fluoroquinolonas	Modificación de la diana	Mutaciones en *gyrA* y *parC*
	Bombas de expulsión	AdeABC, AdeM
Aminoglucósidos	Enzimas modificadores de aminoglucósidos	AAC, ANT, APH
	Bombas de expulsión	AdeABC, AdeM
	Metilación ribosomal	ArmA
Tetraciclinas	Bombas de expulsión	AdeABC, TetA, TetB
	Protección ribosomal	TetM
Glicilglicinas	Bombas de expulsión	AdeABC
Polimixinas (colistina)	Modificación de la diana	Mutaciones en el sistema de dos componentes PmrA/B (modificación LPS), mutaciones en genes de biosíntesis LPS

4.1. Carbapenems.

Los carbapenems son antibióticos β-lactámicos de amplio espectro. Presentan mayor actividad antimicrobiana y mayor estabilidad frente a enzimas β-lactamasas (enzimas que hidrolizan el anillo β-lactámico) que el resto de los antibióticos de su familia [49]. Su mecanismo de acción, al igual que el de todos los antibióticos β-lactámicos, consiste en la **inhibición** de forma **irreversible de la biosíntesis del peptidoglicano (PG)** de la pared celular de las células procariotas. El esqueleto del PG está constituido por cadenas de glúcidos, formadas por la repetición de moléculas de ácido N-acetilmurámico y N-acetilglucosamina. El ácido murámico, a su vez, fija cadenas de tetrapéptidos que forman una malla. El paso final de la síntesis del PG consiste en la formación de estos tetrapéptidos a partir de pentapéptidos mediante la pérdida de uno de los aminoácidos terminales (D-alanil-D-alanina). Este paso, denominado

transpeptidación, es catalizado por las *penicillin binding proteins* (PBPs, proteínas de unión a penicilinas) que son unas enzimas transpeptidasas que se localizan en el periplasma. Los antibióticos β-lactámicos se unen de forma covalente al centro activo de las PBPs bloqueándolas. Esta unión irreversible evita la transpeptidación, interrumpiendo así la síntesis de la pared, y activa enzimas autolíticos de la pared celular bacteriana [50].

Los carbapenems se metabolizan y se excretan en el riñón [51]. En las células del túbulo proximal del riñón se encuentra localizada una metaloenzima de zinc: dehidropeptidasa renal tipo I (DHP-I). Ésta hidroliza dipéptidos, dehidropéptidos, así como antibióticos β-lactámicos de conformación *trans*, por ejemplo, el **imipenem**. Con el fin de evitar la hidrólisis del fármaco por parte de la metaloenzima, se administra el imipenem en combinación con un inhibidor de ésta, denominado cilastatina. La cilastatina es un inhibidor reversible y competitivo de la DHP-I cuya estructura es similar a la de los enlaces escindibles en el imipenem y dehidropéptidos [49].

El **imipenem** deriva de un compuesto denominado tienamicina que es producido por la bacteria *Streptomyces cattley*. Fue comercializado en 1985 y es el tratamiento de elección en sepsis polimicrobianas. El **meropenem** es otro antibiótico carbapenémico. Penetra muy bien en diferentes tejidos y líquidos corporales, por lo que inicialmente la FDA lo aprobó en el año 1996 para el tratamiento de infecciones intraabdominales y meningitis bacteriana. El **ertapenem** fue comercializado en 2001. Es considerado tratamiento de primera línea en infecciones causadas por patógenos Gram negativos productores de β-lactamasas de espectro ampliado (**BLEAs**) y en aquellas causadas por patógenos adquiridos en la comunidad. Tanto el ertapenem como el meropenem son más estables a la DHP-I que el imipenem, por lo que no es necesario administrarlos asociados a cilastatina [51]. Existen otros carbapenems de desarrollo más reciente, como son doripenem, biapenem, panipenem, razupenem o tomopenem.

4.1.1. Mecanismos de resistencia en *A. baumannii* frente a carbapenems.

Las tasas de resistencia a carbapenems superan el 85% en algunas partes del mundo, incluido España [48,52], y vienen dadas por los siguientes mecanismos de resistencia:

- Enzimas β-lactamasas.

Los enzimas β-lactamasas constituyen el principal mecanismo de resistencia a los antibióticos β-lactámicos en *A. baumannii*. Estos enzimas hidrolizan el anillo β-lactámico, presente en todos los antibióticos pertenecientes a este grupo. Existen diferentes tipos de enzimas β-lactamasas. La clasificación de Ambler es la más sencilla y se categoriza a las distintos tipos de enzimas por secuencia proteica, por lo que se clasifican en cuatro clases moleculares: A, B, C y D [53].

β-LACTAMASAS DE CLASE A.

Las β-lactamasas de clase A son enzimas dependientes de serina, al igual que las β-lactamasas de clase C y D. Estos enzimas presentan una serina en su centro activo, la cual, actúa como nucleófilo para atacar el enlace C-N de la β-lactama. Se forma un enzima acil-intermediario, el cual es hidrolizado y el producto liberado del sitio activo de la β-lactamasa, facilitando el ataque nucleofílico [54].

Inhiben penicilinas y cefalosporinas de forma mucho más eficaz que carbapenems, a excepción de las **KPC** que se encuentran ampliamente distribuidas en enterobacterias e hidrolizan eficazmente carbapenems [18].

Las combinaciones de antibióticos β-lactámicos e inhibidores de β-lactamasas que se usan habitualmente en la práctica clínica, por ejemplo, amoxicilina-ácido clavulánico, piperacilina-tazobactam o ampicilina-sulbactam son eficaces frente a las β-lactamasas de clase A [53]; a excepción de las KPC, las cuales, no son inhibidas por ninguna de estas combinaciones terapéuticas. Sin embargo, avibactam y relebactam inhiben eficazmente a todas las β-lactamasas de clase A. Este último muestra gran afinidad frente a las KPC.

β-LACTAMASAS DE CLASE B.

También se denominan metalo-β-lactamasas (MBL) y su mecanismo se basa en una molécula de agua coordinada a un catión divalente (Zn^{2+}), el cual, activa y rompe el anillo β-lactámico. En este tipo de enzimas no se forma el intermediario acilado [54].

Son enzimas de amplio espectro, por lo que inhiben prácticamente a todos los antibióticos β-lactámicos, incluyendo carbapenems [18]. Al contrario que las serin-β-

lactamasas, no presentan afinidad con monobactamas [53]. Las metalo-β-lactamasas con mayor relevancia clínica *en A. baumannii* son las de tipo IMP, VIM, SIM y NDM [55].

Hasta la fecha, no existe ningún inhibidor comercial capaz de inactivar a las metalo-β-lactamasas. En cambio, son inhibidas por quelantes de metales, como el ácido etilendiaminotetraacético (EDTA), ácido dipicolínico o 1,10-o-fenantrolina [53].

β-LACTAMASAS DE CLASE D.

Las β-lactamasas de clase D, también denominadas OXA, son **las que principalmente hidrolizan carbapenems** y la mayoría han sido identificadas en *A. baumannii* [54,56].

Las β-lactamasas de clase D, al igual que las β-lactamasas de clase A y C, son dependientes de serina [54]. Hasta la fecha, se han descrito más de 800 OXAs. Algunas poseen actividad carbapenemasa. Las β-lactamasas hidrolizantes de carbepenems de clase D (**CHDLs**) se reclasificaron recientemente en 12 subgrupos: OXA-23, OXA-24/40, OXA-48, OXA-51, OXA-58, OXA-134a, OXA-143, OXA-211, OXA-213, OXA-214, OXA-229 y OXA-235. Dentro de cada subgrupo, las secuencias genéticas son idénticas en más del 90% y entre subgrupos, las similitudes son inferiores al 70% [54]. La OXA-23, OXA-24/40, OXA-51, OXA-58, OXA-143 y OXA-235 son prevalentes en *A. baumannii* [57], mientras que la OXA-48 sólo ha sido identificada en enterobacterias [56]. La mayoría de estos enzimas están codificados por plásmidos, excepto la OXA-51 cuya localización es cromosómica [55].

Los inhibidores de β-lactamasas utilizados como el ácido clavulánico, tazobactam o sulbactam, no son del todo eficaces frente a CHDLs [57]. El avibactam inhibe de forma eficaz algunas enzimas OXA, como la OXA-48, pero no a las CHDLs producidas por *A. baumannii* [57]. Sin embargo, el LN-1-255, un inhibidor derivado del ácido penicilánico ampliamente estudiado por nuestro grupo inhibe eficazmente a la OXA-48 y a las CHDLs producidas por *A. baumannii* (ver *sección 6.2.1* y *anexo I*).

- Modificaciones de las *Penicillin Binding Proteins* (PBPs).

Las PBPs son la diana de los antibióticos β-lactámicos y son unos enzimas imprescindibles en la formación y en la integridad de la pared bacteriana [58].

Existen diferentes tipos de PBP y, en función del antibiótico, presenta distintos grados de afinidad por unas u otras [59]. La mayoría de las PBPs presentan cierta afinidad por los carbapenems. Por ejemplo, se encontraron 8 PBPs cuyo peso molecular se sitúa en los 94, 65, 49, 40, 30, 24, 22 y 17 kDa que presentaron alteraciones en su expresión en aislamientos de *A. baumannii* resistentes a carbapenems [60].

Las bacterias pueden modificar sus PBP de diversas formas: a) por la mutación de una PBP ya presente en el genoma bacteriano; b) mediante la adquisición de ADN exógeno que codifica una o varias PBP resistentes al antibiótico, las cuales, reemplazan a las PBP sensibles por recombinación génica; y c) por disminución de la afinidad por el antibiótico. De este modo, estos enzimas conservan su función biológica en la bacteria y pierden afinidad por el antibiótico [2].

- Déficit de porinas y bombas de expulsión.

A. baumannii también puede producir resistencia a carbapenems y a otros antibióticos modificando la permeabilidad de la membrana externa, es decir, mediante un déficit en la expresión de porinas y a través de bombas de expulsión. Estos mecanismos de resistencia también están implicados en la patogénesis de *A. baumannii*, por lo que se comentaron en el apartado anterior (ver *secciones 3.5* y *3.6*).

4.2. Sulbactam.

El **sulbactam** es un inhibidor de β-lactamasas, mayoritariamente, de clase C aunque también inactiva algunas de clase A y D [61]. Actualmente, existen diferentes tipos de inhibidores de β-lactamasas. Los primeros compuestos se desarrollaron entre los años 70 y 80 a partir de la estructura química del núcleo penicilánico con modificaciones. Se denominan "inhibidores clásicos", ya que se han comercializado durante las últimas tres décadas. Unas de las características de este grupo es que se unen al centro activo de las β-lactamasas de forma irreversible.

El sulbactam es una sulfona del ácido penicilánico sintetizada por la industria farmacéutica en 1978 [61]. Posee un radical carboxílico en posición 2 que le permite la obtención de ésteres [2]. Se comercializa en combinación con ampicilina, amoxicilina y

cefoperazona [62]. Su uso fue aprobado en 1987 y se administra tanto por vía oral como por vía parenteral [48].

A diferencia de otros inhibidores de β-lactamasas, el sulbactam presenta actividad intrínseca frente a *A. baumannii* debido a la **inhibición irreversible** de la **PBP3** de este patógeno. Sin embargo, sus elevadas tasas de resistencia limitan su uso [57].

4.2.1. Mecanismos de resistencia en *A. baumannii* frente a sulbactam.

A diferencia de otros agentes antimicrobianos pertinentes para el tratamiento de las infecciones causadas por *A. baumannii*, se conoce poco acerca de la base molecular de la resistencia al sulbactam [64].

No obstante, se ha descrito que el principal mecanismo de resistencia a sulbactam en *A. baumannii*, o el de mayor relevancia, es la presencia de la β-lactamasa **TEM-1** en aislamientos clínicos. Ésta es una β-lactamasa de clase A dependiente de serina. Existe una estrecha correlación entre la resistencia a sulbactam y el nivel de expresión del gen $bla_{\text{TEM-1}}$ en *A. baumannii*, así como en la sensibilidad de aquellas cepas que expresen TEM-19 (una variante de la TEM-1 que presenta muy baja actividad) [64].

Otro mecanismo de resistencia a sulbactam en *A. baumannii* es la presencia de la β-lactamasa de clase C **ADC-30**. En cepas de *A. baumannii* resistentes a sulbactam se encontraron incrementados los niveles de expresión del gen $bla_{\text{ADC-30}}$. Este mecanismo de resistencia es inducido a niveles de ARNm y proteínas por otros agentes antimicrobianos, además del sulbactam [65]. Recientemente, se ha demostrado que la β-lactamasa de clase D **OXA-23** también confiere resistencia a sulbactam en *A. baumannii* [66]. Por lo tanto, la resistencia a sulbactam en *A. baumannii* es multifactorial. Las tasas de resistencia a sulbactam en *A. baumannii* se situaron en torno al 65% en el año 2010 en España [52].

4.3. Colistina.

La **colistina** pertenece a una familia de antibióticos denominada polimixinas. La colistina, también denominada **polimixina E**, fue aislada por primera vez del hongo *Paenibacillus polymyxa* var. *colistinus* en 1949 [67]. Las polimixinas se comercializaron durante los años 50 y 60, pero cayeron en desuso hacia la década de los 80 debido a su elevada toxicidad, sobre todo, nefrotoxicidad y neurotoxicidad [68]. Sin embargo, debido a la falta de terapias antimicrobianas eficaces frente a patógenos multirresistentes como *A. baumannii*, *P. aeruginosa* o *K. pneumoniae*, la colistina ha sido reintroducida en los años 90 para el tratamiento de los mismos [67]. Existen 5 tipos de polimixinas, aunque únicamente las polimixinas B y E se utilizan actualmente en la práctica clínica [68]. Las terapias basadas en combinación con colistina son preferibles a la colistina en monoterapia debido a la reducción de la dosis de este antibiótico y, por lo tanto, la reducción de su toxicidad [48].

La colistina es un polipéptido catiónico que actúa interrumpiendo las membranas bacterianas y causando la muerte celular [69]. La molécula de colistina interactúa con el lipopolisacárido (LPS) de la membrana externa, desplazando iones de Mg^{2+} y Ca^{2+}, con carga positiva. De este modo, el LPS queda cargado negativamente, lo que destruye la integridad de la membrana y, como consecuencia, conduce a la muerte celular [67].

4.3.1. Mecanismos de resistencia en *A. baumannii* frente a colistina.

Actualmente, la colistina es un antibiótico considerado como última opción terapéutica cuando el tratamiento con antibióticos de elección no es eficaz. Presenta tasas de resistencia bajas, aunque van aumentando paulatinamente. En un estudio multicéntrico de *A. baumannii* realizado en España entre el 2000 y el 2010, esta ratio pasó de un 0% de resistencias registradas en el año 2000 a un 3%, 10 años más tarde [52] (tabla 1). El informe anual de vigilancia publicado por el Centro Europeo de Prevención y Control de Enfermedades (ECDC), concluyó que en el año 2014 un 4% de las cepas de *A. baumannii* presentaban resistencia a colistina, presentando Grecia e Italia las mayores tasas de resistencia [70].

Un paso crítico en la acción de las polimixinas es la interacción electrostática entre la carga positiva del péptido (polimixina) y la carga negativa del lípido A, el componente endotóxico del LPS. Los mecanismos de resistencia a colistina generalmente implican modificaciones en el lípido A [71].

En el año 2011, nuestro grupo caracterizó por primera vez la base molecular de la resistencia a colistina en *A. baumannii*. La resistencia adquirida a polimixinas en bacterias Gram negativas principalmente se encuentra mediada por el reemplazo del lípido A por arabinosa (L-Ara4N) y **fosfoetanolamina (pEtn)**, mediada por el gen *pmrC*. Estas modificaciones resultan en la eliminación de las cargas negativas del LPS, disminuyendo así la afinidad de las polimixinas por el mismo [72]. Cabe destacar que *A. baumannii* carece de los genes de biosíntesis de L-Ara4N, por lo que utiliza la adición de pEtn como principal mecanismo de resistencia a la colistina, que se encuentra mediado por el operón ***pmrABC*** [67]. En este contexto, se ha descrito el sistema de regulación de dos componentes **PmrAB**, el cual, requiere de al menos dos mutaciones genéticas distintas: un cambio aminoacídico en el gen *pmrB* y la expresión aumentada de los genes *pmrA* y *pmrB* [72]. Finalmente, *pmrC* facilita la adición de la pEtn al lípido A y, por lo tanto, un aumento de la expresión de *pmrC* suele asociarse a mutaciones en los reguladores PmrAB, lo que resulta en una disminución de la sensibilidad de la bacteria a la colistina [67].

Por otra parte, Moffat y col. describieron varios mutantes espontáneos resistentes a colistina de la cepa tipo *A. baumannii* ATCC 19606. Estas cepas presentaron mutaciones dentro de los genes esenciales para la biosíntesis del lípido A, en los genes *lpxA*, *lpxC* o *lpxD*. Estos mutantes de *A. baumannii* ATCC 19606 perdieron la capacidad de producir el lípido A y, por lo tanto, el LPS [71]; confirmando así la implicación de la pérdida del lípido A en la resistencia a colistina. Este segundo mecanismo es muy poco frecuente en cepas clínicas.

4.4. Tigeciclina.

La **tigeciclina** es un agente bacteriostático que deriva de la minociclina, el primer antibiótico de la familia de las glicilciclinas [73]. Las glicilciclinas son nuevos

compuestos semisintéticos que contienen una sustitución en la posición 9 de moléculas derivadas de la tetraciclina. Su mecanismo de acción consiste en la inhibición de la traducción de proteínas en las bacterias uniéndose a la subunidad ribosomal 30S. La tigeciclina se sitúa en el sitio A de la subunidad ribosomal e interacciona con residuos de histidina de ésta, proporcionándole así mayor afinidad. Esta interacción le confiere al antibiótico protección ribosomal, dificultando el desarrollo de los mecanismos de resistencia de la bacteria. Este antibiótico es considerado de amplio espectro y no se ve afectado por los mecanismos clásicos de resistencia a la tetraciclina, incluyendo la protección ribosómica y el flujo por bombas específicas de la tetraciclina [74].

Esta glicilciclina ha sido la primera aprobada en Estados Unidos para el tratamiento de infecciones intraabdominales y cutáneas complicadas, así como para neumonía adquirida en la comunidad. Además, debido a la falta de otras opciones de tratamiento efectivas, la tigeciclina se utiliza a menudo fuera de indicación terapéutica en el tratamiento de neumonía nosocomial, bacteriemias e infecciones del tracto urinario causadas por patógenos Gram negativos multirresistentes [73,74].

La tigeciclina tiene una potente actividad *in vitro* frente a *A. baumannii* y desde el año 2006 se utiliza en el tratamiento de infecciones originadas por cepas resistentes a carbapenems de este patógeno. Sin embargo, presenta algunos problemas farmacocinéticos como niveles plasmáticos bajos, lo que limita su uso en infecciones del torrente sanguíneo [48].

4.4.1. Mecanismos de resistencia en *A. baumannii* frente a tigeciclina.

El desarrollo de resistencia a tigeciclina está mediado, principalmente, por modificaciones en la permeabilidad de la membrana, con el fin de reducir la concentración del antibiótico en el interior de la célula procariota. La expresión de tales mecanismos de resistencia puede requerir una amplia inversión metabólica, lo que a menudo conduce a una reducción de *fitness* de estas bacterias [75]. Las tasas de

resistencias a tigeciclina en *A. baumannii* en España en el año 2010 rondaban el 25% [52].

- Bombas de expulsión.

El principal mecanismo de resistencia a tigeciclina en *A. baumannii* es mediante bombas de expulsión pertenecientes a la familia *resistance-nodulation-cell division* (RND), de modo que se reduce la concentración del antibiótico en el interior de la bacteria [16,75]. Un aumento en la expresión de las bombas de expulsión AdeABC, AdeFGH y AdeIJK se ha relacionado con la resistencia a tigeciclina en *A. baumannii,* de los cuales, AdeABC ha sido descrito como el sistema RND más relevante al exportar tigecilina [61].

La expresión de la bomba AdeABC está regulada por el sistema de dos componentes AdeRS. El incremento de la expresión del gen *adeR* aumenta, a su vez, la expresión de *adeB*, lo que conlleva a un aumento de la resistencia a tigeciclina. No obstante, son más frecuentes las mutaciones en *adeS*, lo que también resulta en una sobreexpresión de AdeABC [75] (ver *sección 3.5*).

- Déficit de porinas.

La tigeciclina entra en las células bacterianas a través de difusión pasiva o transporte activo. Una disminución de la expresión de porinas o transportadores provoca una menor entrada del antibiótico en la bacteria y la imposibilidad de acceder a su diana (ver *sección 3.6*) [16].

4.5. Aminoglucósidos.

Los aminoglucósidos son antibióticos de amplio espectro. El primer antibiótico de esta familia es la estreptomicina, aislada del hongo *Streptomyces* spp. en 1944 y todavía en uso. A la estreptomicina le siguieron la neomicina, la kanamicina o la gentamicina, entre otros [77].

Esta familia de antibióticos ejerce su acción a través de la unión a la subunidad 30S de los ribosomas bacterianos. Mediante esta unión modifica la conformación del sitio A de la subunidad. Como consecuencia, las capacidades de corrección del ribosoma se reducen, lo que resulta en una la mala traducción de las proteínas [77]

Con el fin de evadir los mecanismos de resistencia que las bacterias han ido desarrollando, se comenzaron a diseñar derivados semisintéticos mediante la adición de grupos químicos. Uno de estos derivados es la **amikacina**, cuya estructura proviene de la kanamicina y fue comercializado en 1977. Debido a su propiedad de ser refractario a la mayoría de las enzimas modificadoras de aminoglucósidos, la amikacina es el antibiótico perteneciente a esta familia más utilizado en el tratamiento de infecciones causadas por patógenos resistentes a aminoglucósidos, como *A. baumannii*. En cambio, su nefrotoxicidad y sus crecientes tasas de resistencia limitan su uso [48,77].

4.5.1. Mecanismos de resistencia en *A. baumannii* frente a amikacina.

Las tasas de resistencia en *A. baumannii* a amikacina se sitúan entre el 68 y el 100% [48] y vienen dadas, principalmente, por los siguientes mecanismos:

- Aminoglucósido-acetiltransferasas.

La acetilación del N en la posición 6’ de la amikacina es el principal mecanismo de resistencia a este antibiótico que presentan las bacterias. Esta acetilación se encuentra mediada por enzimas denominadas aminoglucósido-acetiltransferasas (AAC) y se encuentran en diferentes variantes, la mayoría de las cuales, difieren en el N terminal. Además de la amikacina, estos enzimas suelen conferir resistencia a otros aminoglucósidos como la tobramicina y la kanamicina, pero no a la gentamicina [77].

- Metiltransferasas.

Las metiltransferasas son enzimas cuya función es autoprotectora, ya que introducen un grupo metilo en el ribosoma bacteriano con la finalidad de protegerse contra metabolitos secundarios tóxicos. Se transmiten por plásmidos y existen diferentes tipos. En *A. baumannii* el enzima predominante es ArmA [78,79].

5. Búsqueda de nuevas dianas terapéuticas.

El uso incorrecto de antibióticos y la escasa inversión en el desarrollo de nuevos fármacos en este campo han provocado la falta de alternativas reales comercializadas y útiles para el tratamiento de las infecciones causadas por *A. baumannii*. Esto implica la necesidad de buscar nuevas dianas con el objetivo final de diseñar nuevos compuestos antimicrobianos. Áreas como la genómica, proteómica o transcriptómica han sido potenciadas como herramientas adecuadas en el intento de localizar y evaluar nuevas dianas terapéuticas [17].

5.1. Genómica.

La genómica estudia el conjunto de los genes que forman el genoma de los organismos y sus características [80]. Las técnicas de secuenciación dan información de los genomas de los organismos aislados y en su conjunto (*pan-genomes*); lo que nos permite identificar los genes más relevantes y esenciales para la bacteria y por otro lado, los más conservados, como dos grupos claramente diferenciados. La combinación de la información genómica junto con la fenotípica es la clave, tanto para el estudio de factores de virulencia, como de mecanismos de resistencia conservados o emergentes [81].

Durante los últimos años, los avances de la genómica han permitido comprender los mecanismos que intervienen en la patogénesis de *A. baumannii.* Así, el estudio del genoma de *A. baumannii* durante un periodo de tiempo, nos permite evaluar cómo las distintas poblaciones han divergido, revelando un cambio importante en el trasfondo genético predominante en aquellas cepas causantes de infecciones. También nos permite examinar, por ejemplo, el genoma de cepas de *A. baumannii* aisladas en distintos centros hospitalarios, examinando así cuáles son las principales vías de transmisión [6].

5.2. Proteómica.

La proteómica es un área de estudio relativamente reciente y está incluida dentro de la genómica. Consiste en el estudio de las proteínas intra- o extracelulares en un momento y bajo unas condiciones determinadas, independientemente de su secuencia lineal de genes. Además de la identificación de todo el proteoma, esta ciencia también estudia la naturaleza proteica, las interacciones entre las mismas y su localización, así como las modificaciones postraduccionales que se pueden llevar a cabo en la proteína y su implicación en el metabolismo celular [80].

El estudio del proteoma de *A. baumannii* proporciona información muy válida sobre la biología del patógeno. En esta última década se han realizado análisis transcriptómicos y proteómicos utilizando modelos *in vitro*. Por ejemplo, en un estudio de los elementos genéticos involucrados en células sésiles asociadas a la formación de *biofilm* en *A. baumannii*, los autores evaluaron 55 genes que codifican proteínas expresadas exclusivamente durante el desarrollo de *biofilm* [82]. En el año 2009, nuestro grupo realizó un análisis del proteoma citoplasmático y de la membrana de *A. baumannii*. Los datos obtenidos demostraron que este patógeno presenta un metabolismo robusto y versátil capaz de explotar una variedad de fuentes de carbono y energía. Además, reveló la presencia de proteínas de alta expresión que, probablemente, desempeñen un papel crucial no sólo en los mecanismos de virulencia y de resistencia a los antibióticos, sino también en el medio ambiente adaptativo. Estas proteínas seguramente están relacionadas con la persistencia de la bacteria en el entorno hospitalario, una de las señas de identidad de este microorganismo [83].

5.3. Transcriptómica.

Los análisis transcriptómicos estudian el conjunto de ARN mensajero transcrito en una célula. Cada vez se utilizan más en la investigación biomédica y se realizan bajo diferentes condiciones, las cuales, nos dan información de los procesos biológicos que están ocurriendo. Por ejemplo, en los estudios del transcriptoma *in vivo* se analizan muestras de ARN bacteriano extraídas directamente de la infección, las cuales

confieren información relevante sobre los procesos biológicos que se producen durante la patogénesis.

Los análisis previos del transcriptoma de *A. baumannii* proporcionaron información relevante sobre la biología de este género. También se han estudiado los reguladores de las principales rutas transcripcionales. Hasta la fecha se han realizado muy pocos estudios en los que se describa el perfil de expresión génica de *A. baumannii in vivo*, es decir, durante el proceso infeccioso. El primer estudio en el que se describe el perfil de expresión génica de *A. baumannii in vivo* se realizó en el año 2017. En este estudio, Murray y col. analizaron el transcriptoma de *A. baumannii* durante bacteriemia, detectando algunas dianas terapéuticas potenciales, como los genes implicados en la biosíntesis de lipopolisacáridos y cápsulas o en la formación de *biofilm* y pili, así como en el metabolismo [84].

6. Nuevas alternativas terapéuticas frente a *Acinetobacter baumannii.*

El aumento de resistencias a los antimicrobianos actuales en la práctica clínica ha propiciado la necesidad de diseñar y desarrollar nuevos compuestos cuyos mecanismos de acción superen a los mecanismos de resistencia. Actualmente, se encuentran en desarrollo numerosos candidatos y otras opciones terapéuticas que podrían satisfacer estas expectativas [48].

6.1. Nuevos antibióticos en desarrollo.

El desarrollo de nuevos antibióticos se basa en la síntesis de nuevas moléculas o bien, en mejorar las propiedades de los ya existentes; ya sea por unión de radicales a su estructura química que mejoren su eficacia, o mediante la unión a otro compuesto que lo haga más específico y, por lo tanto, menos tóxico.

6.1.1. Cefalosporinas sideróforas.

Los sideróforos son compuestos de bajo peso molecular que sintetizan las propias bacterias. Estas moléculas tienen alta afinidad por el Fe^{3+}; así su función biológica consiste en solubilizar el hierro en el ambiente y enviarlo de vuelta al citoplasma de los microorganismos [17]. Este sistema de captación puede ser utilizado para mejorar la afinidad del fármaco con la bacteria, acoplando el sideróforo al compuesto antimicrobiano.

- Cefiderocol.

El cefiderocol es una cefalosporina de reciente aprobación por la FDA para el tratamiento de infecciones del tracto urinario complicadas. Esta cefalosporina se encuentra conjugada con un catecol en su cadena lateral. La mayoría de los sideróforos tienen en su estructura química un grupo catecol [17,48]. Este grupo catecol le proporciona a la cefalosporina un mecanismo distintivo de absorción activa y, por lo tanto, una mayor penetración de las células bacterianas. El cefiderocol también mostró mayor estabilidad frente a muchas clases de β-lactamasas y actividad contra bacterias Gram negativas altamente resistentes [48].

- Otros sideróforos.

Existen otras cefalosporinas asociadas a sideróforos en desarrollo comercial, como son GSK-3342830 o GT-1. Este último todavía ha sido incluido en fase clínica I recientemente.

La fimsbactina, un sideróforo encontrado en *A. baumannii*, se ha acoplado a la daptomicina. De este modo, la fimsbactina ayudaría a la daptomicina a atravesar la membrana externa y llegar al citoplasma bacteriano [48].

6.1.2. Tetraciclinas.

Las tetraciclinas se unen la subunidad 30S del ribosoma, inhibiendo así la traducción del ARNm y, por lo tanto, la síntesis de proteínas [85]. Actualmente, se encuentran en desarrollo dos tetraciclinas fluoradas.

- Eravaciclina.

La eravaciclina es un agente antibacteriano sintético, cuya estructura es similar a la tigeciclina con dos modificaciones en el anillo D de su núcleo: a) un átomo de flúor reemplaza a la dimetilamina en C-7 y b) un pirrolidin-acetamido reemplaza al 2-terc-butil-gliclamido en C-9 [86].

Al igual que otras tetraciclinas, la eravaciclina inhibe la síntesis de proteínas a través de la unión a la subunidad 30S del ribosoma bacteriano. Este antibiótico demostró actividad frente a una amplia variedad de patógenos, incluyendo MDR o XDR, Gram positivos o anaerobios. La FDA aprobó su uso exclusivo para el tratamiento de infecciones intraabdominales complicadas en mayores de 18 años [48,86].

- **TP-6076.**

Este compuesto se trata de otra tetraciclina fluorada. Demostró su actividad bactericida en un modelo de neumonía murina con cepas de *A. baumannii*. Actualmente, se encuentra en fase clínica I [48].

6.1.3. Otros antibióticos β-lactámicos.

En las dos últimas décadas, apenas se han comercializado nuevos antibióticos β-lactámicos. No obstante, sí que existen varios compuestos en desarrollo, como el **AIC-499** o el **FSI-1671**. Este último se trata de una nueva clase de carbapenems conjugado con sulbactam [48].

6.1.4. Polimixinas.

De manera similar a lo que sucede con los antibióticos β-lactámicos, no hay ninguna polimixina nueva de aprobación reciente; pero sí en fases de desarrollo. Se han estado estudiando moléculas derivadas de la polimixina B, como por ejemplo el **SPR741**. Este péptido catiónico permeabiliza la membrana de bacterias Gram negativas, potenciando así el efecto de otros antibióticos como la rifampicina, claritromicina o la eritromicina frente a *A. baumannii*, entre otros patógenos. Actualmente, SPR741 se encuentra en fase clínica I [48,87].

6.2. Nuevos adyuvantes en desarrollo.

Lamentablemente, no siempre se dan las condiciones óptimas científicas, comerciales o de regulación para el descubrimiento de nuevos fármacos. Por lo tanto, también debemos centrar los estudios en preservar los antibióticos ya existentes. En este punto juegan un papel importante los adyuvantes. Estos compuestos se conciben conjugados a un antibiótico, ya sea para evadir los mecanismos de resistencia de las bacterias frente a dicho antimicrobiano o para incrementar su eficacia antibiótica [88].

6.2.1. Inhibidores de β-lactamasas derivados del ácido penicilánico.

Los inhibidores clásicos de β-lactamasas derivan de la estructura química del ácido penicilánico. Sulbactam y tazobactam, desarrollados en los años 80, son **sulfonas de ácido penicilánico** y son eficaces frente a β-lactamasas de clase A, C y muy pocas de clase D. Dentro de éstas últimas, las denominadas CHDL suponen un paradigma en el tratamiento de las infecciones causadas por *A. baumannii*, puesto que el carbapenem es uno de los antibióticos más utilizados en estos casos en la práctica clínica (ver *sección 4.1*).

Las sulfonas de ácido penicilánico como el **LN-1-255,** presentando en posición 2 una cadena 6-alquilideno, representan unos candidatos prometedores (figura 1) [89]. Estos compuestos fueron diseñador originalmente con el grupo del Dr. Buynak y actualmente continuamos en nuestro grupo esta línea de trabajo.

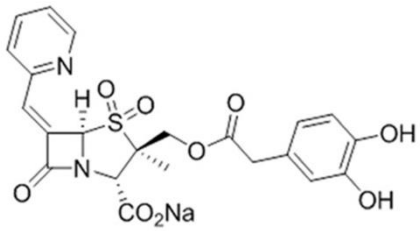

LN-1-255

Figura 1: Estructura química del inhibidor LN-1-255. Figura de Vázquez-Ucha JC., *et al*. (2017) Antimicrob. Agents. Chemother. 61: e01172-17. doi: 10.1128/AAC.01172-17.

El LN-1-255 fue ampliamente estudiado a lo largo de este proyecto (ver *anexo*). Este inhibidor presentó una alta afinidad hacia la OXA-23, OXA-24/40, OXA-51, OXA-58, OXA-143 y OXA-235 de *A. baumannii*, sobre todo la OXA-24/40 con la que demostró mayor eficacia de inhibición [57]. De manera similar, inhibe la OXA-48 de enterobacterias. Cabe destacar que el LN-1-255 también presenta actividad de inhibición frente a β-lactamasas de clase A como SHV y recupera la susceptibilidad antimicrobiana a imipenem, ensalzando su potencial bactericida [90]. Recientemente, evaluamos la eficacia de inhibición del LN-1-255 en modelos *in vivo* obteniendo unos resultados prometedores [91] (ver *anexo*). Hasta la fecha, se trata del único inhibidor de β-lactamasas con capacidad para inhibir a las carbapenemasas de clase D.

6.2.2. Inhibidores de β-lactamasas no derivados del ácido penicilánico.

Recientemente, se han aprobado inhibidores de β-lactamasas no relacionados estructuralmente con el anillo β-lactámico, como por ejemplo el avibactam o el relebactam. Estos dos últimos pertenecen a la familia de los **diazabiciclooctanones (DBO)**, en la cual, también se incluyen otros adyuvantes todavía en desarrollo. Otros inhibidores de β-lactamasas no β-lactámicos son aquellos derivados del **ácido borónico**.

- Diazabicilooctanones (DBO).

Los DBOs son inhibidores de β-lactamasas de "segunda generación" desarrollados a principios de los años 2000 y se han expandido exponencialmente en un período de 15 años (figura 2). Los primeros inhibidores DBO fueron avibactam y relebactam, los cuales, inactivan β-lactamasas de clase A, C y algunas de clase D. Actualmente, se encuentran en fases clínicas inhibidores DBO con "doble acción", ya que son capaces de inhibir PBPs y β-lactamasas, incluidas BLEAs [92].

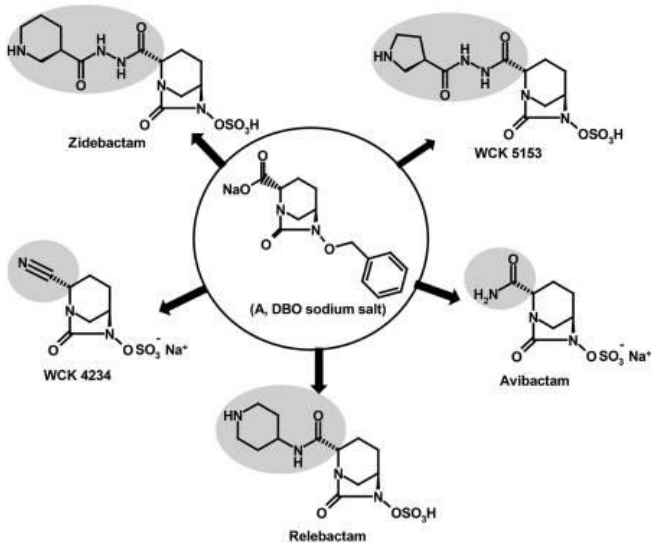

Figura 2: Inhibidores de β-lactamasas DBO. Figura de Papp-Wallace KM., *et al.* (2018) J. Med. Chem. 61:4067–86. doi: 10.1021/acs.jmedchem.8b00091.

- Zidebactam y WCK 5153: Estos inhibidores presentan actividad frente a las PBP2, sobre todo de *A. baumannii*, y potencia la acción bactericida del antibiótico β-lactámico. Cabe destacar su actividad frente a las AmpC más representativas de *P. aeruginosa* [92]. Ambos inhibidores también son activos frente a la OXA-23 y la OXA-51 de *A. baumannii* en modelos murinos y a las MBL de enterobacterias en ensayos *in vitro* [48,93].

- ETX2514: Al igual que los anteriores, este compuesto inhibe a las PBP2 y potencia la actividad del antibiótico β-lactámico. Presenta una serie de modificaciones en la estructura química central de los DBO, que le confiere actividad frente a un amplio abanico de OXAs. El ETX2514 se está desarrollando en combinación con sulbactam [48,92].

- WCK 4234: Este inhibidor de β-lactamasas DBO se está desarrollando en combinación con meropenem. Es activo frente a varias carbapenemasas, incluyendo la OXA-23 y la OXA-51 de *A. baumannii* [48]. La combinación de este inhibidor y meropenem es algo menos eficaz frente a cepas de *A. baumannii* productoras de OXA-24/40 [92].

- Ácidos borónicos.

A finales de la década de 1970, los ácidos borónicos fueron reconocidos como inhibidores de β-lactamasas dependientes de serina en ensayos *in vitro*. El mecanismo de acción de estos inhibidores radica en el boro, el cual, forma un vínculo reversible con el centro activo de la β-lactamasa. No obstante, a pesar de que el boro presenta gran afinidad por las β-lactamasas serin-dependientes, los ácidos borónicos no lograron llegar al desarrollo clínico hasta hace relativamente pocos años [94].

Los representantes de este grupo, como el RPX7009 o el S02030, no presentan actividad frente a *A. baumannii*; sin embargo sí que presentó actividad frente a enterobacterias resistentes a carbapenems o portadoras de KPC [94,95].

6.2.3. Inhibidores de la proteasa del péptido señal.

En las bacterias, alrededor del 20% de todas las proteínas se exportan fuera del citoplasma. El péptido señal es esencial para dirigir a las proteínas hacia la membrana citoplasmática y se escinde del resto de la proteína antes de entrar en el periplasma, finalizando así el proceso de maduración de las mismas [96,97]. Esta escisión la realizan las proteasas del péptido señal (SPasas). Existen dos tipos de SPasas, de tipo I y de tipo II. Las **SPasas de tipo I** son endopeptidasas de membrana que utilizan residuos de serina y lisina como nucleófilos en su centro activo y son las más frecuentes en la mayoría de las bacterias. Son responsables de la ruptura del péptido señal de proteínas excretadas durante la traslocación de la membrana a través de la vía de secreción general *Sec*. Las proteínas entran en el periplasma a través del canal SecYEG, dependiente de energía. Esta energía para la traslocación a través de la membrana proviene de la hidrólisis de ATP procedente de la bomba ATPasa SecA. Por otra parte, las **SPasas de tipo II** utilizan residuos de aspartato en su centro activo [98].

Las características generales de los péptidos señal se conservan a lo largo de la evolución. Tienen una región en la secuencia amino-terminal (1 a 5 residuos de longitud), denominada “región N”, con carga neta positiva. La región N es seguida por un tramo de 7 a 15 residuos hidrofóbicos, con frecuencia leucinas, a los que llamamos “región H”. Seguido de la región H, se encuentran de 3 a 7 residuos denominados la

"región C". Ésta contiene los residuos de especificidad para el reconocimiento y escisión por parte de la SPasa. La secuencia de consenso para el sitio de corte consiste en pequeños residuos alifáticos en las posiciones -3 y -1 en relación con el punto de corte (figura 3) [98].

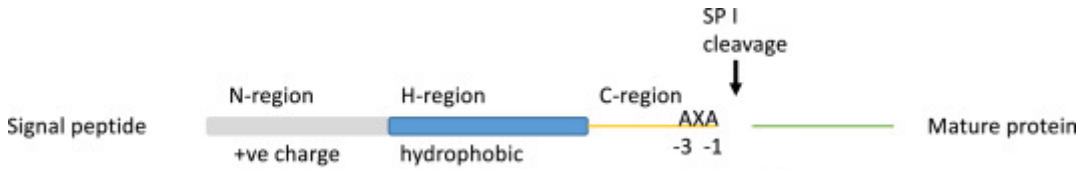

Figura 3: Esquema del péptido señal, dependiente de la vía *Sec*, y del sitio de corte reconocido por la proteasa del péptido señal de tipo I en *E. coli* y *B. subtilis*. Figura de Zalucki YM., *et al.* (2017) Biochem. Biophys. Res. Commun. 483:972–7. doi: 10.1016/j.bbrc.2017.01.044.

Durante las dos últimas décadas, se ha intentado desarrollar algún compuesto inhibidor, pero sin éxito comercial hasta el momento. Cabría esperar que el desarrollo de compuestos inhibidores sería más sencillo en bacterias Gram positivas, ya que el sitio activo del enzima está expuesto en la superficie de la célula. En cambio, en bacterias Gram negativas, el sitio activo se encuentra en el espacio periplásmico, entre la membrana citoplásmica y la membrana externa; por lo que sería inaccesible para moléculas lipófilas y de alto peso molecular, al no poder atravesar la membrana externa [96]. Para solventar este último inconveniente, es necesario el desarrollo de terapias combinadas con el inhibidor y agentes permeabilizadores de membrana, como son la colistina y el hexametafosfato de sodio.

Recientemente, Smith y col. realizaron una serie de modificaciones en la estructura química de las arilomicinas, confiriéndoles así actividad frente a patógenos Gram negativos. Estas modificaciones permitieron identificar análogos, los cuales, presentan mayor afinidad con el objetivo y mejor penetración en la membrana externa que la molécula original. Uno de estos análogos es el **G0775**, una arilomicina sintética con potente actividad antibacteriana *in vitro* frente a los patógenos Gram negativos incluidos en las siglas "ESKAPE" [96].

6.3. Terapias de inmunización: vacunas.

El desarrollo de vacunas contra las enfermedades infecciosas ha sido uno de los logros más notables de la historia de la humanidad. La vacunación ha erradicado enfermedades como la viruela y ha controlado la transmisión de otras, como son la difteria, la poliomielitis, la tos ferina, el sarampión y el tétanos neonatal [99].

La prevención es tan importante como la erradicación de la enfermedad. El patógeno bacteriano interactúa con el huésped y también ha desarrollado varias estrategias para evadir el sistema inmune del mismo. Por lo tanto, la vacunación es una estrategia prometedora para reducir la frecuencia de infecciones por *A. baumannii*, aunque hasta la fecha no existe ninguna comercializada frente a este patógeno [100,101].

La vacunación es una forma de inmunización activa y existen diferentes tipos de vacunas bacterianas en función de la parte antigénica involucrada.

6.3.1. Vacunas de células enteras.

En este tipo de inmunización se administra la célula entera, no sólo la parte antigénica o epítopos. Pueden ser bacterias vivas atenuadas o muertas inactivadas.

- Vacunas vivas atenuadas.

Las vacunas vivas atenuadas pueden ser muy eficaces, ya que son versiones inofensivas de patógenos e imitan la infección natural. Tradicionalmente, la atenuación de la virulencia se logró a través de la selección natural por múltiples pasajes del microorganismo en el medio de cultivo, mutagénesis aleatoria o modificación genética de los genes diana para atenuar la virulencia. En este último modo cabe destacar que no existen dianas genéticas universales para la atenuación bacteriana, por lo que se necesita de los conocimientos básicos de las técnicas moleculares y de los mecanismos de patogenicidad para cada especie o cepa bacteriana [102].

En el año 2017, nuestro grupo diseñó una estrategia para la síntesis de vacunas vivas atenuadas con aplicación para cualquier patógeno bacteriano. Se basaron en un componente esencial del peptidoglicano bacteriano, que se encuentra en la pared

celular de todas las bacterias: el D-glutamato. Manipularon genéticamente las cepas *A. baumannii* ATCC 17978, *P. aeruginosa* PA01 y *S. aureus* 123 con el fin de obtener cepas auxótrofas de D-glutamato. Los resultados fueron muy prometedores, demostrando una eficacia fiable como cepas vivas atenuadas en un modelo murino de infección aguda [102].

- **Vacunas muertas inactivadas.**

Este tipo de vacunas se basan en inactivar a la bacteria por calor o con formaldehído. Se ha sugerido que son más seguras que las vivas atenuadas, pero presentan menos inmunogenicidad.

Existen estudios sobre vacunas inactivadas derivadas de la exposición a antibióticos frente a *A. baumannii*. El pretratamiento con antibióticos de *A. baumannii* ha demostrado que mejora la expresión de aquellas proteínas que le confieren resistencia a los mismos. En todo caso, ya sea una vacuna inactivada derivada de la exposición a antibióticos o no, existe una respuesta robusta de anticuerpos IgG presentes en el suero de ratones inmunizados y que reconocen la cepa de *A. baumannii* utilizada como diana [103].

6.3.2. Vacunas recombinantes de subunidades.

Las vacunas recombinantes de subunidades son aquellas en las que la inmunización se obtiene a partir de epítopos de la bacteria. A diferencia de las vacunas de células enteras, este tipo de vacunas se administran junto con adyuvantes, los cuales, potencian su actividad inmunogénica [99].

Las vacunas recombinantes de subunidades pueden ser de naturaleza proteica, las cuales se diseñan a partir de la identificación de proteínas de membrana antigénicas que contienen factores de virulencia, factores de resistencia y el factor de esencialidad para la bacteria patógena. Esta proteína antigénica identificada se utiliza como diana en el diseño de la proteína recombinante, la cual, se obtiene mediante un proceso de ingeniería genética que consiste en clonar el gen de interés en un vector de expresión y transformarlo en una especie diferente a la original. Después, se procede a la

purificación de la proteína y a la evaluación de su inmunogenicidad en un organismo vivo [101].

Lin y col. clonaron y expresaron una proteína recombinante de OmpA, ésta es la porina más abundante en la membrana externa de *A. baumannii*. Tras la purificación de rOmpA, se administró en ratones con el fin de inmunizarlos y medir la respuesta del sistema inmune. Los resultados demostraron que rOmpA se podría utilizar como una vacuna altamente efectiva, ya que protegió a los ratones de una infección por *A. baumannii* que sería letal [100].

Otro ejemplo de vacuna recombinante de subunidades son las vacunas de extractos proteicos de la membrana externa o complejos de membrana externa (CME). Éstas inducen una respuesta de anticuerpos frente a múltiples antígenos de la membrana externa de bacterias Gram negativas. McConnell y col. desarrollaron en 2011 una vacuna CME frente a *A. baumannii* y los resultados fueron prometedores. Demostraron que las vacunas CME inducen una respuesta específica de antígeno, tanto humoral como celular y que el tratamiento de ratones con esta vacuna fue más que suficiente para conferir inmunidad frente a este patógeno bacteriano [34,104].

6.4. Terapia fágica.

El desarrollo de terapias fágicas es una forma potencial de mejorar el tratamiento de infecciones bacterianas. Los fagos son virus capaces de infectar y matar a las bacterias al final del ciclo lítico de infección, ya que destruyen la pared celular con el fin de liberar nuevos fagos [105].

Para romper la pared celular de la bacteria, algunos bacteriófagos líticos usan proteínas simples, como las amurinas, que inhiben la síntesis del PG. Sin embargo, la mayoría de ellos utilizan dos grupos de proteínas para producir la lisis de la célula huésped. El primero, constituido por holinas, establece sinergia con el segundo, endolisinas. La función de las holinas es perforar el citoplasma del huésped y, por consiguiente, facilitar el acceso de las endolisinas al peptidoglicano bacteriano. Por su parte, las endolisinas son proteínas enzimáticas responsables de la degradación de la

pared celular, las cuales, son utilizadas por los bacteriófagos para hidrolizar el peptidoglicano de las bacterias infectadas [105].

Existen estudios que demuestran que la terapia fágica resulta eficaz frente a *A. baumannii*. Regeimbal y col. aislaron fagos específicos de *A. baumannii*. Realizaron un cóctel con 5 de estos fagos y trataron la infección de *A. baumannii* en un modelo murino de herida quirúrgica, resultando con éxito. También resultó exitoso el mismo cóctel de fagos en una infección de *A. baumannii* en un modelo de *Galleria mellonella*. [106].

Recientemente, Schooley y col. utilizaron un tratamiento terapéutico basado en un cóctel de fagos personalizado para tratar a pacientes diabéticos con pancreatitis necrosante complicada por una infección de *A. baumannii*. La administración de estos bacteriófagos por vía parenteral en las cavidades del absceso se asoció con la reversión de la trayectoria clínica descendente del paciente y la eliminación de la infección producida por *A. baumannii* [107].

6.5. Nanopartículas.

Las nanopartículas son sistemas nanométricos con un núcleo interno y una cubierta externa. Se comenzaron a desarrollar a mediados de los años 80 y se han popularizado como formas farmacéuticas debido a su biocompatibilidad, biodegradabilidad y capacidad para controlar la distribución de medicamentos en el cuerpo [108].

Las nanopartículas han tenido mucha aplicabilidad en el área de oncología, sobre todo, para dirigir los fármacos antineoplásicos a la célula cancerígena y reducir así su toxicidad. Del mismo modo, el hecho de aplicar la nanotecnología en el tratamiento de infecciones causadas por patógenos multirresistentes en una terapia combinada, nos permitiría potenciar la actividad de los antimicrobianos ya existentes y, consecuentemente, reducir su toxicidad.

En el campo de la microbiología, se utilizan diferentes tipos de nanopartículas con múltiples mecanismos de acción para combatir a las bacterias. Entre estos mecanismos se incluyen nanopartículas liberadoras de óxido nítrico (NONPs), nanopartículas que

contienen quitosano (chitosan NPs), nanopartículas de poliarginina (ArgNPs) y nanopartículas de metales, como las de oro y plata (AuNPs y AgNPs, respectivamente) [109].

Recientemente, se ha estudiado la eficacia de las nanopartículas de oro y plata frente a *A. baumannii*. Ambos tipos de nanopartículas fueron conjugados con polimixinas; colistina en el caso de AuNPs y polimixina B con AgNPs [110,111]. Las AuNPs fueron diseñadas para el redireccionamiento con *A. baumannii* mediante la unión de colistina y polietilenglicol (PEG), éste último actuando como ligante. A través de técnicas como la microscopía electrónica de transmisión y la espectroscopía de energía dispersiva de rayos X, se demostró la eficacia de la unión de Col-PEG-AuNPs a la envoltura celular de *A. baumannii* [110]. En el caso de las AgNPs se demostró un efecto sinérgico entre las nanopartículas y la polimixina B, tanto en modelos *in vitro* como *in vivo* [111].

6.6. Agentes antisentido.

La tecnología de interferencia de ARN ha sido estudiada en los últimos años. Los agentes antisentido se basan en el reconocimiento de una secuencia específica de ARN mensajero, lo que conduce a una expresión reducida o alterada de la traducción. Este mecanismo puede ser explotado en estrategias de ingeniería genética para inhibir la síntesis de proteínas esenciales [112]. Los agentes antisentido son oligómeros de 10-30 nucleótidos de longitud, cuya secuencia es complementaria a la del ARNm que queremos inactivar. Modificaciones en la estructura química de estas moléculas conducen a los diferentes tipos de agentes antisentido: *phosphorothioate* (PS), ***peptide nucleic acid*** **(PNA)**, *phosphorodiamidate morpholino oligomers* (PMO) o *locked (bridged) nucleic acids* (LNA/BNA), entre otros [113].

Existen fármacos basados en esta tecnología en ensayos clínicos, e incluso comercializados, para el tratamiento de la distrofia muscular de Duchenne y algunos cánceres; lo que avala el potencial clínico de estos agentes [114]. De modo similar, algunos estudios han demostrado eficacia antibacteriana frente a algunos patógenos como *E. coli*, *K. pneumoniae*, *P. aeruginosa* o *S. aureus* [115–118]. También se ha demostrado que el PNA anti-*gyrA* presentó una inhibición del crecimiento de un

aislamiento clínico de *A. baumannii* [119]. Además, un uso alternativo relevante de la tecnología antisentido es la inactivación de genes de resistencia, modificando el fenotipo de resistencia a antibióticos [120,121]. Por lo tanto, el uso antimicrobiano de esta tecnología ha sido demostrada en los últimos años y podría ser una fuente potencial de nuevos medicamentos.

Los **PNAs** se desarrollaron por primera vez a principios de los años 90 por Nielsen y col. [122]. La estructura química del PNA es similar a la del ADN, en la que el enlace peptídico reemplaza a la estructura azúcar-fosfato. Las unidades de N-(2-aminoetil)-glicina están unidas por enlaces peptídicos para formar la molécula de PNA, y las bases nucleotídicas están unidas a la estructura principal a través de un enlace de metileno carbonilo. La molécula del PNA es eléctricamente neutra y puede hibridarse fuertemente con las moléculas de ADN o ARN sin repulsión de carga [115].

Los PNAs son resistentes a la actividad enzimática de nucleasas y proteasas bacterianas. Estas moléculas deben penetrar adecuadamente a través de la pared celular bacteriana para poder ejercer su acción. No obstante, los PNAs tienen un tamaño superior a la mayoría de antibióticos [112], por lo que requieren de la conjugación de **péptidos permeabilizantes de células (CPPs)** para poder atravesar mejor la pared celular y potenciar su eficacia [115]. La capacidad de permeabilización de los CPPs varía en función de las especies bacterianas, siendo los más comúnmente usados los CPPs $(KFF)_3K$, $(RX)_6B$, $(RXR)_4XB$, o $(RFR)_4X$ [123–125].

7. Síntesis.

Esta Tesis Doctoral está constituida por cuatro capítulos. Los tres primeros se focalizan en la búsqueda de nuevas dianas terapéuticas frente al patógeno multirresistente *A. baumannii*, empleando una metodología novedosa como es la transcriptómica. Los dos últimos se centran en el diseño de nuevos compuestos antimicrobianos y el empleo de nuevas alternativas terapéuticas para el tratamiento de infecciones causadas por *A. baumannii*.

En el **primer capítulo**, presentamos un **análisis transcriptómico** de las cepas de *A. baumannii* ATCC 17978 y AbH12O-A2 utilizando ARN aislado de los pulmones de ratones durante el curso de una infección de neumonía. Tras el análisis transcriptómico, obtuvimos una colección de genes hiperexpresados durante el curso de la infección pulmonar que podrían estar involucrados en la patogenicidad de *A. baumannii*. A partir de la caracterización del transcriptoma durante la infección en pulmón, hemos elaborado 21 mutantes derivados isogénicos de aquellos genes diferencialmente expresados en el pulmón. Finalmente, realizamos un estudio funcional de esta colección de genes mediante ensayos *in vitro* e *in vivo*.

Uno de los genes estudiados es el gen ***hisF*** **(A1S_3245)**. Este gen está implicado en la biosíntesis de purinas e histidina. HisF e HisH forman una proteína heterodimérica imidazol glicerol fosfato sintasa (IGP). Esta enzima heterodimérica cataliza la transformación del intermediario N'-(5'-fosforibosil)-formimino-5-aminoimidazol-4-carboxamida ribonucleótido (PRFAR) en 5'-(5-aminoimidazol-4-carboxamida) ribonucleótido (AICAR) y fosfato de glicerol de imidazol (ImGP), los cuales, se utilizan también en la biosíntesis de purinas y de la histidina, respectivamente [126–128].

AICAR es uno de los productos de HisF y presenta una estructura análoga a la del monofosfato de adenosina (AMP). Este producto es capaz de estimular la actividad de AMPK, una proteína quinasa activada por AMP. Ambas moléculas, monofosfato de AICAR y AMP, desencadenan un cambio conformacional en el complejo AMPK que permite una mayor activación por fosforilación de Thr-172. Este complejo AMPK es un regulador central de la homeostasis energética, el cual, participa en la respuesta celular al estrés metabólico, siendo considerada como una importante diana terapéutica para el control de diferentes enfermedades que afectan al ser humano [129].

Una vez activado, AMPK fosforila a numerosos enzimas metabólicos causando tanto la inhibición global de las vías biosintéticas, como la activación de las vías catabólicas. De este modo, genera y conserva energía [130]. Por otra parte, se ha demostrado que AICAR también es capaz de inhibir la producción de citoquinas proinflamatorias inducida por lipopolisacáridos. Se ha demostrado que el tratamiento con un inhibidor de la adenosina quinasa es capaz de bloquear la capacidad de AICAR para activar la

AMPK, previniendo la inhibición de la inflamación en las células mesangiales en ratones [131,132]. Otros autores también han descrito el papel de AICAR en la regulación de la inflamación [131,133].

La evaluación del gen *hisF* en la patogénesis de *A. baumannii* y su implicación en la respuesta inmune durante la infección por neumonía constituyen el **segundo capítulo** de esta Tesis Doctoral.

Otro gen identificado durante el curso de la infección pulmonar de *A. baumannii* en ratones fue ***lpxB*** **(A1S_1668)**, el cual, está implicado en la formación del lípido A. En la mayoría de las bacterias Gram negativas, el LPS es el principal componente de la membrana externa y está constituido por un dominio hidrofóbico denominado lípido A, un *core* oligosacárido central y el antígeno O [134]. En la vía de síntesis del lípido A, el enzima glicosiltransferasa LpxB cataliza el ataque nucleofílico del 6'-hidroxil del lípido X para formar el disacárido-1-fosfato, el principal componente del lípido A [135]. Por lo tanto, el enzima LpxB parece esencial en las bacterias Gram negativas para desarrollar un LPS intacto, mantener la estructura de la envoltura celular y el crecimiento bacteriano.

Por otra parte, los genes *lpx* están involucrados en la resistencia de *A. baumannii* a colistina (ver *sección 4.3.1*); por lo que cabe esperar que inactivando el gen *lpxB*, se afectará a la actividad de la colistina sobre la bacteria.

En este capítulo utilizamos la tecnología antisentido para la evaluación de LpxB como diana terapéutica y para demostrar la eficacia de los PNA como compuestos antimicrobianos. Por otra parte, comparamos la eficacia del **pPNA anti-*lpxB*** con otros pPNA conjugados, como anti-*murA* y anti-*hisF*, en la inhibición de la traducción, la inhibición del crecimiento bacteriano y la protección de células epiteliales humanas A549 infectadas. También se ha estudiado la sinergia con la colistina tanto en cepas susceptibles como resistentes a la colistina. Cada vez es más preocupante el aumento de resistencias a colistina, considerado un antibiótico de última opción debido a su elevada neurotoxicidad y nefrotoxicidad. Por tanto, es importante el desarrollo de nuevos fármacos que muestren efectos sinérgicos con dicho antibiótico, permitiendo

así disminuir la dosis y, por consiguiente, su toxicidad. Este estudio constituye el **tercer capítulo** de esta Tesis Doctoral.

Por último, el **cuarto capítulo** de esta Tesis Doctoral abarca la evaluación de la actividad antimicrobiana del compuesto **MD3**. Éste es una β-aminocetona con actividad frente a la proteasa del péptido señal de tipo I LepB, de *P. aeruginosa*. Tras la traslocación, LepB corta el péptido señal de la pre-proteína, liberando la proteína madura en el periplasma. El MD3 se sintetizó en el año 2012 e inicialmente se evaluó su eficacia frente a *Mycobacterium tuberculosis*, mostrando inhibición del crecimiento bacteriano y actividad bactericida [136].

La β-aminocetona MD3 fue ampliamente estudiada por nuestro grupo frente al patógeno *A. baumannii* y en combinación con colistina. La colistina desestructura la membrana bacteriana, permitiendo un mejor acceso del compuesto al interior celular. Así esa sinergia entre estas dos moléculas podría reducir las dosis de colistina y, por consiguiente, su toxicidad.

II. OBJETIVOS

Objetivos.

Acinetobacter baumannii es un patógeno nosocomial que se caracteriza por su plasticidad genética, lo que le permite adquirir con facilidad diversos mecanismos de resistencia a los antibióticos. El mal uso de éstos ha propiciado el resurgimiento de estos patógenos multirresistentes y, por consiguiente, el fracaso de las terapias antimicrobianas actuales. Por lo tanto, es necesaria la búsqueda de nuevas dianas y el desarrollo de nuevas alternativas terapéuticas reales.

Esta Tesis Doctoral abarca esta finalidad en cuatro capítulos. Los tres primeros se centran en el estudio de nuevas dianas terapéuticas; mientras que los dos últimos, en la evaluación de nuevas terapias antimicrobianas. Los títulos de los cuatro capítulos que conforman este proyecto, así como los objetivos de cada uno, son los siguientes:

- Capítulo I. **Estudio global del transcriptoma de *Acinetobacter baumannii* durante el desarrollo de neumonía murina.**

Objetivo 1. Determinación de los perfiles de expresión génica de *A. baumannii* durante el desarrollo de neumonía.

Objetivo 2. Evaluación, mediante ensayos *in vitro* e *in vivo*, de la función biológica de aquellos genes de interés y su implicación en la virulencia de *A. baumannii*.

- Capítulo II. **Implicación de HisF en la persistencia en pulmón de *Acinetobacter baumannii* durante una infección por neumonía.**

Objetivo 3. Estudio del papel del gen *hisF* en la patogénesis de *A. baumannii* y en la regulación de la respuesta inflamatoria.

- Capítulo III. **Inhibición del gen *lpxB* de *Acinetobacter baumannii* por conjugados péptido-PNA y evaluación de un efecto sinérgico con colistina.**

Objetivo 4. Evaluación del enzima LpxB como una nueva diana terapéutica de *A. baumannii*.

Objetivo 5. Evaluación del potencial del pPNA anti-*lpxB* para combatir infecciones bacterianas, combinado con colistina o en monoterapia.

- Capítulo IV. **La sinergia entre la colistina y el inhibidor de la proteasa del péptido señal de tipo I MD3 es dependiente del mecanismo de resistencia a colistina en *Acinetobacter baumannii*.**

Objetivo 6. Evaluación de los efectos sinérgicos de la combinación de MD3 y colistina frente a cepas de *A. baumannii* con mecanismos de resistencia a colistina bien caracterizados.

III. CAPÍTULOS

Capítulos

Capítulo I. Estudio global del transcriptoma de *Acinetobacter baumannii* durante el desarrollo de neumonía murina.

Resumen.

En los últimos años, los avances en genómica han permitido comprender los mecanismos implicados en la patogénesis de *A. baumannii* [137,138]. Los estudios de transcriptoma *in vivo* que utilizan muestras de ARN bacteriano extraídas directamente de la infección confieren información relevante sobre los procesos biológicos que se producen durante la patogénesis. Sin embargo, existen muy pocos estudios en los que se describa el perfil de expresión génica de *A. baumannii* durante el proceso infeccioso. En uno de esos estudios, los autores analizaron el transcriptoma de *A. baumannii* durante la bacteriemia, detectando algunas dianas terapéuticas potenciales [84], como los genes implicados en la biosíntesis de lipopolisacáridos y cápsulas o en la formación de *biofilm* y pili, así como en el metabolismo.

En este trabajo presentamos: a) un análisis transcriptómico global de *A. baumannii* ATCC 17978 utilizando ARN aislado de los pulmones de ratones durante el curso de una infección por neumonía, b) la determinación de una colección de genes hiperexpresados durante el curso de la infección pulmonar que podrían estar involucrados en la patogenicidad de *A. baumannii*, c) la construcción de los correspondientes mutantes derivados isogénicos de la cepa de *A. baumannii* ATCC 17978 y d) el estudio funcional de los genes diana mediante ensayos *in vitro* e *in vivo*.

Este primer capítulo constituye un estudio que se encuentra actualmente bajo revisión en la revista *Journal Infectious Diseases*. A continuación, se adjunta el manuscrito enviado a la revista.

Manuscrito.

Global transcriptomic response of *Acinetobacter baumannii* during murine pneumonia.

Marta Martínez-Guitián[#1], Juan C. Vázquez-Ucha[#1], Laura Álvarez-Fraga[#1], Kelly Conde-Pérez[1], Juan A. Vallejo[1], Alejandra Perina[2], Germán Bou[1], Margarita Poza*[1] and Alejandro Beceiro*[1].

[1]Servicio de Microbiología del Complejo Hospitalario Universitario (CHUAC), Instituto de Investigación Biomédica (INIBIC), Centro de Investigaciones Científicas Avanzadas (CICA), Universidad de A Coruña (UDC), A Coruña, Spain.
[2] AllGenetics & Biology SL. Edificio CICA. Campus de Elviña s/n. A Coruña, Spain.

[#] Authors contributed equally to this work.
* Both authors contributed equally for corresponding:
Margarita.Poza.Dominguez@sergas.es (Margarita Poza)
Alejandro.Beceiro.Casas@sergas.es (Alejandro Beceiro)

Address:
Servicio de Microbiología
Complejo Hospitalario Universitario A Coruña (CHUAC)
As Xubias, 15006, A Coruña, Spain.
Telephone: +34 981178000 ext. 292145 Fax: +34 981176097

KEYWORDS: *Acinetobacter baumannii*, *in vivo* transcriptome, animal infection models, murine pneumonia, virulence factors, pathogenesis
RUNNING TITLE: *A. baumannii* transcriptome in lungs

ABSTRACT

Background. Healthcare-associated infections caused by multiresistant pathogens such as *Acinetobacter baumannii* constitute a major health problem worldwide. Here, we present a global transcriptomic analysis of bacterial RNA isolated from lungs of mice infected with the *A. baumannii* ATCC 17978 and AbH12O-A2 strains, with the aim of identifying the genes involved in the development of pneumonia infection.

Material/methods. Total RNA obtained from the infected lungs was analyzed by RNA-sequencing (RNA-seq). Lists of differentially expressed genes were obtained and 21 of these were selected to construct a collection of isogenic mutant strains. The role of the 21 genes in virulence was investigated in a murine pneumonia model. Biofilm formation, motility and adherence abilities, growth rate and antimicrobial susceptibility were analyzed.

Results. Transcriptomic analysis revealed a specific gene expression profile in *A. baumannii* during the lung infection. Mutant strains lacking the *feoA*, *mtnN*, *yfgC*, *basB*, *hisF, oatA* genes and a N-acetyltransferase gene, involved in acinetoferrin biosynthesis, showed a loss of virulence in murine pneumonia. Biofilm formation, adherence abilities and growth rate were decreased in some mutants.

Conclusions. The findings revealed that 7 genes, over-expressed during the course of infection, are involved in virulence in pneumonia models and can be considered new therapeutic targets.

BACKGROUND

Healthcare-associated infections caused by multiresistant pathogens constitute a major problem worldwide and are associated with prolonged medical care, worse outcome and costly therapies. The World Health Organization has recently published a list of antimicrobial resistant "priority" pathogens [1]. Among these, *Acinetobacter baumannii* is included in the category of "critical priority" and is considered one of the most dangerous opportunistic pathogens. This microorganism exhibits an excellent ability to develop antibiotic resistance, readily generating multiresistant strains and outbreaks [2, 3]. It is also known for being highly persistent and for its ability to form biofilms on multiple surfaces [4] and to survive in multiple environments [5, 6].

However, nosocomial environments promote the transmission and persistence of this species, which is particularly well adapted to the antimicrobial pressure in clinical settings such as intensive care units and burns units. The incorrect use of antibiotics and the scarce of investment in the development of new drugs have led to a lack of commercially available alternatives for treating infections caused by this pathogen. This implies an urgent need to search for novel targets for designing new antimicrobial therapies.

For this purpose, we analyzed the transcriptome of *A. baumannii* strain ATCC 17978, which is commonly used in biomedical research and has been studied under multiple conditions, including infectious processes [7-9]. To improve our understanding of the pathogenesis of the species, we also conducted transcriptome analysis of clinical strain AbH12O-A2, which triggered the largest outbreak of *A. baumannii* known worldwide occurred in Madrid [10].

Advances in genomics in recent years have led to an improved understanding of the mechanisms involved in the pathogenesis of *A. baumannii* [9, 10]. Transcriptomic and proteomic analysis have been performed using *in vitro* models, revealing different gene expression or proteomic profiles in planktonic and sessile cells associated with *A. baumannii* biofilms [8, 11]. Similarly, transcriptomic analysis has been used to identify *A. baumannii* genes involved in iron uptake [12]. *In vivo* transcriptome studies of bacterial RNA samples extracted directly from infected tissues provide important information about the biological processes that occur during pathogenesis. Few studies have been reported wherein the gene expression profile of *A. baumannii* during the infection. In one such study, the *A. baumannii* transcriptome was determined in samples obtained from mice with bacteraemia and some potential therapeutic targets were detected [13], including genes involved in lipopolysaccharide and capsule biosynthesis, biofilm and pili formation, and metabolism. Insertion sequencing (INSeq) has also been used with transposon mutagenesis and next-generation sequencing in order to identify novel virulence factors involved in the persistence of *A. baumannii* in the lung [14].

In the present study, we conducted a global transcriptomic analysis of *A. baumannii* ATCC 17978 and AbH12O-A2 strains, using RNA isolated from lungs of mice with

pneumonia caused by these strains. The RNA sequencing procedure yielded a collection of genes differentially expressed during the *in vivo* infection relative to those expressed during *in vitro* conditions. Constructions of the corresponding isogenic derivative mutants of *A. baumannii* ATCC 17978 lacking some of those genes and the application of functional studies allow identifying potential novel therapeutic targets.

METHODS

Bacterial strains and growth media

A. baumannii strains ATCC 17978 and AbH12O-A2 were used to study gene expression in a murine pneumonia infection. A total of 21 differentially expressed genes were selected to construct the corresponding mutant strains (Table 1) derived from the *A. baumannii* ATCC 17978 parental strain, for functional analysis. *Escherichia coli* TG1 was used as the recipient strain for cloning procedures. Strains were routinely grown or maintained in Luria-Bertani (LB) medium supplemented with agar or antibiotic, when needed. All strains were grown at 37 °C and stored in 10% glycerol at -80 °C.

Murine pneumonia infection model

An experimental pneumonia model was used to describe the transcriptome of *A. baumannii* strains during the course of the infection, as previously described [15]. BALB/c male mice were inoculated intratracheally with approximately 5.5 x 10^7 CFUs/mouse of exponentially grown cells of the ATCC 17978 and the AbH12O-A2 strains. Mice that died within the first four hours of inoculation were not included in the final analyses. Mice were euthanized with an overdose of sodium thiopental (Sandoz, Holzkirchen, Germany), 20 h after inoculation. Bronchoalveolar lavage (BAL) was immediately performed to yield bacteria suitable for RNA extraction (*in vivo* samples). Collections of the RNA molecules expressed from bacteria grown in LB flasks (OD_{600}= 1.0) at 37ºC and 180 rpm were isolated and considered *in vitro* samples.

The same pneumonia model was used to compare the virulence of the isogenic derivative mutant strains and that of the parental strain, with the exception that in this case the mice were observed during 140 h.

All experiments with mice were carried out with the approval of and in accordance with the regulatory guidelines and standards established by the Animal Ethics Committee (CHUAC, Spain, project code P2015/82).

Bacterial RNA purification

Total RNA was immediately extracted from both *in vivo* and *in vitro* samples with the RNeasy Mini Kit (Qiagen, Venlo, Netherlands). The RNA was then treated with DNAse I (Invitrogen, California, USA) and purified with the RNeasy MinElute Cleanup Kit (Qiagen). The final concentrations and the purity of the samples were determined spectrophotometrically in a BioDrop µLITE system (Isogen Life Science, Utrecht, Netherlands) and a 2100 Bioanalyzer (Agilent Technologies Inc., California, USA) according to the manufacturers' instructions.

RNA-seq sequencing and bioinformatic analyses of gene expression profiles.

Reads from mRNA libraries were obtained using HiScanSQ (Illumina Inc.). Fifty nucleotide reads were aligned with the complete genome of *A. baumannii* ATCC 17978 and plasmids pAB1 and pAB2 (GenBank codes: NC_009085.1, NC_009083.1, and NC_009084.1, respectively). The gene expression profiles thus obtained were first compared in CIC bioGUNE's genome analysis platform (Bilbao, Spain). To acquire complete information about the differentially expressed genes, the sequences were functionally annotated with Sma3s v.2 software [16], which uses the non-redundant UniRef90 database to assign gene names, descriptions and enzyme commission (EC) numbers to the query sequences and adds gene ontology (GO) terms, UniProt keywords and pathways. Finally, the annotated matrix of gene expression analyses was imported into R v3.5.2. The R packages ggplot2 v3.1.0 [17], plotly v4.8.0 [18] and ggrepel v0.8.0 [19] were used to plot the results of the analyses.

Construction of isogenic derivative mutants

A total of 21 genes differentially expressed *in vivo* and *in vitro* were selected for constructing the corresponding isogenic mutant strains derived from the ATCC 17978 parental strain (Table 1). Briefly, the upstream and downstream regions flanking the selected genes were PCR-amplified and cloned into the pMo130 vector using the

primers listed in Table S1. The construction was then used to transform the ATCC 17978 cells by electroporation [20]. Recombinant colonies representing the first crossover event were selected as previously described [8, 21]. The second crossover event leading to the gene knockout strain was confirmed by PCR, with the primers listed in Table S1, as previously described [20].

Adhesion to epithelial cells

Adherence of the isogenic derivative strains to A549 human alveolar epithelial cells was determined relative to that of the parental ATCC 17978 strain, as previously described [15, 20]. Four independent replicates were conducted.

Quantitative determination of biofilm

Biofilm formation ability was determined following previously established protocols [20, 22]. Eight independent replicates were performed.

Statistical analyses

Student's *t*-tests were performed to evaluate the statistical significance of the observed differences in all assays, except in the survival assays, in which the survival curves were plotted using the Kaplan-Meier method [23] and analyzed using the log-rank (Mantel-Cox) test. Differences were considered statistically significant at $p \leq 0.05$.

RESULTS

***A. baumannii* gene expression varies during lung infection.**

Different gene expression profiles were obtained in *A. baumannii* ATCC 17978 cells grown (*in vivo*) during a lung infection relative to cells grown in flasks *(in vitro*). Raw data were deposited in the GEO database (accession code GSE100552), showing that a total of 1958 genes were up-regulated under *in vivo* conditions (relative to expression at *in vitro* conditions) whereas 1806 were down-regulated during the lung infection (relative to expression at *in vitro* conditions) (document GSE100552_ATCC_ODvsATCC_raton.tsv.gz). Raw data from gene expression profiling

of the AbH12O-A2 strain were also deposited in the GEO database with the same accession code (document GSE100552_AbH12O_A2_ODvsADraton.tsv.gz).

A. baumannii strain ATCC 17978 was used for subsequent procedures while the AbH12O-A2 strain was only used for specific comparison and confirmation of gene expression.

Considering a cut-off point in the Log_2 fold change of more than +1 or less than -1, two lists of respectively 224 up-regulated (Supplementary Material, Table S2) and 126 down-regulated genes (Supplementary Material, Table S3) were obtained for the ATCC 17978 strain (Figure 1). These collections of up-regulated and down-regulated genes were further classified according to their molecular functions, cellular location and the biological process in which they are involved (Figure 2).

The data revealed that *A. baumannii* ATCC 17978 genes that were up-regulated during the lung infection were involved in a broad range of biological processes, mainly biosynthesis (18.6%), cellular nitrogen compound metabolism (17.1%), small molecule metabolism (10.6%), and DNA metabolic (7.54%) or catabolic (6.53%) processes, amongst others (Figure 2A). These up-regulated genes were mainly located in the cytoplasm (31.1%), followed by the plasma membrane (20%), cell wall/envelope (13.3%) and intracellular location (13.3%), amongst other cellular components (Figure 2B). Regarding their molecular function, these over-expressed genes were described as being involved in many processes, particularly DNA binding (18.9%), oxidoreductase activity (13.8%), ion binding (13.38%) and nucleic acid binding transcription factor activity (6.12%), among others (Figure 2C).

The predominant biological processes in which *A. baumannii* ATCC 17978 genes that were down-regulated during the pneumonia are involved included biosynthesis, translation, cellular nitrogen compound metabolism, homeostasis, stress response, small molecule metabolism, transport, protein folding and catabolic processes, amongst others (Figure 2D). These genes were mainly located in the cytoplasm (55.1%), followed by the ribosome (17.4%), the cell wall/envelope (10.1%) and the plasma membrane (5.8%), amongst other cellular components (Figure 2E). Regarding their molecular function, those genes that were down-regulated during the pneumonia infection were found to play a role in many processes, mainly oxidoreductase activity (15%), DNA binding (11.7%) and ion binding (10.8%) (Figure 2F).

With the aim of studying the actual implication of some of these genes in lung infection in mice, a group of 21 *in vivo* over-expressed genes in ATCC 17978 strain (A1S_0094, A1S_0241, A1S_0315, A1S_0318, A1S_0781, A1S_0896, A1S_1013, A1S_1028, A1S_1032, A1S_1146, A1S_1247, A1S_1581, A1S_1657, A1S_2247, A1S_2390, A1S_3032, A1S_3245, A1S_3290, A1S_3363, A1S_3410 and A1S_3879), and previously related to pathogenesis, were selected for functional analysis (Figure 1 and Table 1). When expression was evaluated in the AbH12O-A2 strain, all these genes were also over-expressed during pneumonia relative to the expression in *in vitro* conditions, except genes A1S_1146, A1S_1581, A1S_3363 and A1S_3879, which were not found in the AbH12O-A2 genome (Supplementary Material, Table S4).

Some *A. baumannii* genes are involved in lung infection in mice

Isogenic mutant strains lacking each of these 21 genes were constructed from the ATCC 1978 parental strain (Table 1). Pneumonia infection was induced in mice with these 21 mutant derivative strains in order to determine the involvement of the corresponding genes in virulence. The survival rates of mice infected with the mutant strains were compared with those of mice infected with the parental strain. The survival rates of mice infected with mutant strains Δ0242 (Δ*feoA*), Δ0781 (Δ*mtnN*), Δ1657 (codifying for a membrane protein involved in acinetoferrin biosynthesis), Δ2247 (Δ*yfgC*), Δ2390 (Δ*basB*), Δ3410 (Δ*oatA*) and Δ3245 (Δ*hisF*) were significantly higher than those of mice infected with the wild type strain (i.e. mortality rate of 100% in all assays performed) ($p< 0.02$, Table 1, Figure 3). Infection caused by these mutants increased the average time of survival in mice with pneumonia by between 22 and 81%, relative to that in mice with pneumonia caused by the parental strain. No significant differences in mice survival were observed in the other isogenic mutant strains (data not shown).

Effect of gene deletion on the growth rate

Growth rate and replication ability were evaluated in the different bacterial strains. Of all mutants tested, only the Δ2247 mutant strain showed a lower growth rate, with a

longer mean generation time (30 min, μ=0.023) than for the ATCC 17978 strain (25 min, μ=0.027, $p< 0.05$) (data not shown). The growth rates of Δ0242, Δ2390 and Δ1657 strains (all lacking some component involved in iron uptake) were determined in the absence of iron, and those of strains Δ0242 and Δ2390 (52 min, μ=0.013 and 45 min, μ=0.015, respectively) were significantly lower than in the parental strain (38 min, μ= 0.018, $p< 0.05$), while that of Δ1657 strain did not differ significantly (mean generation time (min, μ=0.017) (Figure 4 and Table 1).

Effect of gene deletion on attachment to eukaryotic cells, biofilm formation and antimicrobial susceptibility

Adherence of strains Δ0094, Δ0242, Δ0315, Δ1028, Δ1581, Δ1657, Δ2390 and Δ3032 to A549 alveolar epithelial cells was significantly weaker than in the wild type ATCC 17978 strain (Fig. 5A and Table 1). By contrast, the Δ3879 strain showed a higher capacity (almost two times higher) to adhere to alveolar cells than the parental strain. The other mutants did not show any differences relative the parental strain (data not shown).

Strains Δ0242, Δ0781, Δ1028, Δ1247, Δ1657, Δ3290, Δ3410, and Δ3879 displayed significantly lower ability to form biofilm than the parental strain, while strain Δ3290 showed a higher (almost two-fold) ability to form biofilm (Figure 5B and Table 1). Deletion of the other selected genes did not lead to any significant differences in biofilm production relative to the wild type strain (data not shown).

Antimicrobial MICs were calculated for all derivative mutants. For all mutants, except for the strain Δ2247, the original MICs of tested antimicrobials were retained. Susceptibility to the cephalosporins (β-lactam antimicrobials) cefoxitin, ceftazidime, cefotaxime and cefepime was four times higher in mutant strain Δ2247 than in the parental strain. However, the penicillins and carbapenem antibiotics, imipenem and meropenem retained their activity. Non-β-lactam antibiotics also retained their activity against Δ2247 (Table 2).

DISCUSSION

Gene expression in *A. baumannii* isolated from lungs of mice with pneumonia (*in vivo* conditions) displays a specific profile, with many genes up or down-regulated relative to expression in the corresponding strains grown in LB medium in flasks (*in vitro* conditions). Some of these genes are involved in the progress and success of the lung infection. Among these, genes A1S_0242 (*feoA*), A1S_0781 (*mtnN*), A1S_1657 (N-acetyltransferase involved in acinetoferrin biosynthesis), A1S_2247 (*yfgC*), A1S_2390 (*basB*), A1S_3245 (*hisF*) and A1S_3410 (*oatA*) were found to be involved in virulence, as their deletion increased the survival rate of the infected mice. The present study highlights the involvement of these genes in pathogenesis and that they could potentially be considered novel targets for designing new antimicrobial agents.

The A1S_0242 gene (*feoA*) belongs to the *feo*ABC system, which has been proposed as the major ferrous iron transport system in prokaryotes. In a previous study, our research team evaluated the role of this gene in iron uptake and virulence in *A. baumannii* [15]. Inactivation of the A1S_0242 gene revealed its involvement in fitness, adhesion, biofilm formation and virulence. The A1S_0242 gene therefore potentially represents a novel therapeutic target [15].

The A1S_0781 gene (*mtnN*) codes for a methylthioadenosine/S-adenosylhomocysteine (MTA/SAH) nucleosidase. This enzyme has different roles, including the recycling of adenine and methionine through S-adenosylmethionine (SAM)-mediated methylation reactions. MtnN also plays a crucial role in maintaining homeostasis in bacteria, and is directly involved in the biosynthesis of autoinducers, such as AI-1 and AI-2 [24]. MtnN inhibition may block the production of both autoinducers, thereby disrupting *quorum sensing* [25]. Inhibition of this enzyme can affect the growth of different bacteria *via* several mechanisms. In particular, deletion of *mtnN* resulted in diminished growth and reduced motility in *Vibrio cholera*, and new inhibitors are currently being explored in relation to the potential development of novel broad-spectrum antimicrobials [26]. Relative to the parental strain, the mutant *mtnN* strain showed a decreased virulence during the pneumonia infection, confirming the importance of this gene in pathogenesis, and the mutant also displayed a weaker biofilm formation ability, possibly due to inhibition of bacterial *quorum sensing* [26].

The gene A1S_1657 encodes a putative membrane protein, a N-acetyltransferase that is possibly implicated in ferric siderophore biosynthesis and which belongs to the A1S_1647-1657 cluster [12]. *Acinetobacter haemolyticus* ATCC 17906 produces the siderophore acinetoferrin under iron-limiting conditions, biosynthesis of which is led by the *acbABCD* operon. Interestingly, the *A. haemolyticus* AcbD protein was very similar (77 % identity, 88% similarity) to the protein encoded by A1S_1657 [27]. In addition, this protein displayed high similarity (39% identity, 69% similarity) to RhbD (the Rhizobactin biosynthesis protein), which is a siderophore produced by *Sinorhizobium meliloti* and present in rhizospheres [28]. The A1S_1657 gene is probably involved in recognition of the siderophore; however, this role may be fulfilled by other siderophore receptors [12]. Inactivation of this gene caused significant loss of virulence in pneumonia, biofilm production, attachment and fitness in the absence of iron [12].

The A1S_2247 gene (*yfgC*, renamed *bepA*) codes for a putative periplasmic metalloprotease. This protein has been suggested to be responsible for maintenance of outer membrane integrity in *E. coli,* both by promoting assembly of outer membrane proteins (OMPs) and by proteolytically eliminating OMPs when their correct assembly is compromised. BepA enhances biogenesis of LptD, an essential OMP involved in outer membrane transport and assembly of lipopolysaccharide, a major outer membrane constituent [29, 30]. Previous studies indicated that inactivation of BepA led to higher susceptibility to several antimicrobials in *E. coli* [31]. Interestingly, in the present study, deletion of this gene also increased susceptibility to all cephalosporins tested, maintaining the susceptibility to penicillins, carbapenems and other antimicrobial families. The involvement of this gene in β-lactam resistance is not fully known, but it may be related to access difficulties of the chromosomal β-lactamase to the β-lactams antimicrobials or to compromised barrier functions of the outer membrane [29]. The Δ2247 mutant showed a slight loss of fitness as well as a significant loss of virulence in the mice infection pneumonia model. Inhibition of this gene would thus have a double objective to combat both virulence and resistance to cephalosporins in these bacteria.

The A1S_2390 gene (*basB*) encodes a protein that is involved in the biosynthesis of acinetobactin, which belongs to the *basABCDEFGIJ* cluster. Acinetobactin has previously been described as the most important *A. baumannii* siderophore [32,33]. Acinetobactin-mediated iron sequestration is necessary for establishment of bacterial infection and cell damage [32]. BasB takes part in the final step of acinetobactin biosynthesis and is involved in obtaining pre-acinetobactin from N-hydroxyhistamine and aminoacyl-BasB. Relative to the parental strain, the Δ2390 mutant showed a loss of adhesion ability, a lower growth rate in the absence of iron and a decrease in virulence in a mice pneumonia infection model.

The A1S_3245 gene (*hisF*) is implicated in purine and histidine biosynthesis. The heterodimeric protein imidazole glycerol phosphate (IGP) synthase HisH/HisF catalyzes the transformation of the intermediate N'-(5'-phosphoribosyl)-formimino-5-aminoimidazol-4-carboxamide ribonucleotide (PRFAR) into 5'-(5-aminoimidazole-4-carboxamide) ribonucleotide (AICAR) and imidazole glycerol phosphate (ImGP), which are further used in purine and histidine biosynthesis, respectively [34, 35]. AICAR can inhibit the lipopolysaccharide-induced production of proinflammatory cytokines, thus regulating the inflammation process [36, 37]. The strain lacking this gene displayed much lower virulence, as we have previously described [38]. However, no other parameters measured in the present study were affected, probably due to the involvement of the gene in the host immune response *in vivo*, preventing appropriate IL-6 secretion and leukocyte recruitment.

The A1S_3410 gene is thought to code for an acyltransferase, and it is possibly involved in the *O*-acetylation of the cell wall polymer peptidoglycan. The *O*-acetylation of peptidoglycan is a major virulence factor identified in many bacteria, including both Gram-positive and Gram-negative bacteria. The peptidoglycan is the target of lytic enzymes (e.g. lysozyme), which are produced by eukaryotic hosts as the first line of defence against pathogens. The *O*-acetylation of peptidoglycan leads to resistance to lysozyme [39]. In some Gram-negative bacteria, the translocation of acetyl groups from the cytoplasm is mediated by PatA, which is transferred to peptidoglycan by PatB, an *O*-acetyltransferase, whereas a single bimodal protein, OatA, catalyzes both reactions in some bacteria [40]. Sequence alignment searches suggested that the

protein encoded by the A1S_3410 gene presents some homology with the *O*-acetyltransferase OatA of *Klebsiella pneumoniae* (94% of identity). Pat and Ape2 are the *O*-acetyltransferases in respectively *Pseudomonas aeruginosa* and *Neisseria gonorrhoeae*, and belong to the two-component system in Gram-negative bacteria involved in peptidoglycan *O*-acetyltransferase activity [41]. In this study, the Δ3410 mutant showed a loss of biofilm production and infection ability in the pneumonia model.

Other mutant strains lacking genes were constructed from the ATCC 17978 strain, but did not decrease the virulence in murine pneumonia. *In vitro* assays were also performed in those mutants, revealing some important features (Table 1). The Δ3290 mutant increased biofilm production relative to the parental strain while decreasing its adhesion efficacy to epithelial alveolar cells. A1S_3290 encodes EsvF2, which is a transcriptional activator of TenA. TenA of *Staphylococcus aureus* is a thiaminase that catalyzes the deamination of aminopyrimidine and the cleavage of thiamine (vitamin B1), with a role in thiamine degradation. In *Bacillus subtilis,* TenA acts as a regulator controlling the secretion of extracellular proteases [42]. In biofilm-bound prokaryotic cells, TenA exhibits increased transcription of the genes involved in thiamine production [43]. Thus, the inactivation of A1S_3290 may cause an excess of intracellular thiamine and an increase in biofilm production. The gene A1S_3879 encodes CorA, a magnesium/nickel/cobalt transporter, which affects virulence and extracellular enzyme production in pathogens such as *Salmonella enterica* and *Pectobacterium carotovorum*. A variety of pathways are affected when CorA is lost, indicating that this transporter may be part of a broader signalling network within the cell [44, 45]. Mg^{2+} homeostasis seems to be related to bacterial virulence. In the present study, the Δ3879 mutant did not cause less virulent lung infection. However, a decrease in biofilm production and an increase (*ca*. two-fold) in the ability to attach to alveolar cells were observed. Finally, the mutant strains deficient in A1S_0094 (*lrp* regulon transcriptional regulator), A1S_0315 (DNA repair system) and A1S_3032 (*tonB*-like) genes displayed a lower ability to adhere to eukaryotic cells (Figure 5A), while mutants Δ1028 (lacking *ligB*, aromatic ring-opening dioxygenase) and Δ1247 (lacking O-methyltransferase) showed a lower biofilm formation ability (Figure 5B).

Considering the worrying increase in antibiotic-resistant strains, particularly multidrug-resistant pathogens such as *A. baumannii*, the search for new antibiotics is an urgent challenge. The description of new mechanisms of action is essential for a better understanding of virulence factors and for the identification of novel series of therapeutic targets that will enable the design of specific new treatments aimed at eradicating serious infections caused by Gram-negative bacteria. The present study demonstrated, through *in vitro* and *in vivo* assays, the key role of some genes detected by deep sequencing procedures in the ability of *A. baumannii* to cause infection. Except for the *feoA* and *hisF* genes, recently described by our research group [15, 38], to our knowledge this is the first time that the relationship between the genes here evaluated and *A. baumannii* virulence has been investigated. This important advancement will potentially provide valuable information that may help drug development in future studies.

Potential conflict of interest.

The authors have no conflicts of interest to declare.

Acknowledgements

We thank M. I. Voskuil (Dept. of Immunology and Microbiology, University of Colorado Medical School, CO, USA) for providing pMo130.

Funding

This work was funded by Projects PI15/00860 awarded to GB and PI14/00059 and PI17/01482 to AB and MP, all within in the National Plan for Scientific Research, Development and Technological Innovation 2013-2016 and funded by the ISCIII - General Subdirection of Assessment and Promotion of the Research-European Regional Development Fund (FEDER) “A way of making Europe”. The study was also funded by project IN607A 2016/22 (GAIN- Agencia Gallega de Innovación - Consellería de Economía, Emprego e Industria) awarded to GB. This work was also supported by Planes Nacionales de I+D+i 2008-2011 / 2013-2016 and Instituto de Salud Carlos III, Subdirección General de Redes y Centros de Investigación Cooperativa, Ministerio de

Economía y Competitividad, Spanish Network for Research in Infectious Diseases (REIPI RD16/0016/006) co-financed by European Development Regional Fund "A way to achieve Europe" and operative program Intelligent Growth 2014-2020. J.C. Vázquez-Ucha was financially supported by the ISCIII project FI18/00315, L. Alvarez-Fraga by the ISCIII project PI14/00059, M. Martínez-Guitián was financially supported by the Grant Clara Roy (Spanish Society of Clinical Microbiology and Infectious Diseases), and K. Conde-Pérez and J.A.Vallejo by IN607A 2016/22.

REFERENCES

[1] "Global priority list of antibiotic-resistant bacteria to guide research, discovery and development of new antibiotics.," ed: World Health Organization, 2017.

[2] A. Y. Peleg, H. Seifert, and D. L. Paterson, "*Acinetobacter baumannii*: emergence of a successful pathogen," (in eng), *Clin Microbiol Rev,* vol. 21, no. 3, pp. 538-82, Jul 2008, doi: 10.1128/CMR.00058-07.

[3] L. L. Maragakis and T. M. Perl, "*Acinetobacter baumannii*: epidemiology, antimicrobial resistance, and treatment options," (in eng), *Clin Infect Dis,* vol. 46, no. 8, pp. 1254-63, Apr 2008, doi: 10.1086/529198.

[4] J. Rodríguez-Baño *et al.*, "Biofilm formation in *Acinetobacter baumannii*: associated features and clinical implications," (in eng), *Clin Microbiol Infect,* vol. 14, no. 3, pp. 276-8, Mar 2008, doi: 10.1111/j.1469-0691.2007.01916.x.

[5] G. Wilharm *et al.*, "Relatedness of wildlife and livestock avian isolates of the nosocomial pathogen *Acinetobacter baumannii* to lineages spread in hospitals worldwide," (in eng), *Environ Microbiol,* vol. 19, no. 10, pp. 4349-4364, 10 2017, doi: 10.1111/1462-2920.13931.

[6] M. Eveillard, M. Kempf, O. Belmonte, H. Pailhoriès, and M. L. Joly-Guillou, "Reservoirs of *Acinetobacter baumannii* outside the hospital and potential involvement in emerging human community-acquired infections," (in eng), *Int J Infect Dis,* vol. 17, no. 10, pp. e802-5, Oct 2013, doi: 10.1016/j.ijid.2013.03.021.

[7] A. Y. Peleg, S. Jara, D. Monga, G. M. Eliopoulos, R. C. Moellering, and E. Mylonakis, "*Galleria mellonella* as a model system to study *Acinetobacter baumannii* pathogenesis and therapeutics," (in eng), *Antimicrob Agents Chemother,* vol. 53, no. 6, pp. 2605-9, Jun 2009, doi: 10.1128/aac.01533-08.

[8] S. Rumbo-Feal *et al.*, "Whole transcriptome analysis of *Acinetobacter baumannii* assessed by RNA-sequencing reveals different mRNA expression profiles in biofilm compared to planktonic cells," (in eng), *PloS one,* vol. 8, no. 8, p. e72968, 2013, doi: 10.1371/journal.pone.0072968.

[9] M. G. Smith *et al.*, "New insights into *Acinetobacter baumannii* pathogenesis revealed by high-density pyrosequencing and transposon mutagenesis," (in eng), *Genes Dev,* vol. 21, no. 5, pp. 601-14, Mar 2007, doi: 10.1101/gad.1510307.

[10] M. Merino *et al.*, "Complete Genome Sequence of the Multiresistant *Acinetobacter baumannii* Strain AbH12O-A2, Isolated during a Large Outbreak in Spain," (in eng), *Genome announcements,* vol. 2, no. 6, 2014, doi: 10.1128/genomeA.01182-14.

[11] M. P. Cabral *et al.*, "Proteomic and functional analyses reveal a unique lifestyle for *Acinetobacter baumannii* biofilms and a key role for histidine metabolism," (in eng), *J Proteome Res,* vol. 10, no. 8, pp. 3399-417, Aug 2011, doi: 10.1021/pr101299j.

[12] B. A. Eijkelkamp, K. A. Hassan, I. T. Paulsen, and M. H. Brown, "Investigation of the human pathogen *Acinetobacter baumannii* under iron limiting conditions," (in eng), *BMC Genomics,* vol. 12, p. 126, Feb 2011, doi: 10.1186/1471-2164-12-126.

[13] G. L. Murray *et al.*, "Global Gene Expression Profile of *Acinetobacter baumannii* During Bacteremia," (in eng), *J Infect Dis,* vol. 215, no. suppl_1, pp. S52-S57, Feb 2017, doi: 10.1093/infdis/jiw529.

[14] N. Wang, E. A. Ozer, M. J. Mandel, and A. R. Hauser, "Genome-wide identification of *Acinetobacter baumannii* genes necessary for persistence in the lung," (in eng), *MBio,* vol. 5, no. 3, pp. e01163-14, Jun 2014, doi: 10.1128/mBio.01163-14.

[15] L. Álvarez-Fraga *et al.*, "Pneumonia infection in mice reveals the involvement of the feoA gene in the pathogenesis of *Acinetobacter baumannii*," (in eng), *Virulence,* vol. 9, no. 1, pp. 496-509, 01 2018, doi: 10.1080/21505594.2017.1420451.

[16] C. S. Casimiro-Soriguer, A. Muñoz-Mérida, and A. J. Pérez-Pulido, "Sma3s: A universal tool for easy functional annotation of proteomes and transcriptomes," (in eng), *Proteomics,* vol. 17, no. 12, Jun 2017, doi: 10.1002/pmic.201700071.

[17] Wickham and H., "ggplot2:elegant graphics for data analysis. Springer.," ed, 2016.

[18] Sievert *et al.*, "Plotly: Create Interactive Web Graphics via 'plotly. js'. R package version 4.8.0.," ed, 2018.

[19] K. Slowikowski, "ggrepel: Repulsive text and label geoms for 'ggplot2'. R package version 0.8.0.," ed, 2019.

[20] L. Álvarez-Fraga *et al.*, "Analysis of the role of the LH92_11085 gene of a biofilm hyper-producing *Acinetobacter baumannii* strain on biofilm formation and attachment to eukaryotic cells," (in eng), *Virulence,* vol. 7, no. 4, pp. 443-55, May 2016, doi: 10.1080/21505594.2016.1145335.

[21] M. A. Hamad, S. L. Zajdowicz, R. K. Holmes, and M. I. Voskuil, "An allelic exchange system for compliant genetic manipulation of the select agents *Burkholderia pseudomallei* and *Burkholderia mallei*," (in eng), *Gene,* vol. 430, no. 1-2, pp. 123-31, Feb 1 2009, doi: 10.1016/j.gene.2008.10.011.

[22] A. P. Tomaras, C. W. Dorsey, R. E. Edelmann, and L. A. Actis, "Attachment to and biofilm formation on abiotic surfaces by *Acinetobacter baumannii*: involvement of a novel chaperone-usher pili assembly system," (in eng), *Microbiology,* vol. 149, no. Pt 12, pp. 3473-84, Dec 2003.

[23] E. L. Kaplan and P. Meier, "Nonparametric Estimation from Incomplete Observations," *Journal of the American Statistical Association,* vol. 53, no. 282, pp. 457-481, 1958, doi: 10.2307/2281868.

[24] N. Parveen and K. A. Cornell, "Methylthioadenosine/S-adenosylhomocysteine nucleosidase, a critical enzyme for bacterial metabolism," (in eng), *Mol Microbiol,* vol. 79, no. 1, pp. 7-20, Jan 2011, doi: 10.1111/j.1365-2958.2010.07455.x.

[25] J. A. Gutierrez, T. Crowder, A. Rinaldo-Matthis, M. C. Ho, S. C. Almo, and V. L. Schramm, "Transition state analogs of 5'-methylthioadenosine nucleosidase disrupt quorum sensing," (in eng), *Nat Chem Biol,* vol. 5, no. 4, pp. 251-7, Apr 2009, doi: 10.1038/nchembio.153.

[26] A. J. Silva, W. B. Parker, P. W. Allan, J. C. Ayala, and J. A. Benitez, "Role of methylthioadenosine/S-adenosylhomocysteine nucleosidase in *Vibrio cholerae* cellular communication and biofilm development," (in eng), *Biochem Biophys Res Commun,* vol. 461, no. 1, pp. 65-9, May 2015, doi: 10.1016/j.bbrc.2015.03.170.

[27] T. Funahashi, T. Tanabe, J. Maki, K. Miyamoto, H. Tsujibo, and S. Yamamoto, "Identification and characterization of a cluster of genes involved in biosynthesis and transport of acinetoferrin, a siderophore produced by *Acinetobacter haemolyticus* ATCC 17906T," (in eng), *Microbiology,* vol. 159, no. Pt 4, pp. 678-90, Apr 2013, doi: 10.1099/mic.0.065177-0.

[28] M. Smith and J. Neilands, "Rhizobactin, a siderophore from *Rhizobium meliloti*," *Journal of Plant Nutrition,* vol. 7:1-5, 449-458, 1984.

[29] S. Narita, C. Masui, T. Suzuki, N. Dohmae, and Y. Akiyama, "Protease homolog BepA (YfgC) promotes assembly and degradation of β-barrel membrane proteins in *Escherichia coli*," (in eng), *Proc Natl Acad Sci U S A,* vol. 110, no. 38, pp. E3612-21, Sep 2013, doi: 10.1073/pnas.1312012110.

[30] E. Oh *et al.*, "Selective ribosome profiling reveals the cotranslational chaperone action of trigger factor in vivo," (in eng), *Cell,* vol. 147, no. 6, pp. 1295-308, Dec 2011, doi: 10.1016/j.cell.2011.10.044.

[31] A. Liu *et al.*, "Antibiotic sensitivity profiles determined with an *Escherichia coli* gene knockout collection: generating an antibiotic bar code," (in eng), *Antimicrob Agents Chemother,* vol. 54, no. 4, pp. 1393-403, Apr 2010, doi: 10.1128/AAC.00906-09.

[32] T. Hasan, C. H. Choi, and M. H. Oh, "Genes Involved in the Biosynthesis and Transport of Acinetobactin in *Acinetobacter baumannii*," (in eng), *Genomics Inform,* vol. 13, no. 1, pp. 2-6, Mar 2015, doi: 10.5808/GI.2015.13.1.2.

[33] J. A. Gaddy, B. A. Arivett, M. J. McConnell, R. López-Rojas, J. Pachón, and L. A. Actis, "Role of acinetobactin-mediated iron acquisition functions in the interaction of *Acinetobacter baumannii* strain ATCC 19606T with human lung epithelial cells, Galleria mellonella caterpillars, and mice," (in eng), *Infect Immun,* vol. 80, no. 3, pp. 1015-24, Mar 2012, doi: 10.1128/IAI.06279-11.

[34] R. Fani, M. Brilli, M. Fondi, and P. Lió, "The role of gene fusions in the evolution of metabolic pathways: the histidine biosynthesis case," (in eng), *BMC Evol Biol,* vol. 7 Suppl 2, p. S4, Aug 2007, doi: 10.1186/1471-2148-7-S2-S4.

[35] P. Alifano *et al.*, "Histidine biosynthetic pathway and genes: structure, regulation, and evolution," (in eng), *Microbiol Rev,* vol. 60, no. 1, pp. 44-69, Mar 1996.

[36] A. Peairs *et al.*, "Activation of AMPK inhibits inflammation in MRL/lpr mouse mesangial cells," (in eng), *Clin Exp Immunol,* vol. 156, no. 3, pp. 542-51, Jun 2009, doi: 10.1111/j.1365-2249.2009.03924.x.

[37] S. Giri, N. Nath, B. Smith, B. Viollet, A. K. Singh, and I. Singh, "5-aminoimidazole-4-carboxamide-1-beta-4-ribofuranoside inhibits proinflammatory response in glial cells: a possible role of AMP-activated protein kinase," (in eng), *J Neurosci,* vol. 24, no. 2, pp. 479-87, Jan 2004, doi: 10.1523/JNEUROSCI.4288-03.2004.

[38] M. Martínez-Guitián *et al.*, "Involvement of HisF in the Persistence of," (in eng), *Front Cell Infect Microbiol,* vol. 9, p. 310, 2019, doi: 10.3389/fcimb.2019.00310.

[39] D. Sychantha *et al.*, "In vitro characterization of the antivirulence target of Gram-positive pathogens, peptidoglycan O-acetyltransferase A (OatA)," (in eng), *PLoS Pathog,* vol. 13, no. 10, p. e1006667, Oct 2017, doi: 10.1371/journal.ppat.1006667.

[40] P. J. Moynihan and A. J. Clarke, "Substrate specificity and kinetic characterization of peptidoglycan O-acetyltransferase B from *Neisseria*

gonorrhoeae," (in eng), *J Biol Chem,* vol. 289, no. 24, pp. 16748-60, Jun 2014, doi: 10.1074/jbc.M114.567388.

[41] P. J. Moynihan and A. J. Clarke, "O-acetylation of peptidoglycan in gram-negative bacteria: identification and characterization of peptidoglycan O-acetyltransferase in *Neisseria gonorrhoeae*," (in eng), *J Biol Chem,* vol. 285, no. 17, pp. 13264-73, Apr 2010, doi: 10.1074/jbc.M110.107086.

[42] A. Begum *et al.*, "*Staphylococcus aureus* thiaminase II: oligomerization warrants proteolytic protection against serine proteases," (in eng), *Acta Crystallogr D Biol Crystallogr,* vol. 69, no. Pt 12, pp. 2320-9, Dec 2013, doi: 10.1107/S0907444913021550.

[43] M. A. Pysz *et al.*, "Transcriptional analysis of biofilm formation processes in the anaerobic, hyperthermophilic bacterium *Thermotoga maritima*," (in eng), *Appl Environ Microbiol,* vol. 70, no. 10, pp. 6098-112, Oct 2004, doi: 10.1128/AEM.70.10.6098-6112.2004.

[44] C. M. Kersey, P. A. Agyemang, and C. K. Dumenyo, "CorA, the magnesium/nickel/cobalt transporter, affects virulence and extracellular enzyme production in the soft rot pathogen *Pectobacterium carotovorum*," (in eng), *Mol Plant Pathol,* vol. 13, no. 1, pp. 58-71, Jan 2012, doi: 10.1111/j.1364-3703.2011.00726.x.

[45] K. M. Papp-Wallace *et al.*, "The CorA Mg^{2+} channel is required for the virulence of *Salmonella enterica* serovar *typhimurium*," (in eng), *J Bacteriol,* vol. 190, no. 19, pp. 6517-23, Oct 2008, doi: 10.1128/JB.00772-08.

Table 1. Compilation of assays performed with the 21 derivative isogenic strains (pneumonia, biofilm, attachment, fitness in presence/absence of iron and antibiotic susceptibility). Differences in bacterial phenotypes observed in the mutant strains compared with the parental ATCC 17978 strain are indicated as follows: (+), decreased by 20-50%; (++), decreased by 50-80%; (+++), decreased by 80-100%; (+++*), increased by 80-100%; (-), no difference. All differences highlighted are statistically significant (p >0.05).

	A. baumannii mutant	Gene description	Mice survival during pneumonia	Biofilm Formation	Attachment	Fitness	Fitness in iron limiting conditions	Increase antibiotic susceptibility	Fold up-regulated during infection (*p*-value)
Virulence loss in murine pneumonia	Δ0242	*feoA*, ferrous iron transport protein A	++	++	+++	-	++	-	1.16 (0.0023)
	Δ0781	*mtnN*, (MTA/SAH) nucleosidase	+	+	-	-	-	-	1.63 (9.04×10^{-9})
	Δ1657	N-acetyltransferase, acinetoferrin biosynthesis	+	++	+++	-	+	-	2.17 (5.06×10^{-08})
	Δ2247	*yfgC* (*bepA*) putative periplasmic metalloprotease	+	-	-	+	-	-	2.06 (5.52×10^{-05})
	Δ2390	*basB*, acinetobactin biosynthesis protein	+	-	+++	-	+++	-	1.05 (0.008)
	Δ3245	*hisF*, imidazole glycerol phosphate synthase cyclase subunit	+++	-	-	-	-	-	2.86 (4.14×10^{-18})
	Δ3410	*oatA*, acyltransferase	+	+	-	-	-	-	2.29 (1.20×10^{-07})
No virulence loss in murine pneumonia	Δ0094	*lrp* regulon transcriptional regulator	-	-	+	-	-	-	3.53 (1.10×10^{-17})
	Δ0315	DNA repair system (2OG-Fe(II)-oxygenase-like)	-	-	+	-	-	-	1.68 (0.00022)
	Δ0318	FusE-MFP/HlyD membrane fusion protein	-	-	-	-	-	-	2.10 (1.57×10^{-07})
	Δ0896	*pilU*, twitching motility	-	-	-	-	-	-	1.13 (0.00635)
	Δ1013	*ureB*, urease beta subunit	-	-	-	-	-	-	1.46 (0.00393)
	Δ1028	*ligB*, aromatic ring-opening dioxygenase	-	+	-	-	-	-	1.29 (0.00326)
	Δ1032	*ata*, Adhesin Ata autotransporter	-	-	-	-	-	-	1.27 (8.76×10^{-07})
	Δ1146	DNA-methyltransferase	-	-	-	-	-	-	1.78 (7.82×10^{-06})
	Δ1247	O-methyltransferase	-	+	-	-	-	-	1.42 (0.00083)
	Δ1581	methyltransferase	-	-	-	-	-	-	2.21 (1.78×10^{-05})
	Δ3032	*tonB*-like, biological transducer activity	-	-	+	-	-	-	1.01 (3.63×10^{-05})
	Δ3290	*esvF2*, thiaminase (transcriptional	-	+++*	+	-	-	-	1.42 (0.00034)
	Δ3363	membrane metalloendopeptidase	-	-	-	-	-	-	1.39 (0.00158)
	Δ3879	*corA*, magnesium and cobalt transporter family	-	+	+++ *	-	-	-	1.55 (0.00188)

Table 2. Minimal inhibitory concentration (mg/L) to β-lactams of *A. baumannii* ATCC 17978 and its derivative mutant strain Δ2247.

β-lactam	ATCC 17978	Δ2247
Ampicillin	16	16
Piperacillin/tazobactam	16	16
Cefoxitin	128	32
Ceftazidime	4	1
Cefotaxime	8	2
Cefepime	2	0.5
Imipenem	0.25	0.25
Meropenem	0.25	0.25

Figure 1. Dispersion plot of genes differentially expressed during lung infection in the murine model. Both collections of 224 up-regulated and 126 down-regulated genes are represented, highlighting the 21 genes selected for construction of the isogenic mutant strains.

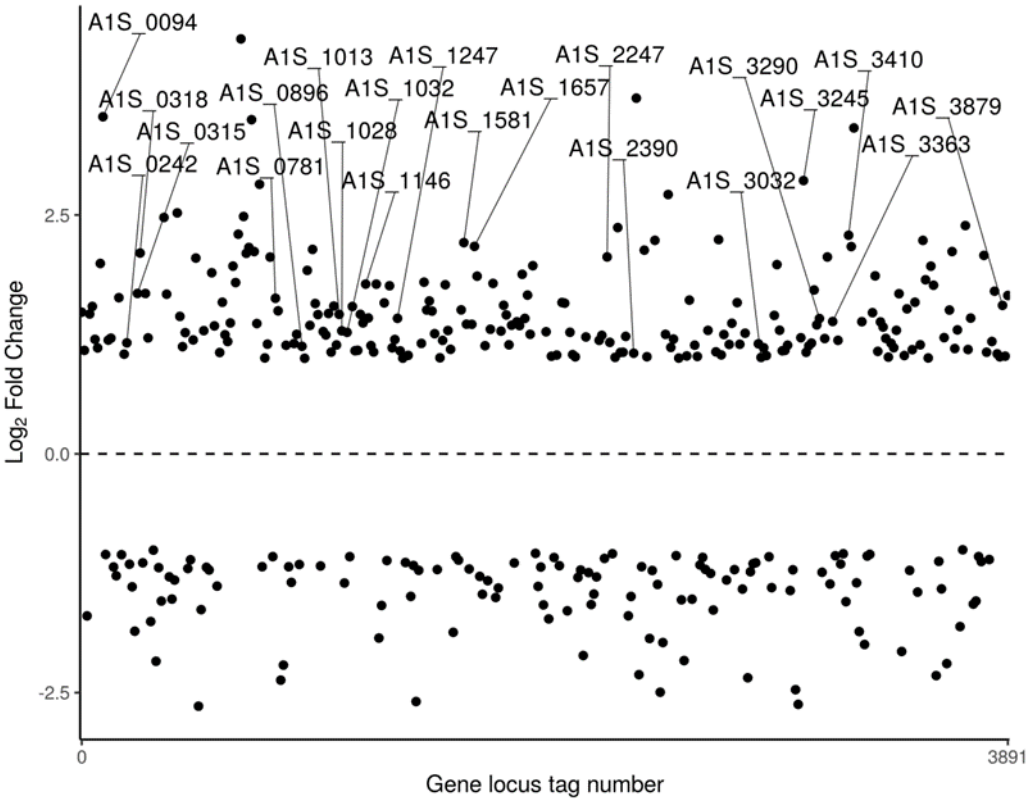

Figure 2. Distribution of sequences of *A. baumannii* ATCC 17978 genes that are up-regulated (A, B, and C) and down-regulated (D, E, and F) during lung infection relative to their expression *in vitro* conditions, by their ontology: biological processes (A and D), cellular components (B and E) and molecular functions (C and F).

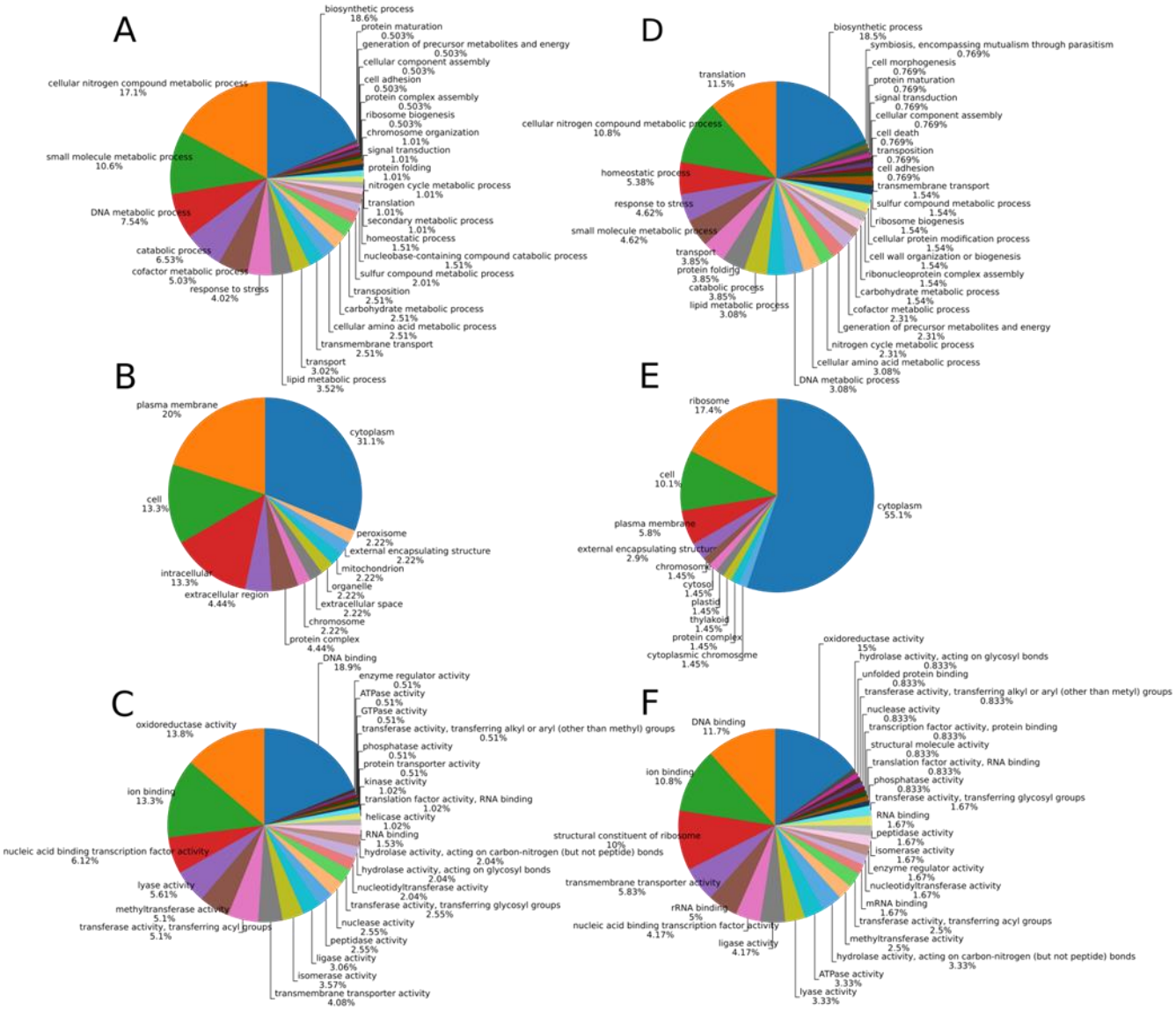

Figure 3. Pneumonia infection in mice. Survival of BALB/c mice (n = 9-11 *per* group) after pneumonia infection with *A. baumannii* ATCC 17978 and the isogenic derivative strains Δ0781, Δ0242, Δ1657, Δ2247, Δ2390, Δ3245 and Δ3410.

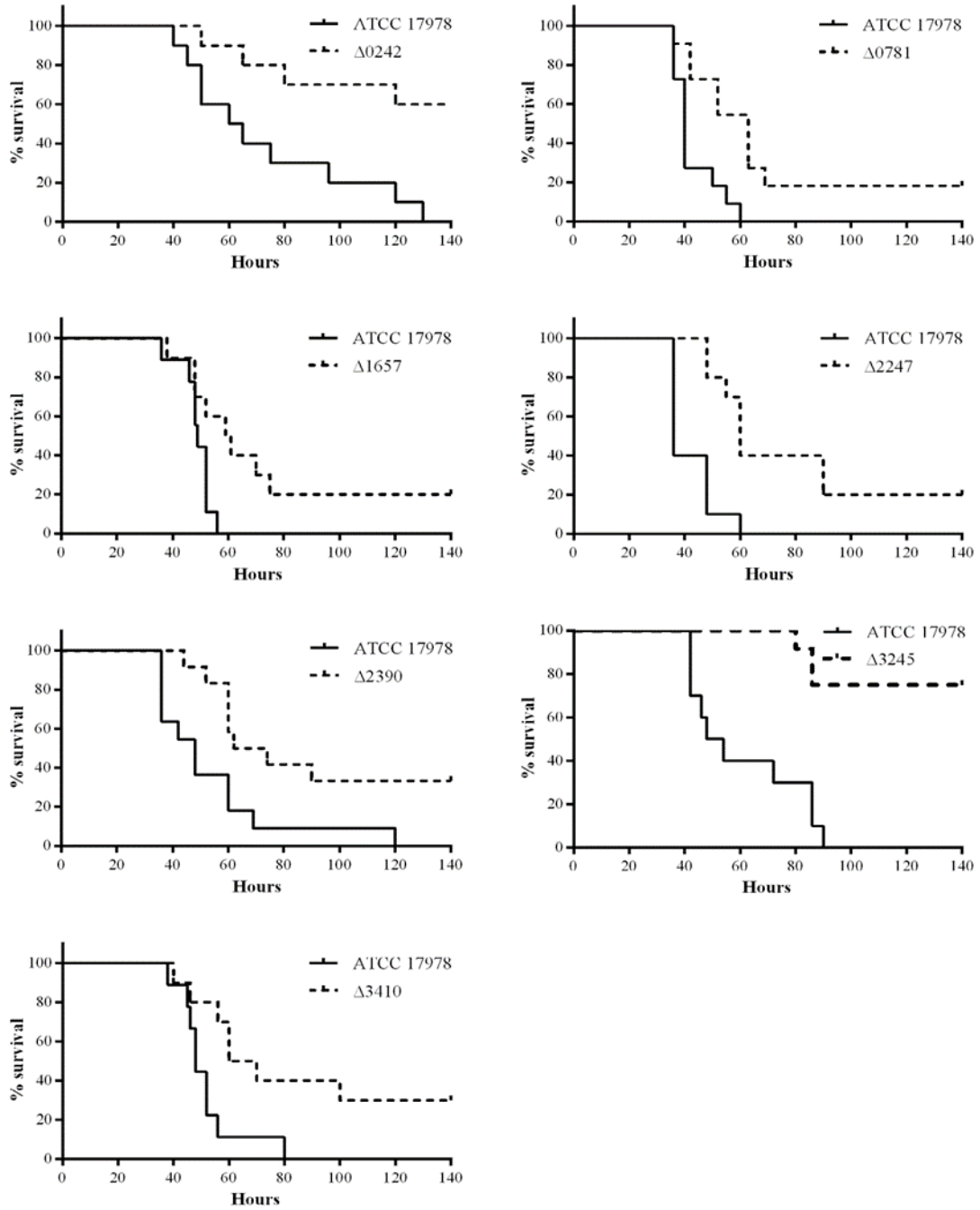

Figure 4. Growth curves and fitness analysis (A: OD_{600} curves; B: time-kill curves) of the ATCC 17978 and the isogenic mutant derivative strains Δ0242, Δ1657 and Δ2390, in the presence of 200 µM of the iron chelator 2,2'-bipyridyl (BIP).

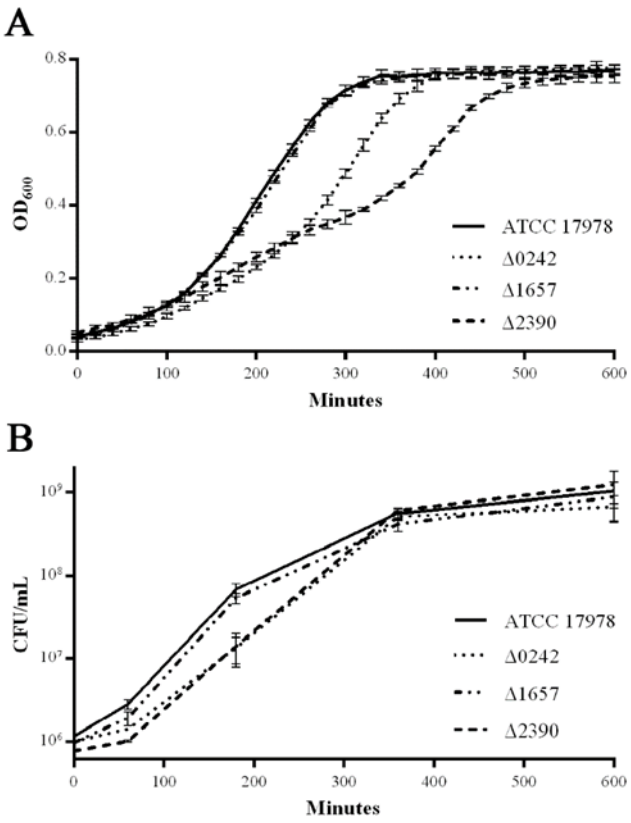

Figure 5. A) Quantification of adhesion to A549 human alveolar epithelial cells of *A. baumannii* ATCC 17978 and the isogenic mutant derivative strains Δ0242, Δ0315, Δ0094, Δ1028, Δ1581, Δ1657, Δ2390, Δ3032 and Δ3879. B) Quantification of biofilm formation capacity of *A. baumannii* ATCC 17978 and the isogenic mutant derivative strains Δ0242, Δ0781, Δ1028, Δ1247, Δ1657, Δ3290, Δ3410 and Δ3879. Significant differences: *, $p<0.05$; ** $p< 0.01$.

A)

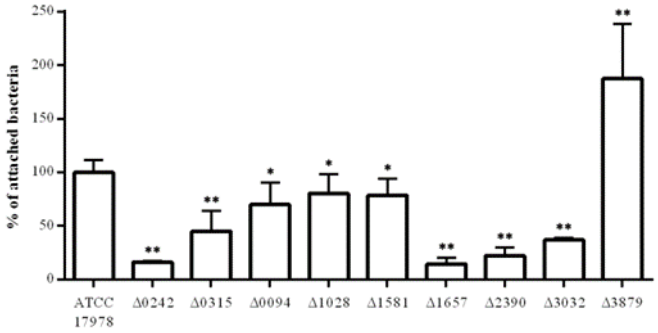

B)

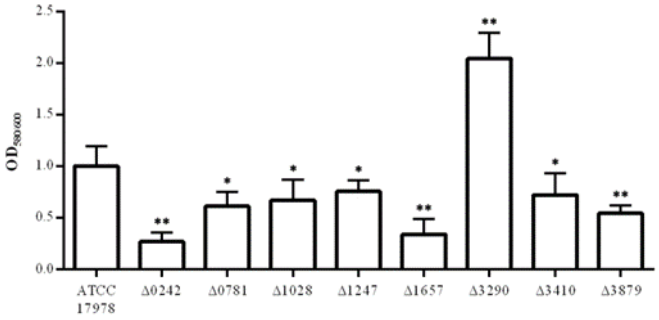

Material suplementario del manuscrito.

Material and Methods

High-throughput sequencing procedures

Transcriptome analysis of the *in vivo* and *in vitro* samples was carried out at CIC bioGUNE's genome analysis platform (Derio, Spain). Three biological replicates were conducted on each sample.

The quantity and quality of the RNAs were evaluated with the Qubit dsDNA Assay Kit (Life Technologies, California, USA) and Agilent RNA Nano Chips (Agilent Technologies, California, USA), respectively. Sequencing libraries were prepared with the Ribo-Zero Magnetic Kit (Illumina, Madison, Wisconsin) and Complete TruSeq Stranded Total RNA kit (Illumina) following the manufacturer's instructions. Bacterial and eukaryotic rRNA was isolated from 1 µg of total RNA, and the remaining RNA was purified, fragmented and primed for cDNA synthesis. First strand cDNA was synthesized with SuperScriptII Reverse Transcriptase (Life Technologies). Second strand cDNA was synthesized with Illumina reagents at 16ºC for 1 h. A-tailing and adaptor ligation were then performed. Finally, libraries were enriched by PCR and then visualized in an Agilent 2100 Bioanalyzer High Sensitivity DNA kit (Agilent Technologies) and quantified by PCR, with a Kapa Library Quantification Kit (Master Mix and DNA Standards, KAPA-Biosystems) and a Qubit dsDNA HS DNA Kit (Life Technologies).

Growth rate analysis under non-limited and limited iron conditions

Growth rate was assessed by measuring the optical density (OD) of the ATCC 17978 and the mutant derivative strains in LB medium, as previously described [1], in the presence or absence of 0.2 mM of the iron chelator 2,2′-bipyridyl (BIP). Growth was monitored at OD_{600} every 20 min until the late-log phase in 24-well plates and an Epoch 2 Microplate Spectrophotometer (BioTek Instruments, Inc., Vermont, USA). The growth rate constant (μ) was calculated on the basis of the exponential segment of the growth curve and defined as ln2/g, where g is the doubling time or mean generation time. Three independent biological replicates were carried out.

Time-kill analysis was also used as described previously to measure the fitness loss of mutants [2]. Strains were inoculated with 10 $x10^5$ CFU/mL into LB medium and grown in 96-well microplates at 37ºC with shaking, using the spectrophotometer. The number of CFUs was determined at 1, 3, 6 and 10h by plating onto LB agar plates and incubating at 37ºC. Independent triplicates were also carried out.

Antibiotic susceptibility assay

The antibiotic susceptibility was determined through microdilution assays, as described by CLSI [3]. The following antibiotics were used: ampicillin, piperacillin-tazobactam, cefoxitin, ceftazidime, cefotaxime, cefepime, imipenem, meropenem, sulbactam, rifampicin, colistin, tetracycline, kanamycin, ciprofloxacin, gentamicin and tigecycline (Sigma). Three independent experiments were performed for each mutant strain of *Acinetobacter baumanni*.

References

[1] L. Álvarez-Fraga *et al.*, "Pneumonia infection in mice reveals the involvement of the feoA gene in the pathogenesis of *Acinetobacter baumannii*," (in eng), *Virulence,* vol. 9, no. 1, pp. 496-509, 01 2018, doi: 10.1080/21505594.2017.1420451.

[2] M. Martínez-Guitián *et al.*, "Antisense inhibition of *lpxB* gene expression in *Acinetobacter baumannii* by peptide-PNA conjugates and synergy with colistin," (in eng), *J Antimicrob Chemother,* Oct 2019, doi: 10.1093/jac/dkz409.

[3] "The M02-A12: Performance Standards for Antimicrobial Disk Susceptibility Tests. Approved Standard Twelfth Edition. CLSI M02-A12 document. Wayne, PA: Clinical and Laboratory Standards Institute. 2015," ed.

Table S1. Oligonucleotides and probes used in the present work.

Primer/Probe name	Sequence	Use in the present study
rpoBRT Fw	tcgtgtatctgcgcttgg	qRT-PCR
rpoBRT Rv	cgtacttcgaagcctgcac	qRT-PCR
rpoB Probe	accaccag	qRT-PCR
A1S_0242RTFw	tcagcgttgaaagtgaagca	qRT-PCR
A1S_0242RTRv	gaattgcgaccaaatcttgc	qRT-PCR
A1S_0242 Probe	catcacca	qRT-PCR
A1S_1657RTFw	gcatgagccacacgttattc	qRT-PCR
A1S_1657RT Rv	cacgtcttgaccattgattcc	qRT-PCR
A1S_1657 Probe	cagtggca	qRT-PCR
A1S_0318RTFw	tgctcaagcacaagcaggt	qRT-PCR
A1S_0318RTRv	tgcgtttttctcggctaact	qRT-PCR
A1S_0318 Probe	agcccaag	qRT-PCR
A1S_0896RT Fw	ttcaatacgacgtagtaccatgc	qRT-PCR
A1S_0896RT Rv	gcgttttcgtgtcagtgct	qRT-PCR
A1S_0896 Probe	gctgctga	qRT-PCR
A1S_1032RTFw	tctgcgtttggtatgacctct	qRT-PCR
A1S_1032RTRv	atttgacatgacgccgaaa	qRT-PCR
A1S_1032 Probe	tggtgatg	qRT-PCR
A1S_3032RTFw	gttactcgacatccgatgagc	qRT-PCR
A1S_3032RT Rv	agctcaagccgatcaacaag	qRT-PCR
A1S_3032 Probe	agctcctg	qRT-PCR
A1S_0094UPFw	gggcggccgcaccggtatttctgcattttta	Construction of the Δ0094 strain
A1S_0094UPRv	cccgagctcagcgagcattactgaactc	Construction of the Δ0094 strain
A1S_0094DOWNFw	ggggagctcgcgcatagatatttcctctt	Construction of the Δ0094 strain
A1S_0094DOWNRv	cccggatccttgtaggtttcatcaagcac	Construction of the Δ0094 strain
A1S_0094intUP	gtcattacaactgagcctc	Confirmation of the deletion of the A1S_0094 gene
A1S_0094intDOWN	gaaatttgacctgcattacc	Confirmation of the deletion of the A1S_0094 gene
A1S_0242UPFw	gggggatccccccactatgacccagtaacatt	Construction of the Δ0242 strain
A1S_0242UPRv	ggggatatccccatccgatcctaaacctttt	Construction of the Δ0242 strain
A1S_0242DOWNFw	ggggatatccccaaattcaagtagaagaagga	Construction of the Δ0242 strain
A1S_0242DOWNRv	ggggcatgccccgaatgaaagcacgtccactt	Construction of the Δ0242 strain
A1S_0242intUPFw	ttcactacattggatcaggt	Confirmation of the deletion of the A1S_0242 gene
A1S_0242intDOWNRv	atcgagcactcgaaccgaa	Confirmation of the deletion of the A1S_0242 gene
A1S_0315UPFw	gggcggccgccccatacctaaagcagccataa	Construction of the Δ0315 strain
A1S_0315UPRv	ggggaattccccgcaatctccccttgctgct	Construction of the Δ0315 strain
A1S_0315DOWNFw	ggggaattcccccaaccacggattaacctga	Construction of the Δ0315 strain
A1S_0315DOWNRv	gggggatccccctttttccgtttcacgaccag	Construction of the Δ0315 strain
A1S_0315intUP	ccgaaagctcagttaaaaaa	Confirmation of the deletion of the A1S_0315 gene
A1S_0315intDOWN	aaacgcggcattgattgag	Confirmation of the deletion of the A1S_0315 gene
A1S_0318UPFw	gggggatccccccttatttgcggtttccatga	Construction of the Δ0318 strain
A1S_0318UPRv	ggggatatccccttaatgcgacaatcaaaatcac	Construction of the Δ0318 strain
A1S_0318DOWNFw	ggggatatccccctgctacagtacatattattg	Construction of the Δ0318 strain
A1S_0318DOWNRv	ggggcatgcccccagaaatggcagatgactttt	Construction of the Δ0318 strain
A1S_0318intUP	atgtctacggtatttacgtg	Confirmation of the deletion of the A1S_0318 gene
A1S_0318intDOWN	gtgaggcaagagaagaactt	Confirmation of the deletion of the A1S_0318 gene
A1S_0781UPFw	gggcggccgccccctaagtctgaaccagatc	Construction of the Δ0781 strain
A1S_0781UPRv	cccgagctcgggcattttccacctgtttctttg	Construction of the Δ0781 strain
A1S_0781DOWNFw	ggggagctccccaacgtagctgaagaatatatg	Construction of the Δ0781 strain
A1S_0781DOWNRv	gggggatcccccctcacaatgtagtcatctca	Construction of the Δ0781 strain
A1S_0781intUP	gactcacatttgttcaaactg	Confirmation of the deletion of the A1S_0781 gene

A1S_0781intDOWN	tatcaggtctcattgtcgaa	Confirmation of the deletion of the A1S_0781 gene
A1S_0896UPFw	ttgcggccgcaataaaattgcttctttggaag	Construction of the Δ0896 strain
A1S_0896UPRv	cggggtaccccgttttgaccgccagtaattt	Construction of the Δ0896 strain
A1S_0896DOWNFw	cggggtaccccgataattgtattctcgctatttt	Construction of the Δ0896 strain
A1S_0896DOWNRv	cgcggatccgcgtccgatttacatctctctg	Construction of the Δ0896 strain
A1S_0896intUP	acagtttaccgtgtgttaa	Confirmation of the deletion of the A1S_0896 gene
A1S_0896intDOWN	aattatgattggtattccgg	Confirmation of the deletion of the A1S_0896 gene
A1S_1013UPFw	ttgcggccgcaaattttagagtggatgccgc	Construction of the Δ1013 strain
A1S_1013UPRv	cccgtcgatgggcaccgggaatcataagtatt	Construction of the Δ1013 strain
A1S_1013DOWNFw	cccgtcgatgggtgggacgtttggatgaaaat	Construction of the Δ1013 strain
A1S_1013DOWNRv	cgcggatccgcgaaatcatcaatcgcctgcaa	Construction of the Δ1013 strain
A1S_1013intUP	ctcatttttactgcaggctt	Confirmation of the deletion of the A1S_1013 gene
A1S_1013intDOWN	cctagacctagtttcaaatg	Confirmation of the deletion of the A1S_1013 gene
A1S_1028UPFw	ttgcggccgcaaggcgctacttcaaggaaaac	Construction of the Δ1028 strain
A1S_1028UPRv	ccggaattccgggctcactaggtatggatata	Construction of the Δ1028 strain
A1S_1028DOWNFw	ccggaattccgggaagggtttgtagttccat	Construction of the Δ1028 strain
A1S_1028DOWNRv	cgcggatccgcgagctcgtctttattcctcaa	Construction of the Δ1028 strain
A1S_1028intUP	gagtgtttgaaactgtttga	Confirmation of the deletion of the A1S_1028 gene
A1S_1028intDOWN	ccacacccttagtacgta	Confirmation of the deletion of the A1S_1028 gene
A1S_1032UPFw	cccgcggccgcggggtgatcaatttcttctgtaa	Construction of the Δ1032 strain
A1S_1032UPRv	cccgaattcgggaaaacttctcagacaaatac	Construction of the Δ1032 strain
A1S_1032DOWNFw	cccgaattcgggagtggtgtgattaattaag	Construction of the Δ1032 strain
A1S_1032intUP	atttattcaattaggatgcc	Confirmation of the deletion of the A1S_1032 gene
A1S_1032intDOWN	tgggtattcataacgtttta	Confirmation of the deletion of the A1S_1032 gene
A1S_1146UPFw	cccgcggccgcgggacgaccagatattaactgg	Construction of the Δ1146 strain
A1S_1146UPRv	cccgatatcgggttggtctcctgaacattta	Construction of the Δ1146 strain
A1S_1146DOWNFw	cccgatatcgggatgaattattaccaacacca	Construction of the Δ1146 strain
A1S_1146DOWNRv	cccggatccgggcctcaatcattggaaactt	Construction of the Δ1146 strain
A1S_1146intUP	gcaaactaatctatcaaatc	Confirmation of the deletion of the A1S_1146 gene
A1S_1146intDOWN	ttcggtagtacattgcaaa	Confirmation of the deletion of the A1S_1146 gene
A1S_1247UPFw	gggcggccgccccttgggttgcgaaagcaac	Construction of the Δ1247 strain
A1S_1247UPRv	ggggaattccccgaaacctttaaagccctaga	Construction of the Δ1247 strain
A1S_1247DOWNFw	ggggaattcccccatagtcaaatttacctgta	Construction of the Δ1247 strain
A1S_1247DOWNRv	gggggatccccccttcaaaaagatcagcaaccg	Construction of the Δ1247 strain
A1S_1247intUP	cgcatttagccatagcaaaa	Confirmation of the deletion of the A1S_1247 gene
A1S_1247intDOWN	ttttcgtattggaccagaag	Confirmation of the deletion of the A1S_1247 gene
A1S_1581UPFw	ccgcggccgcaatcgctttacaaactggaat	Construction of the Δ1581 strain
A1S_1581UPRv	cccgaattcatgaaacacagatcaaagttag	Construction of the Δ1581 strain
A1S_1581DOWNFw	ggggaattcatttttgcattcatccctcag	Construction of the Δ1581 strain
A1S_1581DOWNRv	cccggatccctctctagggaggttcttt	Construction of the Δ1581 strain
A1S_1581intUP	gactcatctagaaataccgt	Confirmation of the deletion of the A1S_1581 gene
A1S_1581intDOWN	cagccatttaatgatgatgc	Confirmation of the deletion of the A1S_1581 gene
A1S_1657UPFw	gggggatcccccgaatatagattagtacagca	Construction of the Δ1657 strain
A1S_1657UPRv	ggggatatcccccatccagcggtgtaatagtg	Construction of the Δ1657 strain
A1S_1657DOWNFw	ggggatatcccccttgtattactgtttccgtgaaa	Construction of the Δ1657 strain
A1S_1657DOWNRv	ggggcatgccccaggaataaattggtcaaggt	Construction of the Δ1657 strain
A1S_1657intUP	taggttatgtcatagcaagg	Confirmation of the deletion of the A1S_1657 gene
A1S_1657intDOWN	agcaatctgttactgaga	Confirmation of the deletion of the A1S_1657 gene
A1S_2247UPFw	ccgcggccgccaccaattgccggtttattt	Construction of the Δ2247 strain
A1S_2247UPRv	cccgagctccgtcttgcaaaaggtaatca	Construction of the Δ2247 strain
A1S_2247DOWNFw	ggggagctcttgcttatgaacttcacgaaa	Construction of the Δ2247 strain
A1S_2247DOWNRv	cccggatccaatctggttagcaaacacac	Construction of the Δ2247 strain
A1S_2247intUP	ggttttatctcagtttctacc	Confirmation of the deletion of the A1S_2247 gene
A1S_2247intDOWN	ctactgctgaaacacgtaag	Confirmation of the deletion of the A1S_2247 gene

A1S_2390UPFw	ttgcggccgcaaagttaacgacactaaaattc	Construction of the Δ2390 strain
A1S_2390UPRv	cggggtaccccgaaacgtcggttaacttgtt	Construction of the Δ2390 strain
A1S_2390DOWNFw	cggggtaccccgaaccttagctcaaatctag	Construction of the Δ2390 strain
A1S_2390DOWNRv	cgcggatccgcgaatttggagtatatggcat	Construction of the Δ2390 strain
A1S_2390intUP	gacatcaactcattagaaaa	Confirmation of the deletion of the A1S_2390 gene
A1S_2390intDOWN	cttctaaaacacagtcatc	Confirmation of the deletion of the A1S_2390 gene
A1S_3032UPFw	gggctgcagccctgcaccacttgcttatatgc	Construction of the Δ3032 strain
A1S_3032UPRv	gggtctagacccctgaagctgaatttgaagttc	Construction of the Δ3032 strain
A1S_3032DOWNFw	gggtctagacccgaataccatctactgttttt	Construction of the Δ3032 strain
A1S_3032DOWNRv	gggggatccccccccagtcatgataaagatctg	Construction of the Δ3032 strain
A1S_3032intUP	accgttgggtgatttagtaa	Confirmation of the deletion of the A1S_3032 gene
A1S_3032intDOWN	agggaaaaggcatctatatg	Confirmation of the deletion of the A1S_3032 gene
A1S_3245UPFw	ttgcggccgcaagtcacggaacaaatctgag	Construction of the Δ3245 strain
A1S_3245UPRv	ccggaattccgggttaatactcactttgtctg	Construction of the Δ3245 strain
A1S_3245DOWN	ccggaattccggtatcgaaatgcgcttgtaag	Construction of the Δ3245 strain
A1S_3245DOWNRv	cgcggatccgcggtttggcaatttctagccc	Construction of the Δ3245 strain
A1S_3245intUP	gcctgtgtaggaactttca	Confirmation of the deletion of the A1S_3245 gene
A1S_3245intDOWN	ccactctctcaagctgta	Confirmation of the deletion of the A1S_3245 gene
A1S_3290UPFw	gggcggccgccccattttcatcaatttcaggc	Construction of the Δ3290 strain
A1S_3290UPRv	ggggaattccccgttgccagagttcttgaga	Construction of the Δ3290 strain
A1S_3290DOWNFw	ggggaattccccgttaggtttagatcagatcta	Construction of the Δ3290 strain
A1S_3290DOWNRv	gggggatccccccttcctgtagaaggtgtatt	Construction of the Δ3290 strain
A1S_3290intUP	atggatcagacctataccaa	Confirmation of the deletion of the A1S_3290 gene
A1S_3290intDOWN	ctggagttgtcctcattatt	Confirmation of the deletion of the A1S_3290 gene
A1S_3363UPFw	ccgcggccgcggataaccaccaacgatatgca	Construction of the Δ3363 strain
A1S_3363UPRv	ggggaattcgctttgaaaggaataaaaataag	Construction of the Δ3363 strain
A1S_3363DOWNFw	ggggaattccttatccccttattattta	Construction of the Δ3363 strain
A1S_3363DOWNRv	gggggatccatacacccagcctgaattg	Construction of the Δ3363 strain
A1S_3363intUP	tttcttctgagtacactgga	Confirmation of the deletion of the A1S_3363 gene
A1S_3363intDOWN	aggtttcttatgaggttcct	Confirmation of the deletion of the A1S_3363 gene
A1S_3410UPFw	ttgcggccgcaaaaataatctggaatcagtgct	Construction of the Δ3410 strain
A1S_3410UPRv	cccgtcgacgggtggtgacgccataatttcc	Construction of the Δ3410 strain
A1S_3410DOWNFw	cccgtcgacgggataagccccttgaaaatagg	Construction of the Δ3410 strain
A1S_3410DOWNRv	cgcggatccgcgattagtacgcgaaggtggg	Construction of the Δ3410 strain
A1S_3410intUP	cttctgccacacagtatatt	Confirmation of the deletion of the A1S_3410 gene
A1S_3410intDOWN	gtcaggagctggttttaatt	Confirmation of the deletion of the A1S_3410 gene
A1S_3879UPFw	gggcggccgcccatcaatttccatcagactgc	Construction of the Δ3879 strain
A1S_3879UPRv	ggggaattccccaccatagatactggcgatta	Construction of the Δ3879 strain
A1S_3879DOWNFw	ggggaattccccagagattactcccgcaaatt	Construction of the Δ3879 strain
A1S_3879DOWNRv	gggggatcccccaaaaagctcctgcaagtact	Construction of the Δ3879 strain
A1S_3879intUP	gattcttacttgatacaacgt	Confirmation of the deletion of the A1S_3879 gene
A1S_3879intDOWN	gctgaaaatcattcaagcct	Confirmation of the deletion of the A1S_3879 gene
pMo130 site2 Fw	attcatgaccgtgctgac	Confirmation the plasmid construction
pMo130 site2 Rv	cttgtctgtaagcggatg	Confirmation the plasmid construction

Table S2. Up-regulated genes.

Gene	Function	Gene Name	Description
A1S_0007	putative transport protein	*yheS*	ABC transporter, ATP-binding protein YheS
A1S_0008	putative RND type efflux pump	*adeT*	RND type efflux pump involved in aminoglycoside resistance
A1S_0016	site-specific tyrosine recombinase	*xerC*	Int
A1S_0066	hypothetical protein	*pgm*	Pgm
A1S_0069	L-lactate dehydrogenase FMN linked	*lldD*	L-lactate dehydrogenase
A1S_0071	tyrosine aminotransferase tyrosine repressible%2C PLP-dependent	*tyrB*	Aromatic amino acid aminotransferase
A1S_0091	hypothetical protein	BN1002_00790	Pyruvate kinase
A1S_0094	lrp regulon transcriptional regulator (AsnC family)	*lrp*	AsnC family protein
A1S_0127	putative integral membrane protein (DedA)	*dedA*	Cytochrome O ubiquinol oxidase
A1S_0128	putative membrane protein	*yqjF*	DoxX family protein
A1S_0213	hypothetical protein	*tniE*	TniE
A1S_0234	type 4 fimbriae expression regulatory protein	*pilR*	Chemotaxis protein CheY
A1S_0242	putative ferrous iron transport protein A	*feoA*	FeoA domain protein
A1S_0315	DNA repair system	*alkB*	Alkylated DNA repair protein
A1S_0318	Putative FusE-MFP/HlyD membrane fusion protein	*aaeA*	Efflux transporter, RND family, MFP subunit
A1S_0339	pH adaptation potassium efflux system protein G	*phaG*	pH adaptation potassium efflux system protein G
A1S_0347	putative oxidoreductase%3B putative flavoprotein monooxygenase	*xlnD*	3-hydroxybenzoate 6-hydroxylase 1
A1S_0389	hypothetical protein	*crcB*	Putative fluoride ion transporter CrcB
A1S_0394	putative acyl-CoA dehydrogenase	*sfnA*	Acyl-CoA dehydrogenase/oxidase family protein
A1S_0451	formyltetrahydrofolate deformylase	*purU*	Formyltetrahydrofolate deformylase
A1S_0452	hypothetical protein	*tonB*	Protein TonB
A1S_0466	Sec-independent protein translocase protein	*tatA*	Sec-independent protein translocase protein TatA
A1S_0517	hypothetical protein	N/A	N/A
A1S_0554	peptide chain release factor 3	*prfC*	Peptide chain release factor 3
A1S_0560	putative transcriptional regulator	*alsR*	LysR family transcriptional regulatory protein
A1S_0580	putative short-chain dehydrogenase	*budC*	Diacetyl reductase [(S)-acetoin forming]
A1S_0624	putative lipoprotein	*yfgC_2*	TPR repeat-containing protein YfgC
A1S_0627	hypothetical protein	AB988_2879	
A1S_0630	hypothetical protein	*smc*	Chromosome partition protein Smc
A1S_0631	hypothetical protein	*traW*	TraW
A1S_0636	DNA polymerase V component	*umuD*	DNA polymerase V

A1S_0642	hypothetical protein	*stbA*	StbA
A1S_0648	hypothetical protein	*nucH*	Nuclease
A1S_0663	putative DNA helicase	*repA*	Regulatory protein RepA
A1S_0664	replication C family protein	*repC*	RepC
A1S_0665	putative mating pair formation protein	*trbJ*	Conjugal transfer protein TrbJ
A1S_0666	TrbL/VirB6 plasmid conjugal transfer protein	*trbL*	Putative mating pair formation protein
A1S_0667	hypothetical protein	N/A	N/A
A1S_0669	Bile acid:sodium symporter	*acr3*	Arsenite efflux pump
A1S_0672	Resolvase	*parA*	ParA
A1S_0673	putative transposase	*insE*	Putative transposase
A1S_0674	putative transposase	*insA*	Transposase
A1S_0676	putative transposase	*tnpA*	TnpA
A1S_0677	transposase		Transposase DDE domain protein
A1S_0736	hypothetical protein		
A1S_0739	putative transcriptional regulator	ACX60_14695	TetR family transcriptional regulator
A1S_0769	ferredoxin--NADP+ reductase	*fpr*	Ferredoxin--NADP+ reductase
A1S_0781	putative MTA/SAH nucleosidase	*mtnN*	MTA/SAH nucleosidase
A1S_0793	putative transcriptional regulator	*coaX*	Type III pantothenate kinase
A1S_0809	dethiobiotin synthetase x	*bioD*	ATP-dependent dethiobiotin synthetase BioD
A1S_0842	hypothetical protein	X781_11720	Laccase domain protein
A1S_0855	dioxygenase beta subunit	*yeaX*	Putative dioxygenase subunit beta YeaX
A1S_0896	twitching motility protein	*pilU*	Twitching motility protein
A1S_0898	hypothetical protein	*yggS*	YggS
A1S_0901	hypothetical protein	Pat9b_5877	OsmC family protein
A1S_0917	Transcriptional regulator	*cynR*	Transcription activator of glutamate synthase(LysR family)
A1S_0946	hypothetical protein	N/A	N/A
A1S_0947	putative vanillate O-demethylase oxygenase subunit (VanA-like)	*vanA*	Vanillate O-demethylase oxygenase subunit VanA
A1S_0956	putative dinucleotide-utilizing enzyme	*nadX*	Probable L-aspartate dehydrogenase
A1S_0969	transketolase	*tkt*	Putative transketolase
A1S_0979	putative membrane-bound protein in GNT I transport system (GntY)	*nfuA*	Fe/S biogenesis protein NfuA
A1S_0982	hypothetical protein	N/A	N/A
A1S_0992	transcriptional regulator (LysR family)	*oxyR*	Bacterial regulatory helix-turn-helix, lysR family protein
A1S_0997	hypothetical protein	N/A	N/A
A1S_0999	putative signal peptide	*wzi*	Wzi capsule assembly protein
A1S_1013	urease beta subunit	*ureB*	Urease subunit beta
A1S_1028	hypothetical protein	*ygiD*	Aromatic ring-opening dioxygenase
A1S_1032	hypothetical protein	*ata*	Adhesin Ata autotransporter
A1S_1049	hypothetical protein	A1S_1049	UPF0102 protein A1S_1049
A1S_1090	putative transcription regulator (AsnC family)	*lrp*	AsnC/Lrp family transcriptional regulator
A1S_1100	D-glucarate dehydratase	*gudD*	D-glucarate dehydratase
A1S_1140	RNAse HII	*rnhB*	Ribonuclease HII

A1S_1145	putative Cro protein	ACX60_12595	Cro/Cl family transcriptional regulator
A1S_1146	site-specific DNA-methyltransferase	*ydiP*	Putative BsuMI modification methylase subunit YdiP
A1S_1147	Site-specific DNA methylase-like protein	N/A	N/A
A1S_1166	hypothetical protein	N/A	N/A
A1S_1170	hypothetical protein	N/A	N/A
A1S_1171	hypothetical protein	STY0016	Glycosyl hydrolase lysozyme (N-acetylmuramidase)
A1S_1201	alkyl hydroperoxide reductase subunit F	*ahpF*	Alkyl hydroperoxide reductase subunit F
A1S_1216	LysR regulator	*benM*	Aromatic hydrocarbon utilization transcriptional regulator CatR
A1S_1218	heavy metal regulator HmrR	*hmrR*	HTH-type transcriptional regulator (Copper efflux regulator) (Copper export regulator)
A1S_1232	EsvB	*yybR_5*	Uncharacterized HTH-type transcriptional regulator yybR
A1S_1247	putative O-methyltransferase protein	*mdmC*	O-methyltransferase mdmC
A1S_1284	ABC-type nitrate/sulfonate/bicarbonate transport system	*ssuA*	ABC transporter substrate-binding protein
A1S_1316	MFS transporter%3B MFS transporter cyanate permease family	*yeaN*	Inner membrane transport protein YeaN
A1S_1342	putative enoyl-CoA hydratase II	*paaG*	1,2-epoxyphenylacetyl-CoA isomerase
A1S_1410	putative LysR-family transcriptional regulator	*yhjC*	YhjC
A1S_1422	2-(5''-triphosphoribosyl)-3'-dephosphocoenzyme-A synthase	*citG*	Probable 2-(5''-triphosphoribosyl)-3'-dephosphocoenzyme-A synthase
A1S_1423	malonate decarboxylase delta subunit	*mdcC*	Malonate decarboxylase acyl carrier protein
A1S_1427	malonate decarboxylase epsilon subunit	*mdcH*	Malonyl CoA-acyl carrier protein transacylase
A1S_1458	alkyl hydroperoxide reductase subunit F	*ahpF*	Alkyl hydroperoxide reductase subunit F
A1S_1463	serine acetyltransferase	*cysE*	Serine acetyltransferase
A1S_1489	putative glutathione S-transferase	ACIAD2062	Putative glutathione S-transferase
A1S_1495	putative transcriptional regulator	ACIAD2053	Putative transcriptional regulator
A1S_1496	hypothetical protein	*pmpR*	Probable transcriptional regulatory protein yebC
A1S_1511	biotin synthase	*bioB*	Biotin synthase
A1S_1516	putative antibiotic resistance	*yncA*	Acetyltransferase
A1S_1580	integrase	*xerC_3*	Phage integrase family protein 5
A1S_1581	methyltransferase putative	*gp24*	DNA cytosine methyltransferase
A1S_1585	putative replicative DNA helicase	*dnaB*	Replicative DNA helicase
A1S_1646	hypothetical protein	*ybaK*	Cys-tRNA(Pro)/Cys-tRNA(Cys) deacylase
A1S_1657	putative siderophore biosynthesis protein%3B putative acetyltransferase	*mbtK*	Lysine N-acyltransferase MbtK

A1S_1668	lipid A-disaccharide synthase	*lpxB*	Lipid-A-disaccharide synthase
A1S_1680	hypothetical protein	N/A	N/A
A1S_1685	recombination protein gap repair	*recR*	Recombination protein RecR
A1S_1687	Transcriptional regulator	*osmB*	Osmotically inducible lipoprotein B
A1S_1748	replication protein		Phage/plasmid replication family protein
A1S_1752	AdeA membrane fusion protein	*acrA*	Efflux transporter, RND family, MFP subunit
A1S_1796	aldehyde dehydrogenase	*aldH*	Aldehyde dehydrogenase family protein
A1S_1806	Senescence marker protein-30 (SMP-30)	*araB*	Calcium-binding protein
A1S_1817	Acyl-CoA dehydrogenase	*bcd*	Butyryl-CoA dehydrogenase
A1S_1839	Dihydroxy-acid dehydratase	*ilvD*	Dihydroxy-acid dehydratase
A1S_1840	transcriptional regulator GntR family	*pdhR*	Pyruvate dehydrogenase complex repressor
A1S_1847	3-oxoadipate CoA-transferase subunit B	*catJ*	3-oxoadipate CoA-transferase
A1S_1848	Beta-ketoadipyl CoA thiolase	*catF*	Beta-ketoadipyl CoA thiolase
A1S_1869	putative porin for benzoate transport (BenP)	*benP*	Outer membrane porin, OprD family
A1S_1892	Beta-ketoadipyl CoA thiolase	*catF*	Beta-ketoadipyl CoA thiolase
A1S_1893	3-oxoadipate CoA-transferase subunit B	*catJ*	3-oxoadipate CoA-transferase
A1S_1943	putative membrane protein	AB895_3785	Membrane protein
A1S_2003	putative nitrate reductase	*nasB*	Nitrite reductase
A1S_2018	tail tape meausure protein	15	Tape measure domain protein
A1S_2021	hypothetical protein	N/A	N/A
A1S_2027	hypothetical protein	ERS370012_01389	Uncharacterised protein
A1S_2100	hypothetical protein		Alpha/beta hydrolase fold family protein
A1S_2118	hypothetical protein		
A1S_2120	16S rRNA pseudouridylate 516 synthase	*rsuA*	Pseudouridine synthase
A1S_2149	putative acyl CoA dehydrogenase oxidoreductase protein	*mmgC*	Acyl-CoA dehydrogenase
A1S_2220	hypothetical protein	MW7_3113	Atp-dependent protease subunit
A1S_2226	putative glycosyl transferase related protein	*Smlt2543*	Putative glycosyl transferase
A1S_2247	putative signal peptide	*yfgC_1*	Putative beta-barrel assembly-enhancing protease
A1S_2265	thiamine biosynthesis protein thiazole moiety	*thiG*	Thiazole synthase
A1S_2271	rtcb protein	*rtcB*	RNA-splicing ligase RtcB
A1S_2274	aminoacyl-histidine dipeptidase	*pepD*	Aminoacyl-histidine dipeptidase
A1S_2286	hypothetical protein	*mutT_2*	8-oxo-dGTP diphosphatase
A1S_2330	putative acyl-CoA dehydrogenase	*fadE*	Acyl-CoA dehydrogenase
A1S_2336	hypothetical protein	*rsmE*	Ribosomal RNA small subunit

			methyltransferase E
A1S_2390	putative acinetobactin biosynthesis protein	*lgrD*	Non-ribosomal peptide synthetase module protein, siderophore biosynthesis
A1S_2393	hypothetical protein	ECA2041	Putative DNA-binding protein
A1S_2456	transcriptional regulator lysR family	*lysR*	Transcriptional regulator
A1S_2468	hypothetical protein	N/A	N/A
A1S_2512	hypothetical protein	N/A	N/A
A1S_2563	putative siderophore-interacting protein	N/A	N/A
A1S_2569	hypothetical protein	*orf2*	Transposase
A1S_2573	23-dihydroxybenzoate-AMP ligase	*entE*	(2,3-dihydroxybenzoyl) adenylate synthase
A1S_2574	23-dihydroxybenzoate-AMP ligase	*entE*	2,3-dihydroxybenzoate-AMP ligase
A1S_2618	Putative RND family drug transporter	ACIAD2648	Transporter
A1S_2643	oxidoreductase short chain dehydrogenase/reductase family	*isfD*	AraC family transcriptional regulator
A1S_2655	hypothetical protein	N/A	N/A
A1S_2685	hypothetical protein	ACIAD2857	
A1S_2689	transcriptional regulator TetR family	*acnR*	Transcriptional regulator, TetR family
A1S_2709	hypothetical protein	N/A	N/A
A1S_2771	putative transcriptional regulator (AraC family)	*appY*	DNA-binding transcriptional activator
A1S_2776	hypothetical protein	*atfA*	Diacylglycerol O-acyltransferase
A1S_2794	putative nitroreductase	*pnbA*	Nitroreductase
A1S_2839	hypothetical protein	*rtcB*	RNA-splicing ligase RtcB
A1S_2880	putative signal peptide	J596_0277	META domain protein
A1S_2883	transcriptional regulator protein (OmpR family)	*baeR*	Transcriptional regulator protein (OmpR family), response regulator in two-component regulatory system with BaeS, regulates RNA synthesis
A1S_2931	hypothetical protein	*cusF*	Cation efflux system protein CusF
A1S_2944	hypothetical protein	N/A	N/A
A1S_2952	putative pyridine nucleotide-disulfide oxidoreductase class I	*lpd*	Dihydrolipoamide dehydrogenase
A1S_3009	oxidoreductase short-chain dehydrogenase/reductase family	*pECR*	Peroxisomal trans-2-enoyl-CoA reductase
A1S_3032	TonB-like protein	*tonB*	Periplasmic protein TonB
A1S_3044	hypothetical protein	*cicA*	HAD-superfamily subfamily IB, PSPase-like protein
A1S_3053	acyl coenzyme A dehydrogenase	*fadE*	Acyl coenzyme A dehydrogenase
A1S_3128	succinylglutamate desuccinylase	*astE*	Succinylglutamate desuccinylase
A1S_3145	putative membrane protein	*yccS*	TIGR01666 family membrane protein
A1S_3149	hypothetical protein	*ygiN*	Putative quinol monooxygenase YgiN
A1S_3155	hypothetical protein	Psyr_2501	Hemerythrin
A1S_3159	lipase foldase	*lipB*	Lipase chaperone

A1S_3160	lipase	*lip*	Lactonizing lipase
A1S_3198	23S ribosomal RNA G745 methyltransferase	*rrm*	23S ribosomal RNA G745 methyltransferase
A1S_3245	imidazole glycerol phosphate synthase cyclase subunit	*hisF*	Imidazole glycerol phosphate synthase subunit HisF
A1S_3246	hypothetical protein	J610_2193	Fatty acid hydroxylase superfamily protein
A1S_3259	putative transcriptional regulator YdzF	BH0655	Uncharacterized HTH-type transcriptional regulator BH0655
A1S_3266	aldo/keto reductase family oxidoreductase	*plr1*	Aldo/keto reductase
A1S_3277	putative pirin-like protein	PA2418	Putative quercetin 2,3-dioxygenase PA2418
A1S_3284	putative transcriptional regulator	*ydcN*	YdcN
A1S_3290	EsvF2	*tenA*	TenA family transcriptional regulator
A1S_3303	hypothetical protein	ACIAD3468	
A1S_3338	hypothetical protein	N/A	N/A
A1S_3363	membrane metalloendopeptidase protein	N/A	N/A
A1S_3383	D-tyrosyl tRNA(tyr) deacylase	*dtd*	D-aminoacyl-tRNA deacylase
A1S_3410	putative acyltransferase	*oatA*	Acyltransferase
A1S_3411	Putative GTPases (G3E family)	*cobW*	Cobalamin synthesis protein/P47K
A1S_3412	hypothetical protein	AMQ28_13705	Peptidase M15
A1S_3483	hypothetical protein	*wzy*	Beta-carotene 15,15'-monooxygenase
A1S_3509	hypothetical protein	*nemR_3*	Bacterial regulatory s, tetR family protein
A1S_3510	hypothetical protein	N/A	N/A
A1S_3511	hypothetical protein	ACX60_18915	
A1S_3512	hypothetical protein	N/A	N/A
A1S_3513	hypothetical protein	ACX60_18940	
A1S_3519	hypothetical protein	N/A	N/A
A1S_3536	hypothetical protein	*resP*	Integrase
A1S_3537	hypothetical protein	LV38_01156	
A1S_3546	hypothetical protein	AB988_2953	
A1S_3552	hypothetical protein	AB988_3023	
A1S_3553	hypothetical protein	N/A	N/A
A1S_3581	hypothetical protein	N/A	N/A
A1S_3591	hypothetical protein	AB895_2571	Signal peptide protein
A1S_3607	hypothetical protein	ACX60_12590	
A1S_3624	hypothetical protein	ABAYE2581	
A1S_3629	hypothetical protein	N/A	N/A
A1S_3630	hypothetical protein	ABSDF1052	Putative bacteriophage protein
A1S_3636	hypothetical protein	N/A	N/A
A1S_3637	hypothetical protein	N/A	N/A
A1S_3653	hypothetical protein	J530_2256	Reverse transcriptase family protein
A1S_3656	hypothetical protein	N/A	N/A
A1S_3677	hypothetical protein	N/A	N/A
A1S_3684	hypothetical protein	N/A	N/A
A1S_3686	hypothetical protein		Peptidase S24
A1S_3697	hypothetical protein	J530_1967	Terminase small subunit
A1S_3700	hypothetical protein	N/A	N/A
A1S_3750	hypothetical protein	N/A	N/A
A1S_3760	hypothetical protein	N/A	N/A

A1S_3761	hypothetical protein	N/A	N/A
A1S_3818	hypothetical protein	N/A	N/A
A1S_3819	hypothetical protein	N/A	N/A
A1S_3827	hypothetical protein	ERS370000_04104	Limonene-1,2-epoxide hydrolase
A1S_3844	hypothetical protein	N/A	N/A
A1S_3845	hypothetical protein	N/A	N/A
A1S_3877	hypothetical protein	N/A	N/A
A1S_3879	hypothetical protein	*corA*	Magnesium and cobalt transport protein
A1S_3884	hypothetical protein	N/A	N/A
A1S_3891	hypothetical protein		

Table S3. Down-regulated genes.

Gene	Function	Gene Name	Description
A1S_0565	putative membrane protein	NE0381	Integral membrane protein, DUF6
A1S_3176	putative membrane protein	*pglL1*	General O-oligosaccharyltransferase
A1S_1377	transcriptional regulator acrR family	*fadR*	Fatty acid metabolism regulator protein
A1S_2532	sulfate transport protein	*cysP*	Sulfate ABC transporter, sulfate-binding protein
A1S_3175	bacterioferritin	*bfr1*	Ferroxidase
A1S_0800	bacterioferritin	*bfr*	Ferroxidase
A1S_2959	Hsp 24 nucleotide exchange factor	*grpE*	Protein GrpE
A1S_3657	hypothetical protein	N/A	N/A
A1S_2423	50S ribosomal protein L31	*rpmE*	50S ribosomal protein L31
A1S_0803	trehalose-6-phosphate synthase	*otsA*	Trehalose-6-phosphate synthase
A1S_3679	hypothetical protein	N/A	N/A
A1S_0373	apolipoprotein N-acyltransferase copper homeostasis protein	*cutE*	Apolipoprotein N-acyltransferase
A1S_2628	electron transfer flavoprotein beta-subunit	*etfB*	Electron transfer flavodomain protein
A1S_2147	Flavin reductase-like protein	*flr*	FMN-binding protein
A1S_3567	hypothetical protein	N/A	N/A
A1S_3486	hypothetical protein	ABAYE3785	
A1S_2549	hypothetical protein	*rtxA*	Structural toxin protein RtxA
A1S_2481	FKBP-type peptidyl-prolyl cis-trans isomerase	*slyD*	Peptidyl-prolyl cis-trans isomerase
A1S_1186	ATP-dependent protease Hsp 100	*clpB*	Chaperone protein ClpB
A1S_1518	putative suppressor of F exclusion of phage T7	*fxsA*	Putative suppressor of F exclusion of phage T7 (FxsA)
A1S_3443	heat shock protein Hsp40	*dnaJ*	Chaperone protein DnaJ
A1S_0292	putative outer membrane protein W	ACIAD0314	Putative outer membrane protein W
A1S_3736	hypothetical protein	N/A	N/A
A1S_0360	30S ribosomal protein S15	*rpsO*	30S ribosomal protein S15
A1S_1961	heat shock protein 15	*hslR*	Heat shock protein 15
A1S_0011	hypothetical protein	*erpA*	Iron-sulfur cluster insertion protein ErpA
A1S_2351	glutamine synthetase	*glnA*	Glutamine synthetase

A1S_2072	putative universal stress protein family	ACIAD1238	Universal stress protein
A1S_2731	50S ribosomal protein L21	*rplU*	50S ribosomal protein L21
A1S_0570	hypothetical protein	*rsfS*	Ribosomal silencing factor RsfS
A1S_1187	CinA-like protein	*pncC*	CinA-like protein
A1S_1926	putative membrane protein	*ybgE*	Cyd operon YbgE family protein
A1S_2181	transcriptional factor	*mdcH*	Malonate decarboxylase, epsilon subunit
A1S_3780	hypothetical protein	J810_2980	
A1S_3407	Urocanase	*hutU*	Imidazolonepropionate hydrolase
A1S_0380	glutamate racemase	*murI*	Glutamate racemase
A1S_3790	hypothetical protein	N/A	N/A
A1S_2627	electron transfer flavoprotein alpha-subunit	*etfA*	Electron transfer flavoFAD-binding domain protein
A1S_2665	chaperone Hsp10	*groS*	10 kDa chaperonin
A1S_0447	50S ribosomal protein L33	*rpmG*	50S ribosomal protein L33
A1S_1688	hypothetical protein	N/A	N/A
A1S_2352	glutamine synthetase	*glnA*	Glutamine synthetase
A1S_1355	p-hydroxybenzoate hydroxylase transcriptional activator	*pobR*	IclR family transcriptional regulator, pca regulon regulatory protein
A1S_1679	putative signal peptide	ACIAD2317	Signal peptide protein
A1S_2186	DNA-binding protein	*fis*	DNA-binding protein Fis
A1S_3628	hypothetical protein	N/A	N/A
A1S_3164	30S ribosomal protein S16	*rpsP*	30S ribosomal protein S16
A1S_2948	thioredoxin C-3	*thi3*	Thioredoxin C-3
A1S_3675	hypothetical protein	ABSDF2139	
A1S_1738	putative transcriptional regulator	ACIAD2678	Putative transcriptional regulator
A1S_3113	hypothetical protein	*yvlC*	PspC domain protein
A1S_0282	transcription antitermination protein	*nusG*	Transcription termination/antitermination protein NusG
A1S_1924	cytochrome d terminal oxidase polypeptide subunit I	*cydA*	Cytochrome bd ubiquinol oxidase subunit 1
A1S_0628	putative transposase	*tnpA*	Transposase
A1S_2531	sulfate transport protein	*cysP*	Sulfate transporter subunit
A1S_3342	putative arsenate reductase	*arsC1*	ArsC1
A1S_1031	DNA-binding ATP-dependent protease La	*lon*	ATP-dependent protease La
A1S_3431	putative histidine triad family protein	ACIAD3604	Putative histidine triad family protein
A1S_0828	50S ribosomal protein L25	*rplY*	50S ribosomal protein L25
A1S_1681	putative methyltransferase	*ycgJ*	Putative methyltransferase YcgJ
A1S_0448	50S ribosomal protein L28	*rpmB*	50S ribosomal protein L28
A1S_2840	outer membrane protein A	*omp38*	Outer membrane protein Omp38
A1S_2126	aconitate hydratase 2	*acnB*	Aconitate hydratase 2
A1S_2218	CsuA/B	*csuA/B*	CsuA/B
A1S_0445	hypothetical protein	N/A	N/A
A1S_1675	hypothetical protein	N/A	N/A
A1S_0200	inorganic pyrophosphatase	*ppa*	Inorganic pyrophosphatase
A1S_2730	50S ribosomal protein L27	*rpmA*	50S ribosomal protein L27
A1S_2171	30S ribosomal protein S6	*rpsF*	30S ribosomal protein S6

A1S_3297	putative outer membrane protein	*omp33-36*	33-36 kDa outer membrane protein
A1S_2984	50S ribosomal protein L34	*rpmH*	50S ribosomal protein L34
A1S_2507	hypothetical protein	N/A	N/A
A1S_3601	hypothetical protein	N/A	N/A
A1S_1382	putative transcriptional regulator	*yafC*	Transcriptional regulator, LysR family
A1S_0597	50S ribosomal protein L20	*rplT*	50S ribosomal protein L20
A1S_2132	putative outer membrane protein	*tamA*	Translocation and assembly module TamA
A1S_3171	RNA polymerase omega subunit	*rpoZ*	DNA-directed RNA polymerase subunit omega
A1S_2886	acyl-CoA dehydrogenase	*acdB*	Acyl-CoA dehydrogenase
A1S_1471	putative transcriptional regulator (AraC family)	*ada_2*	Bacterial regulatory helix-turn-helix s, AraC family protein
A1S_2706	sigma D (sigma 70) factor of RNA polymerase major sigma factor during exponential growth	*rpoD*	RNA polymerase sigma factor RpoD
A1S_1620	hypothetical protein	*gst*	Glutathione S-transferase
A1S_0520	putative oxidoreductase protein%3B putative dehydrogenase (flavoprotein)	*mhpA*	3-(3-hydroxy-phenyl)propionate/3-hydroxycinnamic acid hydroxylase
A1S_0379	hypothetical protein	N/A	N/A
A1S_0593	protein chain initiation factor IF-3	*infC*	Translation initiation factor IF-3
A1S_1925	cytochrome d terminal oxidase polypeptide subunit II	*cydB*	Cytochrome d terminal oxidase polypeptide subunit II
A1S_0168	Zinc(II) binding peptide deformylase 1	*def*	Peptide deformylase
A1S_0819	acyl carrier protein (ACP)	*acpP*	Acyl carrier protein
A1S_2425	putative Na+-dependent transporter	*yfeH*	Bile acid:sodium symporter
A1S_0684	putative toluene tolerance protein Ttg2F	N/A	N/A
A1S_0960	putative permease (MFS superfamily)	*proP*	Putative transport protein
A1S_2020	hypothetical protein	*plpl0035*	YcfA family protein
A1S_1376	Acyl-CoA dehydrogenase	*iVD*	Isovaleryl-CoA dehydrogenase, mitochondrial
A1S_2697	multifunctional protein	*cobA*	Siroheme synthase
A1S_0891	hemerythrin-like metal-binding protein	*dcrH3*	Putative hemerythrin-like protein
A1S_0248	DnaK suppressor protein	*dksA*	RNA polymerase-binding transcription factor DksA
A1S_3385	putative membrane protein	ABSDF3576	0
A1S_2985	hypothetical protein	ABSDF2848	0
A1S_1831	hypothetical protein	*lys*	Putative integral membrane protein
A1S_0323	hypothetical protein	N/A	N/A
A1S_2998	S-adenosylmethionine-6-N'N'-adenosyl	*rsmA*	Ribosomal RNA small subunit methyltransferase A
A1S_1331	major facilitator superfamily MFS_1	*shiA*	MFS transporter, MHS family, shikimate and dehydroshikimate transport protein
A1S_3809	hypothetical protein	*aapA*	Aromatic amino acid transporter
A1S_3661	hypothetical protein	N/A	N/A
A1S_1205	alkyl hydroperoxide reductase C22 subunit	*ahpC*	Peroxiredoxin
A1S_1573	integration host factor beta subunit	*himD*	Integration host factor subunit beta
A1S_0529	glutaredoxin	*grxC*	Glutaredoxin

A1S_3821	hypothetical protein	J810_0823	Prokaryotic lipo-attachment site family protein
A1S_2245	30S ribosomal protein S21	*rpsU*	30S ribosomal protein S21
A1S_2005	nitrite reductase	*nasD*	Nitrite reductase, large subunit, nucleotide-and Fe/S-cluster binding
A1S_2704	lipoate-protein ligase B	*lipB*	Octanoyltransferase
A1S_3103	toluene tolerance efflux transporter	*ttg*	Toluene tolerance protein Ttg2A
A1S_1531	putative cobalamin biosynthetic protein (CobB)	*npdA*	NAD-dependent deacetylase (Regulatory protein sirtuin family)
A1S_1042	hypothetical protein	N/A	N/A
A1S_0776	putative transcriptional regulator (TetR-family)	*ACIAD0757*	Putative transcriptional regulator (TetR-family)
A1S_3795	hypothetical protein	N/A	N/A
A1S_3494	hypothetical protein	N/A	N/A
A1S_3378	phosphatidylserine decarboxylase	*psd*	Phosphatidylserine decarboxylase proenzyme
A1S_2590	putative thioesterase	*ybgC*	Tol-pal system-associated acyl-CoA thioesterase
A1S_0226	DNA polymerase III chi subunit	*holC*	DNA polymerase III, chi subunit
A1S_0095	D-amino acid dehydrogenase	*dadA*	D-amino acid dehydrogenase
A1S_3497	hypothetical protein	N/A	N/A
A1S_3397	hypothetical protein	*rhtB*	RhtB family transporter
A1S_2270	Metal-dependent Hydrolase of the beta-lactamase superfamily III	*rbn*	Ribonuclease Z
A1S_1901	hypothetical protein	APD31_15465	Metal-dependent hydrolase
A1S_0366	heat shock protein Hsp33	*hslO*	33 kDa chaperonin
A1S_3742	hypothetical protein	N/A	N/A

Table S4. Gene expression of the *A. baumannii* ATCC 17978 and AbH12O-A2 strains by RNA-seq.

A. baumannii ATCC 17978 gene	Expression level by RNA-seq[a]	*A. baumannii* AbH12O-A2 gene	Expression level by RNA-seq[a]
A1S_0242	2.23	LX00_01305	3.43
A1S_0781	3.07	LX00_03635	1.8
A1S_1657	4.5	LX00_08360	41.93
A1S_2247	4.17	LX00_12175	2.03
A1S_2390	2.07	LX00_13160	1.62
A1S_3245	7.26	LX00_17405	15.67
A1S_3410	4.89	LX00_18390	59.3
A1S_0094	11.47	LX00_00645	24.59
A1S_0315	3.18	LX00_01660	5.1
A1S_0318	4.29	LX00_01680	6.54
A1S_0896	2.18	LX00_04470	3.68
A1S_1013	2.75	LX00_05115	1.73
A1S_1028	2.43	LX00_05200	2.17
A1S_1032	2.41	LX00_05215	1.47
A1S_1146	3.41	-	-
A1S_1247	2.67	LX00_06110	1.37
A1S_1581	4.63	-	-
A1S_3032	2.01	LX00_16260	2.31
A1S_3290	2.66	LX00_17795	2.13
A1S_3363	2.6	-	-
A1S_3879	2.93	-	-

Capítulo II. Implicación de HisF en la persistencia en pulmón de *Acinetobacter baumannii* durante una infección por neumonía.

Resumen.

Los patógenos nosocomiales como *A. baumannii* son capaces de adquirir y desarrollar mecanismos de resistencia a antibióticos, lo que representa un problema importante tanto a nivel clínico como económico. Por lo tanto, es una necesidad urgente la búsqueda de nuevas dianas terapéuticas frente *A. baumannii.* En el presente capítulo se demuestra el potencial de HisF como una nueva diana terapéutica para combatir las infecciones producidas por dicho patógeno.

HisF es una proteína de la ruta de biosíntesis de la histidina y purinas. HisF forma un heterodímero con HisH, el cual, cataliza una reacción produciendo ImGP y AICAR. AICAR, por una parte, induce la activación de AMPK, implicado en la regulación de la homeostasis inhibiendo rutas de biosíntesis y activando rutas catabólicas; por otra parte, es capaz de inhibir la producción de citoquinas proinflamatorias inducida por lipopolisacáridos, como la IL-6.

El gen *hisF* de *A. baumannii* se ha encontrado hiperexpresado en la cepa tipo ATCC 17978 y en el aislamiento clínico AbH12O-A2 durante el curso de una infección por neumonía murina. Se obtuvo una cepa de *A. baumannii* ATCC 17978 mutante mediante la deleción del gen *hisF.* La comparación de ambas cepas, cepa salvaje y su derivado isogénico, en ensayos de neumonía murina resultó en la inducción de una infección subletal por parte de la cepa mutante. Sin embargo, al utilizar un modelo murino de sepsis y en *G. mellonella* no se observaron diferencias significativas en la supervivencia de ratones y larvas infectadas por ambas cepas.

También se realizaron ensayos fenotípicos como producción de *biofilm*, adhesión y supervivencia en células eucariotas y sensibilidad a antibióticos sin observarse diferencias significativas entre la cepa de *A. baumannii* ATCC 17978 y su derivado isogénico Δ*hisF*. En cuanto al crecimiento y *fitness* de la bacteria tampoco se

observaron diferencias entre ambas cepas, pero sí se demostró la auxotrofía del mutante para histidina.

Por otra parte, se realizaron inmunoensayos con el fin de comparar los niveles de secreción de IL-6, porcentaje de fagocitosis y reclutamiento de leucocitos en infecciones provocadas por la cepa de *A. baumannii* ATCC 17978 y su derivado isogénico Δ*hisF*. Para ello se realizaron infecciones *in vitro* (sobre una monocapa de macrófagos murinos RAW 264.7) e *in vivo* (se provocó una neumonía en ratones BALB/c). Los datos obtenidos demostraron un incremento en la secreción de IL-6, en el porcentaje fagocitosis y en el número de leucocitos recluidos en aquellas infecciones producidas por la cepa mutante en comparación con la cepa salvaje.

La información obtenida sugiere que el gen *hisF*, además de estar involucrado en la respuesta inmune innata y en la inflamación, se encuentra implicado en la virulencia durante una infección por neumonía; lo que explica en parte la habilidad de esta cepa de persistir en el pulmón. Este trabajo sienta las bases del diseño de terapias antimicrobianas que bloquean la actividad de HisF en *A. baumannii*.

Este trabajo se recoge en la publicación Martínez-Guitián M., Vázquez-Ucha J.C., Álvarez-Fraga L., Conde-Pérez K., Lasarte-Monterrubio C., Vallejo J.A., Bou G., Poza M., Beceiro A. (2019) Involvement of HisF in the persistence of *Acinetobacter baumannii* during a pneumonia infection. Front. Cell. Infect. Microbiol. 9:310. doi: 10.3389/fcimb.2019.00310, la cual, se adjunta a continuación.

Artículo publicado.

frontiers in Cellular and Infection Microbiology

BRIEF RESEARCH REPORT
published: 29 August 2019
doi: 10.3389/fcimb.2019.00310

Involvement of HisF in the Persistence of *Acinetobacter baumannii* During a Pneumonia Infection

Marta Martínez-Guitián†, Juan C. Vázquez-Ucha†, Laura Álvarez-Fraga†, Kelly Conde-Pérez, Cristina Lasarte-Monterrubio, Juan Andrés Vallejo, Germán Bou, Margarita Poza† and Alejandro Beceiro†*

Servicio de Microbiología Do Complexo Hospitalario Universitario da Coruña (CHUAC), Instituto de Investigación Biomédica da Coruña (INIBIC), Universidade da Coruña (UDC), A Coruña, Spain

OPEN ACCESS

Edited by:
D. Scott Merrell, Uniformed Services University, United States

Reviewed by:
Eric P. Skaar, Vanderbilt University, United States
Luis R. Martinez, The University of Texas at El Paso, United States

****Correspondence:***
Margarita Poza
margarita.poza.dominguez@sergas.es

† These authors have contributed equally to this work

Specialty section:
This article was submitted to Molecular Bacterial Pathogenesis, a section of the journal Frontiers in Cellular and Infection Microbiology

Received: *05 June 2019*
Accepted: *15 August 2019*
Published: *29 August 2019*

Citation:
Martínez-Guitián M, Vázquez-Ucha JC, Álvarez-Fraga L, Conde-Pérez K, Lasarte-Monterrubio C, Vallejo JA, Bou G, Poza M and Beceiro A (2019) Involvement of HisF in the Persistence of Acinetobacter baumannii During a Pneumonia Infection. Front. Cell. Infect. Microbiol. 9:310. doi: 10.3389/fcimb.2019.00310

Acinetobacter baumannii is currently considered one of the most problematic nosocomial microorganisms. In the present work the *hisF* gene from the ATCC 17978 strain and the AbH12O-A2 clinical isolate of *A. baumannii* was found over-expressed during the course of murine pneumonia infections. The study demonstrated that the *A. baumannii* ATCC 17978 mutant strain lacking the *hisF* gene induces a sub-lethal pneumonia infection in mice, while the complemented mutant strain increased its virulence. This histidine auxotroph mutant showed an increase on IL-6 secretion and leukocytes recruitment during infections. Furthermore, data revealed that the *hisF* gene, implicated in the innate immunity and inflammation, is involved in virulence during a pneumonia infection, which may partly explain the ability of this strain to persist in the lung. We suggest that HisF, essential for full virulence in this pathogen, should be considered a potential target for developing new antimicrobial therapies against *A. baumannii*.

IMPORTANCE

Nosocomial pathogens such as *A. baumannii* are able to acquire and develop multi-drug resistance and represent an important clinical and economic problem. There is therefore an urgent need to find new therapeutic targets to fight against *A. baumannii*. In the present work, the potential of HisF from *A. baumannii* as a therapeutic target has been addressed since this protein is involved in the innate inmunity and the inflamatory response and seems essential to develop a pneumonia in mice. This work lays the groundwork for designing antimicrobial therapies that block the activity of HisF.

Keywords: HisF, mice pneumonia model, lung infection, *Acinetobacter baumannii*, virulence

INTRODUCTION

Acinetobacter baumannii is included in a list published by the WHO of the most important antibiotic-resistant bacteria (World Health Organization, 2017). This species shows a high capacity to persist in hospital environments and to develop antimicrobial resistance. There is therefore an urgent need to find new therapeutic targets for designing novel strategies for fighting against this pathogen.

The *hisF* gene of *A. baumannii* is involved in histidine and *de novo* purine biosynthesis. The *hisH* and *hisF* products shape the heterodimeric protein imidazole glycerol phosphate (ImGP) synthase. This heterodimeric enzyme catalyzes transformation of the intermediate N′-(5′-phosphoribosyl)-formimino-5-aminoimidazol-4-carboxamide ribonucleotide (PRFAR) into 5′-(5-aminoimidazole-4-carboxamide) ribonucleotide (AICAR) and ImGP, which are further used in *de novo* purine and histidine biosynthesis, respectively (**Figure S1**).

One of the products of HisF, AICAR, an analog of adenosine monophosphate (AMP), is capable of stimulating AMP-activated protein kinase (AMPK) activity. Both AICAR monophosphate and AMP, which are small molecules, trigger a conformational change in the AMPK complex that allows further activation by phosphorylation of Thr-172 (Kim et al., 2016). The AMPK enzyme, the central regulator of energy homeostasis, participates in the cellular response to metabolic stress and is considered an important therapeutic target for controlling different human diseases (Kim et al., 2016). Once activated, AMPK phosphorylates numerous metabolic enzymes, causing global inhibition of biosynthetic pathways and activation of catabolic pathways and thus generating and conserving energy (Ruderman et al., 2003). As well as stimulating AMPK, AICAR can also inhibit the lipopolysaccharide-induced production of proinflammatory cytokines (Giri et al., 2004). Treatment with an adenosine kinase inhibitor was able to block the ability of AICAR to activate AMPK, preventing inhibition of inflammation in mice mesangial cells (Jhun et al., 2004; Peairs et al., 2009). Other authors have also described the role of AICAR in regulating inflammation (Giri et al., 2004; Jhun et al., 2004; Peairs et al., 2009).

In the present study, we found that the *hisF* gene was over-expressed in the lungs of mice with pneumonia caused by the ATCC 17978 strain and the multiresistant AbH12O-A2 clinical isolate of *A. baumannii*. The aim of the study was to investigate the involvement of the *hisF* gene in the pathogenesis of *A. baumannii* by using *in vitro* and *in vivo* assays.

TABLE 1 | Bacterial strains and plasmids used in this study.

Strain or plasmid	Relevant characteristics	Source or references
STRAIN		
A. baumannii		
ATCC 17978	Clinical isolate	ATCC*
Δ*hisF*	A1S_3245 gene (*hisF*) deletion mutant obtained from the ATCC 17978 strain	This study
ATCC 17978 + pWH1266-Km	ATCC 17978 harboring the empty pWH1266-Km plasmid; Km^R, Tet^R	This study
Δ*hisF* + pWH1266-Km	Δ*hisF* harboring the empty pWH1266-Km plasmid; Km^R, Tet^R	This study
Δ*hisF* complemented	Δ*hisF* harboring the pWH1266-Km-*hisF* plasmid; Km^R	This study
AbH12O-A2	Multiresistant clinical isolate, which caused a large nosocomial outbreak	Merino et al., 2014; Pérez et al., 2017
E. coli TG1	Used for DNA recombinant methods	Lucigen
PLASMID		
pWH1266-Km	*A. baumannii* shuttle vector; Km^R, Tet^R	Álvarez-Fraga et al., 2016
pWH1266-Km-*hisF*	pWH1266-Km harboring the A1S_*hisF* gene; Km^R	This study
pMo130	Suicide vector for the construction of *A. baumannii* isogenic derivative; Km^R, SacB, XylE	Hamad et al., 2009

*American Type Culture Collection.

MATERIALS AND METHODS

Microbial Strains and Culture Conditions

A. baumannii ATCC 17978 and its mutant derivative strains, as well as the AbH12O-A2 clinical isolate of *A. baumannii* and *E. coli* TG1 (**Table 1**) were routinely grown or maintained in Luria-Bertani (LB) or Mueller-Hinton (MH) media supplemented with 2% agar when necessary. All strains were grown at 37°C and stored at −80°C in LB broth with 10% glycerol. When appropriate, cultures were supplemented with kanamycin (km) at a final concentration of 50 mg/L (Sigma-Aldrich, USA).

Determination of the *hisF* Gene Expression

An experimental model of pneumonia in mice was used to describe the transcriptome of the ATCC 17978 and the multiresistant AbH12O-A2 clinical strains of *A. baumannii* during the course of infection, as previously reported (Álvarez-Fraga et al., 2018). Briefly, BALB/c male mice were intratracheally inoculated with ~6×10^7 bacteria *per* mouse. Bronchoalveolar lavage (BAL) was performed at 20 h to obtain bacteria for RNA extraction (*in vivo* samples). RNA extracted from bacteria grown in LB medium was used as an experimental control (*in vitro* samples). Total RNA was used for RNAseq analysis (Illumina, Biogune, Spain). Reads from each mRNA library were obtained using HiScanSQ (Illumina Inc., CIC bioGUNE, Bilbao, Spain). Gene expression analysis was done at CIC bioGUNE's genome analysis platform (Derio, Spain). Raw data were deposited in the GEO database with the accession code GSE100552 (document named GSE100552_ATCC_ODvsATCC _raton.tsv.gz).

Construction of the Isogenic Mutant Strain

The *hisF* gene was identified as A1S_3245 in the first genome sequence of *A. baumannii* ATCC 17978 (CP000521) (Fernando et al., 2014) and later annotated as AU097_05240 in a recent genome sequence of this strain (CP018664.1). The isogenic mutant strain (Δ*hisF*), lacking the *hisF* gene, was derived from the *A. baumannii* ATCC 17978 strain by double crossover recombination using the suicide vector pMo130 (Genbank: EU862243), as previously described (Álvarez-Fraga et al., 2016). Briefly, the Δ*hisF* isogenic mutant derivative was constructed by deleting a fragment of the A1S_3245 gene. The upstream and downstream regions flanking the A1S_3245 gene were

PCR-amplified and cloned into the vector pMo130 using the primers shown in **Table S1**. The construction obtained was used to transform wild type cells by electroporation. Recombinant colonies were selected as previously described (Álvarez-Fraga et al., 2016). The second crossover event was checked by PCR using primers listed in **Table S1**.

Complementation of the Mutant Strain

In order to obtain the complemented strain, the A1S_3245 gene was PCR-amplified from the genome of the ATCC 17978 strain and cloned into vector pWH1266-Km using the primers shown in **Table S1**. The pWH1266-Km plasmid was constructed as previously described (Hamad et al., 2009; Álvarez-Fraga et al., 2016). The genetic construction obtained was used to transform the Δ*hisF* isogenic mutant strain. The complemented Δ*hisF* mutant strain was selected in kanamycin-containing plates. The ATCC 17978 and the Δ*hisF* strains harboring the empty pWH1266-Km vector were used as experimental controls.

Biofilm Formation Assay

Biofilm formation ability was assessed as described by Tomaras et al. (2003) and modified by Álvarez-Fraga et al. (2016). Briefly, cells of *A. baumannii* centrifuged from an overnight culture were washed and resuspended in LB medium. Then, samples were stagnant incubated at 37°C for 48 h. Growth was monitored at OD_{600nm} and the amount of biofilm formed was quantified by crystal violet staining using ethanol-acetone. The OD_{580nm}/OD_{600nm} ratio was used to normalize the amount of biofilm formed to the total cell content of each sample.

Adhesion to A549 Human Alveolar Epithelial Cells

The ability of the strains to adhere to A549 human epithelial cells was evaluated as described by Gaddy et al. (2009) and modified by Álvarez-Fraga et al. (2016). Briefly, A549 human cells were grown at 37°C and 5% CO_2 in Dulbecco modified Eagle medium (DMEM) (Sigma-Aldrich) containing 1% of penicillin-streptomycin (Fisher Scientific, UK) and 10% of fetal bovine serum. Monolayers were washed with HBSS (Hank's balanced salt solution, Fisher Scientific) without glucose (mHBSS). A549 cells (1×10^5 cells/well) were then infected with 10^7 bacteria in 24-well plates and incubated for 3 h in mHBSS at 37°C. Finally, A549 cells were washed and lysed with sodium deoxycholate. Lysates were plated and incubated at 37°C for 24 h. Colony forming units (CFUs) were counted to determine the number of bacteria adhered to cells.

Growth Curve Analysis

Fitness was assessed by measuring the growth rates of the ATCC 17978 strain, the isogenic mutant strain Δ*hisF*, the ATCC 17978 + pWH1266-Km, the Δ*hisF* + pWH1266-Km, and the Δ*hisF* mutant strain complemented as described before. Briefly, 1.5 ml of LB medium was inoculated with ~5×10^7 CFU of each strain, previously grown until the stationary phase, and incubated at 37°C with shaking. Growth was monitored in an Epoch 2 Microplate Spectrophotometer (BioTek Instruments, Inc.) and OD_{600nm} values were recorded every 20 min as previously described (Álvarez-Fraga et al., 2018).

Growth curves were also performed to demonstrate the histidine auxotrophy of the Δ*hisF* mutant. To perform these assays, 10×10^5 CFUs/well of the ATCC 17978 strain and the isogenic mutant strain Δ*hisF* were grown in M9 minimal medium in presence or absence of 0.5 mM of histidine. Cultures were inoculated as above described. Samples were collected at 3, 6, 24, and 48 h and the number of viable bacteria present in the medium was checked by colonies counting in LB agar plates.

Determination of A549 Cells Survival Infected With *A. baumannii* Strains

An experimental model of infection of A549 human alveolar epithelial cells was used to study the *in vitro* virulence of *A. baumannii* strains as previously described (González-Bello et al., 2015). Briefly, cells were cultured in DMEM suplemented with 10% fetal bovine serum and 1% of penicillin-strptomycin. Later, 1×10^5 cells per well were infected with 5×10^7 CFUs of parental and Δ*hisF* mutant strain and incubated 20 h at 37°C. The number of inoculated bacteria was determined by direct plating. A LIVE/DEAD fluorescence microscopy kit (Cellstain Double-staining Kit; Fluka, Switzerland) was used according to the manufacturer's instructions to measure cell viability post-infection. The A549 cells were incubated for 15 min at 37°C with the two fluorescent molecules to obtain simultaneous fluorescent staining; calcein-AM, to stain viable cells (green), and propidium iodide, to stain only dead cells (red). Microscopic images of the stained cells were obtained using an inverted fluorescence microscope (Nikon Eclipse Ti) and analyzed with the NIS Elements Br software package.

Susceptibility Testing

Antimicrobial susceptibility analyses, done by the disk diffusion method, were performed using ampicillin, cefoxitin, ceftazidime, cefepime, imipenem, tigecycline, rifampicin, colistin, ciprofloxacin, and gentamicin disks (Sigma-Aldrich) (Clinical and Laboratory Standards Institute, 2018).

Murine Pneumonia Model

A murine pneumonia model was used to examine the role of the *hisF* gene in *in vivo* virulence. Briefly, BALB/c mice were intratracheally inoculated with 40 μL of a bacterial suspension containing 3×10^9 CFU/mL sterile saline solution and 10% of porcine mucin (wt/vol) (Sigma-Aldrich) mixed at 1:1 ratio (Álvarez-Fraga et al., 2018).

To ascertain the relevance of the *hisF* gene in virulence using a murine pneumonia model, a second assay was performed to determine the bacterial burden in lungs. Groups of 8 mice were intratracheally inoculated, as above described, with ATCC 17978 wild type and Δ*hisF* mutant strains. Mice were sacrificed at 20 h and lung samples were obtained and processed as previously described (Rodríguez-Hernández et al., 2000).

Murine Sepsis Model

A murine sepsis model was also constructed using BALB/c mice. Mice were inoculated intraperitoneally with 100 μL of a

bacterial suspension containing 75 × 10^7 CFU/mL, as previously described (Beceiro et al., 2014). The survival rate was assessed during 7 days post-infection.

Galleria mellonella Infection Model

The virulence of the ATCC 17978 wild type and Δ*hisF* mutant strains was assessed using a *Galleria mellonella* infection model as previously described (Álvarez-Fraga et al., 2018). Briefly, *G. mellonella* caterpillars (Bio Systems Technology, UK) were infected with 2 × 10^4 bacteria and incubated at 37°C in the dark. Death was determined every 8 h during 6 days to obtain the larval survival rates.

IL-6 Production Determination

Cell-free supernatants from infected RAW 264.7 cells and from BAL fluid from infected mice were used to analyse cytokine IL-6. RAW 264.7 macrophages were grown at 37°C and 5% CO_2 in DMEM medium (Sigma-Aldrich) containing 10% fetal bovine serum and 1% penicillin-streptomycin (Fisher Scientific). An amount of 1 × 10^5 RAW 264.7 cells *per* well were infected with 3.5 × 10^7 CFU of the parental or mutant strains using 24-well plates. Cell supernatants were collected at 2, 6, and 20 h post-infection, centrifuged at 1,000x *g* for 10 min and stored at −80°C prior to IL-6 production determination.

BAL fluids from lungs of mice infected as above described with the wild type or the mutant strain were extracted at 6 and 24 h after the challenge. A protease inhibitor cocktail was added and immediately centrifuged at 1,000x *g* for 10 min.

IL-6 was measured in both macrophages and lung samples by ELISA using the Murine IL-6 ELISA Kit (Diaclone, France) as previously described (Alnahas et al., 2017).

Leukocyte Counts

In the murine pneumonia model, BAL fluid was obtained 6 and 24 h after the challenge, to determine the total leukocyte cell counts. Cells were fixed and stained with Diff-Quick Stain (Thermo-Scientific, USA). Counts were performed using a microscope (Olympus, Japan) and the software cellSens Dimension (Olympus).

Phagocytic Assays

The phagocytic activity was assessed against the *A. baumannii* strains used in this study. RAW 264.7 murine cells were maintained in DMEM supplemented with 10% fetal bovine serum and 1% of penicillin-streptomycin. Macrophages were activated RAW 264.7 during 3 days in presence of phorbol 12-myristate 13-acetate (PMA, Sigma-Aldrich) at 100 nM. Then macrophages RAW 264.7 were scraped and seeded into 48-well plates (4 × 10^4 cells/well). Bacterial strains were cultured in LB or LB with 50 mg/L of kanamycin at 37°C until 0.7 OD_{600nm}, washed twice in saline solution and adjusted at 10 × 10^6 CFU/mL in DMEM + 10% FBS. Additionally, AICAR at 1 mM was added to the Δ*hisF* mutant and incubated 30 min at room temperature. Infections were performed adding 200 μL of bacterial inoculum to each well with cells and incubated 1 h at 37°C. Finally, supernatants were aspirated and plated onto LB or LB plus kanamycin plates. The determination of phagocytosis activity was calculated by comparison with control wells with bacterial inoculum without the presence of macrophages.

Statistical Analysis

A student's *t*-test was used to evaluate the statistical significance of the observed differences in all assays, except in the survival assays, in which the survival curves were plotted by the Kaplan-Meier method and analyzed with the log-rank test. Differences were considered statistically significant at $p \leq 0.05$. All assays were performed at least in triplicate.

Ethics Statement

All experiments with mice were performed in accordance with regulatory guidelines and standards established by the Animal Ethics Committee (CHUAC, Spain, project code P82).

RESULTS AND DISCUSSION

Expression analysis of the *hisF* gene was performed using the *A. baumannii* ATCC 17978 strain, one of the best-studied strains of this species, and the multiresistant AbH12O-A2 clinical isolate, that caused more than 300 colonizations/infections in a hospital in Madrid, Spain (Merino et al., 2014; Pérez et al., 2017). Transcriptomic analysis using RNAseq Illumina procedures revealed that, relative to bacteria grown *in vitro*, the *hisF* gene was over-expressed in both the ATCC 17978 (7.2-fold) and the AbH12O-A2 clinical (19.2-fold) *A. baumannii* strains, causing lung infection in mice.

Expression of other genes involved in histidine biosynthesis was also checked. The pathway of histidine biosynthesis is complex and involves nine genes (*hisG*, *hisI*, *hisE*, *hisA*, *hisF*, *hisH*, *hisB*, *hisC*, and *hisD*) (Fani et al., 1998). Among these genes, only *hisF* was found to be over-expressed during the lung infection, in both the ATCC 17978 and the AbH12O-A2 clinical strains. A key step occurs when the formation of two products is catalyzed by the heterodimeric enzyme complex ImGP synthase, which consists of *hisH* and *hisF*. One of the products, ImGP, is further used in histidine biosynthesis, and the other, AICAR, is used in *de novo* synthesis of purines and AMPK activation (Fani et al., 1998; O'Donoghue et al., 2001) (**Figure S1**). Thus, AICAR synthesis mainly depends on HisH and HisF. The mechanism whereby HisH produces ammonia (NH_3) from glutamine involves hydrolysis to release NH_3 and glutamate (Chittur et al., 2001). The sequential HisH and HisF reactions are strongly coupled in order to facilitate the necessary transfer of NH_3 to the HisF active site and to produce ImGP and AICAR. In our *in vivo* transcriptomic analysis, we detected over-expression of the *hisF* gene whereas the expression level of the *hisH* gene remained unaltered. The different speed of reaction of these enzymes could explain the relevance of HisF in AICAR production and in virulence during the lung infection. Thus, it has been demonstrated that a 5,300-fold increase in basal glutamine hydrolysis produced by HisH is observed in the presence of the substrate PRFAR (Myers et al., 2003). In this case, over-expression of *hisH* may not be as important as over-expression of *hisF* for increasing the AICAR synthesis.

An isogenic mutant strain lacking *hisF* gene (Δ*hisF*) derived from the ATCC 17978 strain was constructed in order to investigate the function of *hisF*. No significant differences between the ATCC 17978 strain and its derivate isogenic mutant Δ*hisF* were observed in biofilm formation or capacity for adherence to A549 human alveolar epithelial cells (**Figures S2A,B**). There was also no difference in growth rate between the parental and the Δ*hisF* mutant strain (**Figure S2C**) or in the survival rate of human alveolar epithelial A549 cells infected with the mutant and the wild type strains (**Figure S2D**). No changes in susceptibility to any of the tested antimicrobials were detected when the *hisF* gene was deleted (**Table S2**).

Remarkably, the murine pneumonia model showed that the survival rate of mice infected with the Δ*hisF* mutant strain was significantly higher than that of mice infected with the parental strain ($p < 0.001$, **Figure 1A**). The lack of the *hisF* gene led to an important loss of virulence in the *A. baumannii* ATCC 17978 strain. Conversely, no such differences were observed in the murine sepsis or in the *G. mellonella* infection models (**Figure S3**). When bacterial burden in lungs was analyzed at 20 h, results confirmed the relevant decrease of virulence in the experimental murine pneumonia. The lungs of mice infected with the Δ*hisF* mutant showed two logarithms less bacterial burden than those infected with the parental strain ($p < 0.01$, **Figure S4**).

Then, complementation of the mutant strain with the A1S_3245 gene (Δ*hisF* complemented strain) was performed by expressing the *hisF* gene from the pWH1266-Km vector. In a parallel assay, virulence of both the mutant and the parental strains harboring the empty plasmid and the mutant containing the plasmid harboring the *hisF* gene were analyzed using the murine pneumonia model. No significant differences were observed between the *A. baumannii* wild type strain harboring the empty pWH1266-Km vector and the Δ*hisF* mutant strain complemented. However, the virulence of the Δ*hisF* mutant strain complemented was higher than that of the Δ*hisF* mutant strain harboring the empty plasmid ($p < 0.05$, **Figure 1B**). Overall the data indicated that the *hisF* gene expressed from the plasmid partly restored the wild type phenotype. It should be noted that carrying the pWH1266-Km plasmid implies an important metabolic load to the bacterium, which affects its growth rate and its fitness (Álvarez-Fraga et al., 2018). As shown in **Figure S2C**, the strains carrying the pWH1266-Km plasmid decreased their fitness, which, in turn, affects their virulence. Therefore, the survival rate of mice infected with strains harboring the pWH1266-Km plasmid was higher than that of mice infected with strains without plasmids, for the same bacterial inoculum. However, as shown in **Figure S2C** no fitness differences were observed between the ATCC 17978 and the Δ*hisF* strains or between the ATCC 17978 carrying pWH1266-Km, the Δ*hisF* mutant strain carrying pWH1266-Km and the Δ*hisF* mutant strain complemented. Thus, the decreased virulence of Δ*hisF* mutants in murine pneumonia assays is exclusively attributable to the inactivation of *hisF* gene and not to the presence/absence of the pWH1266-Km plasmid.

The transformation of PRFAR by HisF produces AICAR, used in *de novo* purine biosynthesis and ImGP, used in histidine biosynthesis (**Figure S1**). Purine nucleotides can be synthesized trough two distinct pathways. First, purines can be synthesized *de novo*, attaching a formyl group to AICAR to produce IMP (inosine monophosphate) and later AMP and GMP (guanosine monophosphate). Alternatively, purine bases can be salvaged and recycled by the hydrolytic degradation of nucleic acids and nucleotides. However, to synthetize histidine the HisF protein and ImGP are essential. Thus, histidine auxotrophy assays were performed to demonstrate the implication of A1S_3245 in AICAR and ImGP production. As reflected in **Figure S5**, while the ATCC 17978 strain was able to grow in M9 minimal medium, the Δ*hisF* mutant strain was unable to grow, decreasing the number of viable bacteria at 24 h. The addition of 0.5 mM of histidine to the M9 medium does not affected the growth rate

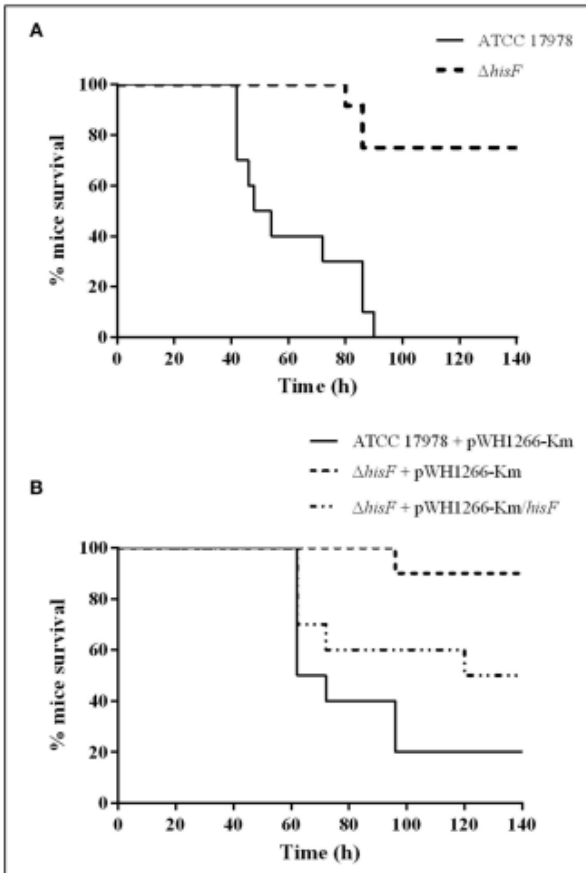

FIGURE 1 | Survival rate of mice in a pneumonia model ($N = 10$). **(A)** The parental ATCC 17978 and the mutant Δ*hisF A. baumannii* strains. Survival was significantly higher in mice infected with the Δ*hisF* mutant ($p < 0.01$). **(B)** The ATCC 17978 + pWH1266-Km (empty plasmid), the Δ*hisF* + pWH1266-Km, and the complemented Δ*hisF A. baumannii* strains. Survival was significantly lower in mice infected with the complemented than in the Δ*hisF* strain harboring the empty plasmid ($p < 0.05$). There were no significant differences in survival between mice infected with ATCC 17978 + pWH1266-km and Δ*hisF* complemented strains.

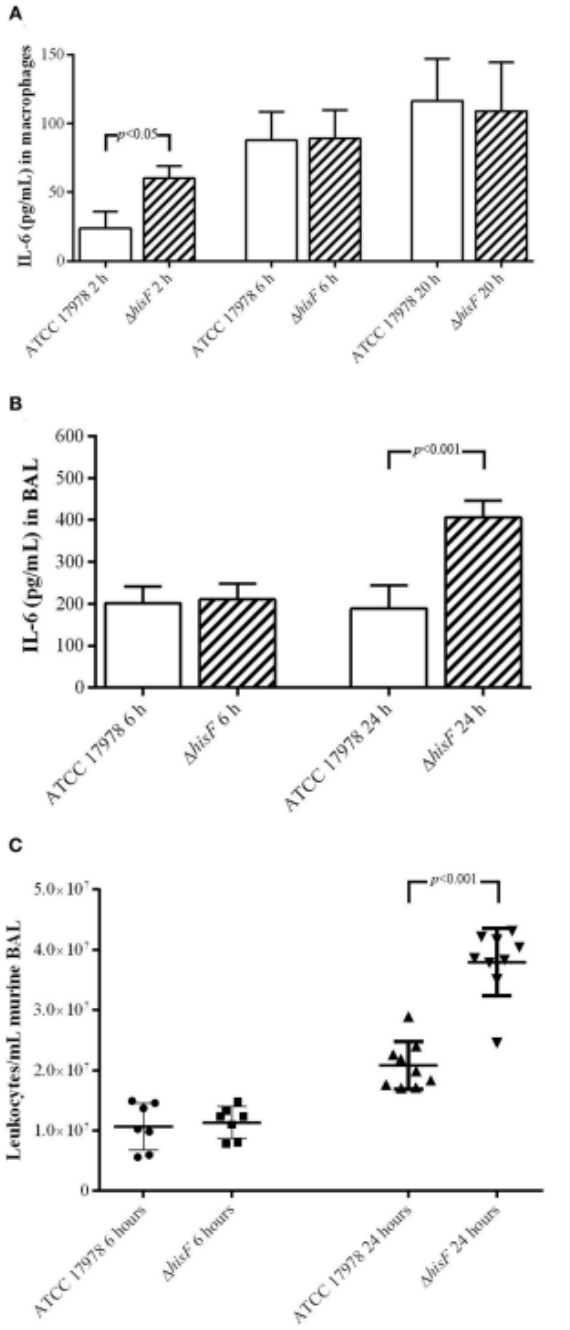

FIGURE 2 | (A) Amount of IL-6 at 2, 6, and 20 h post-infection in the cell-free supernatant of macrophages RAW 264.7 ($N = 5$) infected with the parental ATCC 17978 and the Δ*hisF* mutant *A. baumannii* strains. **(B)** Amount of IL-6 at 6 and 24 h post-infection in BAL fluid from mice lungs ($N = 7$) infected with the parental ATCC 17978 and the Δ*hisF* mutant *A. baumannii* strains. **(C)** Total leukocyte counts in BAL fluid from mice lungs infected with the parental ATCC 17978 and the Δ*hisF* mutant *A. baumannii* strains, at 6 h ($N = 7$) and 24 h ($N = 9$) post-infection.

of the parental strain but increased the growth rate of the Δ*hisF* mutant. The mutant showed a growth rate very similar to the parental strain, thus displaying the later auxotrophy by histidine.

Lungs are particularly susceptible to infection because of the huge epithelial surface in contact with inspired air. Thus, the respiratory tract must possess defense mechanisms such as the anatomical barriers of the nose or the phagocytes in alveoli. The cytokine IL-6 is involved in regulating inflammatory responses during bacterial infection, and high IL-6 concentrations are detected in BAL fluids from patients with pneumonia (Dehoux et al., 1994). In murine models of pneumonia, IL-6 has been described as being involved in antibacterial host defense and in regulating the cytokine network in lungs (van der Poll et al., 1997). Thus, the acute pulmonary inflammatory response caused by local exposure to bacterial lipopolysaccharide is regulated by inflammatory mediators such as IL-6.

In this study, immunoassays performed to detect the cytokine IL-6 in macrophages RAW 264.7 infected with the parental and the mutant strains, indicated that the macrophages differentially secreted IL-6 at 2 h ($p < 0.01$). In this model of *in vitro* infection the mutant strain was able to induce faster the IL-6 secretion, starting the pro-inflammatory response before than the parental strain. However, at 6 and 20 h, the IL-6 levels secreted by macrophages RAW 264.7 were similar in infections caused by both strains (**Figure 2A**). Thus, the increase of AICAR biosynthesis is involved in a delayed IL-6 secretion. ELISA analysis of BAL fluids from the murine pneumonia model revealed that the IL-6 concentration was higher in BAL fluids from mice infected with the Δ*hisF* mutant strain than in those infected with the parental strain ($p < 0.001$) at 24 h post-infection, whereas, no significant difference was were observed in murine BAL fluids obtained at an earlier stage post-infection (6 h) (**Figure 2B**).

IL-6 is one of the most discriminative markers for definition and evaluation of recovery in patients with pneumonia, being the serum levels of IL-6 in mild or severe pneumonia infections higher (de Brito et al., 2016). During the initial phases of pneumonia, alveolar macrophages produce a variety of pro-inflammatory cytokines such as IL-6, whose role is to both attract and activate polymorphonuclear leukocytes, necessary for local bacterial defense and clearance (Bordon et al., 2013). Thus, noticing an increase of IL-6 secretion in the infection of the Δ*hisF* mutant, we performed a study of leukocytes recruitment in lung infection caused by the parental ATCC 17978 and the Δ*hisF* mutant strains. Leukocyte counts in BAL fluids obtained from the lungs of mice infected with the Δ*hisF* mutant were almost two times higher than in those infected with the parental strain ($p < 0.001$) at 24 h (**Figure 2C**). Microscopic visualization also allowed identifying the different types of leukocytes. However, although differences were found in the total number of leukocytes in the infections, no differences were observed between each cell type in infections caused by the parental (neutrophils 69%, lymphocytes 16%, macrophages 8%, eosinophils 6%, or basophils 1%) and the mutant strain (neutrophils 61%, lymphocytes 26%, macrophages 3%, eosinophils 7%, or basophils 3%). In contrast to the infection in macrophages, which showed differences at the very early stage post-infection, in the pneumonia model the significant

differences were observed at 24 h post-infection, both in IL-6 production and in leukocyte cells counts. Thus, expression and recruitment of cytokines take longer in the *in vivo* model of infection than in the *in vitro* model of cultured macrophages.

In order to correlate with protection, IL-6 measured by ELISA was compared with the implication of *hisF* and AICAR in phagocytic activity assays. As illustrated in **Figure 3A**, there was higher phagocytosis of the Δ*hisF* mutant strain (28% phagocytosis) than of the parental strain (14%, $p < 0.01$). The protective effect of HisF was confirmed in assays with the *A. baumannii* strains carrying the plasmid pWH1266-Km. Thus, the Δ*hisF* + pWH1266-Km mutant showed more susceptibility to macrophages (39% phagocytosis) that the ATCC 17978 + pWH1266-Km (6%, $p > 0.01$), concordantly with the previous result. Relevantly the complementation with the *hisF* gene increased the resistance to the phagocytosis, the Δ*hisF* complemented strain showed very similar number of viable bacteria (2% phagocytosis) to the ATCC 17978 + pWH1266-Km strain (**Figure 3B**). Finally, significant phagocytosis protection was observed when AICAR at 1 mM was used in the assays with the Δ*hisF* + pWH1266-km mutant showing phagocytosis percentages similar to those of the parental ATCC 17978 in absence of AICAR (**Figure 3A**). Thus, it is clear than both the genetic complementation with the *hisF* gene or the AICAR addition to the culture medium, increase the resistance to macrophages of the *A. baumannii* strain with the inactivated *hisF* gene.

The results of infection of RAW 264.7 macrophages and of *in vivo* pneumonia experiments using the parental and the isogenic mutant strains suggested that HisF participates in the early and acute inflammatory responses and host defense against *A. baumannii* infection, inhibiting initiation of the innate immune cell recruitment in lungs. Moreover, the data obtained in this study suggest that conversion of PRFAR by the heterodimeric protein HisHF, in ImGP and AICAR, plays a key role in lung infection caused by *A. baumannii*. AICAR expression, which is involved in AMPK phosphorylation, can be used by the bacteria to reduce the host immune response and favor infection. The role of AICAR and AMPK in inflammation has previously been described (Jhun et al., 2004; Peairs et al., 2009), although AICAR is known to exert various other effects such as regulation of cell proliferation and apoptosis, *via* both AMPK-dependent and independent mechanisms (Campàs et al., 2003; López et al., 2003). The adenosine kinase inhibitor 5′-iodotubercidin has been used to prevent the AICAR-mediated inhibition of inflammation cascade signaling, suggesting that AMPK activation may be considered a potential therapeutic target in inflammatory diseases (Peairs et al., 2009).

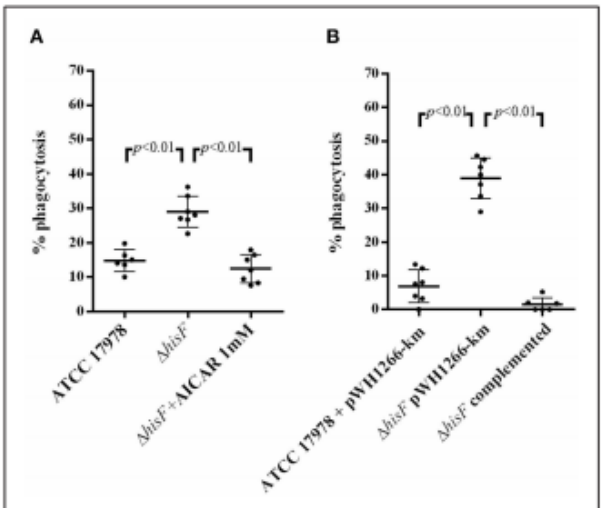

FIGURE 3 | *In vitro* phagocytosis assays with macrophages RAW 264.7. **(A)** Per cent killing of *A. baumannii* ATCC 17978, the Δ*hisF* mutant, and the Δ*hisF* mutant in presence of AICAR 1 mM ($N = 6$). **(B)** Per cent killing of *A. baumannii* ATCC 17978 + pWH1266-Km (empty plasmid), the Δ*hisF* + pWH1266-Km, and the Δ*hisF* complemented strains ($N = 6$).

Significant differences between the wild-type and the Δ*hisF* mutant strains were observed in relation to survival in the murine pneumonia model, but not in the sepsis model. Inactivation of the *hisF* gene led to disappearance of *A. baumannii*-associated virulence, which did not happen in the bacteraemia model. This can be attributed to the differences between the local and the systemic inflammation due to the immune response. The importance of pro-inflammatory cytokines in host defense during pneumonia, which have different roles in local inflammation than in the systemic compartment, has been well-described (Schultz and Poll, 2005; Madigan et al., 2014). Neutrophils are the first inflammatory cells to arrive at the infection site, attracted by chemoattractants such as interleukins. Neutrophils ingest the damaged cells and also attract macrophages, which carry out phagocytosis. The macrophages release inflammation-inducing cytokines, such as IL-1 or IL-6, which increase vascular permeability, swelling, and local heat. As a result, the pathogen is rapidly located and destroyed by the recruited macrophages and neutrophils. However, in bacteraemia models, the infection is not localized, leading to extended systemic inflammation. Septic shock occurs when the inflammatory response disseminates inflammatory cells and mediators through the circulatory and lymphatic systems. Thus, although local production of pro-inflammatory cytokines contributes greatly to host defense during local infections in the lung, the excessive production of pro-inflammatory cytokines at the systemic level causes organ failure and death in animal models (Schultz and Poll, 2005; Madigan et al., 2014). We suggest that the different virulence phenotypes found in both infection models are at least partly due to the different consequences of the pro-inflammatory interleukin-mediated inflammatory processes.

To the best of our knowledge, this is the first study describing the interplay between HisF and the innate immune response in lungs during bacterial pathogenesis. Further studies and detailed analysis of the inflammatory response are needed for a better understanding of the role of HisF in the *A. baumannii* pathogenesis and host defense.

In conclusion, the study findings demonstrated that the lack of HisF in the pneumonia infection of immunocompetent BALB/c mice caused by ATCC 17978 *A. baumannii* induces a sub-lethal infection. Complementation with the original *hisF*

gene in the Δ*hisF* mutant increased its virulence in the experimental pneumonia model. HisF is involved in inhibition of the recruitment of innate immune cells, as well as in the production of the proinflammatory cytokine IL-6. Thus, the *hisF* gene from *A. baumannii* ATCC 17978, which is over-expressed during the course of a pneumonia infection, is essential for full virulence of the strain in lung infection. The *hisF* gene is therefore an alternative and useful tool for future pathogenesis studies of *A. baumannii*-associated pneumonia and for identifying and characterizing important virulence factors, and it thus represents a potential target for evaluating new antimicrobial therapies. In light of the study findings, expression of the *hisF* gene seems to decrease the innate immunity and the inflammatory responses, which may partly explain the ability of the pathogen to persist in the lung.

DATA AVAILABILITY

Publicly available datasets were analyzed in this study. This data can be found here: https://www.ncbi.nlm.nih.gov/geo/query/acc.cgi?acc=GSE100552.

AUTHOR CONTRIBUTIONS

MM-G, KC-P, and CL-M performed phenotypic experiments and inmunoassays. JV-U and JV performed animal models. LÁ-F performed transcriptomics and mutant construction. GB supervised the experiments. AB and MP designed and supervised the experiments and wrote the manuscript. All authors discussed the results and contributed to the final manuscript.

FUNDING

This work was funded by Projects PI15/00860 awarded to GB and PI14/00059 and PI17/01482 to AB and MP, all within in the National Plan for Scientific Research, Development and Technological Innovation 2013–2016 and funded by the ISCIII—General Subdirection of Assessment and Promotion of the Research-European Regional Development Fund (FEDER) A way of making Europe. The study was also funded by project IN607A 2016/22 (GAIN-Agencia Gallega de Innovación - Consellería de Economía, Emprego e Industria) awarded to GB. This work was also supported by Planes Nacionales de I+D+i 2008–2011/2013–2016 and Instituto de Salud Carlos III, Subdirección General de Redes y Centros de Investigación Cooperativa, Ministerio de Economía y Competitividad, Spanish Network for Research in Infectious Diseases (REIPI RD12/0015/0014 and REIPI RD16/0016/006) co-financed by European Development Regional Fund A way to achieve Europe and operative program Intelligent Growth 2014-2020. JV-U was financially supported by the ISCIII (FI18/00315), MM-G was financially supported by the Grant Clara Roy (Spanish Society of Clinical Microbiology and Infectious Diseases), CL-M by Consellería de Cultura, Xunta de Galicia (IN606A-2019/029) and KC-P and JV by IN607A 2016/22.

SUPPLEMENTARY MATERIAL

The Supplementary Material for this article can be found online at: https://www.frontiersin.org/articles/10.3389/fcimb.2019.00310/full#supplementary-material

REFERENCES

Alnahas, S., Hagner, S., Raifer, H., Kilic, A., Gasteiger, G., Mutters, R., et al. (2017). IL-17 and TNF-α are key mediators of *Moraxella catarrhalis* triggered exacerbation of allergic airway inflammation. *Front. Immunol.* 8:1562. doi: 10.3389/fimmu.2017.01562

Álvarez-Fraga, L., Pérez, A., Rumbo-Feal, S., Merino, M., Vallejo, J. A., Ohneck, E. J., et al. (2016). Analysis of the role of the LH92_11085 gene of a biofilm hyper-producing *Acinetobacter baumannii* strain on biofilm formation and attachment to eukaryotic cells. *Virulence* 7, 443–455. doi: 10.1080/21505594.2016.1145335

Álvarez-Fraga, L., Vázquez-Ucha, J. C., Martínez-Guitián, M., Vallejo, J. A., Bou, G., Beceiro, A., et al. (2018). Pneumonia infection in mice reveals the involvement of the *feoA* gene in the pathogenesis of *Acinetobacter baumannii*. *Virulence* 9, 496–509. doi: 10.1080/21505594.2017.1420451

Beceiro, A., Moreno, A., Fernández, N., Vallejo, J. A., Aranda, J., Adler, B., et al. (2014). Biological cost of different mechanisms of colistin resistance and their impact on virulence in *Acinetobacter baumannii*. *Antimicrob. Agents Chemother.* 58, 518–526. doi: 10.1128/AAC.01597-13

Bordon, J., Aliberti, S., Fernandez-Botran, R., Uriarte, S. M., Rane, M. J., Duvvuri, P., et al. (2013). Understanding the roles of cytokines and neutrophil activity and neutrophil apoptosis in the protective versus deleterious inflammatory response in pneumonia. *Int. J. Infect. Dis.* 17, e76–e83. doi: 10.1016/j.ijid.2012.06.006

Campàs, C., López, J. M., Santidrián, A. F., Barragán, M., Bellosillo, B., Colomer, D., et al. (2003). Acadesine activates AMPK and induces apoptosis in B-cell chronic lymphocytic leukemia cells but not in T lymphocytes. *Blood* 101, 3674–3680. doi: 10.1182/blood-2002-07-2339

Chittur, S. V., Klem, T. J., Shafer, C. M., and Jo Davisson, V. (2001). Mechanism for acivicin inactivation of triad glutamine amidotransferases. *Biochemistry* 40, 876–887. doi: 10.1021/bi0014047

Clinical and Laboratory Standards Institute (2018). *M02. Performance Standards for Antimicrobial Disk Susceptibility Tests.* Retrieved from: https://clsi.org/media/1925/m02ed13_sample.pdf

de Brito, R. C. C. M., Lucena-Silva, N., Torres, L. C., Luna, C. F., Correia, J. B., and da Silva, G. A. (2016). The balance between the serum levels of IL-6 and IL-10 cytokines discriminates mild and severe acute pneumonia. *BMC Pulm. Med.* 16, 19–21. doi: 10.1186/s12890-016-0324-z

Dehoux, M. S., Boutten, A., Ostinelli, J., Seta, N., Dombret, M. C., Crestani, B., et al. (1994). Compartmentalized cytokine production within the human lung in unilateral pneumonia. *Am. J. Respir. Crit. Care Med.* 150, 710–716. doi: 10.1164/ajrccm.150.3.8087341

Fani, R., Mori, E., Tamburini, E., and Lazcano, A. (1998). Evolution of the structure and chromosomal distribution of histidine biosynthetic genes. *Origins Life Evol. Biosph.* 28, 555–570. doi: 10.1023/A:1006531526299

Fernando, D. M., Xu, W., Loewen, P. C., Zhanel, G. G., and Kumar, A. (2014). Triclosan can select for an AdeIJK-overexpressing mutant of *Acinetobacter baumannii* ATCC 17978 that displays reduced susceptibility to multiple antibiotics. *Antimicrob. Agents Chemother.* 58, 6424–6431. doi: 10.1128/AAC.03074-14

Gaddy, J. A., Tomaras, A. P., and Actis, L. A. (2009). The *Acinetobacter baumannii* 19606 OmpA protein plays a role in biofilm formation on abiotic surfaces and

in the interaction of this pathogen with eukaryotic cells. *Infect. Immun.* 77, 3150–3160. doi: 10.1128/IAI.00096-09

Giri, S., Nath, N., Smith, B., Viollet, B, Singh, A.K., and Singh, I. (2004). 5-aminoimidazole-4-carboxamide-1-−4-ribofuranoside inhibits proinflammatory response in glial cells: a possible role of AMP-activated protein kinase. *J. Neurosci.* 24, 479–487. doi: 10.1523/JNEUROSCI.4288-03.2004

González-Bello, C., Tizón, L., Lence, E., Otero, J. M., Van Raaij, M. J., Martínez-Guitian, M., et al. (2015). Chemical modification of a dehydratase enzyme involved in bacterial virulence by an ammonium derivative: evidence of its active site covalent adduct. *J. Am. Chem. Soc.* 137, 9333–9343. doi: 10.1021/jacs.5b04080

Hamad, M. A., Zajdowicz, S. L., Holmes, R. K., and Voskuil, M. I. (2009). An allelic exchange system for compliant genetic manipulation of the select agents *Burkholderia pseudomallei* and *Burkholderia mallei*. *Gene* 430, 123–131. doi: 10.1016/j.gene.2008.10.011

Jhun, B. S., Jin, Q., Oh, Y. T., Kim, S. S., Kong, Y., Cho, Y. H., et al. (2004). 5-aminoimidazole-4-carboxamide riboside suppresses lipopolysaccharide-induced TNF-α production through inhibition of phosphatidylinositol 3-kinase/Akt activation in RAW 264.7 murine macrophages. *Biochem. Biophys. Res. Commun.* 318, 372–380. doi: 10.1016/j.bbrc.2004.04.035

Kim, J., Yang, G., Kim, Y., Kim, J., and Ha, J. (2016). AMPK activators: mechanisms of action and physiological activities. *Exp. Mol. Med.* 48:e224. doi: 10.1038/emm.2016.16

López, J.M., Santidrián, A.F., Campàs, C., and Gil, J. (2003). 5-aminoimidazole-4-carboxamide riboside induces apoptosis in Jurkat cells, but the AMP-activated protein kinase is not involved. *Biochem. J.* 370(Pt 3), 1027–1032. doi: 10.1042/bj20021053

Madigan, M., Martinko, J., Stahl, D., and Clark, D. (2014). *Brock Biology of Microorganisms, 13th Edn.* (Harlow: Pearson).

Merino, M., Alvarez-Fraga, L., Gomez, M. J., Aransay, A. M., Lavin, J. L., Chaves, F., et al. (2014). Complete genome sequence of the multiresistant *Acinetobacter baumannii* strain AbH12O-A2, isolated during a large outbreak in Spain. *Genome Announc.* 2, e01182–14. doi: 10.1128/genomeA.01182-14

Myers, R. S., Jensen, J. R., Deras, I. L., Smith, J. L., and Davisson, V. J. (2003). Substrate-induced changes in the ammonia channel for imidazole glycerol phosphate synthase. *Biochemistry* 42, 7013–7022. doi: 10.1021/bi034314l

O'Donoghue, P., Amaro, R., and Luthey-Schulten, Z. (2001). On the structure of *hisH*: protein structure prediction in the context of structural and functional genomics. *J. Struct. Biol.* 134, 257–268. doi: 10.1006/jsbi.2001.4390

Peairs, A., Radjavi, A., Davis, S., Li, L., Ahmed, A., Giri, S., et al. (2009). Activation of AMPK inhibits inflammation in MRL/lpr mouse mesangial cells. *Clin. Exp. Immunol.* 156, 542–551. doi: 10.1111/j.1365-2249.2009.03924.x

Pérez, A., Merino, M., Rumbo-Feal, S., Álvarez-Fraga, L., Vallejo, J. A., Beceiro, A., et al. (2017). The FhaB/FhaC two-partner secretion system is involved in adhesion of *Acinetobacter baumannii* AbH12o-A2 strain. *Virulence* 8, 959–974. doi: 10.1080/21505594.2016.1262313

Rodríguez-Hernández, M. J., Pachón, J., Pichardo, C., Cuberos, L., Ibáñez-Martínez, J., García-Curiel, A., et al. (2000). Imipenem, doxycycline and amikacin in monotherapy and in combination in *Acinetobacter baumannii* experimental pneumonia. *J. Antimicrob. Chemother.* 45, 493–501. doi: 10.1093/jac/45.4.493

Ruderman, N. B., Park, H., Kaushik, V. K., Dean, D., Constant, S., Prentki, M., et al. (2003). AMPK as a metabolic switch in rat muscle, liver and adipose tissue after exercise. *Acta Physiol Scand.* 178, 435–442. doi: 10.1046/j.1365-201X.2003.01164.x

Schultz, M., and Poll, T. (2005). Modulation of innate immune responses in the treatment of sepsis and pneumonia. *Curr. Drug Targets Inflamm. Allergy* 3, 11–17. doi: 10.2174/1568010043483962

Tomaras, A. P., Dorsey, C. W., Edelmann, R. E., and Actis, L. A. (2003). Attachment to and biofilm formation on abiotic surfaces by *Acinetobacter baumannii*: involvement of a novel chaperone-usher pili assembly system. *Microbiology* 149(Pt 12), 3473–3484. doi: 10.1099/mic.0.26541-0

van der Poll, T., Keogh, C. V., Guirao, X., Buurman, W. A., Kopf, M., and Lowry, S. F. (1997). Interleukin-6 gene-deficient mice show impaired defense against pneumococcal pneumonia. *J. Infect. Dis.* 176, 439–444. doi: 10.1086/514062

World Health Organization (2017). *Global Priority List of Antibiotic-Resistant Bacteria to Guide Research, Discovery and Development of New Antibiotics.* Retrieved from: http://www.who.int/medicines/publications/WHO-PPL-Short_Summary_25Feb-ET_NM_WHO.pdf

Conflict of Interest Statement: The authors declare that the research was conducted in the absence of any commercial or financial relationships that could be construed as a potential conflict of interest.

Material suplementario del artículo.

Table S1. Oligonucleotides used in the present work.

Primer name	Sequence	Use in the study
A1S_3245UPFw	ttgcggccgcaagtcacggaacaaatctgag	Construction of the Δ*hisF* mutant
A1S_3245UPRv	ccggaattccgggttaatactcactttgtctg	Construction of the Δ*hisF* mutant
A1S_3245DOWN	ccggaattccggtatcgaaatgcgcttgtaag	Construction of the Δ*hisF* mutant
A1S_3245DOWNRv	cgcggatccgcggtttggcaatttctagccc	Construction of the Δ*hisF* mutant
A1S_3245intUP	gcctgtgtaggaactttca	Confirmation the deletion of the A1S_3245 gene
A1S_3245intDOWN	ccactctctcaagctgta	Confirmation the deletion of the A1S_3245 gene
A1S_3245FwEcoRVCompl	cccgatatcatgcttgctaaacgtattat	Cloning the A1S_3245gene into the pWH1266-Km plasmid to complement the Δ*hisF* strain
A1S_3245RvBamHICompl	cccggatccttacaagcgcatttcgatac	Cloning the A1S_3245gene into the pWH1266-Km plasmid to complement the Δ*hisF* strain

Table S2. Antibiotic susceptibility profile of ATCC 17978 and Δ*hisF* mutant.

	Zone diameter mean difference (mm)	
Antibiotic	**ATCC 17978**	***ΔhisF***
Ampicillin	9	9
Cefoxitin	9	9
Ceftazidime	20	21
Cefepime	22	23
Imipenem	29	31
Tigecycline	22	24
Rifampicin	11	11
Colistin	13	14
Ciprofloxacin	25	27
Gentamicin	24	26

Figure S1. Reactions catalyzed by HisH and HisF. The ammonia molecule required for this reaction is provided by the glutaminase HisH which transfers nitrogen from L-glutamine to form L-glutamate. Later, PRFAR is converted by HisF into ImGP and AICAR. The second product of the reaction, AICAR, is further used in de novo purine biosynthesis and AMPK activation.

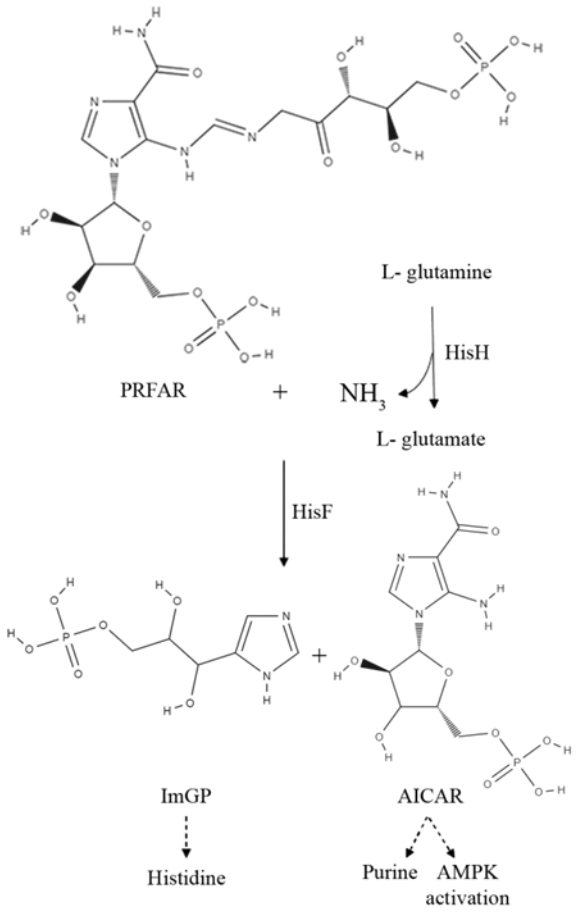

Figure S2. *In vitro* assays. A) Quantification of the biofilm formation ability *of A. baumannii* ATCC 17978 strain and the mutant derivative strain Δ*hisF* (N=6, bars represent the standard deviations). B) Quantification of the bacterial adhesion ability to A549 cells of *A. baumannii* ATCC 17978 strain and the mutant derivative strain Δ*hisF* (N=6, bars represent the standard deviations). C) Growth curves of the ATCC 17978 strain and the isogenic mutant derivative strain Δ*hisF*. Data correspond to the mean of four replicates and bars represent the standard deviations. D) Fluorescence microscopy images of human alveolar A549 cells infected by ATCC 17978 and Δ*hisF* strains after 16 h post infection.

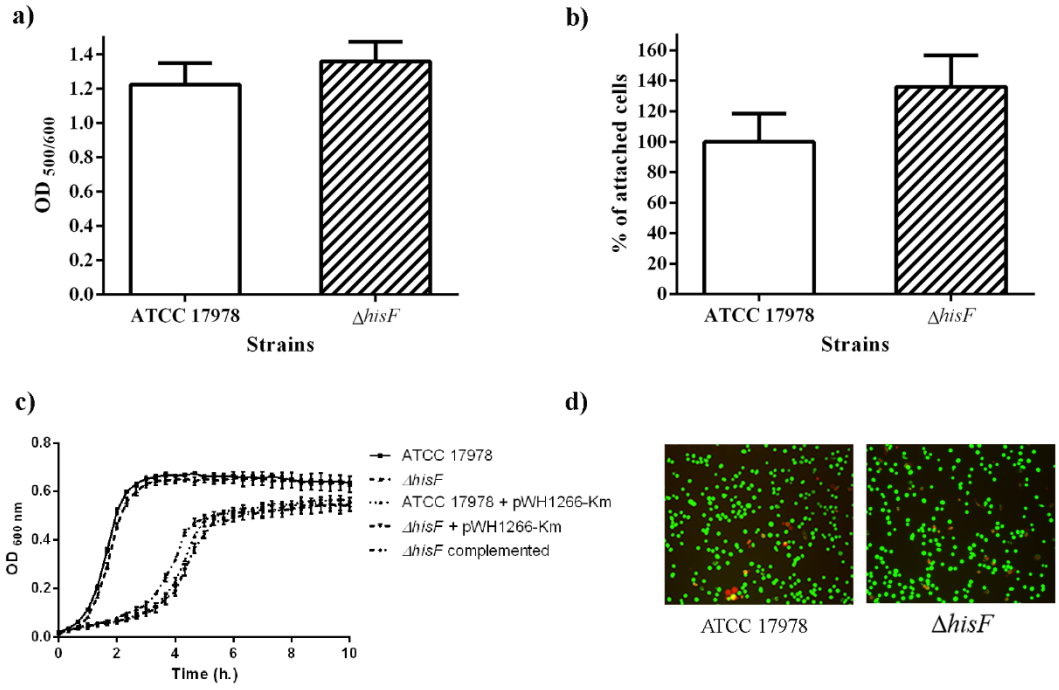

Figure S3. *In vivo* assays. A) Experimental murine model of bacteraemia performed with the *A. baumannii* ATCC 17978 and the isogenic mutant Δ*hisF* strains (N=10). B) *G. mellonella* larvae infection model using the *A. baumannii* ATCC 17978 and the isogenic mutant strains. Non-infected larvae (PBS) were used as control (N=10).

a)

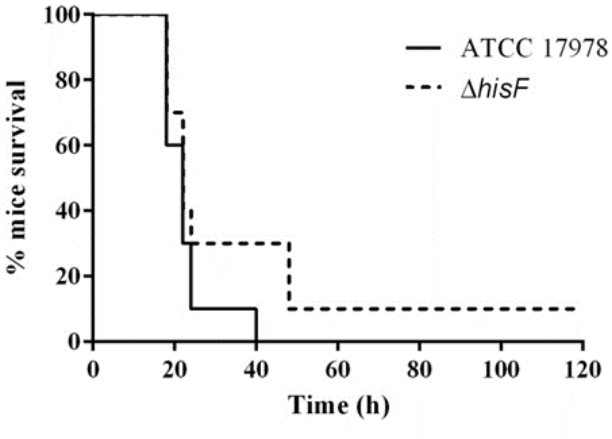

b)

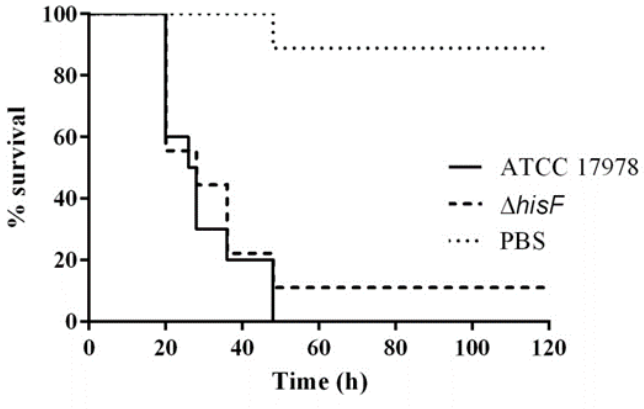

Figure S4. Bacterial burden in lungs from mice infected with both strains ATCC 17978 and Δ*hisF* mutant of *A. baumannii*.

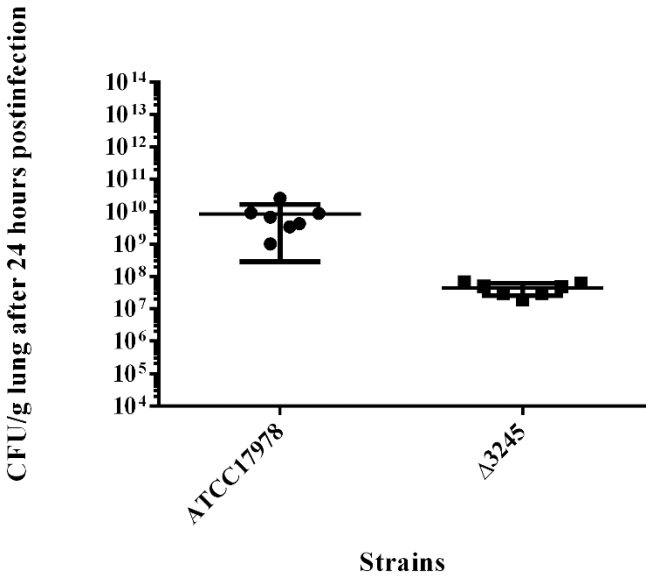

Figure S5. Auxotrophy assay in M9 medium.

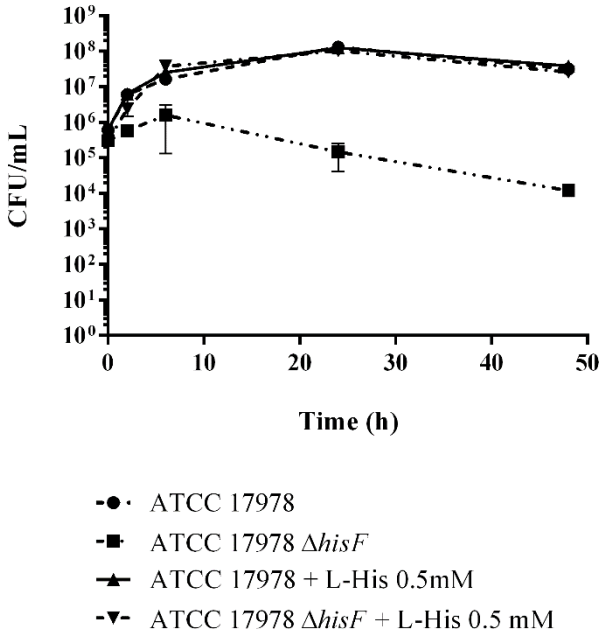

Capítulo III. Inhibición del gen *lpxB* de *Acinetobacter baumannii* por conjugados de péptido-PNA y evaluación de un efecto sinérgico con colistina.

Resumen.

La resistencia a los antimicrobianos de los patógenos nosocomiales es una prioridad en la agenda de la mayoría de los gobiernos y comunidades de investigación de todo el mundo. Debido a este aumento progresivo de las tasas de resistencia, muchos agentes antimicrobianos en desuso tuvieron que ser rescatados y utilizados de nuevo. Este es el caso de la colistina, la cual, ha sido reintroducida en el tratamiento de patógenos multirresistentes como *A. baumannii*, a pesar de su elevada nefrotoxicidad y neurotoxicidad. Por lo tanto, los esfuerzos deben estar dirigidos a desarrollar nuevas alternativas terapéuticas debido a la escasez de nuevos antibióticos.

Los PNAs son un tipo de agentes antisentido cuya secuencia nucleotídica es complementaria a un lugar de reconocimiento en el ARNm de la proteína seleccionada, lo que conduce a una expresión reducida o alterada de la traducción. De este modo, utilizamos esta tecnología para inhibir proteínas esenciales para la supervivencia bacteriana. Los PNAs requieren una entrada adecuada a través de la pared celular, por lo tanto, se suelen conjugar con péptidos penetrantes de células (CPPs) para mejorar la penetración intracelular y la potencia antisentido.

En este capítulo se demostró la eficacia de la tecnología antisentido como una nueva alternativa terapéutica frente a patógenos multirresistentes. También se evaluó el potencial del gen *lpxB* de *A. baumannii* como una nueva diana terapéutica.

El gen *lpxB* de *A. baumannii* ATCC 17978 resultó hiperexpresado durante el transcurso de una neumonía murina. Se realizaron ensayos de expresión de la proteína LpxB en presencia y en ausencia del pPNA anti-*lpxB*, resultando en un 80% de la inhibición de la expresión. También se evaluó la eficacia inhibitoria del pPNA anti-*lpxB* mediante ensayos de infección en células epiteliales alveolares A549 y en curvas de letalidad; comparando dicho agente antisentido frente a la inhibición proteica que presentó el

pPNA anti-*murA* (utilizado como control positivo) y el pPNA anti-*hisF* (utilizado como control negativo).

Con la finalidad de intentar reducir la dosis de colistina en el tratamiento de las infecciones producidas por *A. baumannii*, se evaluó la eficacia inhibitoria del pPNA anti-*lpxB* en conjunto con colistina, resultando en un efecto sinérgico en aquellas cepas sensibles a dicho antibiótico. En cuanto a las cepas que presentan mecanismos de resistencia a colistina, se observó una bajada de la CMI de este péptido antimicrobiano en conjunto con el PNA, pero sin llegar a catalogarlo como sinergia. Los ensayos *in vivo* confirmaron que un tratamiento combinado de pPNA anti-*lpxB* y colistina era más efectivo que la colistina en monoterapia.

Este trabajo se recoge en la publicación Martínez-Guitián M., Vázquez-Ucha J.C., Álvarez-Fraga L., Conde-Pérez K., Bou G., Poza M., Beceiro A. (2019) Antisense inhibition of *lpxB* gene by peptide-PNA conjugates and synergy with colistin in *Acinetobacter baumannii*. J Antimicrob Chemother doi:10.1093/jac/dkz409, adjuntada a continuación.

Artículo publicado.

J Antimicrob Chemother
doi:10.1093/jac/dkz409

Journal of Antimicrobial Chemotherapy

Antisense inhibition of *lpxB* gene expression in *Acinetobacter baumannii* by peptide–PNA conjugates and synergy with colistin

Marta Martínez-Guitián, Juan Carlos Vázquez-Ucha, Laura Álvarez-Fraga, Kelly Conde-Pérez, Germán Bou, Margarita Poza*† and Alejandro Beceiro†

Servicio de Microbiología do Complexo Hospitalario Universitario da Coruña (CHUAC), Instituto de Investigación Biomédica da Coruña (INIBIC), Centro de Investigacións Cientificas Avanzadas (CICA), Universidade da Coruña (UDC), A Coruña, Spain

*Corresponding author: E-mail: margarita.poza.dominguez@sergas.es
†These authors contributed equally to this work.

Received 29 April 2019; returned 17 July 2019; revised 28 August 2019; accepted 3 September 2019

Background: LpxB is an enzyme involved in the biosynthesis pathway of lipid A, a component of LPS.

Objectives: To evaluate the *lpxB* gene in *Acinetobacter baumannii* as a potential therapeutic target and to propose antisense agents such as peptide nucleic acids (PNAs) as a tool to combat bacterial infection, either alone or in combination with known antimicrobial therapies.

Methods: RNA-seq analysis of the *A. baumannii* ATCC 17978 strain in a murine pneumonia model was performed to study the *in vivo* expression of *lpxB*. Protein expression was studied in the presence or absence of anti-*lpxB* $(KFF)_3K$-PNA (pPNA). Time–kill curve analyses and protection assays of infected A549 cells were performed. The chequerboard technique was used to test for synergy between pPNA and colistin. A *Galleria mellonella* infection model was used to test the *in vivo* efficacy of pPNA.

Results: The *lpxB* gene was overexpressed during pneumonia. Treatment with a specific pPNA inhibited LpxB expression *in vitro*, decreased survival of the ATCC 17978 strain and increased the survival rate of infected A549 cells. Synergy was observed between pPNA and colistin in colistin-susceptible strains. *In vivo* assays confirmed that a combination treatment of anti-*lpxB* pPNA and colistin was more effective than colistin in monotherapy.

Conclusions: The *lpxB* gene is essential for *A. baumannii* survival. Anti-*lpxB* pPNA inhibits LpxB expression, causing bacterial death. This pPNA showed synergy with colistin and increased the survival rate in *G. mellonella*. The data suggest that antisense pPNA molecules blocking the *lpxB* gene could be used as antibacterial agents.

Introduction

Acinetobacter baumannii is an important nosocomial pathogen that has shown a great capacity for persistence in the hospital environment and readily causes outbreaks.[1] The frequency of MDR clinical isolates has steadily increased over the last few decades and it is becoming especially difficult to manage *A. baumannii* infections owing to the lack of treatment options.[2,3] Antimicrobial resistance in nosocomial pathogens is at the top of the agenda of most governments and research communities worldwide. Owing to the progressive increase in resistance rates, many antimicrobial agents that had previously fallen into disuse have had to be rescued and used again. So, colistin, in spite of its high nephrotoxicity and neurotoxicity, was reintroduced for the treatment of MDR pathogens such as *A. baumannii*.[4,5] The scarcity of new antibiotics in the pipeline makes it imperative that efforts be directed toward the development of new therapeutic alternatives.

Recent advances have been made in antisense RNA technology. This strategy, using sequence-specific mRNA recognition leading to reduced or altered expression of transcripts, can be exploited to inhibit the synthesis of selected essential proteins.[6] Antisense oligomers (ASOs) are typically 10–30 nt in length and have nucleotide sequences that are complementary to their target mRNA.

The inhibitory efficiency of antisense molecules depends on various factors such as their length, structure, binding rate, intracellular concentrations and resistance to degradation by nucleases and proteases. Antisense molecules are specifically designed to address these issues and improve their inhibitory efficiency. Rasmussen *et al.*[6] have reviewed these strategies.

The chemical structure of antisense molecules can be optimized using a combination of sugar, backbone, nucleobase and 3′- and 5′-terminal modifications that lead to different types of

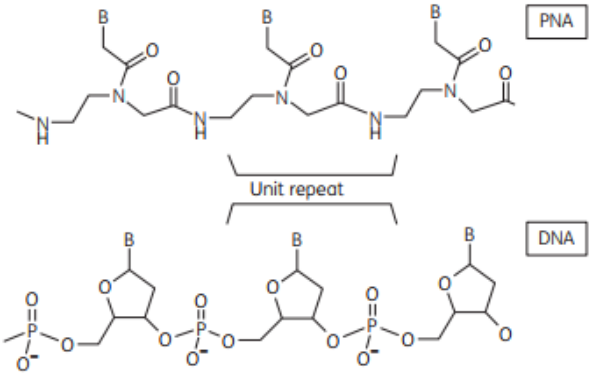

Figure 1. Chemical structure of PNA and DNA oligomers. B indicates adenine, guanine, cytosine or thymine.

ASO including: phosphorothioate (PS, in which one of the non-bridging oxygen molecules of the phosphodiester bond of DNA is replaced with sulphur); phosphorodiamidate morpholino oligomers (PMOs, in which the deoxyribose of DNA has been replaced by morpholine rings coupled by non-ionic phosphorodiamidate intersubunit linkages); locked/bridged nucleic acids (LNAs/BNAs, bicyclic nucleotide analogues with a furanose ring modified by the introduction of a methylene group); and peptide nucleic acids (PNAs), among others.[6–8] It is necessary therefore to carefully consider parameters such as degradation resistance, binding efficiency, solubility and cellular delivery before any of these modifications are selected.

PNA antisense agents, first developed in 1991,[9] are able to inhibit gene expression with sequence specificity.[10] A PNA is a DNA analogue in which the sugar–phosphate backbone has been replaced by a synthetic peptide bond (Figure 1). *N*-(2-aminoethyl)-glycine units are linked by peptide bonds to form the PNA molecule and the nucleobases are attached to the backbone through methylene carbonyl linkages. The PNA backbone is both flexible and electrically neutral. These oligomers can strongly hybridize to DNA or RNA; the reason for this is the lack of electrostatic repulsion because of the total absence of negative charge on the PNA oligomer. Hence they show higher affinity and specificity when targeting DNA and RNA strands compared with natural DNA or RNA.[11,12]

For efficient antisense inhibition, PNAs also require a suitable entry point to penetrate the protective barrier of the cell wall. PNAs are larger than most drugs[6] and are usually conjugated to cell-penetrating peptides (CPPs), used as membrane-permeable delivery vehicles in order to increase the intracellular concentrations.[10] The permeabilizing capacity of CPPs varies according to the bacterial species. The most commonly used CPPs are: $(KFF)_3K$; $(RX)_6B$; $(RXR)_4XB$; and $(RFR)_4X$.[13–15]

The binding of ASOs to complementary mRNA sequences is now a well-established strategy in mammalian systems. Some antisense drugs have been approved or are undergoing clinical trials, mainly for the treatment of cancer and other human diseases.[6,11,16,17] Likewise, a few studies have reported their efficacy against bacterial pathogens such as *Escherichia coli*, *Klebsiella pneumoniae*, *Pseudomonas aeruginosa* and *Staphylococcus aureus*.[10,18–20] Growth inhibition of *A. baumannii* by anti-*gyrA* PNAs has been demonstrated.[21] Silencing resistance genes is an important alternative use of antisense technology and one that has made it possible to modify the phenotype of strains from antibiotic resistant to antibiotic susceptible.[22,23] Indeed, the antimicrobial use of this technology has been proven in recent years and could be a potential source of new drugs.[24,25]

Bacterial transcriptomic analysis allows identification of essential genes that can be selected as therapeutic targets, which paves the way for the design and development of new antibacterial drugs. In most Gram-negative bacteria, LPS is the major component of the outer membrane, which contains a lipid A membrane anchor, core oligosaccharide and O-antigen polysaccharide.[26] In the lipid A biosynthesis pathway, the glycosyltransferase enzyme LpxB catalyses the nucleophilic attack of the 6′-hydroxyl of lipid X to form disaccharide-1-phosphate, the main component of lipid A.[27] Thus, in Gram-negative bacteria, LpxB is essential for the development of an intact LPS, so maintaining the structure of the bacterial cell envelope and its growth.[27]

In this study, two other genes were selected for inhibition using peptide–pPNA conjugates (pPNAs): *murA* and *hisF* genes. MurA (A1S_0685 gene in the ATCC 17978 strain) is an essential enzyme that catalyses the transfer of enolpyruvate from phosphoenolpyruvate to uridine-diphospho-*N*-acetylglucosamine, which is the first committed step of peptidoglycan biosynthesis, a fundamental component of bacterial cell wall survival.[28] This enzyme is also a target of fosfomycin, whose mechanism of action has been well studied.[29] Anti-*murA* pPNA was used in this study for comparison of antisense inhibition. HisF (A1S_3245 gene in the ATCC 17978 strain), an imidazole glycerol phosphate synthase, is involved in histidine metabolism[30] and we have observed that it is also involved in the persistence of *A. baumannii* in lung infection, but is not essential for prokaryotic survival. A Δ*hisF* mutant derivative of *A. baumannii* (strain ATCC 17978) created by our group did not show differences in growth rate when compared with the parental strain.[31] Consequently, the anti-*hisF* pPNA was used as a negative control.

In the present study, increased expression of the A1S_1668 gene (*lpxB*) was identified during the course of *A. baumannii* lung infection in mice. We evaluated the potential of the pPNA anti-*lpxB* to combat bacterial infection, used alone or in combination with colistin. Finally, we evaluated the LpxB enzyme as a new target using pPNA antisense technology against laboratory strains and clinical isolates of *A. baumannii*.

Materials and methods

Bacterial strains, cell lines and pPNAs

Bacterial strains of *A. baumannii* were cultured at 37°C in LB medium (a nutrient-rich medium designed for growth of pure cultures) or M9 minimal salts medium (a highly referenced minimal growth medium containing only salts and 20% glucose as carbon source; Becton Dickinson) supplemented with colistin 15 mg/L when necessary. Strains were frozen in LB with 10% glycerol and maintained at −80°C until analysis. Antimicrobial activity assays using antisense molecules were performed in two different culture media to evaluate two extreme conditions with an excess and deficit of bacterial nutrients: LB and M9. The strains used and a description of main characteristics are listed in Table 1.

Table 1. Description of *A. baumannii* strains and MICs of anti-*lpxB* pPNA, colistin and both in combination[a]

	MIC (mg/L) in LB medium					MIC (mg/L) in M9 medium						
Strains	colistin	pPNA[b]	COL_{pPNA}	$pPNA_{COL}$	FIC_{index}	colistin	pPNA[b]	COL_{pPNA}	$pPNA_{COL}$	FIC_{index}	Description	Ref.
ATCC 17978	0.5	100 (20)	0.06	6.2 (1.2)	0.18, synergy	1	12.5 (2.5)	0.25	1.5 (0.3)	0.37, synergy	*A. baumannii* reference strain	ATCC
ATCC 19606	2	100 (20)	0.25	25 (5)	0.375, synergy	2	12.5 (2.5)	0.12	1.5 (0.3)	0.18, synergy	*A. baumannii* type strain	ATCC
ATCC 19606 *pmrB*	32	100 (20)	4	25 (5)	0.375, synergy	32	12.5 (2.5)	16	1.5 (0.3)	0.62, no interaction	Col-R isogenic mutant derivative of ATCC 19606. Single amino acid substitution (Ala227Val) in PmrB	34
ABRIM	2	100 (20)	0.25	25 (5)	0.375, synergy	1	12.5 (2.5)	0.25	1.5 (0.3)	0.37, synergy	*A. baumannii* clinical isolate	55
ABRIM *pmrB*	64	100 (20)	32	6.2 (1.2)	0.56, no interaction	64	12.5 (2.5)	64	12.5 (2.5)	2, no interaction	Col-R isogenic mutant derivative of ABRIM. Single amino acid substitution (Asn353Tyr) in PmrB	34
AB248	0.5	100 (20)	0.06	12.5 (2.5)	0.245, synergy	0.5	12.5 (2.5)	0.06	3 (0.6)	0.36, synergy	*A. baumannii* clinical isolate	42
AB249 *pmrB*	128	100 (20)	128	100 (20)	2, no interaction	64	12.5 (2.5)	32	1.5 (0.3)	0.62, no interaction	Col-R isogenic clinical isolate derivative of AB248. Single amino acid substitution (Pro233Ser) in PmrB	42

Col-R, colistin-resistant; Ref., reference.
[a]COL_{pPNA}, colistin MICs in the presence of anti-*lpxB* pPNA; $pPNA_{COL}$, pPNA MICs in the presence of colistin.
[b]pPNA MIC values in brackets are expressed in μM.

Table 2. Sequences of the PNA antisense molecules used in this study conjugated with the CPP $(KFF)_3K$

PNA designation	Sequence	Length (bp)
anti-*lpxB*	KFFKFFKFFK-CCAAGGCGATTTA	13
anti-*murA*	KFFKFFKFFK-CCATTAATATTTAAGC	16
anti-*hisF*	KFFKFFKFFK-GCATAGCTTTTTCC	14

A549 human alveolar epithelial cells were maintained at 37°C in the presence of 5% CO_2 in DMEM (Sigma-Aldrich) supplemented with 10% FBS and 1% penicillin/streptomycin (Thermo Fisher, Waltham, MA, USA).

The PNA antisense molecules (anti-*lpxB*, anti-*murA* and anti-*hisF*) were covalently conjugated in all cases with the CPP $(KFF)_3K$ (Biomers, Ulm, Germany) using solid-phase peptide synthesis. The sequences of the antisense conjugates are shown in Table 2.

Transcriptomic analysis in a murine pneumonia infection model

A murine pneumonia model allowed us to study the transcriptome of the *A. baumannii* ATCC 17978 strain during the course of an infection. Transcriptomic analysis compared RNA extracted from bacteria infecting mouse lungs with that from bacteria growing *in vitro*. The experimental model, deep sequencing procedures and bioinformatics analysis were performed as described previously.[32] Briefly, male BALB/c mice were inoculated intratracheally with ~6×10^7 bacteria per mouse. Bronchoalveolar lavage was performed after 20 h to obtain bacteria for RNA extraction (*in vivo* samples) and for comparison with RNA extracted from bacteria grown in LB medium (*in vitro* samples). Total RNA was used for RNA-seq analysis (Illumina, bioGUNE, Spain). The genome analysis platform at CIC bioGUNE (Derio, Spain) was used for gene expression analysis.

Construction of isogenic deletion derivatives

The mutant derivative strain lacking the *lpxB* gene was constructed following the protocol described previously.[32] Briefly, following the double-crossover recombination method, an isogenic mutant strain lacking the *lpxB* gene was derived from the *A. baumannii* ATCC 17978 strain using the pMo130 suicide vector (GenBank: EU862243). The upstream and downstream regions flanking the *lpxB* gene were PCR-amplified and cloned into the pMo130 vector using the following primers: UPFw: TTGCGGCCGCAACAGGATTCGTATTATTATAG; DOWNFw: CCGGAATTCCGGAGATTCTTTTCTTTGATACT; UPRv: CCGGAATTCCGGATTTTTAAGATTTGATTGGCTA; and DOWNRv: CGCGGATCCGCGTCTTGAACTAAAAGTTTCTG. The genetic construction obtained was used to transform the ATCC 17978 strain. Selection of the Δ*lpxB* mutant strain was performed on plates containing kanamycin.

In vitro inhibition of LpxB expression

lpxB and *murA* genes of the *A. baumannii* ATCC 17978 strain were amplified and cloned into the pEXP5-CT/TOPO bacterial expression vector (Invitrogen, Carlsbad, CA, USA). Following the protocols of the Expressway Cell-Free *E. coli* Expression System (Invitrogen), with some modifications, LpxB and MurA proteins were synthesized together using the pEXP5-CT/TOPO-*lpxB* and pEXP5-CT/TOPO-*murA* vectors with the C-terminal polyhistidine tag (HHHHHH-COOH). Reactions were incubated at 37°C with shaking (300 rpm) and 15 μL aliquots were collected at 5, 15, 25 and 45 min. pPNA (5 μM) targeted at *lpxB* was added to the reactions to demonstrate specific inhibition of LpxB translation. Aliquots with total proteins were separated on 12% SDS-PAGE gel and transferred onto polyvinylidene difluoride (PVDF) membranes to be resolved by western blotting. Membranes were revealed with Anti-His (C-term)-HRP Antibody (Thermo Fisher), using the Amersham Imager-600 system (GE Healthcare, Chicago, IL, USA).

Inhibition of A. baumannii growth by antisense pPNAs

Time–kill analysis was used to measure the *in vitro* bactericidal activity of anti-*lpxB*, anti-*murA* and anti-*hisF* pPNAs, as described previously with some modifications.[33] Strains were grown overnight and ~1×10^6 cfu/mL were inoculated into LB or M9 medium. Bacteria were grown in 96-well microplates at 37°C with shaking, using the Epoch-2 Microplate Spectrophotometer (BioTek Instruments, Winooski, VT, USA). pPNAs were added at concentrations of 2.5, 5 and 35 μM. The number of cfu was

determined at 1, 3, 6, 24 and 48 h by plating onto LB agar plates and incubating at 37°C for 24 h.

Infection of A549 monolayers

The viability of infected A549 human alveolar epithelial cells in the presence or absence of pPNA was compared. Cell monolayers (2×10^4 cells/well) were infected with 11×10^6 cfu/well of *A. baumannii* strain ATCC 17978 at an moi of 550 for 30 h in glucose-free Hank's balanced salt solution (HBSS, Gibco), supplemented with 2.5 μM or 5 μM anti-*lpxB* pPNA. The same protocol was followed in the absence of pPNA and in the presence of an inactivated ATCC 17978 strain, which was incubated for 3 h in 4% paraformaldehyde, washed with saline solution by centrifugation, then used as a toxicity control of pPNA. The viability of the infected cells was examined with the Cell Counting Kit-8 (CCK-8, Sigma–Aldrich), following the manufacturer's instructions.

Susceptibility testing of colistin and pPNA

The combination of anti-*lpxB* pPNA and colistin (Sigma–Aldrich) was tested against different *A. baumannii* strains, with and without lipid A modifications mediated by mutations in the *pmrB* gene.[34] The strain types and clinical strains used, as well as their previously characterized mechanisms of colistin resistance, are listed in Table 1. Colistin MICs were determined by broth microdilution, following CLSI criteria.[35] The activity of the pPNA in combination with colistin was assessed by chequerboard assay in LB and M9 media.[36,37] After 20 h of incubation, 10 μL of alamarBlue reagent (Thermo Fisher) was added to all wells and incubated for 4 h at 37°C to identify wells containing viable bacteria. The FIC index (FIC_{index}) was calculated as follows: $FIC_{index} = FIC_{COL} + FIC_{pPNA} = MIC[COL_{pPNA}]/[COL] + MIC[pPNA_{COL}]/[pPNA]$. FIC data were interpreted as follows: $FIC_{index} \leq 0.5$, synergy; $FIC_{index} > 0.5$ to 4, no interaction; and $FIC_{index} > 4$, antagonism. The MIC values for anti-*murA* pPNA in both growth media were also tested for all *A. baumannii* strains listed in Table 1.

Galleria mellonella virulence assay

The efficacy of the anti-*lpxB* pPNA treatment was tested in a *G. mellonella* survival assay. Caterpillars were obtained from BioSystems Technology (Exeter, UK). *A. baumannii* strain ATCC 17978 was grown to an OD_{600} of 0.7, collected by centrifugation and resuspended in sterile PBS. *G. mellonella* survival assays were performed by injecting groups of 15 larvae with 10 μL of suspension containing ~3×10^3 cfu/larva as bacterial inoculum, as previously described.[32,38] Treatments were injected 1 h post-infection. Treatments evaluated were: colistin (2 mg/kg), anti-*lpxB* pPNA (75 mg/kg) and a combination of colistin (2 mg/kg) and anti-*lpxB* pPNA (75 mg/kg). A group of larvae injected with 10 μL of sterile PBS was included as control. Treatments using lower anti-*lpxB* pPNA concentrations (25 and 50 mg/kg) were also tested. After inoculation, the larvae were incubated at 37°C in the dark and death was assessed over 4 days.

Statistical significance

At least three independent replicates were done for each assay. Student's *t*-tests were performed to evaluate the statistical significance of observed differences, except in the survival assays, where survival curves were plotted using the Kaplan–Meier method and analysed using the log-rank (Mantel–Cox) test.[39] *P* values of ≤0.05 were considered statistically significant.

Results

Transcriptomic analysis revealed increased expression of the lpxB gene

A collection of genes found by RNA-seq analysis in an experimental murine pneumonia model were differentially expressed compared with genes detected in bacteria grown in artificial conditions (LB medium). The raw data obtained were deposited in the GEO database under the accession code GSE100552. The *lpxB* gene increased its expression 3.63-fold in the course of murine pneumonia relative to *in vitro* conditions.

An attempt was made to construct an isogenic mutant lacking the *lpxB* gene derived from the ATCC 17978 strain. All attempts to obtain a viable Δ*lpxB* mutant yielded negative results, thus supporting that modification of lipid X by LpxB to form disaccharide-1-phosphate is essential for bacterial viability.

Inhibition of LpxB expression by anti-lpxB pPNA

Expression cloning of LpxB and MurA into the pEXP5-CT/TOPO-*lpxB* and pEXP5-CT/TOPO-*murA* vectors using the cell-free *E. coli* expression system showed two clearly visible bands in western blot, at 44 and 53 kDa, respectively (Figure 2). When anti-*lpxB* pPNA was added to the reaction, significant inhibition of LpxB expression was shown. No expression of LpxB was observed at 5 or 15 min of reaction and only 5%–10% of expression was observed at 25 and 45 min compared with MurA protein expression.

Antibacterial effect of anti-lpxB pPNA

To determine whether the presence of a pPNA affects bacterial growth, time–kill curves were performed in LB or M9 media. Different behaviours were observed, depending on the culture medium. In LB medium, the addition of 2.5 or 5 μM anti-*lpxB* pPNA led to a 1 $\log_{10}$ cfu/mL decrease after 24 h, compared with cultures grown in the absence of pPNA, and the antimicrobial effect increased at 48 h (Figure 3). Anti-*murA* pPNA showed lower antimicrobial activity and the negative anti-*hisF* control did not show growth inhibition. Remarkably, when a high concentration of pPNA (35 μM) was added to the LB, antimicrobial activity increased significantly and 6.1 and 5 $\log_{10}$ cfu/mL decreases were observed at 6 h in the presence of the anti-*lpxB* and anti-*murA* pPNAs, respectively. At a concentration of 35 μM, the anti-*lpxB* pPNA showed bactericidal activity, defined as a reduction of 99.9% (≥3 $\log_{10}$) of the total number of cfu/mL in the original inoculum.[40] The anti-*hisF* pPNA, used as a negative control, showed no antimicrobial activity at 2.5 and 5 μM, but showed slight antimicrobial activity at 35 μM. This was probably due to the high concentration of antimicrobial peptide, which can show moderate non-specific CPP-related toxicity, as previously described.[41]

Interestingly, the antimicrobial activity of the anti-*lpxB* and anti-*murA* pPNAs increased in M9 minimal medium compared with LB (Figure 4). Indeed, 2.5 μM anti-*lpxB* pPNA showed a strong bactericidal effect, with no viable bacteria remaining at 24 h (an ~7.5 $\log_{10}$ decrease in the bacterial population). Similar results were obtained when 5 μM anti-*lpxB* pPNA was used, with the complete absence of viable bacteria at 3 h. The anti-*murA* pPNA

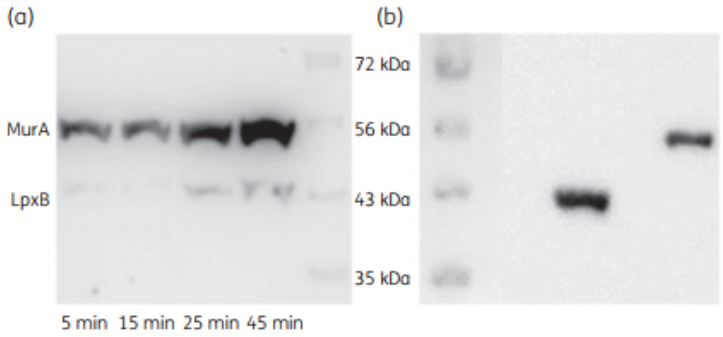

Figure 2. LpxB inhibition assay by anti-*lpxB* pPNA. (a) Western blot showing MurA and LpxB expression. Anti-*lpxB* pPNA 5 μM was added to the reaction. Aliquots of 15 μL were taken at 5, 15, 25 and 45 min. (b) Protein expression controls. Western blot of LpxB and MurA proteins in different reactions without antisense molecules. Aliquots of 15 μL were taken at 25 min.

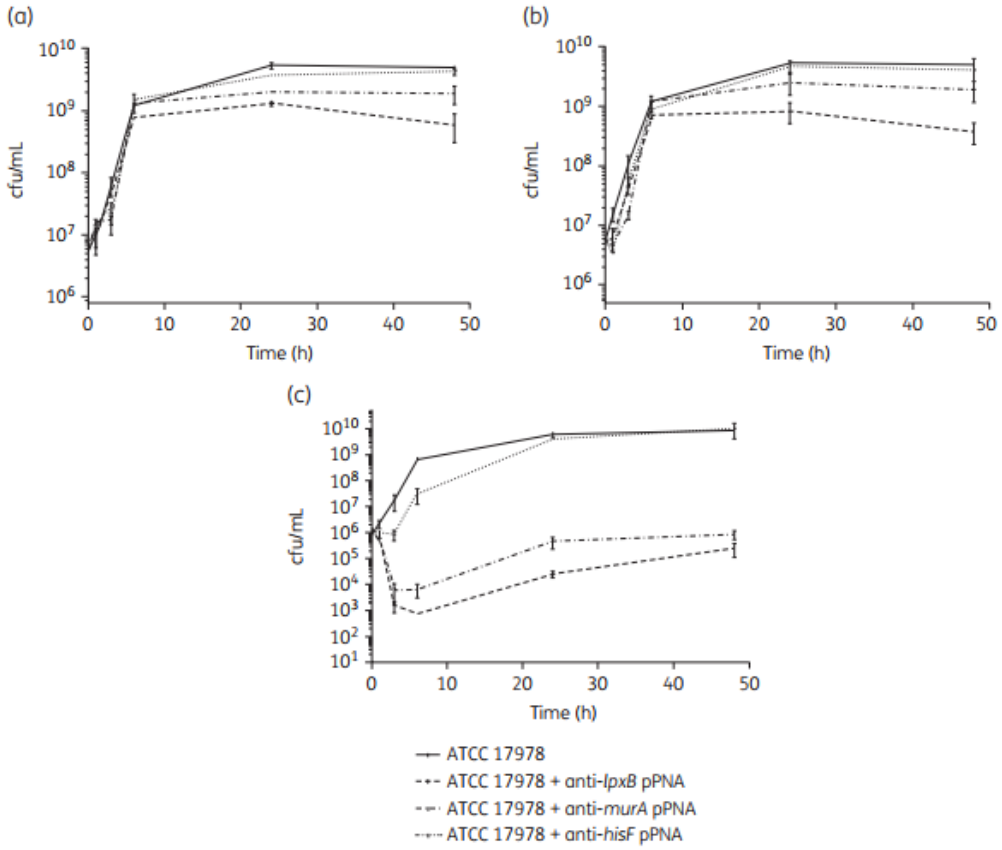

Figure 3. Antimicrobial activity of pPNAs in LB medium. Antisense molecules were added at (a) 2.5 μM, (b) 5 μM and (c) 35 μM.

showed lower antimicrobial activity, decreasing by ~3.1 and 4.6 $\log_{10}$ cfu/mL in the presence of 2.5 μM and 5 μM pPNA, respectively. At 2.5 μM, anti-*hisF* pPNA barely affected bacterial growth and at 5 μM, the bacterial population was reduced by only 1.1 $\log_{10}$. Time–kill curves performed in M9 with anti-*lpxB* pPNA at concentrations higher than 5 μM showed similar results (data not shown). Growth inhibition was dose-dependent in both media tested.

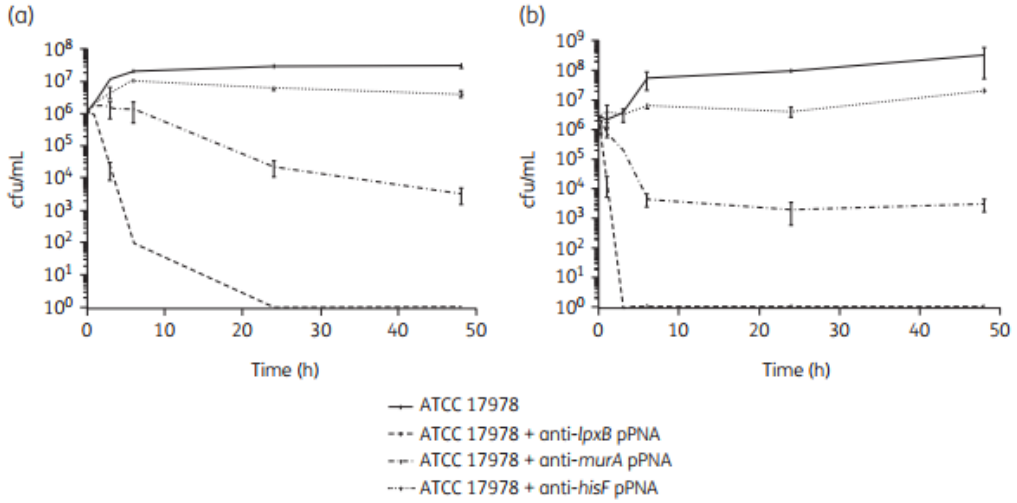

Figure 4. Antimicrobial activity of pPNAs in M9 minimal medium. Antisense molecules were added at (a) 2.5 μM and (b) 5 μM.

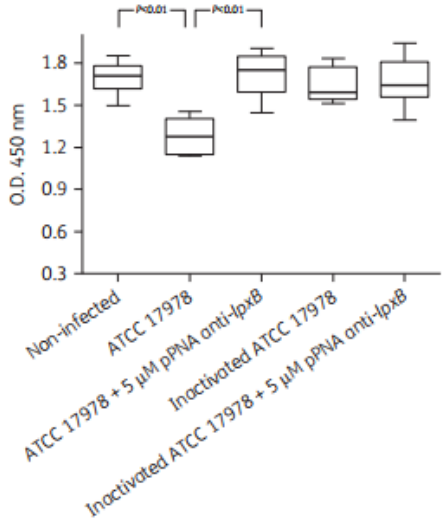

Figure 5. Infection of A549 human epithelial cells with *A. baumannii* ATCC 17978 and treatment with anti-*lpxB* pPNA. The *x*-axis represents the survival rate of: (i) uninfected A549 cells; (ii) infected and untreated A549 cells; (iii) infected A549 cells treated with 5 μM pPNA. The last two conditions (iv and v) indicate the lack of toxicity of the pPNA for A549 alveolar cells using inactivated *A. baumannii* in the absence and presence of 5 μM pPNA.

Anti-lpxB pPNA treatment of A549 human alveolar epithelial cells infected with A. baumannii

A549 alveolar cells were infected with *A. baumannii* ATCC 17978 and 5 μM pPNA was immediately added to the glucose-free HBSS medium. As shown in Figure 5, untreated *A. baumannii* infection led to a 27% decrease in survival in the human A549 cells compared with the uninfected cells ($P<0.01$). However, when anti-*lpxB* pPNA was added, the survival rate of infected A549 cells was the same as the cells without infection and showed significant differences compared with the infected but untreated group ($P<0.01$). pPNA-related toxicity was not observed in the A549 cells when 5 μM anti-*lpxB* pPNA was used in the presence of inactivated *A. baumannii*. pPNA concentrations lower than 2.5 μM were also used, but with no improvement in epithelial cell survival.

Synergy between colistin and pPNAs

The MICs of anti-*lpxB* pPNA, colistin and the two agents in combination were studied in a collection of colistin-susceptible and colistin-resistant *A. baumannii* strains in LB and M9. The results are shown in Table 1, Table S1 and Figure S1 (both available as Supplementary data at *JAC* Online). The MICs of colistin showed concordance with those previously published.[42,43] The MICs of colistin-susceptible and colistin-resistant strains were 0.5–2 mg/L and 32–128 mg/L, respectively, in both media. Importantly, the MICs of anti-*lpxB* pPNA in LB and M9 were 20 μM and 2.5 μM, respectively, for all strains. With respect to the anti-*murA* pPNA, the MICs of the anti-*murA* pPNA were 20 to ≥80 μM in LB medium and 2.5–10 μM in M9 medium.

Similar results were obtained in the two culture media by the chequerboard method, as shown in Table 1. Colistin and anti-*lpxB* pPNA showed clear synergy against all colistin-susceptible strains. Conversely, no synergy (no interaction) was observed against colistin-resistant strains; although in LB the colistin-resistant strains ATCC 19606 *pmrB* and ABRIM *pmrB* decreased the MICs of anti-*lpxB* pPNA 4- and 16-fold, respectively, in the presence of colistin. Regarding the colistin MICs, the anti-*lpxB* pPNA led to an 8-fold decrease in the MIC of colistin for all colistin-susceptible strains grown in LB, whereas for colistin-resistant strains, the decrease was only 0–2-fold. Similarly, in M9 medium, anti-*lpxB* pPNA lowered the MIC of colistin 4–16-fold for colistin-susceptible strains and 0–2-fold for colistin-resistant strains.

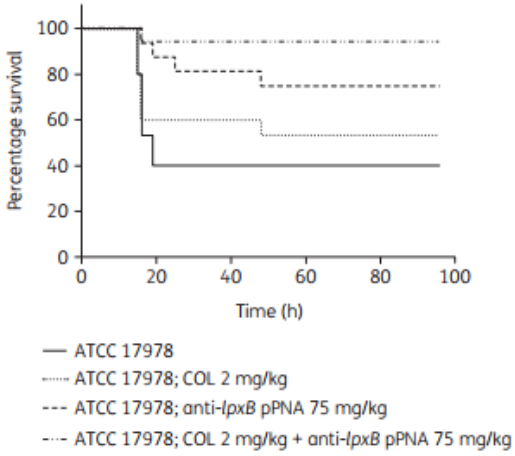

Figure 6. Survival of *G. mellonella* larvae (n=15 per group) following infection with *A. baumannii* strain ATCC 17978 and treatment with colistin and anti-*lpxB* pPNA. A 75 mg/kg concentration of anti-*lpxB* pPNA corresponds to 15 μM.

G. mellonella combined treatment

The efficacy of anti-*lpxB* pPNA, alone and in combination with colistin, was tested in a *G. mellonella* virulence assay, as shown in Figure 6. The survival rate in infected but not treated *G. mellonella* was 40%, while the survival of those treated with colistin was 60%. Interestingly, the survival rate following treatment with 75 mg/kg of anti-*lpxB* pPNA was 75%, higher than that of colistin monotherapy (P<0.03). Nevertheless, the best results were obtained with the combination therapy of anti-*lpxB* pPNA and colistin, showing a survival rate of 95% of the caterpillars (P<0.001). When lower concentrations of anti-*lpxB* pPNA were tested (25 and 50 mg/kg), statistical differences were either not observed or were lower. No mortality was observed in the control group of larvae injected with sterile PBS.

Discussion

The emergence of bacterial resistance and the scarce arsenal of antimicrobials available have led to an urgent need to design alternative strategies to combat infections caused by MDR pathogens. One approach as a potential novel therapy against resistant pathogens is the use of antisense molecules such as PNAs, BNAs and PMOs, which have shown promising results and could, in time, become a new medical weapon against MDR bacteria.[6] Given the significant problem of MDR *A. baumannii* and the potential benefits of pPNAs, we think that greater effort and attention should be paid to the development of these new antibacterial agents. In recent years, studies have investigated oligomers that target essential bacterial genes conjugated to carrier peptides for delivery.[44–46] In the present study, the cell-penetrating peptide $(KFF)_3K$ was covalently conjugated to PNAs to facilitate the intracellular delivery of the antisense molecule into *A. baumannii* and to induce damage by disorganization of the outer membrane.[15] These peptides did not show toxicity in animal assays[47] and, at concentrations up to 64 μM, the $(KFF)_3K$ peptide was not toxic to mammalian cells.[48]

In the battle against bacterial multiresistance, a description of new bacterial targets is also needed for the development of novel antimicrobial strategies. Transcriptomic analysis revealed that the *lpxB* gene was overexpressed in *A. baumannii* during lung infection. Our attempts to construct an *A. baumannii lpxB* mutant strain were unsuccessful, suggesting that it is involved in key metabolic steps. Both our group and others have previously described the relevance of *lpx* genes (*lpxA*, *lpxC* and *lpxD*) to the maintenance of LPS structure, fitness and virulence of *A. baumannii*[43,49,50] and LpxC inhibitors have also been developed.[51] These issues encourage us therefore to further investigate LpxB as a new bacterial target. Antisense inhibition has also been studied and compared with a second target, MurA. This key protein was already included as a possible target in earlier studies of antisense PNA inhibition. Different anti-*murA* PNA sequences conjugated to $(KFF)_3K$ were tested against *E. coli*, *K. pneumoniae* and *Salmonella enterica* serotype Typhimurium and some of the antisense molecules showed promising MIC values (1.2–3.2 μM).[29,45] In this study, we took essential target genes such as *murA* and *lpxB*, whose silencing led to the inhibition of bacterial growth.

Importantly, inhibition of LpxB expression resulted in better antibacterial activity than MurA inhibition, showing the high potential of LpxB as a new target. The use of anti-*lpxB* pPNA specifically reduces expression of LpxB, as was demonstrated by western blot assays where MurA inhibition was not observed, showing that bacterial death is exclusively due to LpxB inhibition. Western blotting detected slight LpxB expression at 25 and 45 min. This was probably due to the design of the expression system, which exponentially increased the amount of target mRNA and maximized the yield of synthesized proteins, so preventing total inhibition of mRNA translation by the anti-*lpxB* pPNA.

Time–kill curves to determine the bactericidal activity of anti-*lpxB* pPNA against the ATCC 17978 strain showed that the anti-*lpxB* antisense molecule presented a bactericidal effect at 35 μM in LB, with an ~3 $\log_{10}$ decrease in the initial inoculum at 6 h and likewise at 2.5 μM in M9 media. These results correlate with the MIC assays, which showed anti-*lpxB* pPNA growth inhibition at 20 μM and 2.5 μM in LB and M9, respectively (Table 1). The anti-*murA* pPNA showed a lower bactericidal effect in time–kill curves against the ATCC 17978 strain, with an ~2 $\log_{10}$ decrease in the initial inoculum at 35 μM in LB and at 2.5 or 5 μM in M9 medium. The results obtained with the anti-*murA* pPNA also correlate with the MICs obtained, which were 40 μM in LB and 5 μM in M9 (Table S1). So, although anti-*murA* pPNA presented a bacteriostatic effect at these concentrations, its bactericidal activity was lower than that of anti-*lpxB* pPNA.

In time–kill curves and MIC assays, the anti-*murA* and anti-*lpxB* pPNAs both showed higher antimicrobial activity in the M9 medium than in LB. This increased activity in M9 is probably related to the lower bacterial growth rate due to lack of nutrients. The lower growth rate can be observed in the ATCC 17978 strain in the absence of pPNAs (used as control) grown in M9 medium (Figure 4) rather than in LB (Figure 3) in the first hours of growth. Lower population densities were also observed in the stationary phase (24–48 h) in M9 medium compared with the LB medium (~1–1.5 log). The lower growth rate and bacterial density could facilitate the entry of the pPNAs and increase their bactericidal activity.

Colistin is an old antibiotic that was recovered as a last-resort antimicrobial alternative for the treatment of MDR pathogens.

The main mechanism of colistin resistance in *A. baumannii* involves phosphoethanolamine modifications that alter the LPS.[34,52] Since this antimicrobial agent presents high toxicity, the lower the dose administered, the fewer the adverse reactions, and a large number of studies are currently developing optimal pharmacokinetic/pharmacodynamic (PK/PD) parameters for treatment.[5] Reducing the colistin dosage would be an excellent way to improve its usefulness. In this study, we tested the synergistic activity of colistin in combination with anti-*lpxB* pPNA. The outer membrane of the bacteria is the first line of defence against PNA penetration.[53] Colistin leads to disruption of the bacterial membrane and pore formation, which promotes uptake into the cell and permits passage of different molecules, so facilitating the entry of the pPNA into the prokaryotic cell.[54] The chequerboard assays confirmed this synergy in colistin-susceptible strains. Nevertheless, although the MICs of both compounds decreased when used alone, no synergy was observed when tested against colistin-resistant *A. baumannii* strains. Here we suggest that the modified lipid A in the colistin-resistant strains[34] could prevent the increase in membrane permeability.

Infected A549 human lung epithelial cells grown as monolayers and *G. mellonella* virulence assays both showed the efficacy of treatment with anti-*lpxB* pPNA against *A. baumannii* infection. The viability of A549 cells treated with anti-*lpxB* pPNA was identical to that of non-infected cells, while the survival rates of caterpillars treated with pPNA or colistin were higher than those of non-infected larvae. The combination of colistin and anti-*lpxB* pPNA, however, showed greater efficacy than the two compounds used as monotherapy. The *in vitro* and *in vivo* results obtained here showed that the combination of colistin and PNA antisense molecules conjugated with small cationic CPPs is a successful strategy to increase the penetration ability of PNAs on their own. In conclusion, our study provides evidence to support the importance of the *lpxB* gene, which increased its expression significantly during murine pneumonia, as an essential gene for *A. baumannii* survival. Furthermore, LpxB expression was inhibited by anti-*lpxB* pPNA, causing bacterial death, which represents a protective effect against infection. Synergy between anti-*lpxB* pPNA and colistin was demonstrated. This is the first study to describe the importance of this gene in *A. baumannii* and it may be considered an interesting therapeutic target for the design of new antimicrobial therapies.

Funding

This study was funded by projects PI15/00860 and PI18/00501 to G.B., CP13/00226 to A.B., and PI14/00059 and PI17/01482 to A.B. and M.P. (Instituto de Salud Carlos III). The study was also funded by project IN607A 2016/22 (GAIN- Agencia Gallega de Innovación - Consellería de Economía, Emprego e Industria) to G.B. Support was also provided by Planes Nacionales de I+D+i 2013–2016 and ISCIII, Subdirección General de Redes y Centros de Investigación Cooperativa, Ministerio de Economía y Competitividad, Spanish Network for Research in Infectious Diseases (REIPI RD16/0016/006) co-financed by European Development Regional Fund 'A way to achieve Europe' and the operative programme Intelligent Growth 2014–2020. J.C.V.U. was financially supported by the Miguel Servet Programme (ISCIII, Spain CP13/00226) and the pFIS Programme (FI18/00315) and M.M.G. was financially supported by a Clara Roy grant (SEIMC) and K.C.P. by IN607A 2016/22.

Transparency declarations

Nothing to declare.

Supplementary data

Table S1 and Figure S1 are available as Supplementary data at *JAC* Online.

References

1 Dijkshoorn L, Nemec A, Seifert H. An increasing threat in hospitals: multidrug-resistant *Acinetobacter baumannii*. *Nat Rev Microbiol* 2007; **5**: 939–51.

2 Peleg AY, Seifert H, Paterson DL. *Acinetobacter baumannii*: emergence of a successful pathogen. *Clin Microbiol Rev* 2008; **21**: 538–82.

3 Magiorakos AP, Srinivasan A, Carey RB *et al*. Multidrug-resistant, extensively drug-resistant and pandrug-resistant bacteria: an international expert proposal for interim standard definitions for acquired resistance. *Clin Microbiol Infect* 2012; **18**: 268–81.

4 Gerson S, Betts JW, Lucaßen K *et al*. Investigation of novel *pmrB* and *eptA* mutations in isogenic *Acinetobacter baumannii* isolates associated with colistin resistance and increased virulence *in vivo*. *Antimicrob Agents Chemother* 2019; **63**: pii=e01586-18.

5 Stein A, Raoult D. Colistin: an antimicrobial for the 21st century? *Clin Infect Dis* 2002; **35**: 901–2.

6 Rasmussen LC, Sperling-Petersen HU, Mortensen KK. Hitting bacteria at the heart of the central dogma: sequence-specific inhibition. *Microb Cell Fact* 2007; **6**: 24.

7 Hegarty JP, Stewart DB. Advances in therapeutic bacterial antisense biotechnology. *Appl Microbiol Biotechnol* 2018; **102**: 1055–65.

8 Soler-Bistué A, Zorreguieta A, Tolmasky ME. Bridged nucleic acids reloaded. *Molecules* 2019; **24**: pii=E2297.

9 Nielsen PE, Egholm M, Berg RH *et al*. Peptide nucleic acids (PNAs): potential antisense and anti-gene agents. *Anticancer Drug Des* 1993; **8**: 53–63.

10 Good L, Awasthi SK, Dryselius R *et al*. Bactericidal antisense effects of peptide-PNA conjugates. *Nat Biotechnol* 2001; **19**: 360–4.

11 Montazersaheb S, Hejazi MS, Nozad Charoudeh H. Potential of peptide nucleic acids in future therapeutic applications. *Adv Pharm Bull* 2018; **8**: 551–63.

12 Nielsen PE, Egholm M, Berg RH *et al*. Sequence-selective recognition of DNA by strand displacement with a thymine-substituted polyamide. *Science* 1991; **254**: 1497–500.

13 Ghosal A. Peptide nucleic acid antisense oligomers open an avenue for developing novel antibacterial molecules. *J Infect Dev Ctries* 2017; **11**: 212–4.

14 Bai H, You Y, Yan H *et al*. Antisense inhibition of gene expression and growth in gram-negative bacteria by cell-penetrating peptide conjugates of peptide nucleic acids targeted to *rpoD* gene. *Biomaterials* 2012; **33**: 659–67.

15 Vaara M, Porro M. Group of peptides that act synergistically with hydrophobic antibiotics against gram-negative enteric bacteria. *Antimicrob Agents Chemother* 1996; **40**: 1801–5.

16 Woodford N, Wareham DW on behalf of the UK Antibacterial Antisense Study Group. Tackling antibiotic resistance: a dose of common antisense? *J Antimicrob Chemother* 2009; **63**: 225–9.

17 Wacheck V, Zangemeister-Wittke U. Antisense molecules for targeted cancer therapy. *Crit Rev Oncol Hematol* 2006; **59**: 65–73.

18 Ghosal A, Nielsen PE. Potent antibacterial antisense peptide-peptide nucleic acid conjugates against *Pseudomonas aeruginosa*. *Nucleic Acid Ther* 2012; **22**: 323–34.

19 Kurupati P, Tan KS, Kumarasinghe G *et al*. Inhibition of gene expression and growth by antisense peptide nucleic acids in a multiresistant

β-lactamase-producing *Klebsiella pneumoniae* strain. *Antimicrob Agents Chemother* 2007; **51**: 805–11.

20 Nekhotiaeva N, Awasthi SK, Nielsen PE *et al.* Inhibition of *Staphylococcus aureus* gene expression and growth using antisense peptide nucleic acids. *Mol Ther* 2004; **10**: 652–9.

21 Wang H, He Y, Xia Y *et al.* Inhibition of gene expression and growth of multidrug-resistant *Acinetobacter baumannii* by antisense peptide nucleic acids. *Mol Biol Rep* 2014; **41**: 7535–41.

22 Lopez C, Arivett BA, Actis LA *et al.* Inhibition of AAC(6')-Ib-mediated resistance to amikacin in *Acinetobacter baumannii* by an antisense peptide-conjugated 2',4'-bridged nucleic acid-NC-DNA hybrid oligomer. *Antimicrob Agents Chemother* 2015; **59**: 5798–803.

23 Soler Bistué AJ, Martín FA, Vozza N *et al.* Inhibition of *aac(6')-Ib*-mediated amikacin resistance by nuclease-resistant external guide sequences in bacteria. *Proc Natl Acad Sci USA* 2009; **106**: 13230–5.

24 Kole R, Krainer AR, Altman S. RNA therapeutics: beyond RNA interference and antisense oligonucleotides. *Nat Rev Drug Discov* 2012; **11**: 125–40.

25 McClorey G, Wood MJ. An overview of the clinical application of antisense oligonucleotides for RNA-targeting therapies. *Curr Opin Pharmacol* 2015; **24**: 52–8.

26 Raetz CR, Whitfield C. Lipopolysaccharide endotoxins. *Annu Rev Biochem* 2002; **71**: 635–700.

27 Bohl TE, Shi K, Lee JK, Aihara H. Crystal structure of lipid A disaccharide synthase LpxB from *Escherichia coli*. *Nat Commun* 2018; **9**: 377.

28 Sonkar A, Shukla H, Shukla R *et al.* UDP-*N*-acetylglucosamine enolpyruvyl transferase (MurA) of *Acinetobacter baumannii* (AbMurA): structural and functional properties. *Int J Biol Macromol* 2017; **97**: 106–14.

29 Goh S, Boberek JM, Nakashima N *et al.* Concurrent growth rate and transcript analyses reveal essential gene stringency in *Escherichia coli*. *PLoS One* 2009; **4**: e6061.

30 Rieder G, Merrick MJ, Castorph H *et al.* Function of *hisF* and *hisH* gene products in histidine biosynthesis. *J Biol Chem* 1994; **269**: 14386–90.

31 Martínez-Guitián M, Vázquez Ucha JC, Álvarez-Fraga L *et al.* Involvement of HisF in the persistence of *Acinetobacter baumannii* during a pneumonia infection. *Front Cell Infect Microbiol* 2019; **9**: 310.

32 Álvarez-Fraga L, Vázquez-Ucha JC, Martínez-Guitián M *et al.* Pneumonia infection in mice reveals the involvement of the *feoA* gene in the pathogenesis of *Acinetobacter baumannii*. *Virulence* 2018; **9**: 496–509.

33 Beceiro A, López-Rojas R, Domínguez-Herrera J *et al.* *In vitro* activity and *in vivo* efficacy of clavulanic acid against *Acinetobacter baumannii*. *Antimicrob Agents Chemother* 2009; **53**: 4298–304.

34 Beceiro A, Llobet E, Aranda J *et al.* Phosphoethanolamine modification of lipid A in colistin-resistant variants of *Acinetobacter baumannii* mediated by the *pmrAB* two-component regulatory system. *Antimicrob Agents Chemother* 2011; **55**: 3370–9.

35 CLSI. *Performance Standards for Antimicrobial Susceptibility Testing—Ninth Edition: M07*. 2012.

36 Hsieh MH, Yu CM, Yu VL *et al.* Synergy assessed by checkerboard. A critical analysis. *Diagn Microbiol Infect Dis* 1993; **16**: 343–9.

37 Odds FC. Synergy, antagonism, and what the chequerboard puts between them. *J Antimicrob Chemother* 2003; **52**: 1.

38 Hornsey M, Longshaw C, Phee L *et al.* *In vitro* activity of telavancin in combination with colistin versus Gram-negative bacterial pathogens. *Antimicrob Agents Chemother* 2012; **56**: 3080–5.

39 Kaplan EL, Meier P. Nonparametric estimation from incomplete observations. *J Am Stat Assoc* 1958; **53**: 457–81.

40 Silva F, Lourenço O, Queiroz JA *et al.* Bacteriostatic versus bactericidal activity of ciprofloxacin in *Escherichia coli* assessed by flow cytometry using a novel far-red dye. *J Antibiot* 2011; **64**: 321–5.

41 Patenge N, Pappesch R, Krawack F *et al.* Inhibition of growth and gene expression by PNA-peptide conjugates in *Streptococcus pyogenes*. *Mol Ther Nucleic Acids* 2013; **2**: e132.

42 Poumaras S, Poulou A, Dafopoulou K *et al.* Growth retardation, reduced invasiveness, and impaired colistin-mediated cell death associated with colistin resistance development in *Acinetobacter baumannii*. *Antimicrob Agents Chemother* 2014; **58**: 828–32.

43 Beceiro A, Moreno A, Fernández N *et al.* Biological cost of different mechanisms of colistin resistance and their impact on virulence in *Acinetobacter baumannii*. *Antimicrob Agents Chemother* 2014; **58**: 518–26.

44 Hansen AM, Bonke G, Larsen CJ *et al.* Antibacterial peptide nucleic acid-antimicrobial peptide (PNA-AMP) conjugates: antisense targeting of fatty acid biosynthesis. *Bioconjug Chem* 2016; **27**: 863–7.

45 Mondhe M, Chessher A, Goh S *et al.* Species-selective killing of bacteria by antimicrobial peptide-PNAs. *PLoS One* 2014; **9**: e89082.

46 Mellbye BL, Weller DD, Hassinger JN *et al.* Cationic phosphorodiamidate morpholino oligomers efficiently prevent growth of *Escherichia coli in vitro* and *in vivo*. *J Antimicrob Chemother* 2010; **65**: 98–106.

47 Rustici A, Velucchi M, Faggioni R *et al.* Molecular mapping and detoxification of the lipid A binding site by synthetic peptides. *Science* 1993; **259**: 361–5.

48 Mohamed MF, Hammac GK, Guptill L *et al.* Antibacterial activity of novel cationic peptides against clinical isolates of multi-drug resistant *Staphylococcus pseudintermedius* from infected dogs. *PLoS One* 2014; **9**: e116259.

49 Carretero-Ledesma M, García-Quintanilla M, Martín-Peña R *et al.* Phenotypic changes associated with colistin resistance due to lipopolysaccharide loss in *Acinetobacter baumannii*. *Virulence* 2018; **9**: 930–42.

50 Moffatt JH, Harper M, Harrison P *et al.* Colistin resistance in *Acinetobacter baumannii* is mediated by complete loss of lipopolysaccharide production. *Antimicrob Agents Chemother* 2010; **54**: 4971–7.

51 Lin L, Tan B, Pantapalangkoor P *et al.* Inhibition of LpxC protects mice from resistant *Acinetobacter baumannii* by modulating inflammation and enhancing phagocytosis. *MBio* 2012; **3**: pii=e00312-12.

52 Adams MD, Nickel GC, Bajaksouzian S *et al.* Resistance to colistin in *Acinetobacter baumannii* associated with mutations in the PmrAB two-component system. *Antimicrob Agents Chemother* 2009; **53**: 3628–34.

53 Good L, Sandberg R, Larsson O *et al.* Antisense PNA effects in *Escherichia coli* are limited by the outer-membrane LPS layer. *Microbiology* 2000; **146**: 2665–70.

54 Hancock RE. Peptide antibiotics. *Lancet* 1997; **349**: 418–22.

55 Bou G, Oliver A, Martínez-Beltrán J. OXA-24, a novel class D β-lactamase with carbapenemase activity in an *Acinetobacter baumannii* clinical strain. *Antimicrob Agents Chemother* 2000; **44**: 1556–61.

Material suplementario del artículo publicado.

Table S1. MICs (mg/L) a of *A. baumannii* strains to anti-*murA* and anti-*hisF* pPNAs.

***A. baumannii* strains**	**anti-*hisF* pPNA**		**anti-*murA pPNA***	
	LB medium	**M9 medium**	**LB medium**	**M9 medium**
ATCC 17978	≥400 (≥80)	≥400 (≥80)	230 (40)	28.7 (5)
ATCC 19606	≥400 (≥80)	≥400 (≥80)	115 (20)	28.7 (5)
ATCC 19606 *pmrB*	≥400 (≥80)	≥400 (≥80)	460 (≥80)	28.7 (5)
ABRIM	≥400 (≥80)	≥400 (≥80)	115 (20)	57.5 (10)
ABRIM *pmrB*	≥400 (≥80)	≥400 (≥80)	460 (≥80)	57.5 (10)
AB248	≥400 (≥80)	≥400 (≥80)	115 (20)	14.4 (2.5)
AB249 *pmrB*	≥400 (≥80)	≥400 (≥80)	460 (≥80)	14.4 (2.5)

[a]pPNA MICs values in brackets are expressed in µM.

Figure S1. Assessment of synergy between colistin and anti-*lpxB* pPNA. Checkerboard assays using colistin and anti-*lpxB* pPNA on cultures of ATCC 17978, ATCC 19606, ABRIM, and AB248 strains (colistin-susceptible strains). Pink wells indicate growth and blue wells indicate growth inhibition in a) LB medium and b) M9 medium.

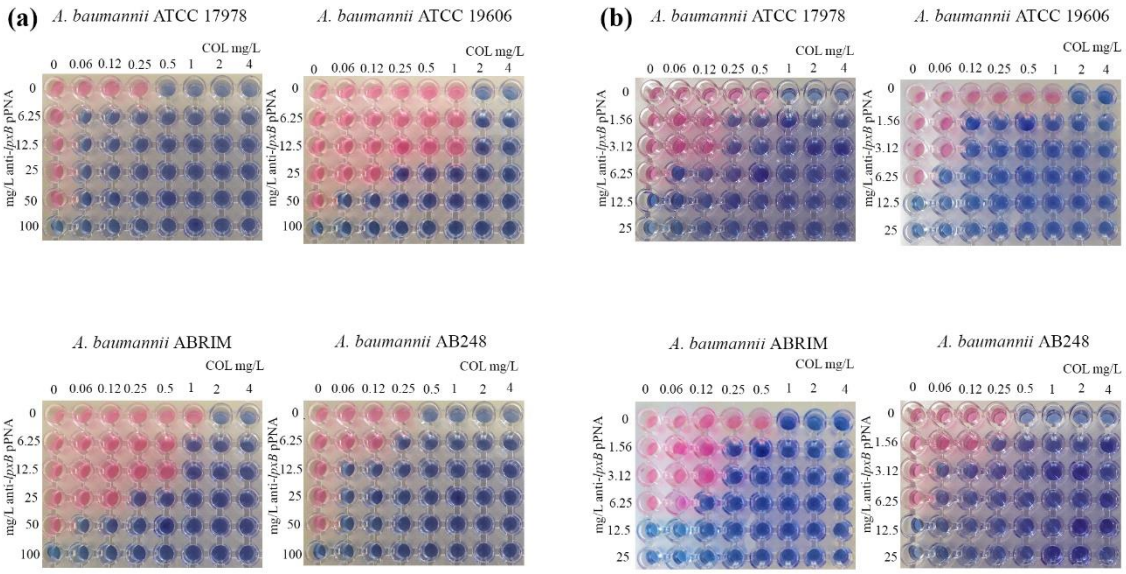

Capítulo IV. La sinergia entre la colistina y el inhibidor de la proteasa del péptido señal de tipo I MD3 es dependiente del mecanismo de resistencia a colistina en *Acinetobacter baumannii*.

Resumen.

La colistina es un antibiótico de última opción terapéutica en el tratamiento de *A. baumannii* MDR, debido a su elevada toxicidad. El diseño de nuevos compuestos que presenten sinergia con la colistina permitiría reducir la dosis de dicho antibiótico y, por tanto, la recuperación del mismo en terapias antimicrobianas.

La colistina es un péptido antimicrobiano policatiónico cuya diana es el lipopolisacárido bacteriano polianiónico. Hasta el momento se han estudiado dos mecanismos de resistencia a colistina en *A. baumannii*. El primero consiste en la pérdida total del LPS mediante la inactivación de la ruta de biosíntesis del lípido A. Mutaciones en cualquiera de los tres primeros genes implicados en esta ruta (*lpxA*, *lpxC* y *lpxD*) previenen la interacción con la colistina y dan lugar a una resistencia de alto nivel. Un segundo mecanismo, previamente estudiado por nuestro grupo, implica mutaciones y aumento de la expresión de los genes *pmrAB*. Esto da lugar a la adición de residuos de fosfoetanolamina al lípido A, lo que disminuye la carga negativa del LPS.

En este cuarto y último capítulo de esta Tesis Doctoral evaluamos los efectos sinérgicos de la colistina con una β-aminocetona sintética denominada MD3. Este compuesto es un inhibidor de la proteasa del péptido señal de tipo I. Estos enzimas bacterianos están implicados en la maduración de proteínas a través de la separación del péptido de señalización amino-terminal de las proteínas traslocadas. La permeabilización de la membrana externa permite un acceso más eficiente de MD3 a las SPasas localizadas en el citoplasma.

Se realizaron ensayos de *checkerboard* y curvas de crecimiento en distintas cepas de *A. baumannii*, entre las cuales, se incluyen cepas sensibles y resistentes a colistina, cepas

tipo y aislamientos clínicos. Estos ensayos confirmaron la sinergia entre ambos compuestos en función del mecanismo de resistencia a colistina que presente la bacteria.

Este trabajo se recoge en la publicación Martínez-Guitián M., Vázquez-Ucha J.C., Odingo J., Parish T., Poza M., Waite R.D., Bou G., Wareham D.W., Beceiro A. (2016) Synergy between colistin and the signal peptidase inhibitor MD3 is dependent on the mechanism of colistin resistance in *Acinetobacter baumannii*. Antimicrob. Agents Chemother. 60:4375–4379. doi:10.1128/AAC.00510-16, adjuntada a continación.

Artículo publicado.

AMERICAN SOCIETY FOR MICROBIOLOGY | Antimicrobial Agents and Chemotherapy

Synergy between Colistin and the Signal Peptidase Inhibitor MD3 Is Dependent on the Mechanism of Colistin Resistance in *Acinetobacter baumannii*

Marta Martínez-Guitián,[a] Juan C. Vázquez-Ucha,[a] Joshua Odingo,[b] Tanya Parish,[b] Margarita Poza,[a] Richard D. Waite,[c] German Bou,[a] David W. Wareham,[c] Alejandro Beceiro[a]

Servicio de Microbiología-Instituto de Investigación Biomédica (INIBIC), Coruña, Spain[a]; TB Discovery Research, Infectious Disease Research Institute, Seattle, Washington, USA[b]; Antimicrobial Research Group, Barts & The London School of Medicine and Dentistry, Queen Mary University of London, London, United Kingdom[c]

Synergy between colistin and the signal peptidase inhibitor MD3 was tested against isogenic mutants and clinical pairs of *Acinetobacter baumannii* isolates. Checkerboard assays and growth curves showed synergy against both colistin-susceptible strains (fractional inhibitory concentration index [FIC_{index}] = 0.13 to 0.24) and colistin-resistant strains with mutations in *pmrB* and phosphoethanolamine modification of lipid A (FIC_{index} = 0.14 to 0.25) but not against colistin-resistant Δ*lpx* strains with loss of lipopolysaccharide (FIC_{index} = 0.75 to 1). A colistin/MD3 combination would need to be targeted to strains with specific colistin resistance mechanisms.

Acinetobacter baumannii is an important nosocomial pathogen that is able to acquire or develop resistance to multiple antibiotics (1). The frequency of multidrug-resistant (MDR) clinical isolates has increased in recent years. One of "agents of last resort" with activity against *A. baumannii* MDR strains is colistin (COL) (polymyxin E) (2), a polycationic antimicrobial peptide which targets the polyanionic bacterial lipopolysaccharide (LPS) (3). Two mechanisms of resistance to colistin are the most studied in *A. baumannii* (4, 5). One involves the total loss of LPS by means of inactivation of the lipid A biosynthetic pathway. Mutations in any of the first three genes involved in lipid A biosynthesis (*lpxA*, *lpxC*, and *lpxD*) prevent interaction with colistin and result in high-level resistance (6). A second mechanism, previously studied by our group, involves mutations and increased expression of *pmrAB* genes. These result in the addition of phosphoethanolamine residues to lipid A, which decreases the negative charge displayed on the LPS (7, 8). Colistin resistance is concerning; with no new commercial antimicrobials available for use against MDR isolates, there is an urgent need to develop compounds to address this clinical issue (9, 10).

Recently, enhanced antimicrobial activity of colistin in combination with a synthetic β-aminoketone, MD3 [1-(2,5-dichlorophenyl)-3-(dimethylamino)propan-1-one], an inhibitor of bacterial type I signal peptidases (SPases), was described. It was demonstrated that SPase inhibition by MD3 in combination with outer membrane permeabilizing agents (colistin or sodium hexametaphosphate [NaHMP]) was increased in *A. baumannii* and other species (11). Bacterial SPases are involved in the maturation of proteins through cleavage of the amino-terminal signal peptides of translocated proteins (12). Permeabilization of the outer membrane should enable more-efficient access of MD3 to cytoplasm-located SPases. The aim of the present study was therefore to evaluate the synergistic effects of the combination of MD3 and colistin against strains of *A. baumannii* harboring well-characterized mechanisms of colistin resistance.

The combination of MD3 and colistin (COL) was tested against *A. baumannii* strains with deficits in LPS biosynthesis (inactivating mutations in *lpx* genes) and strains with lipid A modifications (mutations in *pmrB*). The bacterial strains used were the antibiotic-susceptible *A. baumannii* ATCC 19606 type strain and isogenically derived colistin-resistant (Col^r) mutants ATCC 19606Δ*lpxA*, ATCC 19606Δ*lpxC*, ATCC 19606Δ*lpxD* (6), and ATCC 19606*pmrB* (7). Also tested were the MDR but colistin-susceptible (Col^s) clinical isolate *A. baumannii* ABRIM (13) and its derived Col^r ABRIM*pmrB* mutant (7). Finally, two pairs of Col^s/Col^r *A. baumannii* isolates, AB248/AB249*pmrB* and AB299/AB347*pmrB*, recovered consecutively from two intensive-care units (ICU) patients before and after colistin therapy, were studied (14). Molecular mechanisms of colistin resistance in each of these strains have been extensively characterized previously (Table 1). The MICs of COL and MD3 were determined by broth microdilution following CLSI criteria (15). Colistin MICs were also confirmed by Etest (bioMérieux, France) in the presence of 1 to 4 mg/liter of MD3. The activity of COL in combination with MD3 was assessed in checkerboard assays (16, 17). After 20 h of incubation, 10-μl volumes of alamarBlue reagent (Thermo-Scientific, USA) were added to all wells to identify those containing viable bacteria. The fractional inhibitory concentration index (FIC_{index}) was calculated as follows: $FIC_{index} = FIC_{COL} + FIC_{MD3}$ = MIC [COL_{MD3}]/[COL] + MIC [$MD3_{COL}$]/[MD3]. The FIC data were interpreted as follows: FIC_{index} = ≤0.5, synergy; FIC_{index} = >0.5 to 4, no interaction (17). The MD3 compound was obtained from the Infectious Disease Research Institute of Seattle (USA).

Growth curve analyses were performed using COL and MD3 at

Received 8 March 2016 Returned for modification 3 April 2016
Accepted 24 April 2016
Accepted manuscript posted online 2 May 2016
Citation Martínez-Guitián M, Vázquez-Ucha JC, Odingo J, Parish T, Poza M, Waite RD, Bou G, Wareham DW, Beceiro A. 2016. Synergy between colistin and the signal peptidase inhibitor MD3 is dependent on the mechanism of colistin resistance in *Acinetobacter baumannii*. Antimicrob Agents Chemother 60:4375–4379. doi:10.1128/AAC.00510-16.
Address correspondence to Alejandro Beceiro, alejandro.beceiro.casas@sergas.es.

TABLE 1 Descriptions of bacterial strains and MICs of colistin and MD3 alone and in combination[a]

A. baumannii strain	MIC (mg/liter)				FIC_{index}	Description	Source or reference
	Colistin	MD3	COL_{MD3}	$MD3_{COL}$			
ATCC 19606	0.5	32	0.06	2	Synergy	*A. baumannii* type strain	ATCC
ATCC 19606*pmrB*	64	16	0.5	4	Synergy	Isogenic derivative mutant of ATCC 19606; single amino acid substitution (Ala227Val) in PmrB	7
ATCC 19606Δ*lpxA*	64	2	16	1	No interaction	Isogenic derivative mutant of ATCC 19606; 445-bp deletion at nucleotide 364 within the *lpxA* gene and frameshift after H121	6
ATCC 19606Δ*lpxC*	128	2	64	1	No interaction	Isogenic derivative mutant of ATCC 19606; 84-bp deletion within the *lpxC* gene	6
ATCC 19606Δ*lpxD*	2,056	2	1,028	1	No interaction	Isogenic derivative mutant of ATCC 19606; single-base deletion at nucleotide 364 of the *lpxD* gene and frameshift after K317	6
ABRIM	0.5	32	0.06	4	Synergy	*A. baumannii* clinical isolate	13
ABRIM*pmrB*	32	8	0.5	1	Synergy	Isogenic derivative mutant of ABRIM; single amino acid substitution (Asn353Tyr) in PmrB	7
AB248	0.25	64	0.03	1	Synergy	*A. baumannii* clinical isolate	14
AB249*pmrB*	256	32	0.25	8	Synergy	Isogenic clinical isolate derivative of AB248; single amino acid substitution (Pro233Ser) in PmrB	14
AB299	0.25	64	0.03	4	Synergy	*A. baumannii* clinical isolate	14
AB347*pmrB*	64	16	0.25	4	Synergy	Isogenic clinical isolate derivative of AB299; single amino acid substitution (Pro170Leu) in PmrB	14

[a] COL_{MD3}, colistin MICs in the presence of MD3; $MD3_{COL}$, MD3 MICs in the presence of colistin; ATCC, American Type Culture Collection.

the fixed concentrations that resulted in synergy when COL and MD3 were combined in checkerboards. *A. baumannii* cultures were grown overnight, and 5×10^5 CFU/ml was used to inoculate 100 μl of Mueller-Hinton II broth in 96-well plates. Optical density was monitored using an Epoch-2 Microplate Spectrophotometer for 18 h (BioTek, USA).

Synergy observed in Col^s and Col^r strains with amino acid modifications in PmrB. The MICs of colistin and MD3 for the studied strains are shown in Table 1. The MICs of colistin were concordant with those previously published (14, 18). MD3 alone had little activity against any of the *A. baumannii* strains tested. However, there was a clear inverse relationship between susceptibility to MD3 and the MIC of COL, which could have been due in part to easier transport of MD3 through a modified outer membrane. All the Col^r mutants showed a MD3 MIC 2-fold to 16-fold lower than that seen with the wild-type parents (Table 1).

Clear synergy was seen against the Col^s ATCC 19606 parental strain (FIC_{index} = 0.18), the Col^s clinical strains (FIC_{index} = 0.13 to 0.24), and all the Col^r strains with modifications in *pmrB* (including both the ATCC 19606*pmrB* strain [FIC_{index} = 0.26] and the clinical isolates [FIC_{index} = 0.14 to 0.25]). However, no synergy (interpreted as no interaction) was observed against the Δ*lpx* strains (FIC_{index} = 0.75 to 1) (Table 1 and Fig. 1A). In Col^r Δ*lpx* mutants, the use of MD3 resulted in a reduction in the MIC of COL of only 2-fold to 4-fold. This was in contrast to 128-fold and 1,028-fold reductions at 4 mg/liter and 8 mg/liter of MD3 for the ATCC 19606*pmrB* mutant (from 64 mg/liter to 0.5 and 0.06 mg/liter, respectively). Similarly, assays performed using the ABRIM*pmrB*, AB249*pmrB*, and AB347*pmrB* Col^r clinical strains showed reductions in the COL MIC from 32 to 0.5 mg/liter, 256 to 0.25 mg/liter, and 64 to 0.25 mg/liter, respectively (64-fold to 256-fold), with MD3 added at 1 mg/liter. A decrease in the COL MIC of 8-fold to 16-fold was also observed with the Col^s clinical strains. These results confirm a potent synergistic effect of MD3 in combination with COL against Col^r strains with *pmrB* gene mutations promoting phosphoethanolamine modifications but not against Col^r strains with complete loss of the LPS.

The effects of MD3 and COL on the growth and fitness of *A. baumannii* ATCC 19606, ATCC 19606*pmrB*, and ATCC 19606Δ*lpxD* are shown in Fig. 1B. When *A. baumannii* ATCC 19606 was grown in the presence of concentrations of COL and MD3 that were below the MICs of the compounds (0.06 mg/liter and 2 mg/liter, respectively), the strain was able to grow, although its fitness was affected. However, when the two compounds were combined at those concentrations, synergy and complete inhibition of growth were observed. Similarly, the ATCC 19606*pmrB* mutant was able to grow in the presence of 1 mg/liter of COL or 4 mg/liter of MD3 (64-fold below the MIC for COL and 4-fold below the MIC for MD3) but growth was totally inhibited in the presence of COL and MD3 in combination. In contrast, in the case of ATCC 19606Δ*lpxD* (COL and MD3 MICs of 2,056 mg/liter and 2 mg/liter, respectively), no synergistic inhibition of growth was seen even with COL at 512 mg/liter. Against the clinical pairs ABRIM/ABRIM*pmrB*, AB248/AB249*pmrB*, and AB299/AB347*pmrB*, the combination of the two compounds at subinhibitory concentrations inhibited growth, while with the Δ*lpxA* and Δ*lpxC* Col^r mutants, the growth was not affected, as seen with the Δ*lpxD* mutant (data not shown). These assays confirmed the results obtained using the checkerboard method.

This study confirmed that combining MD3 and COL increases the susceptibility of Col^s *A. baumannii* strains, as previously reported (11). Moreover, we have demonstrated that there is also a significant synergistic effect against Col^r isolates that is dependent on the mechanism of colistin resistance. In Col^r *A. baumannii* strains harboring phosphoethanolamine modifications in lipid A, potent synergy between MD3 and COL was observed, but no interaction was seen when colistin resistance was mediated by lipid A deficiency. We also observed that the acquisition of colistin

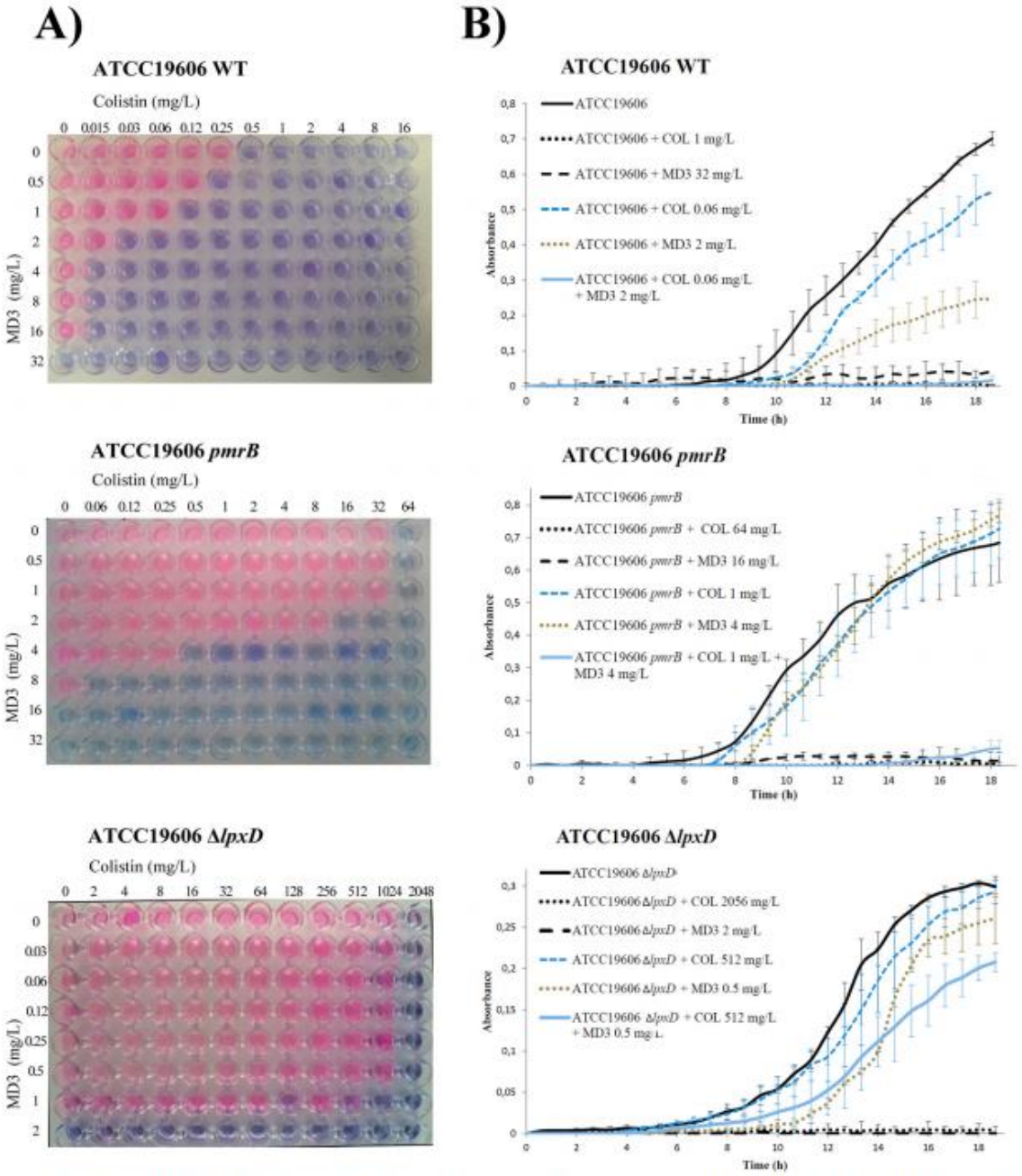

FIG 1 Assessment of synergy. (A) Checkerboard assays using colistin and MD3 performed on cultures of ATCC 19606, ATCC 19606*pmrB*, and ATCC 19606Δ*lpxD A. baumannii* strains. Pink wells indicate growth. Blue wells indicate growth inhibition. (B) Growth curves of the same strains in the absence of antimicrobials (black line) and in the presence of colistin at their MIC (black dotted line), of MD3 at their MIC (black dashed line), of colistin at their COL_{MD3} MIC (blue dashed line), of MD3 at their $MD3_{COL}$ MIC (green dotted line), and of colistin and MD3 at the COL_{MD3} and$MD3_{COL}$ MICs (blue line). COL_{MD3}, MICs of colistin in the presence of MD3; $MD3_{COL}$, MICs of MD3 in the presence of colistin. Because of the different methodologies used in the two assays, for the growth curve assays, strains ATCC 19606 and ATCC 19606*pmrB* were grown in 1 mg/liter of colistin instead 0.5 mg/liter as MIC controls. Independent assays were performed at least three times.

resistance in *A. baumannii* by means of a loss of LPS paradoxically increases the susceptibility to MD3.

In most published reports from studies of Col^r *A. baumannii* clinical isolates, resistance has been found to be mediated by modifications of the *pmrAB* genes (14, 19–22), as in those included in this study. Although clinical isolates with loss of LPS have been described (6, 23), complete loss of LPS promotes drastic changes in bacterial cellular architecture and significant loss of fitness (24),

whereas colistin resistance due to lipid A modifications leads a low or null fitness cost in the presence of antimicrobial selective pressure (18, 25). The relevant fitness burdens may affect the ability of Col^r *A. baumannii* to persist and spread in the clinical environment; therefore, it is most likely that Col^r clinical isolates of *A. baumannii* carry mutations in *pmrAB* genes rather than in *lpx* genes.

Colistin resistance due to phosphoethanolamine modification mediated by a plasmid-encoded enzyme, MCR-1, has recently been described in *Enterobacteriaceae* (26). This highlights the need for compounds, alone or in combination, able to target Col^r bacteria. We conclude that the MD3 compound could be used in the future for development of therapy against infections caused by Col^r *A. baumannii* and other MDR Gram-negative pathogens.

ACKNOWLEDGMENTS

We thank J. D. Boyce for the kind gift of the *A. baumannii* ATCC 19606Δ*lpxA* (AL1851), ATCC 19606Δ*lpxC* (AL1842), and ATCC 19606Δ*lpxD* (AL1852) strains. We also thank S. Pournaras for the kind gift of the *A. baumannii* AB248, AB249, AB299, and AB347 strains.

We declare that we have no conflicts of interest.

FUNDING INFORMATION

This work, including the efforts of German Bou, was funded by MINECO | Instituto de Salud Carlos III (ISCIII) (PI12/00552). This work, including the efforts of Margarita Poza and Alejandro Beceiro, was funded by MINECO | Instituto de Salud Carlos III (ISCIII) (PI14/00059). This work, including the efforts of Juan C. Vázquez-Ucha and Alejandro Beceiro, was funded by MINECO | Instituto de Salud Carlos III (ISCIII) (CP13/00226).

This work was supported by the Spanish National Plans for Scientific Research, Development and Technological Innovation 2008-2011 and 2013-2016 and funded by the ISCIII-General Subdirection of Assessment and Promotion of the Research European Regional Development Fund (ERDF) "A way of making Europe" and also by the Spanish Network for Research in Infectious Diseases (REIPI RD12/0015).

REFERENCES

1. **Peleg AY, Seifert H, Paterson DL.** 2008. *Acinetobacter baumannii*: emergence of a successful pathogen. Clin Microbiol Rev 21:538–582. http://dx.doi.org/10.1128/CMR.00058-07.
2. **Huttner B, Jones M, Rubin MA, Neuhauser MM, Gundlapalli A, Samore M.** 2012. Drugs of last resort? The use of polymyxins and tigecycline at US Veterans Affairs medical centers, 2005–2010. PLoS One 7:e36649.
3. **Hancock RE.** 1997. Peptide antibiotics. Lancet 349:418–422. http://dx.doi.org/10.1016/S0140-6736(97)80051-7.
4. **Cai Y, Chai D, Wang R, Liang B, Bai N.** 2012. Colistin resistance of *Acinetobacter baumannii*: clinical reports, mechanisms and antimicrobial strategies. J Antimicrob Chemother 67:1607–1615. http://dx.doi.org/10.1093/jac/dks084.
5. **Olaitan AO, Morand S, Rolain JM.** 2014. Mechanisms of polymyxin resistance: acquired and intrinsic resistance in bacteria. Front Microbiol 5:643.
6. **Moffatt JH, Harper M, Harrison P, Hale JD, Vinogradov E, Seemann T, Henry R, Crane B, St Michael F, Cox AD, Adler B, Nation RL, Li J, Boyce JD.** 2010. Colistin resistance in *Acinetobacter baumannii* is mediated by complete loss of lipopolysaccharide production. Antimicrob Agents Chemother 54:4971–4977. http://dx.doi.org/10.1128/AAC.00834-10.
7. **Beceiro A, Llobet E, Aranda J, Bengoechea JA, Doumith M, Hornsey M, Dhanji H, Chart H, Bou G, Livermore DM, Woodford N.** 2011. Phosphoethanolamine modification of lipid A in colistin-resistant variants of *Acinetobacter baumannii* mediated by the *pmrAB* two-component regulatory system. Antimicrob Agents Chemother 55:3370–3379. http://dx.doi.org/10.1128/AAC.00079-11.
8. **Adams MD, Nickel GC, Bajaksouzian S, Lavender H, Murthy AR, Jacobs MR, Bonomo RA.** 2009. Resistance to colistin in *Acinetobacter baumannii* associated with mutations in the PmrAB two-component system. Antimicrob Agents Chemother 53:3628–3634. http://dx.doi.org/10.1128/AAC.00284-09.
9. **Kempf M, Rolain JM.** 2012. Emergence of resistance to carbapenems in *Acinetobacter baumannii* in Europe: clinical impact and therapeutic options. Int J Antimicrob Agents 39:105–114. http://dx.doi.org/10.1016/j.ijantimicag.2011.10.004.
10. **Durante-Mangoni E, Utili R, Zarrilli R.** 2014. Combination therapy in severe *Acinetobacter baumannii* infections: an update on the evidence to date. Future Microbiol 9:773–789. http://dx.doi.org/10.2217/fmb.14.34.
11. **Personne Y, Curtis MA, Wareham DW, Waite RD.** 2014. Activity of the type I signal peptidase inhibitor MD3 against multidrug-resistant Gram-negative bacteria alone and in combination with colistin. J Antimicrob Chemother 69:3236–3243. http://dx.doi.org/10.1093/jac/dku309.
12. **Paetzel M, Karla A, Strynadka NC, Dalbey RE.** 2002. Signal peptidases. Chem Rev 102:4549–4580. http://dx.doi.org/10.1021/cr010166y.
13. **Bou G, Oliver A, Martínez-Beltrán J.** 2000. OXA-24, a novel class D beta-lactamase with carbapenemase activity in an *Acinetobacter baumannii* clinical strain. Antimicrob Agents Chemother 44:1556–1561. http://dx.doi.org/10.1128/AAC.44.6.1556-1561.2000.
14. **Pournaras S, Poulou A, Dafopoulou K, Chabane YN, Kristo I, Makris D, Hardouin J, Cosette P, Tsakris A, Dé E.** 2014. Growth retardation, reduced invasiveness, and impaired colistin-mediated cell death associated with colistin resistance development in *Acinetobacter baumannii*. Antimicrob Agents Chemother 58:828–832. http://dx.doi.org/10.1128/AAC.01439-13.
15. **Clinical and Laboratory Standards Institute.** 2012. Performance standards for antimicrobial susceptibility testing: 17th informational supplement M07-A9. CLSI, Wayne, PA, USA.
16. **Hsieh MH, Yu CM, Yu VL, Chow JW.** 1993. Synergy assessed by checkerboard. A critical analysis. Diagn Microbiol Infect Dis 16:343–349. http://dx.doi.org/10.1016/0732-8893(93)90087-N.
17. **Odds FC.** 2003. Synergy, antagonism, and what the chequerboard puts between them. J Antimicrob Chemother 52:1. http://dx.doi.org/10.1093/jac/dkg301.
18. **Beceiro A, Moreno A, Fernández N, Vallejo JA, Aranda J, Adler B, Harper M, Boyce JD, Bou G.** 2014. Biological cost of different mechanisms of colistin resistance and their impact on virulence in *Acinetobacter baumannii*. Antimicrob Agents Chemother 58:518–526. http://dx.doi.org/10.1128/AAC.01597-13.
19. **Kim Y, Bae IK, Jeong SH, Yong D, Lee K.** 2015. *In vivo* selection of pan-drug resistant *Acinetobacter baumannii* during antibiotic treatment. Yonsei Med J 56:928–934. http://dx.doi.org/10.3349/ymj.2015.56.4.928.
20. **Lesho E, Yoon EJ, McGann P, Snesrud E, Kwak Y, Milillo M, Onmus-Leone F, Preston L, St Clair K, Nikolich M, Viscount H, Wortmann G, Zapor M, Grillot-Courvalin C, Courvalin P, Clifford R, Waterman PE.** 2013. Emergence of colistin-resistance in extremely drug-resistant *Acinetobacter baumannii* containing a novel *pmrCAB* operon during colistin therapy of wound infections. J Infect Dis 208:1142–1151. http://dx.doi.org/10.1093/infdis/jit293.
21. **Mavroidi A, Likousi S, Palla E, Katsiari M, Roussou Z, Maguina A, Platsouka ED.** 2015. Molecular identification of tigecycline- and colistin-resistant carbapenemase-producing *Acinetobacter baumannii* from a Greek hospital from 2011 to 2013. J Med Microbiol 64:993–997. http://dx.doi.org/10.1099/jmm.0.000127.
22. **Durante-Mangoni E, Del Franco M, Andini R, Bernardo M, Giannouli M, Zarrilli R.** 2015. Emergence of colistin resistance without loss of fitness and virulence after prolonged colistin administration in a patient with extensively drug-resistant *Acinetobacter baumannii*. Diagn Microbiol Infect Dis 82:222–226. http://dx.doi.org/10.1016/j.diagmicrobio.2015.03.013.
23. **Selasi GN, Nicholas A, Jeon H, Lee YC, Yoo JR, Heo ST, Lee JC.** 2015. Genetic basis of antimicrobial resistance and clonal dynamics of carbapenem-resistant *Acinetobacter baumannii* sequence type 191 in a Korean hospital. Infect Genet Evol 36:1–7. http://dx.doi.org/10.1016/j.meegid.2015.09.001.
24. **Soon RL, Nation RL, Cockram S, Moffatt JH, Harper M, Adler B, Boyce JD, Larson I, Li J.** 2011. Different surface charge of colistin-susceptible and -resistant *Acinetobacter baumannii* cells measured with zeta potential

as a function of growth phase and colistin treatment. J Antimicrob Chemother 66:126–133. http://dx.doi.org/10.1093/jac/dkq422.
25. **Wand ME, Bock LJ, Bonney LC, Sutton JM.** 2015. Retention of virulence following adaptation to colistin in *Acinetobacter baumannii* reflects the mechanism of resistance. J Antimicrob Chemother 70:2209–2216. http://dx.doi.org/10.1093/jac/dkv097.
26. **Liu YY, Wang Y, Walsh TR, Yi LX, Zhang R, Spencer J, Doi Y, Tian G, Dong B, Huang X, Yu LF, Gu D, Ren H, Chen X, Lv L, He D, Zhou H, Liang Z, Liu JH, Shen J.** 2016. Emergence of plasmid-mediated colistin resistance mechanism MCR-1 in animals and human beings in China: a microbiological and molecular biological study. Lancet Infect Dis 16:161–168. http://dx.doi.org/10.1016/S1473-3099(15)00424-7.

IV. DISCUSIÓN

Discusión.

Acinetobacter baumannii ha evolucionado como un patógeno hospitalario de gran relevancia por su capacidad para resistir la desecación, los desinfectantes y los principales agentes antimicrobianos [48]. El aumento de las tasas de resistencia es un problema sanitario y económico a nivel global, no sólo por la morbilidad y mortalidad que produce, sino también por los costes que acarrea.

Ante estas circunstancias, la necesidad de nuevas opciones terapéuticas para el tratamiento de las infecciones por patógenos multirresistentes es indiscutible. Dado que el descubrimiento y la aparición de resistencias a los nuevos antimicrobianos son casi simultáneos, es necesario el desarrollo de fármacos con nuevos mecanismos de acción que superen los actuales mecanismos de resistencia y, por lo tanto, la búsqueda de nuevas dianas terapéuticas [48]. Esta Tesis Doctoral se centra en el estudio de nuevas dianas terapéuticas y en la evaluación de nuevos compuestos antimicrobianos, que podrían sentar las bases de las terapias antibióticas futuras.

En este trabajo nos apoyamos en la transcriptómica para la selección de genes candidatos de *A. baumannii* como dianas terapéuticas potenciales. En el año 2017 Murray y col. realizaron el primer análisis transcriptómico de la cepa *A. baumannii* ATCC 17978 *in vivo*, en un modelo de bacteriemia. En esta Tesis Doctoral se determinaron los perfiles de expresión génica de este patógeno en un modelo de **neumonía murina** y se compararon frente a la cepa cultivada en matraz, esta última utilizada como control. En este modelo *in vivo*, *A. baumannii* mostró unos perfiles de expresión génica muy específicos, donde 144 genes presentaron alterada su expresión en la infección pulmonar con respecto a la cepa cultivada en matraz. Algunos de estos genes son A1S_0242 (*feoA*), A1S_0781 (*mtnN*) A1S_1657 (N-acetiltransferasa de biosíntesis de sideróforo 1), A1S_2247 (*yfgC)*, A1S_2390 (*basB*), A1S_3245 (*hisF*), A1S_3410 (*oatA*) y A1S_1668 (*lpxB*). Tras estudiar la bibliografía de todos aquellos genes que resultaron con una expresión incrementada en el transcriptoma durante la infección *in vivo*, se escogieron 21 genes en los que se encontró cierta implicación en la virulencia en cualquier especie bacteriana. Se delecionaron cada uno de éstos por recombinación homóloga, realizando así 21 derivados isogénicos de la cepa ATCC

17978, con la finalidad de evaluar su función y su implicación en la patogénesis de *A. baumannii*.

Algunos de estos genes o bien ya han sido estudiados en profundidad por nuestro grupo, o a día de hoy todavía se están estudiando, como es el caso de A1S_0242 (*feoA*) [19] y de A1S_2390 (*basB*). El gen **A1S_0242 (*feoA*)** pertenece al sistema *feo*ABC, que se propone como el principal sistema de transporte de hierro ferroso conocido en procariotas. Nuestro grupo demostró que la inactivación del gen *feoA* juega un papel importante en *fitness*, adherencia a células eucariotas, formación de *biofilm* y virulencia [19]. Por otra parte, el gen **A1S_2390 (*basB*)** codifica una proteína implicada en la biosíntesis de acinetobactina. Esta última ha sido descrita como el sideróforo más relevante de *A. baumannii* [139,140]. El secuestro de hierro por parte de la acinetobactina es imprescindible para el establecimiento de la infección bacteriana y el daño celular [139].

Otro gen implicado en la absorción del hierro por parte de la bacteria y cuya expresión se vio incrementada durante el modelo de neumonía murina es el gen **A1S_1657**. Este gen codifica una supuesta proteína de membrana, la N-acetiltransferasa, implicada en la biosíntesis del sideróforo férrico y en el reconocimiento del mismo [141]. El gen A1S_1657 se estudió en profundidad en el **primer capítulo** de esta Tesis Doctoral. Se demostró que la inactivación de este gen causó una pérdida significativa de virulencia en neumonía, producción de *biofilm*, adherencia a células eucariotas y *fitness* en ausencia de hierro.

Cabe destacar que los genes pertenecientes a los clústeres de la acinetobactina (del gen A1S_2372 al A1S_2390) y del sideróforo férrico (del gen A1S_1647 al A1S_1657) también vieron incrementada su expresión en el análisis transcriptómico realizado por Murray y col. Esto sugiere la importancia de la captación de hierro en el éxito de una infección producida por este patógeno nosocomial [84].

Además de los genes citados anteriormente, en el primer capítulo de esta Tesis Doctoral se realizó una evaluación de los genes A1S_0781 (*mtnN*), A1S_2247 (*yfgC)* y A1S_3410 (*oatA*) y su implicación en la virulencia de *A. baumannii*. Las cepas mutantes de todos ellos mostraron una disminución significativa de la virulencia en el modelo de

neumonía murina. Por su parte, el gen **A1S_0781 (*mtnN*)** juega un papel crucial en el mantenimiento de la homeostasis bacteriana y está directamente involucrado en la biosíntesis de autoinductores del *quorum sensing*, como por ejemplo, AI-1 y AI-2 [142]. La inhibición de este enzima produce el bloqueo en la producción de ambos autoinductores y, por lo tanto, interrumpe la detección del *quorum sensing* [143]. Esto explicaría que la cepa mutante en *mtnN* mostró una disminución en la producción de *biofilm*, probablemente, debido a la inhibición del *quorum sensing*.

El gen **A1S_2247 (*yfgC*, renombrado *bepA*)** codifica para una metaloproteasa periplásmica. Esta proteína es responsable del mantenimiento de la integridad de la membrana externa en *E. coli* [144,145]. La inactivación de *bepA* en *E. coli* resultó en una mayor sensibilidad a diferentes antimicrobianos [146]. Nuestra cepa mutante Δ2247 presentó mayor susceptibilidad a cefalosporinas; sin embargo, mantuvo intacta la sensibilidad a otras familias de antimicrobianos. Este incremento en la sensibilidad a cefalosporinas puede estar relacionado con dificultades de acceso de la β-lactamasa cromosómica a los antimicrobianos, o debido a funciones de barrera comprometidas de la membrana externa [144].

A su vez, el gen **A1S_3410 (*oatA*)** codifica para una aciltransferasa y, posiblemente, se encuentre implicado en la O-acetilación del peptidoglicano de la pared celular. Éste es el principal factor de virulencia identificado en muchas bacterias, tanto Gram positivas como Gram negativas. El peptidoglicano es la diana de enzimas líticas, como la lisozima, que son producidas por huéspedes eucariotas como primera línea de defensa contra patógenos bacterianos. La O-acetilación del peptidoglicano conduce a la resistencia a la lisozima. En este estudio, la cepa mutante Δ3410, además de disminuir la capacidad de infección en el modelo de neumonía murina, mostró una pérdida de producción de *biofilm*.

Los genes **A1S_3245 (*hisF*)** y **A1S_1668 (*lpxB*)** de *A. baumannii* se estudiaron en mayor profundidad dedicándole un capítulo de esta Tesis Doctoral a cada uno de ellos. En estos genes, al igual que los comentados anteriormente, su expresión se vio incrementada durante la infección por neumonía, tanto en la cepa tipo ATCC 17978 como en el aislamiento clínico AbH12O-A2. En el caso de la cepa mutante Δ*hisF* fue sorprendente la disminución de la virulencia en el modelo de neumonía murina,

resultando casi inocua. Esto nos llevó a profundizar más en las funciones del gen *hisF*. Este estudio se recoge en el segundo capítulo.

Por otra parte, los intentos frustrados de conseguir una cepa mutante delecionando el gen A1S_1668 (*lpxB*) resultan en utilizar una tecnología novedosa para inactivar químicamente al gen y así estudiar su implicación en la virulencia de *A. baumannii*. Esta nueva tecnología son los oligómeros antisentido, muy utilizados en el campo de la Oncología y en distrofias musculares, pero muy poco explorados en el área microbiológica. Este trabajo constituye el tercer capítulo de esta Tesis Doctoral.

En el **segundo capítulo** de esta Tesis Doctoral estudiamos en profundidad el **gen *hisF*** de *A. baumannii*. Este gen está implicado en la biosíntesis de purinas y de la histidina. Esta ruta es compleja e incluye 9 genes [147], de los cuales, el gen *hisF* vio incrementada su expresión durante la neumonía. HisF junto con HisH producen ImGP y AICAR. El ImGP se utiliza en la biosíntesis de la histidina; mientras que AICAR se utiliza en la síntesis *de novo* de purinas y activación de AMPK [148,149]. Se ha demostrado que AICAR también puede inhibir la producción de citoquinas proinflamatorias inducida por lipopolisacáridos, regulando así el proceso inflamatorio [126,127]. Se ha demostrado que AICAR inactiva el ARNm, inhibiendo así la expresión de las citoquinas proinflamatorias IL-6 y el factor de necrosis tumoral-*alpha* (TNF-α). En cuanto a las citoquinas antiinflamatorias, sería inactivada en mayor medida la IL-10 [150].

Como se ha comentado anteriormente, se construyó una cepa mutante isogénica que carece de dicho gen (Δ*hisF*) derivada de la cepa ATCC 17978. Esta cepa mutante mostró una clara disminución de la virulencia en una infección pulmonar en ratones.

Además, se realizaron otros ensayos *in vivo*, un modelo de sepsis murina y en *G. mellonella*; pero no se observaron diferencias entre la virulencia de la cepa mutante Δ*hisF* y la cepa parenteral. Del mismo modo, se realizaron numerosos ensayos *in vitro* para estudiar la implicación del gen *hisF* en la virulencia de *A. baumannii*. Sin embargo, tampoco se observó ningún otro parámetro afectado por la deleción del gen medido *in vitro*; probablemente, debido a su implicación en la respuesta inmune del huésped *in vivo*.

Durante las fases iniciales de una infección por neumonía, los macrófagos alveolares producen una variedad de citoquinas proinflamatorias, implicadas en la respuesta inmune inespecífica, cuya función es atraer y activar a los leucocitos polimorfonucleares, necesarios para la defensa y la eliminación local de patógenos [151]. Por lo tanto, realizamos una serie de inmunoensayos para determinar y comparar la producción de citoquinas proinflamatorias durante una infección con la cepa parental y con la cepa mutante Δ*hisF*. Las citoquinas proinflamatorias que dependen de la inactivación de AICAR son la IL-6 y TNF-α [150], por lo que medimos los niveles de éstas en los diferentes ensayos mediante la técnica ELISA.

Los inmunoensayos, tanto *in vitro* (infectando macrófagos RAW 264.7) como *in vivo* (mediante el modelo de neumonía murina), demostraron una mayor producción de IL-6 cuando originaba la infección la cepa mutante Δ*hisF* que cuando la originaba la cepa parenteral. Sin embargo, no observamos diferencias significativas en los niveles de TNF-α entre ambas cepas.

El TNF-α es producido principalmente por células *natural killer,* implicadas en la respuesta inmune adaptativa celular, encargada de la eliminación de patógenos intracelulares como son virus y hongos. Esto explicaría la inexistencia de diferencias significativas en los niveles de TNF-α en los ensayos realizados con la cepa ATCC 17978 y su derivado isogénico Δ*hisF* [152,153].

La IL-6, producida principalmente por macrófagos, favorece la diferenciación de linfocitos B a células plasmáticas productoras de anticuerpos en los folículos secundarios de los ganglios linfáticos. Es decir, la IL-6 media en la respuesta inmune adaptativa **humoral**, implicada sobre todo en la eliminación de patógenos extracelulares, como son las bacterias. Además, la IgM secretada en esta respuesta primaria activa con gran potencia la vía clásica del sistema de complemento, liberándose factores de complemento que actúan como quimiotácticos, favoreciendo el reclutamiento de macrófagos, y como opsoninas, facilitando la fagocitosis [152,153]. Esta teoría también explicaría el mayor porcentaje de fagocitosis observado en los macrófagos infectados con la cepa Δ*hisF* frente al observado en la infección por la cepa salvaje.

Por otra parte, sería interesante comprobar si aquellos ratones supervivientes tras la infección con la cepa mutante desarrollaron linfocitos B de memoria que protegiesen al ratón en una segunda infección por *A. baumannii*. De este modo, la deleción del gen *hisF* sería una forma de atenuar a la cepa con fines preventivos, como es el desarrollo de una vacuna.

Los datos obtenidos en este estudio sugieren que la conversión PRFAR, por la proteína heterodimérica HisH/HisF, en ImGP y AICAR, juega un papel clave en la infección pulmonar causada por *A. baumannii*. Por lo tanto, HisF es un buen candidato para el desarrollo de fármacos.

En el **tercer capítulo** de esta Tesis Doctoral se utilizó la tecnología antisentido para inactivar al gen **A1S_1668 (*lpxB*)**, una glicosiltransferasa implicada en la síntesis del lípido A. Esta tecnología se basa en la inhibición de la traducción, uniéndose estas moléculas al ARNm. Empleamos esta metodología debido a los numerosos intentos fallidos de construir una cepa mutante por la deleción del gen *lpxB*; lo que sugiere la participación de este gen en pasos metabólicos clave para la supervivencia bacteriana. Otros grupos y el nuestro han descrito previamente la relevancia de los genes *lpx* (*lpxA*, *lpxC* y *lpxD*) en el mantenimiento estructural del LPS, en *fitness* y en la virulencia de *A. baumannii* [71,154,155]. En el transcriptoma realizado por Murray y col., el gen *lpxC* (A1S_3330) vio incrementada su expresión 3,8 veces durante la bacteriemia. El LPS es uno de los principales factores de virulencia de *A. baumannii.* Por lo tanto, resulta interesante estudiar los genes *lpx* por ser genes de síntesis del lípido A, uno de los principales componentes del LPS [84]. En este capítulo hemos estudiado en profundidad LpxB como una nueva diana bacteriana y la utilizamos para el desarrollo de nuevas estrategias antimicrobianas.

En este trabajo hemos seleccionado los oligómeros antisentido PNAs para el desarrollo de compuestos antimicrobianos. Éstos se diseñaron a partir de la secuencia nucleotídica de los genes de estudio, en este caso los genes *lpxB*, *murA* e *hisF*, y se les conjugó covalentemente el péptido $(KFF)_3K$, para facilitar su liberación intracelular. Esta unión del péptido al PNA afecta negativamente a la bacteria debido a la

desorganización de su membrana externa [125]. Estos péptidos no mostraron toxicidad en ensayos con animales y el péptido $(KFF)_3K$ no fue tóxico para las células eucariotas hasta concentraciones superiores a 64μM [156].

En todos los ensayos realizados *in vitro*, el pPNA anti-*lpxB* mostró mayor actividad antimicrobiana que el pPNA anti-*murA* frente a *A. baumannii*. MurA es la diana de la fosfomicina, por lo tanto, es muy probable que el pPNA anti-*murA* sea eficaz frente a otras especies. Del mismo modo, el gen *lpxB* se encuentra altamente conservado [135]; por lo que con toda probabilidad la actividad antimicrobiana mostrada del pPNA anti-*lpxB* frente a *A. baumannii* también se mantenga en otras especies bacterianas.

El gen *hisF* está implicado en la respuesta inmune del hospedador, pero no es esencial para la supervivencia de la bacteria, salvo en unas condiciones muy limitadas. Por esta razón se utilizó el pPNA anti-*hisF* como control negativo interno. No obstante, es probable que este PNA presente actividad antimicrobiana en un modelo de neumonía murina.

La tecnología antisentido resultó en una estrategia eficaz frente a infecciones bacterianas, tal como pudimos observar en ensayos *in vitro* e *in vivo*. Por lo tanto, es probable que se pudiesen diseñar PNAs para la mayoría de las posibles dianas comentadas a lo largo de esta Tesis Doctoral. Una de estas dianas interesantes es el gen *feoA* (A1S_0242), el cual, participa en el sistema de captación de hierro Feo. El éxito de una infección pulmonar depende parcialmente de la capacidad de la bacteria para adquirir el hierro disponible en el medio. El sistema Feo capta el Fe^{2+}, muy abundante en condiciones anaerobias. En cambio, el Fe^{3+} es captado por moléculas quelantes, como el citrato, y reducido a Fe^{2+} antes del transporte al citosol a través del sistema Feo. *A. baumannii* presenta sideróforos basados en el citrato, por ejemplo, la acinetobactina. Nuestro grupo ha demostrado que la deleción del gen *feoA* inhibió la captación de hierro, provocando una disminución en *fitness*, adhesión a células eucariotas y producción de *biofilm*. También se observó una disminución de la virulencia en un modelo de neumonía murina y en *G. mellonella*, al inactivar este gen [19].

Otra estrategia interesante sería inhibir el gen *basB* (A1S_2390) implicado en el último paso de la síntesis de la acinetobactina, el principal sideróforo de *A. baumannii* y responsable de la captación del Fe^{3+} disponible en el medio. La inactivación del gen *basB* produce una disminución importante de la virulencia de *A. baumannii* en ensayos *in vivo*. Tanto un pPNA anti-*feoA* como un pPNA anti-*basB* presentarían posiblemente actividad antimicrobiana frente a *A. baumannii*, tanto en ensayos *in vitro* como *in vivo*. Del mismo modo, serían eficaces frente a otras especies bacterianas, ya que estos sistemas de captación de hierro se han descrito en otras especies.

Sin embargo, el gen A1S_1657 también relacionado con la síntesis de sideróforos en *A. baumannii*, no sería una diana óptima para el diseño de PNAs debido a que su función podría ser complementada por otros sideróforos. La especie *A. baylyi* carece de los genes análogos a A1S_1656 y A1S_1657; sin embargo, presenta una aciltransferasa entre los genes análogos a A1S_1654 y A1S_1655. Es decir, el clúster de este sideróforo se encuentra en la misma posición en todas las cepas de *A. baumannii,* pero en A. *baylyi* presenta una reorganización genética [141], por lo que no sería probable que un pPNA dirigido a esta diana fuese eficaz frente a otras especies bacterianas.

Por otra parte, el aumento de las tasas de resistencias a antibióticos y las pocas alternativas terapéuticas conllevan a la reintroducción de antibióticos en desuso en la práctica clínica. Este es el caso de la colistina, un antibiótico recuperado como última opción terapéutica en el tratamiento de patógenos multirresistentes. Este agente antimicrobiano presenta una toxicidad elevada, por lo tanto, cuanto menor sea la dosis administrada, se producirán menores reacciones adversas. Es importante poder rescatar la colistina en el tratamiento de cepas resistentes a colistina, por lo que el diseño de compuestos que presenten efectos sinérgicos con la colistina u otros antibióticos es de vital importancia.

En esta Tesis Doctoral hemos evaluado la actividad sinérgica entre la colistina y el pPNA anti-*lpxB*. Hemos escogido la colistina por su acción sobre la membrana externa, la cual, proporciona la primera línea de defensa de la bacteria frente a la penetración de agentes antimicrobianos [157]. No obstante, ésta se ve deformada por acción de la colistina debido la formación de poros, que permiten el paso de diferentes moléculas al interior celular procariota, entre las cuales, se incluyen los PNAs [158].

Los ensayos de *checkerboard* realizados confirmaron esta sinergia en las cepas sensibles a la colistina. Sin embargo, aunque las concentraciones mínimas inhibitorias (CMIs) disminuyeron para ambos compuestos utilizados en monoterapia, no se observó ninguna sinergia en las cepas de *A. baumannii* resistentes a la colistina. Aquí sugerimos que el lípido A modificado de estas cepas resistentes a la colistina podría prevenir el aumento de la permeabilidad de la membrana externa. Los ensayos de virulencia en *G. mellonella* confirmaron el efecto protector del pPNA anti-*lpxB* frente a la infección causada por *A. baumannii* y la sinergia de éste con colistina. Los resultados *in vitro* e *in vivo* obtenidos mostraron que la combinación de colistina y PNAs es una estrategia exitosa para aumentar la capacidad de penetración de éstos últimos.

Del mismo modo, en el **cuarto capítulo** de esta Tesis Doctoral, evaluamos otro compuesto con propiedades antimicrobianas y su sinergia con la colistina, el MD3. El MD3 es una β-aminocetona inhibidora de las proteasas del péptido señal de tipo I (SPasa I). El péptido señal dirige a la proteína madura hacia el citoplasma. Una vez que se produce la traslocación, la SPasa escinde el péptido señal del resto de la proteína, finalizando así la maduración de las mismas. En el análisis transcriptómico *in vivo* de *A. baumannii*, se encontraron dos genes que codifican para SPasas, A1S_0019 y A1S_2608. El gen A1S_0019 codifica para una SPasa de tipo II y el gen A1S_2608, para una SppA que es una SPasa perteneciente a la familia S49, de tipo I [159]. En ambos casos, su expresión no se vio alterada durante el curso de la infección por neumonía, al igual que en el análisis transcriptómico en bacteriemia. A pesar de que su expresión se mantenga sin alteraciones durante los procesos infecciosos, las SPasas son unas buenas dianas terapéuticas. Su mecanismo consiste en inhibir la maduración de proteínas, que pueden ser esenciales o no para la supervivencia bacteriana; por otra parte, se produce una acumulación proteica importante en el interior celular que puede provocar la apoptosis. No obstante, hay que tener en cuenta que las células eucariotas también presentan SPasas, por lo que se debe dirigir muy bien el compuesto hacia los enzimas bacterianos para evitar problemas de toxicidad.

La colistina permeabiliza la membrana externa, por lo que facilita la entrada del MD3 al interior celular procariota. En este trabajo la combinación de MD3 y colistina fue

evaluada frente a cepas de *A. baumannii* sensibles y resistentes a colistina. Las cepas resistentes a colistina presentaban mutaciones en los genes *lpx* (genes implicados en la biosíntesis del LPS) o cepas con modificaciones del lípido A (mutaciones en *pmrB*). El MD3 en monoterapia presenta poca actividad frente a las cepas de *A. baumannii* utilizadas en este trabajo. Sin embargo, existe una clara relación inversa entre la sensibilidad al MD3 y la CMI a colistina, que se debe en parte a un transporte facilitado del MD3 a través de una membrana externa modificada. Todas las cepas mutantes resistentes a colistina mostraron una CMI al MD3 inferior a la CMI observada en la cepa tipo.

La sinergia se determinó, al igual que en el capítulo anterior, mediante ensayos de *checkerboard*. La combinación colistina y MD3 presentó una clara sinergia frente a las cepas sensibles a colistina, tanto clínicas como tipo, y frente a todas las cepas resistentes a colistina con modificaciones en *pmrB*. Sin embargo, no se observaron efectos sinérgicos en las cepas deficitarias de *lpx*. Se realizaron curvas de crecimiento que confirmaron estos efectos sinérgicos y el daño que producían en *fitness*.

En esta Tesis Doctoral realizamos los estudios de sinergia entre la colistina y ambas moléculas, PNAs y MD3. No obstante, podría presentar sinergia con otros antibióticos en función de su mecanismo de acción. Los PNAs inhiben la traducción de una proteína determinada y el MD3, el proceso de traslocación y maduración de aquellas proteínas que tienen que ser dirigidas al periplasma por un péptido señal. Por lo tanto, cabe esperar que cualquier antibiótico que afecte a la síntesis de proteínas y actúe a nivel de los ribosomas como es el caso de la tigeciclina y amikacina, antibióticos de rutina en la práctica clínica para el tratamiento de infecciones originadas por *A. baumannii*, presentará sinergia con estos compuestos. Por otra parte, cabe destacar, por ejemplo, la cepa mutante Δ2247 aumentó la sensibilidad de cefalosporinas en comparación con la cepa salvaje, por lo que es probable que un pPNA anti-*yfgC* (A1S_2247) presente efectos sinérgicos con éstas.

En conclusión, el análisis transcriptómico *in vivo* de *A. baumannii* nos dio una visión general de todos aquellos procesos biológicos que transcurren durante la infección en

pulmón. Del mismo modo, nos permitió conocer aquellos genes que presentaron alterada su expresión. El estudio exhaustivo de los mismos nos sugiere cuáles serían los mejores candidatos para el desarrollo de nuevas estrategias antimicrobianas.

De los genes con un incremento en su expresión en el transcriptoma de la infección por neumonía, se profundizó en mayor medida en los genes *hisF* y *lpxB* de *A. baumannii*. En el caso del gen *hisF* está implicado en un aumento de la persistencia de la bacteria en pulmón y en la respuesta inflamatoria aguda. El gen *lpxB* es esencial para la supervivencia de la bacteria y se encuentra altamente conservado en otras especies bacterianas. Estas propiedades intrínsecas de estos genes, los convierte en dianas farmacológicas idóneas para el diseño de nuevos fármacos.

En esta Tesis Doctoral, demostramos la eficacia de la tecnología antisentido en el tratamiento de infecciones originadas por *A. baumannii*. Se utilizaron PNAs con la secuencia específica del gen *lpxB*, confirmando así su potencial como diana terapéutica. También evaluamos las posibles sinergias entre la colistina y nuevos compuestos antimicrobianos para reducir su toxicidad y mejorar así su utilidad. Demostramos la eficacia de la sinergia entre el pPNA anti-*lpxB* y la colistina, tanto en ensayos *in vitro* como en ensayos *in vivo*. Por otra parte, confirmamos la actividad antimicrobiana y la sinergia con colistina del MD3, un inhibidor de SPasas I.

En definitiva, se han localizado nuevos genes esenciales para la infección en pulmón originada por *A. baumannii*, que pueden ser considerados dianas terapéuticas potenciales. También se han evaluado con éxito nuevas alternativas terapéuticas frente a este patógeno multirresistente.

V. CONCLUSIONES

Conclusiones.

- Capítulo I. Estudio global del transcriptoma de *Acinetobacter baumannii* durante el desarrollo de neumonía murina.

1. Las cepas de *A. baumannii* ATCC 17978 y AbH12O-A2 presentaron una expresión génica diferencial durante el curso de la infección por neumonía.

2. Aproximadamente un 5% de los genes analizados en el estudio transcriptómico experimentaron un incremento en su expresión en el modelo de neumonía murina, siendo alguno de ellos posibles candidatos a nuevas dianas terapéuticas.

- Capítulo II. Implicación de HisF en la persistencia en pulmón de *Acinetobacter baumannii* durante una infección por neumonía.

3. El gen *hisF* de *A. baumannii* está implicado en la inhibición del reclutamiento de células del sistema inmune de la respuesta innata y en la producción de la citoquina proinflamatoria IL-6. Este gen codifica una proteína esencial en el desarrollo de la infección pulmonar.

- Capítulo III. Inhibición del gen *lpxB* de *Acinetobacter baumannii* por conjugados péptido-PNA y evaluación de un efecto sinérgico con colistina.

4. El enzima LpxB, esencial para la supervivencia de *A. baumannii*, puede considerarse una diana interesante para el diseño de nuevas terapias antimicrobianas.

5. El pPNA anti-*lpxB*, que inhibe la expresión del enzima LpxB, presentó actividad antimicrobiana en modelos *in vitro* e *in vivo*, y podría ser evaluada como una nueva alternativa terapéutica, combinado a colistina o en monoterapia.

- Capítulo IV. **La sinergia entre la colistina y el inhibidor de la peptidasa de señalización de tipo I MD3 es dependiente del mecanismo de resistencia a colistina en *Acinetobacter baumannii*.**

6. El compuesto MD3 presentó actividad antimicrobiana y sinergia con colistina frente a *A. baumannii*. Podría utilizarse en el desarrollo de terapias contra infecciones causadas por este patógeno, incluyendo aquellas cepas resistentes a colistina.

VI. BIBLIOGRAFÍA

Bibliografía.

[1] Kardos N, Demain AL. Penicillin: The medicine with the greatest impact on therapeutic outcomes. Appl Microbiol Biotechnol 2011;92:677–87. https://doi.org/10.1007/s00253-011-3587-6.

[2] García Rodríguez JA, García Sánchez JE, Gobernado M, Picazo JJ, Prieto J, editors. Antimicrobianos en Medicina. 2ª edición. Sociedad Española de Quimioterapia; 2006.

[3] Antimicrobial Resistance: Tackling a crisis for the health and wealth of nations. Review on Antimicrobial Resistance. n.d.

[4] Organization WH. Global priority list of antibiotic-resistant bacteria to guide research, discovery and development of new antibiotics n.d. http://www.who.int/medicines/publications/WHO-PPL-Short_Summary_25Feb-ET_NM_WHO.pdf.

[5] Wong D., Nielsen T.B., Bonomo R.A., Pantapalangkor P., *et al*. Clinical and Pathophysiological Overview of *Acinetobacter* Infections: a Century of Challenges. Clin Microbiol Rev 2017;30:409–47. https://doi.org/http://dx.doi.org/10.1128/CMR.00058-16.

[6] Adams MD, Wright MS, Karichu JK, Venepally P, Fouts DE, Chan AP, *et al*. Rapid Replacement of *Acinetobacter baumannii* Strains Accompanied by Changes in Lipooligosaccharide Loci and Resistance Gene Repertoire . MBio 2019;10:1–14. https://doi.org/10.1128/mbio.00356-19.

[7] Pendleton JN, Gorman SP, Gilmore BF. Patogenos Eskape Er 2013;11:297–308. https://doi.org/10.1586/eri.13.12.

[8] Xia J, Gao J, Tang W. Nosocomial infection and its molecular mechanisms of antibiotic resistance. Biosci Trends 2016;10:14–21. https://doi.org/10.5582/bst.2016.01020.

[9] Chatterjee N, Bhattacharyya K, Dam S. *Acinetobacter baumannii*: An emerging unique multi-drug resistant pathogen. Eur J Biomed Pharm Sci 2016;3:117–30.

[10] Baumann P. Isolation of *Acinetobacter* from soil and water. J Bacteriol 1968;96:39–42.

[11] LPSN bacterio.net n.d. http://www.bacterio.net/acinetobacter.html (accessed October 8, 2019).

[12] Dijkshoorn L, Nemec A, Seifert H. An increasing threat in hospitals: Multidrug-resistant *Acinetobacter baumannii*. Nat Rev Microbiol 2007. https://doi.org/10.1038/nrmicro1789.

[13] Antunes LCS, Visca P, Towner KJ. *Acinetobacter baumannii*: Evolution of a global pathogen. Pathog Dis 2014;71:292–301. https://doi.org/10.1111/2049-

632X.12125.

[14] McConnell MJ, Actis L, Pachón J. *Acinetobacter baumannii*: Human infections, factors contributing to pathogenesis and animal models. FEMS Microbiol Rev 2013;37:130–55. https://doi.org/10.1111/j.1574-6976.2012.00344.x.

[15] Dijkshoorn L, Nemec A, Seifert H. An increasing threat in hospitals: Multidrug-resistant *Acinetobacter baumannii*. Nat Rev Microbiol 2007;5:939–51. https://doi.org/10.1038/nrmicro1789.

[16] Beceiro A, Tomás MDM, Bou G. Antimicrobial resistance and virulence: a successful or deleterious association in the bacterial world? Clin Microbiol Rev 2013;26:185–230. https://doi.org/10.1128/CMR.00059-12.

[17] Ferreira D, Seca AML, Pinto DCGA, Silva AMS. Targeting human pathogenic bacteria by siderophores: A proteomics review. J Proteomics 2016;145:153–66. https://doi.org/10.1016/j.jprot.2016.04.006.

[18] Lee C-R, Lee JH, Park M, Park KS, Bae IK, Kim YB, *et al*. Biology of *Acinetobacter baumannii*: Pathogenesis, Antibiotic Resistance Mechanisms, and Prospective Treatment Options. Front Cell Infect Microbiol 2017;7. https://doi.org/10.3389/fcimb.2017.00055.

[19] Álvarez-Fraga L, Vázquez-Ucha JC, Martínez-Guitián M, Vallejo JA, Bou G, Beceiro A, *et al*. Pneumonia infection in mice reveals the involvement of the *feoA* gene in the pathogenesis of *Acinetobacter baumannii*. Virulence 2018. https://doi.org/10.1080/21505594.2017.1420451.

[20] Clemmer KM, Bonomo RA, Rather PN. Genetic analysis of surface motility in *Acinetobacter baumannii*. Microbiology 2011;157:2534–44. https://doi.org/10.1099/mic.0.049791-0.

[21] Roca I, Espinal P, Vila-Fanés X, Vila J. The *Acinetobacter baumannii* oxymoron: Commensal hospital dweller turned pan-drug-resistant menace. Front Microbiol 2012;3:1–30. https://doi.org/10.3389/fmicb.2012.00148.

[22] Harding CM, Tracy EN, Carruthers MD, Rather PN, Actis LA, Munson RSJ. *Acinetobacter baumannii* Strain M2 Produces Type IV Pili Which Play. Am Soc Microbiol 2013;4:1–10. https://doi.org/10.1128/mBio.00360-13.Editor.

[23] Costerton JW, Stewart PS, Greenberg EP. Bacterial biofilms: A common cause of persistent infections. Science (80-) 1999. https://doi.org/10.1126/science.284.5418.1318.

[24] Pasmore M, Costerton JW. Biofilms, bacterial signaling, and their ties to marine biology. J Ind Microbiol Biotechnol 2003;30:407–13. https://doi.org/10.1007/s10295-003-0069-6.

[25] Gaddy JA, Tomaras AP, Actis LA. The *Acinetobacter baumannii* 19606 OmpA protein plays a role in biofilm formation on abiotic surfaces and in the interaction of this pathogen with eukaryotic cells. Infect Immun 2009;77:3150–60. https://doi.org/10.1128/IAI.00096-09.

[26] Chu BC, Garcia-Herrero A, Johanson TH, Krewulak KD, Lau CK, Peacock RS, *et al*. Siderophore uptake in bacteria and the battle for iron with the host; a bird's eye view. BioMetals 2010;23:601–11. https://doi.org/10.1007/s10534-010-9361-x.

[27] Dashper SG, Butler CA, Lissel JP, Paolini RA, Hoffmann B, Veith PD, *et al*. A novel *Porphyromonas gingivalis* FeoB plays a role in manganese accumulation. J Biol Chem 2005. https://doi.org/10.1074/jbc.M503896200.

[28] Stevenson B, Wyckoff EE, Payne SM. *Vibrio cholerae* FeoA , FeoB , and FeoC Interact To Form a Complex 2016;198:1160–70. https://doi.org/10.1128/JB.00930-15.Editor.

[29] Antunes CS, Imperi F, Towner KJ, Visca P. Genome-assisted identification of putative iron-utilization genes in *Acinetobacter baumannii* and their distribution among a genotypically diverse collection of clinical isolates 2011;162:279–84. https://doi.org/10.1016/j.resmic.2010.10.010.

[30] Nairz M, Schroll A, Sonnweber T, Weiss G. The struggle for iron - a metal at the host-pathogen interface. Cell Microbiol 2010. https://doi.org/10.1111/j.1462-5822.2010.01529.x.

[31] Shapiro JA, Wencewicz TA. Acinetobactin Isomerization Enables Adaptive Iron Acquisition in *Acinetobacter baumannii* through pH-Triggered Siderophore Swapping. ACS Infect Dis 2016;2:157–68. https://doi.org/10.1021/acsinfecdis.5b00145.

[32] Luke NR, Sauberan SL, Russo TA, Beanan JM, Olson R, Loehfelm TW, *et al*. Identification and characterization of a glycosyltransferase involved in *Acinetobacter baumannii* lipopolysaccharide core biosynthesis. Infect Immun 2010;78:2017–23. https://doi.org/10.1128/IAI.00016-10.

[33] García A, Salgado F, Solar H, González CL, Zemelman R, Onate A. Some immunological properties of lipopolysaccharide from *Acinetobacter baumannii*. J Med Microbiol 1999;48:479–83. https://doi.org/10.1099/00222615-48-5-479.

[34] McConnell MJ, Domínguez-Herrera J, Smani Y, López-Rojas R, Docobo-Pérez F, Pachón J. Vaccination with outer membrane complexes elicits rapid protective immunity to multidrug-resistant *Acinetobacter baumannii*. Infect Immun 2011;79:518–26. https://doi.org/10.1128/IAI.00741-10.

[35] Russo TA, Luke NR, Beanan JM, Olson R, Sauberan SL, MacDonald U, *et al*. The K1 capsular polysaccharide of *Acinetobacter baumannii* strain 307-0294 is a major virulence factor. Infect Immun 2010;78:3993–4000. https://doi.org/10.1128/IAI.00366-10.

[36] Sandkvist M, Hol WGJ, Korotkov K V. The type II secretion system: biogenesis, molecular architecture and mechanism. Nat Rev Microbiol 2012;10:336–51. https://doi.org/10.1038/nrmicro2762.

[37] Johnson TL, Waack U, Smith S, Mobley H, Sandkvist M. *Acinetobacter baumannii* Is Dependent on the Type II Secretion System and Its Substrate LipA for Lipid Utilization and *In Vivo* Fitness . J Bacteriol 2016;198:711–9.

https://doi.org/10.1128/jb.00622-15.

[38] Repizo GD, Gagné S, Foucault-Grunenwald ML, Borges V, Charpentier X, Limansky AS, *et al*. Differential role of the T6SS in *Acinetobacter baumannii* virulence. PLoS One 2015;10:1–20. https://doi.org/10.1371/journal.pone.0138265.

[39] Pérez-cruz C, Delgado L, López-iglesias C, Mercade E. Outer-Inner Membrane Vesicles Naturally Secreted by Gram-Negative Pathogenic Bacteria 2015:1–18. https://doi.org/10.1371/journal.pone.0116896.

[40] Rumbo C, Ferna E, Merino M, Poza M, Mendez JA, Soares NC, *et al*. Horizontal Transfer of the OXA-24 Carbapenemase Gene via Outer Membrane Vesicles : a New Mechanism of Dissemination of Carbapenem Resistance Genes in *Acinetobacter baumannii*. Antimicrob Agents Chemother 2011;55:3084–90. https://doi.org/10.1128/AAC.00929-10.

[41] Fernández L, Hancock REW. Adaptive and mutational resistance: Role of porins and efflux pumps in drug resistance. Clin Microbiol Rev 2012;25:661–81. https://doi.org/10.1128/CMR.00043-12.

[42] Pérez A, Carrie D, Latasa C, Poza M, Beceiro A, Tomás MDM, *et al*. Cloning, nucleotide sequencing, and analysis of the AcrAB-TolC efflux pump of *Enterobacter cloacae* and determination of its involvement in antibiotic resistance in a clinical isolate. Antimicrob Agents Chemother 2007;51:3247–53. https://doi.org/10.1128/AAC.00072-07.

[43] Coyne S, Rosenfeld N, Lambert T, Courvalin P, Périchon B. Overexpression of resistance-nodulation-cell division pump AdeFGH confers multidrug resistance in *Acinetobacter baumannii*. Antimicrob Agents Chemother 2010;54:4389–93. https://doi.org/10.1128/AAC.00155-10.

[44] Smani Y, Fa̍brega A, Roca I, Sańchez-Encinales V, Vila J, Pachón J. Role of OmpA in the multidrug resistance phenotype of *Acinetobacter baumannii*. Antimicrob Agents Chemother 2014;58:1806–8. https://doi.org/10.1128/AAC.02101-13.

[45] Iyer R, Moussa SH, Durand-Réville TF, Tommasi R, Miller A. *Acinetobacter baumannii* OmpA Is a Selective Antibiotic Permeant Porin. ACS Infect Dis 2018;4:373–81. https://doi.org/10.1021/acsinfecdis.7b00168.

[46] Catel-ferreira M, Nehmé R, Molle V, Aranda J, Bouffartigues E, Chevalier S, *et al*. Deciphering the Function of the Outer Membrane Protein OprD Homologue of *Acinetobacter baumannii*. Antimicrob Agents Chemother 2012;56:3826–32. https://doi.org/10.1128/AAC.06022-11.

[47] Rumbo C, Tomás M, Moreira EF, Soares NC, Carvajal M, Santillana E, *et al*. The *Acinetobacter baumannii* Omp33-36 porin is a virulence factor that induces apoptosis and modulates autophagy in human cells. Infect Immun 2014;82:4666–80. https://doi.org/10.1128/IAI.02034-14.

[48] Isler B, Doi Y, Bonomo RA, Paterson DL. New Treatment Options against Carbapenem-Resistant *Acinetobacter baumannii* Infections. Antimicrob Agents

Chemother 2019;63:1–43. https://doi.org/10.1128/AAC.01110-18.

[49] Keynan S, Hooper NM, Felici A, Amicosante G, Turner AJ. The renal membrane dipeptidase (dehydropeptidase I) inhibitor, cilastatin, inhibits the bacterial metallo-β-lactamase enzyme CphA. Antimicrob Agents Chemother 1995;39:1629–31. https://doi.org/10.1128/AAC.39.7.1629.

[50] Marín M, Gudiol F. Antibióticos betalactámicos. Enferm Infecc Microbiol Clin 2003;21:42–55. https://doi.org/10.1157/13042137.

[51] Mohammed H, Hisham N, Brahim I, El-Gamal MI, Bahaaeldin A, Aladdin R. Recent updates of carbapenem antibiotics. Eur J Med Chem 2017;131:185–95. https://doi.org/10.1016/j.ejmech.2017.03.022.

[52] Fernández-Cuenca F, Tomás-Carmona M, Caballero-Moyano F, Bou G, Martínez-Martínez L, Vila J, *et al*. [*In vitro* activity of 18 antimicrobial agents against clinical isolates of *Acinetobacter* spp.: multicenter national study GEIH-REIPI-Ab 2010]. Enferm Infecc Microbiol Clin 2013. https://doi.org/10.1016/j.eimc.2012.06.010.

[53] Bush K, Jacoby GA. Updated functional classification of β-lactamases. Antimicrob Agents Chemother 2010;54:969–76. https://doi.org/10.1128/AAC.01009-09.

[54] Jeon JH, Lee JH, Lee JJ, Park KS, Karim AM, Lee CR, *et al*. Structural basis for carbapenem-hydrolyzing mechanisms of carbapenemases conferring antibiotic resistance. Int J Mol Sci 2015;16:9654–92. https://doi.org/10.3390/ijms16059654.

[55] Bonnin RA, Nordmann P, Poirel L. Screening and deciphering antibiotic resistance in *Acinetobacter baumannii*: A state of the art. Expert Rev Anti Infect Ther 2013. https://doi.org/10.1586/eri.13.38.

[56] Poirel L, Bonnin RA, Nordmann P. Genetic features of the widespread plasmid coding for the carbapenemase OXA-48. Antimicrob Agents Chemother 2012;56:559–62. https://doi.org/10.1128/AAC.05289-11.

[57] Vázquez-Ucha JC, Maneiro M, Martínez-Guitián M, Buynak J, Bethel CR, Bonomo RA, *et al*. Activity of the ß-Lactamase inhibitor LN-1-255 against carbapenem-hydrolyzing class D ß-Lactamases from *Acinetobacter baumannii*. Antimicrob Agents Chemother 2017. https://doi.org/10.1128/AAC.01172-17.

[58] Levy N, Bruneau J-M, Le Rouzic E, Bonnard D, Le Strat F, Caravano A, *et al*. Structural basis for *E. coli* Penicillin Binding Protein (PBP) 2 inhibition, a platform for drug design. J Med Chem 2019:acs.jmedchem.9b00338. https://doi.org/10.1021/acs.jmedchem.9b00338.

[59] Lacasse E, Brouillette E, Larose A, Parr TR, Rubio A, Malouin F. *In Vitro* Activity of Tebipenem (SPR859) Against Penicillin-Binding Proteins of Gram-negative and Gram-positive Bacteria. Antimicrob Agents Chemother 2019. https://doi.org/10.1128/aac.02181-18.

[60] Vashist J, Tiwari V, Das R, Kapil A, Rajeswari MR. Analysis of penicillin-binding proteins (PBPs) in carbapenem resistant *Acinetobacter baumannii*. Indian J Med

Res 2011.

[61] Drawz SM, Bonomo RA. Three decades of β-lactamase inhibitors. Clin Microbiol Rev 2010;23:160–201. https://doi.org/10.1128/CMR.00037-09.

[62] Vademecum n.d.

[63] McLeod SM, Shapiro AB, Moussa SH, Johnstone M, McLaughlin RE, De Jonge BLM, *et al*. Frequency and mechanism of spontaneous resistance to sulbactam combined with the novel β-lactamase inhibitor ETX2514 in clinical isolates of *Acinetobacter baumannii*. Antimicrob Agents Chemother 2018;62:1–5. https://doi.org/10.1128/AAC.01576-17.

[64] Krizova L, Poirel L, Nordmann P, Nemec A. TEM-1 β-lactamase as a source of resistance to sulbactam in clinical strains of *Acinetobacter baumannii*. J Antimicrob Chemother 2013;68:2786–91. https://doi.org/10.1093/jac/dkt275.

[65] Kuo SC, Lee YT, Lauderdale TLY, Huang WC, Chuang MF, Chen CP, *et al*. Contribution of *Acinetobacter*-derived cephalosporinase-30 to sulbactam resistance in *Acinetobacter baumannii*. Front Microbiol 2015. https://doi.org/10.3389/fmicb.2015.00231.

[66] Yang Y, Xu Q, Li T, Fu Y, Shi Y, Lan P, *et al*. OXA-23 is a prevalent mechanism contributing to sulbactam resistance in diverse *Acinetobacter baumannii* clinical strains. Antimicrob Agents Chemother 2019. https://doi.org/10.1128/AAC.01676-18.

[67] Gerson S, Betts JW, Lucaßen K, Nodari CS, Wille J, Josten M, *et al*. Investigation of Novel *pmrB* and *eptA* Mutations in Isogenic *Acinetobacter baumannii* Isolates Associated with Colistin Resistance and Increased Virulence In Vivo . Antimicrob Agents Chemother 2019;63. https://doi.org/10.1128/aac.01586-18.

[68] Berenguer N, Horcajada JP, Montero MM, Grau S, Salas E, Luque S, *et al*. Luces y sombras en el uso de colistina: falta mucho por conocer. Enferm Infecc Microbiol Clin 2011;29:287–96. https://doi.org/10.1016/j.eimc.2011.02.003.

[69] Bialvaei AZ, Samadi Kafil H. Colistin, mechanisms and prevalence of resistance. Curr Med Res Opin 2015. https://doi.org/10.1185/03007995.2015.1018989.

[70] Karaiskos I, Souli M, Galani I, Giamarellou H. Colistin: still a lifesaver for the 21st century? Expert Opin Drug Metab Toxicol 2017. https://doi.org/10.1080/17425255.2017.1230200.

[71] Vinogradov E, Seemann T, Moffatt JH, St. Michael F, Harrison P, Nation RL, *et al*. Colistin Resistance in *Acinetobacter baumannii* Is Mediated by Complete Loss of Lipopolysaccharide Production. Antimicrob Agents Chemother 2010;54:4971–7. https://doi.org/10.1128/aac.00834-10.

[72] Beceiro A, Llobet E, Aranda J, Bengoechea JA, Doumith M, Hornsey M, *et al*. Phosphoethanolamine Modification of Lipid A in Colistin-Resistant Variants of *Acinetobacter baumannii* Mediated by the *pmrAB* Two-Component Regulatory System. Antimicrob Agents Chemother 2011;55:3370–9. https://doi.org/10.1128/aac.00079-11.

[73] Ni W, Han Y, Zhao J, Wei C, Cui J, Wang R, *et al*. Tigecycline treatment experience against multidrug-resistant *Acinetobacter baumannii* infections: A systematic review and meta-analysis. Int J Antimicrob Agents 2016;47:107–16. https://doi.org/10.1016/j.ijantimicag.2015.11.011.

[74] Olson MW, Ruzin A, Feyfant E, Iii TSR, Connell JO, Bradford PA. Functional, Biophysical, and Structural Bases for Antibacterial Activity of Tigecycline 2006;50:2156–66. https://doi.org/10.1128/AAC.01499-05.

[75] Trebosc V, Gartenmann S, Royet K, Manfredi P, Tötzl M, Schellhorn B, *et al*. A novel genome-editing platform for drug-resistant *Acinetobacter baumannii* reveals an *AdeR*-unrelated tigecycline resistance mechanism. Antimicrob Agents Chemother 2016;60:7263–71. https://doi.org/10.1128/AAC.01275-16.

[76] Yang YS, Chen HY, Hsu WJ, Chou YC, Perng CL, Shang HS, *et al*. Overexpression of AdeABC efflux pump associated with tigecycline resistance in clinical *Acinetobacter nosocomialis* isolates. Clin Microbiol Infect 2019;25:512.e1-512.e6. https://doi.org/10.1016/j.cmi.2018.06.012.

[77] Ramirez MS, Tolmasky ME. Amikacin: Uses, Resistance, and Prospects for Inhibition 2017. https://doi.org/10.3390/molecules22122267.

[78] McConnell MJ, Actis L, Pachón J. *Acinetobacter baumannii*: Human infections, factors contributing to pathogenesis and animal models. FEMS Microbiol Rev 2013;37:130–55. https://doi.org/10.1111/j.1574-6976.2012.00344.x.

[79] Zarubica T, Baker MR, Wright HT, Rife JP. The aminoglycoside resistance methyltransferases from the ArmA/Rmt family operate late in the 30S ribosomal biogenesis pathway. Rna 2011;17:346–55. https://doi.org/10.1261/rna.2314311.

[80] Klug WS, Cummings MR, Spencer CA, Palladino MA. Conceptos de genética. 2013.

[81] Galata V, Laczny CC, Backes C, Hemmrich-Stanisak G, Schmolke S, Franke A, *et al*. Integrating Culture-based Antibiotic Resistance Profiles with Whole-genome Sequencing Data for 11,087 Clinical Isolates. Genomics Proteomics Bioinformatics 2019. https://doi.org/10.1016/j.gpb.2018.11.002.

[82] Rumbo-Feal S, Gómez MJ, Gayoso C, Álvarez-Fraga L, Cabral MP, Aransay AM, *et al*. Whole Transcriptome Analysis of *Acinetobacter baumannii* Assessed by RNA-Sequencing Reveals Different mRNA Expression Profiles in Biofilm Compared to Planktonic Cells. PLoS One 2013. https://doi.org/10.1371/journal.pone.0072968.

[83] Soares NC, Cabral MP, Parreira JR, Gayoso C, Barba MJ, Bou G. 2-DE analysis indicates that *Acinetobacter baumannii* displays a robust and versatile metabolism. Proteome Sci 2009;7:37. https://doi.org/10.1186/1477-5956-7-37.

[84] Murray GL, Kostoulias XP, Boyce JD, Peleg AY, Tsyganov K, Powell D, *et al*. Global Gene Expression Profile of *Acinetobacter baumannii* During Bacteremia. J Infect Dis 2017.

[85] Chukwudi CU. Harvey_Ions&FS_ScanElectronMicrosc1972II,409-419.1980.pdf

2016;60:4433–41. https://doi.org/10.1128/AAC.00594-16.Address.

[86] Zhanel GG, Cheung D, Adam H, Zelenitsky S, Golden A, Schweizer F, *et al*. Review of Eravacycline, a Novel Fluorocycline Antibacterial Agent. Drugs 2016;76:567–88. https://doi.org/10.1007/s40265-016-0545-8.

[87] Corbett D, Wise A, Langley T, Skinner K, Trimby E 8, Birchall S, *et al*. Title: Potentiation of Antibiotic Activity by a Novel Cationic Peptide: Potency and 1 Spectrum of Activity of SPR741 2 3 4 Running Title: Potency and Spectrum of Activity of SPR741 5 6 7. AAC Accept Manuscr Posted Online Antimicrob Agents Chemother 2017;22:1–10. https://doi.org/10.1128/AAC.00200-17.

[88] Wright GD. Antibiotic Adjuvants: Rescuing Antibiotics from Resistance. Trends Microbiol 2016;24:862–71. https://doi.org/10.1016/j.tim.2016.06.009.

[89] Buynak JD, A Srinivasa R, Doppalapudi VR, Adam G, Petersen PJ, Nidamarthy SD. The synthesis and evaluation of 6-alkylidene-2'β-substituted penam sulfones as β-lactamase inhibitors. Bioorganic Med Chem Lett 1999;9:1997–2002. https://doi.org/10.1016/S0960-894X(99)00325-X.

[90] Vallejo JA, Martínez-Guitián M, Vázquez-Ucha JC, González-Bello C, Poza M, Buynak JD, *et al.* LN-1-255, a penicillanic acid sulfone able to inhibit the class D carbapenemase OXA-48. J Antimicrob Chemother 2016;71:2171–80. https://doi.org/10.1093/jac/dkw105.

[91] Vázquez-Ucha JC, Martínez-Guitián M, Maneiro M, Conde-Pérez K, Álvarez-Fraga L, Torrens G, *et al*. Therapeutic Efficacy of LN-1-255 in Combination with Imipenem in Severe Infection Caused by Carbapenem-Resistant *Acinetobacter baumannii*. Antimicrob Agents Chemother 2019. https://doi.org/10.1128/AAC.01092-19.

[92] Papp-Wallace KM, Nguyen NQ, Jacobs MR, Bethel CR, Barnes MD, Kumar V, *et al*. Strategic Approaches to Overcome Resistance against Gram-Negative Pathogens Using β-Lactamase Inhibitors and β-Lactam Enhancers: Activity of Three Novel Diazabicyclooctanes WCK 5153, Zidebactam (WCK 5107), and WCK 4234. J Med Chem 2018;61:4067–86. https://doi.org/10.1021/acs.jmedchem.8b00091.

[93] Moya B, Barcelo IM, Bhagwat S, Patel M, Bou G, Papp-Wallace KM, *et al*. Potent ß-lactam enhancer activity of zidebactam and WCK 5153 against *Acinetobacter baumannii*, including carbapenemase-producing clinical isolates. Antimicrob Agents Chemother 2017. https://doi.org/10.1128/AAC.01238-17.

[94] Papp-Wallace KM, Bonomo RA. New β-Lactamase Inhibitors in the Clinic. Infect Dis Clin North Am 2016. https://doi.org/10.1016/j.idc.2016.02.007.

[95] Livermore DM, Mushtaq S. Activity of biapenem (RPX2003) combined with the boronate β-lactamase inhibitor RPX7009 against carbapenem-resistant *Enterobacteriaceae*. J Antimicrob Chemother 2013;68:1825–31. https://doi.org/10.1093/jac/dkt118.

[96] Smith PA, Koehler MFT, Girgis HS, Yan D, Chen Y, Chen Y, *et al*. Optimized

arylomycins are a new class of Gram-negative antibiotics. Nature 2018;561:189–94. https://doi.org/10.1038/s41586-018-0483-6.

[97] Zalucki YM, Jennings MP. Signal peptidase I processed secretory signal sequences: Selection for and against specific amino acids at the second position of mature protein. Biochem Biophys Res Commun 2017;483:972–7. https://doi.org/10.1016/j.bbrc.2017.01.044.

[98] Lukaszczyk M, Pradhan B, Remaut H. Bacterial Cell Walls and Membranes. vol. 92. Springer International Publishing; 2019. https://doi.org/10.1007/978-3-030-18768-2.

[99] Sarkar I, Garg R, van Drunen Littel-van den Hurk S. Selection of adjuvants for vaccines targeting specific pathogens. Expert Rev Vaccines 2019;18:505–21. https://doi.org/10.1080/14760584.2019.1604231.

[100] Lin L, Tan B, Pantapalangkoor P, Ho T, Hujer AM, Taracila MA, *et al*. *Acinetobacter baumannii* rOmpA vaccine dose alters immune polarization and immunodominant epitopes. Vaccine 2013;31:313–8. https://doi.org/10.1016/j.vaccine.2012.11.008.

[101] Solanki V, Tiwari V. Subtractive proteomics to identify novel drug targets and reverse vaccinology for the development of chimeric vaccine against *Acinetobacter baumannii*. Sci Rep 2018;8:1–19. https://doi.org/10.1038/s41598-018-26689-7.

[102] Cabral MP, García P, Beceiro A, Rumbo C, Pérez A, Moscoso M, *et al*. Design of live attenuated bacterial vaccines based on D-glutamate auxotrophy. Nat Commun 2017;8. https://doi.org/10.1038/ncomms15480.

[103] Shu MH, Matrahim N, Noramdan N, Pang SP, Hashim SH, Phoon WH, *et al*. An Inactivated Antibiotic-Exposed Whole-Cell Vaccine Enhances Bactericidal Activities Against Multidrug-Resistant *Acinetobacter baumannii*. Sci Rep 2016;6:1–8. https://doi.org/10.1038/srep22332.

[104] Pulido MR, García-Quintanilla M, Pachón J, McConnell MJ. Immunization with lipopolysaccharide-free outer membrane complexes protects against *Acinetobacter baumannii* infection. Vaccine 2018;36:4153–6. https://doi.org/10.1016/j.vaccine.2018.05.113.

[105] Cisek AA, Dąbrowska I, Gregorczyk KP, Wyżewski Z. Phage Therapy in Bacterial Infections Treatment: One Hundred Years After the Discovery of Bacteriophages. Curr Microbiol 2017;74:277–83. https://doi.org/10.1007/s00284-016-1166-x.

[106] Regeimbal JM, Jacobs AC, Corey BW, Henry MS, Thompson MG, Pavlicek RL, *et al*. Personalized Therapeutic Cocktail of Wild Environmental Phages Rescues Mice from *Acinetobacter baumannii* Wound Infections. Antimicrob Agents Chemother 2016;60:5806–16. https://doi.org/10.1128/aac.02877-15.

[107] Mateczun AJ, Lancaster J, Quinones J, Strathdee SA, Picel AC, Henry MS, *et al*. Development and Use of Personalized Bacteriophage-Based Therapeutic

Cocktails To Treat a Patient with a Disseminated Resistant *Acinetobacter baumannii* Infection. Antimicrob Agents Chemother 2017;61:1–14. https://doi.org/10.1128/aac.00954-17.

[108] Alonso MJ, Sanchez A, Torres D, Seijo B, Vila-Jato JL. Joint effects of monomer and stabilizer concentrations on physico-chemical characteristics of poly(butyl 2-cyanoacrylate) nanoparticles. J Microencapsul 1990;7:517–26. https://doi.org/10.3109/02652049009040475.

[109] Pelgrift RY, Friedman AJ. Nanotechnology as a therapeutic tool to combat microbial resistance. Adv Drug Deliv Rev 2013;65:1803–15. https://doi.org/10.1016/j.addr.2013.07.011.

[110] Miller SE, Bell CS, Mejias R, McClain MS, Cover TL, Giorgio TD. Colistin-functionalized nanoparticles for the rapid capture of *Acinetobacter baumannii*. J Biomed Nanotechnol 2016. https://doi.org/10.1166/jbn.2016.2273.

[111] Wan G, Ruan L, Yin Y, Yang T, Ge M, Cheng X. Effects of silver nanoparticles in combination with antibiotics on the resistant bacteria *Acinetobacter baumannii*. Int J Nanomedicine 2016. https://doi.org/10.2147/IJN.S104166.

[112] Rasmussen LCV, Sperling-Petersen HU, Mortensen KK. Hitting bacteria at the heart of the central dogma: Sequence-specific inhibition. Microb Cell Fact 2007. https://doi.org/10.1186/1475-2859-6-24.

[113] Hegarty JP, Stewart DB. Advances in therapeutic bacterial antisense biotechnology. Appl Microbiol Biotechnol 2018. https://doi.org/10.1007/s00253-017-8671-0.

[114] Kole R, Krainer AR, Altman S. RNA therapeutics: Beyond RNA interference and antisense oligonucleotides. Nat Rev Drug Discov 2012. https://doi.org/10.1038/nrd3625.

[115] Good L, Awasthi SK, Dryselius R, Larsson O, Nielsen PE. Bactericidal antisense effects of peptide-PNA conjugates. Nat Biotechnol 2001. https://doi.org/10.1038/86753.

[116] Kurupati P, Tan KSW, Kumarasinghe G, Poh CL. Inhibition of gene expression and growth by antisense peptide nucleic acids in a multiresistant β-lactamase-producing *Klebsiella pneumoniae* strain. Antimicrob Agents Chemother 2007;51:805–11. https://doi.org/10.1128/AAC.00709-06.

[117] Nekhotiaeva N, Awasthi SK, Nielsen PE, Good L. Inhibition of *Staphylococcus aureus* gene expression and growth using antisense peptide nucleic acids. Mol Ther 2004. https://doi.org/10.1016/j.ymthe.2004.07.006.

[118] Ghosal A, Nielsen PE. Potent Antibacterial Antisense Peptide–Peptide Nucleic Acid Conjugates Against *Pseudomonas aeruginosa*. Nucleic Acid Ther 2018;22:323–34. https://doi.org/10.1089/nat.2012.0370.

[119] Wang H, He Y, Xia Y, Wang L, Liang S. Inhibition of gene expression and growth of multidrug-resistant *Acinetobacter baumannii* by antisense peptide nucleic acids. Mol Biol Rep 2014. https://doi.org/10.1007/s11033-014-3643-2.

[120] Lopez C, Arivett BA, Actis LA, Tolmasky ME. Inhibition of AAC(6')-Ib-Mediated Resistance to Amikacin in Acinetobacter baumannii by an Antisense Peptide-Conjugated 2',4'-Bridged Nucleic Acid-NC-DNA Hybrid Oligomer. Antimicrob Agents Chemother 2015;59:5798–803. https://doi.org/10.1128/aac.01304-15.

[121] Soler Bistue AJC, Martin FA, Vozza N, Ha H, Joaquin JC, Zorreguieta A, *et al*. Inhibition of aac(6')-Ib-mediated amikacin resistance by nuclease-resistant external guide sequences in bacteria. Proc Natl Acad Sci 2009;106:13230–5. https://doi.org/10.1073/pnas.0906529106.

[122] Nielsen P, Egholm M, Berg R, Buchardt O. Peptide nucleic acids (PNAs): potential antisense and anti-gene agents. Anticancer Drug Des n.d.;8:53-63.

[123] Ghosal A. Peptide nucleic acid antisense oligomers open an avenue for developing novel antibacterial molecules. J Infect Dev Ctries 2017. https://doi.org/10.3855/jidc.9159.

[124] Bai H, You Y, Yan H, Meng J, Xue X, Hou Z, *et al*. Antisense inhibition of gene expression and growth in gram-negative bacteria by cell-penetrating peptide conjugates of peptide nucleic acids targeted to rpoD gene. Biomaterials 2012. https://doi.org/10.1016/j.biomaterials.2011.09.075.

[125] Vaara M, Porro M. Group of peptides that act synergistically with hydrophobic antibiotics against Gram-negative enteric bacteria. Antimicrob Agents Chemother 1996.

[126] Alifano P, Fani R, Liò P, Lazcano A, Bazzicalupo M, Carlomagno MS, *et al*. Histidine biosynthetic pathway and genes: structure, regulation, and evolution. Microbiol Rev 1996.

[127] Fani R, Brilli M, Fondi M, Lió P. The role of gene fusions in the evolution of metabolic pathways: The histidine biosynthesis case. BMC Evol Biol 2007. https://doi.org/10.1186/1471-2148-7-S2-S4.

[128] Klem TJ, Davisson VJ. Imidazole Glycerol Phosphate Synthase: The Glutamine Amidotransferase in Histidine Biosynthesis. Biochemistry 1993. https://doi.org/10.1021/bi00070a029.

[129] Kim J, Yang G, Kim Y, Kim J, Ha J. AMPK activators: Mechanisms of action and physiological activities. Exp Mol Med 2016. https://doi.org/10.1038/emm.2016.16.

[130] Ruderman NB, Park H, Kaushik VK, Dean D, Constant S, Prentki M, *et al*. AMPK as a metabolic switch in rat muscle, liver and adipose tissue after exercise. Acta Physiol. Scand., 2003. https://doi.org/10.1046/j.1365-201X.2003.01164.x.

[131] Jhun BS, Jin Q, Oh YT, Kim SS, Kong Y, Cho YH, *et al*. 5-Aminoimidazole-4-carboxamide riboside suppresses lipopolysaccharide- induced TNF-α production through inhibition of phosphatidylinositol 3-kinase/Akt activation in RAW 264.7 murine macrophages. Biochem Biophys Res Commun 2004. https://doi.org/10.1016/j.bbrc.2004.04.035.

[132] Peairs A, Radjavi A, Davis S, Li L, Ahmed A, Giri S, *et al*. Activation of AMPK

inhibits inflammation in MRL/lpr mouse mesangial cells. Clin Exp Immunol 2009. https://doi.org/10.1111/j.1365-2249.2009.03924.x.

[133] Giri S. 5-Aminoimidazole-4-Carboxamide-1- -4-Ribofuranoside Inhibits Proinflammatory Response in Glial Cells: A Possible Role of AMP-Activated Protein Kinase. J Neurosci 2004. https://doi.org/10.1523/jneurosci.4288-03.2004.

[134] Raetz CRH, Whitfield C. Lipopolysaccharide Endotoxins. Annu Rev Biochem 2002. https://doi.org/10.1146/annurev.biochem.71.110601.135414.

[135] Bohl TE, Shi K, Lee JK, Aihara H. Crystal structure of lipid A disaccharide synthase LpxB from *Escherichia coli*. Nat Commun 2018. https://doi.org/10.1038/s41467-017-02712-9.

[136] Ollinger J, O'Malley T, Ahn J, Odingo J, Parish T. Inhibition of the sole type I signal peptidase of *Mycobacterium tuberculosis* is bactericidal under replicating and nonreplicating conditions. J Bacteriol 2012;194:2614–9. https://doi.org/10.1128/JB.00224-12.

[137] Smith MG, Gianoulis TA, Pukatzki S, Mekalanos JJ, Ornston LN, Gerstein M, *et al*. New insights into *Acinetobacter baumannii* pathogenesis revealed by high-density pyrosequencing and transposon mutagenesis. Genes Dev 2007. https://doi.org/10.1101/gad.1510307.

[138] Merino M, Alvarez-Fraga L, Gomez MJ, Aransay AM, Lavin JL, Chaves F, *et al*. Complete Genome Sequence of the Multiresistant *Acinetobacter baumannii* Strain AbH12O-A2, Isolated during a Large Outbreak in Spain. Genome Announc 2014. https://doi.org/10.1128/genomea.01182-14.

[139] Hasan T, Choi CH, Oh MH. Genes Involved in the Biosynthesis and Transport of Acinetobactin in *Acinetobacter baumannii*. Genomics Inform 2015. https://doi.org/10.5808/gi.2015.13.1.2.

[140] Gaddy JA, Arivett BA, McConnell MJ, López-Rojas R, Pachón J, Actis LA. Role of Acinetobactin-Mediated Iron Acquisition Functions in the Interaction of *Acinetobacter baumannii* Strain ATCC 19606 ^{T} with Human Lung Epithelial Cells, *Galleria mellonella* Caterpillars, and Mice. Infect Immun 2012. https://doi.org/10.1128/IAI.06279-11.

[141] Eijkelkamp BA, Hassan KA, Paulsen IT, Brown MH. Investigation of the human pathogen *Acinetobacter baumannii* under iron limiting conditions. BMC Genomics 2011. https://doi.org/10.1186/1471-2164-12-126.

[142] Parveen N, Cornell KA. Methylthioadenosine/S-adenosylhomocysteine nucleosidase, a critical enzyme for bacterial metabolism. Mol Microbiol 2011. https://doi.org/10.1111/j.1365-2958.2010.07455.x.

[143] Gutierrez JA, Crowder T, Rinaldo-Matthis A, Ho MC, Almo SC, Schramm VL. Transition state analogs of 5'-methylthioadenosine nucleosidase disrupt quorum sensing. Nat Chem Biol 2009. https://doi.org/10.1038/nchembio.153.

[144] Narita S -i., Masui C, Suzuki T, Dohmae N, Akiyama Y. Protease homolog BepA

(YfgC) promotes assembly and degradation of β-barrel membrane proteins in *Escherichia coli*. Proc Natl Acad Sci 2013. https://doi.org/10.1073/pnas.1312012110.

[145] Oh E, Becker AH, Sandikci A, Huber D, Chaba R, Gloge F, et al. Selective ribosome profiling reveals the cotranslational chaperone action of trigger factor *in vivo*. Cell 2011. https://doi.org/10.1016/j.cell.2011.10.044.

[146] Liu A, Tran L, Becket E, Lee K, Chinn L, Park E, *et al*. Antibiotic sensitivity profiles determined with an *Escherichia coli* gene knockout collection: Generating an antibiotic bar code. Antimicrob Agents Chemother 2010. https://doi.org/10.1128/AAC.00906-09.

[147] Fani R, Mori E, Tamburini E, Lazcano A. Evolution of the structure and chromosomal distribution of histidine biosynthetic genes. Orig Life Evol Biosph 1998;28:555–70. https://doi.org/10.1023/A:1006531526299.

[148] Fani R, Mori E, Tamburini E, Lazcano A. Evolution of the structure and chromosomal distribution of histidine biosynthetic genes. Orig Life Evol Biosph 1998;28(4-6):55.

[149] O'Donoghue P, Amaro R, Luthey-Schulten Z. On the structure of HisH: protein structure prediction in the context of structural and functional genomics. J Struct Biol 2001;134(2-3):257–68. https://doi.org/10.1006/jsbi.2001.4390.

[150] Kirchner J, Brüne B, Namgaladze D. AICAR inhibits NFκB DNA binding independently of AMPK to attenuate LPS-triggered inflammatory responses in human macrophages. Sci Rep 2018;8:1–9. https://doi.org/10.1038/s41598-018-26102-3.

[151] Bordon J, Aliberti S, Fernandez-Botran R, Uriarte SM, Rane MJ, Duvvuri P, *et al*. Understanding the roles of cytokines and neutrophil activity and neutrophil apoptosis in the protective *versus* deleterious inflammatory response in pneumonia. Int J Infect Dis 2013. https://doi.org/10.1016/j.ijid.2012.06.006.

[152] Delves PJ, Martin SJ, Burton DR, Roitt IM, Aparicio Alonso P. Roitt. Inmunología. Fundamentos (11a edición). Inmunología 2008. https://doi.org/10.1016/s0213-9626(08)70069-6.

[153] Abul K. Abbas. Inmunología celular y molecular. 2012. https://doi.org/10.1017/CBO9781107415324.004.

[154] Beceiro A, Moreno A, Fernández N, Vallejo JA, Aranda J, Adler B, *et al*. Biological cost of different mechanisms of colistin resistance and their impact on virulence in *Acinetobacter baumannii*. Antimicrob Agents Chemother 2014. https://doi.org/10.1128/AAC.01597-13.

[155] Carretero-Ledesma M, García-Quintanilla M, Martín-Peña R, Pulido MR, Pachón J, McConnell MJ. Phenotypic changes associated with colistin resistance due to lipopolysaccharide loss in *Acinetobacter baumannii*. Virulence 2018. https://doi.org/10.1080/21505594.2018.1460187.

[156] Rustici A, Velucchi M, Faggioni R, Sironi M, Ghezzi P, Quataert S, *et al*. Molecular

mapping and detoxification of the lipid A binding site by synthetic peptides. Science (80-) 1993. https://doi.org/10.1126/science.8420003.

[157] Good L, Sandberg R, Larsson O, Nielsen PE, Wahlestedt C. Antisense PNA effects in *Escherichia coli* are limited by the outer-membrane LPS layer. Microbiology 2000. https://doi.org/10.1099/00221287-146-10-2665.

[158] Hancock REW. Peptide antibiotics. Lancet (North Am Ed 1997. https://doi.org/10.1016/S0140-6736(97)80051-7.

[159] MEROPS n.d. https://www.ebi.ac.uk/merops/cgi-bin/famsum?family=S49 (accessed October 15, 2019).

VII. ANEXO

Otras publicaciones de primera autoría **NO INCLUIDAS** en esta Tesis Doctoral.

J Antimicrob Chemother 2016; **71**: 2171–2180
doi:10.1093/jac/dkw105 Advance Access publication 28 April 2016

Journal of Antimicrobial Chemotherapy

LN-1-255, a penicillanic acid sulfone able to inhibit the class D carbapenemase OXA-48

Juan A. Vallejo[1]†, Marta Martínez-Guitián[1]†, Juan C. Vázquez-Ucha[1], Concepción González-Bello[2], Margarita Poza[1], John D. Buynak[3], Christopher R. Bethel[4], Robert A. Bonomo[4,5], German Bou[1]‡ and Alejandro Beceiro[1]*‡

[1]*Servicio de Microbiología-Instituto de Investigación Biomédica (INIBIC), 15006 A Coruña, Spain;* [2]*Centro Singular de Investigación en Química Biolóxica e Materiais Moleculares (CIQUS), Universidad de Santiago de Compostela, 15782 Santiago de Compostela, Spain;* [3]*Department of Chemistry, Southern Methodist University, Dallas, TX 75275, USA;* [4]*Research Service, Louis Stokes Cleveland Veterans Affairs Medical Center, Cleveland, OH 44106, USA;* [5]*Departments of Biochemistry, Molecular Biology and Microbiology, Pharmacology and Medicine, Case Western Reserve University, Cleveland, OH 44106, USA*

*Corresponding author. Servicio de Microbiología-Instituto de Investigación Biomédica (INIBIC), Complejo Hospitalario Universitario A Coruña (CHUAC), As Xubias, 15006 A Coruña, Spain. Tel: +34-981178000, ext. 292145; Fax: +34-981176097; E-mail: alejandro.beceiro.casas@sergas.es
†Contributed equally to this work.
‡Contributed equally to this work.

Received 1 December 2015; returned 18 January 2016; revised 29 February 2016; accepted 4 March 2016

Objectives: Carbapenemases are the most important mechanism responsible for carbapenem resistance in Enterobacteriaceae. Among carbapenemases, OXA-48 presents unique challenges as it is resistant to β-lactam inhibitors. Here, we test the capacity of the compound LN-1-255, a 6-alkylidene-2′-substituted penicillanic acid sulfone, to inhibit the activity of the carbapenemase OXA-48.

Methods: The OXA-48 gene was cloned and expressed in *Klebsiella pneumoniae* and *Escherichia coli* in order to obtain MICs in the presence of inhibitors (clavulanic acid, tazobactam and sulbactam) and LN-1-255. OXA-48 was purified and steady-state kinetics was performed with LN-1-255 and tazobactam. The covalent binding mode of LN-1-255 with OXA-48 was studied by docking assays.

Results: Both OXA-48-producing clinical and transformant strains displayed increased susceptibility to carbapenem antibiotics in the presence of 4 mg/L LN-1-255 (2–32-fold increased susceptibility) and 16 mg/L LN-1-255 (4–64-fold increased susceptibility). Kinetic assays demonstrated that LN-1-255 is able to inhibit OXA-48 with an acylation efficiency (k_2/K) of $10 \pm 1 \times 10^4$ M^{-1} s^{-1} and a slow deacylation rate (k_{off}) of $7 \pm 1 \times 10^{-4}$ s^{-1}. IC_{50} was 3 nM for LN-1-255 and 1.5 μM for tazobactam. Lastly, k_{cat}/k_{inact} was 500-fold lower for LN-1-255 than for tazobactam.

Conclusions: In these studies, carbapenem antibiotics used in combination with LN-1-255 are effective against the carbapenemase OXA-48, an important emerging mechanism of antibiotic resistance. This provides an incentive for further investigations to maximize the efficacy of penicillin sulfone inhibition of class D plasmid-carried Enterobacteriaceae carbapenemases.

Introduction

Antimicrobial resistance rates of bacterial pathogens have steadily increased in recent years and are now considered a world health crisis by major international agencies.[1] Enterobacteriaceae are a bacterial family in which significantly increased rates of resistance have been observed. The main resistance mechanism—as for Gram-negative bacteria in general—is β-lactamase-mediated hydrolysis of antimicrobial compounds.[2] The prevalence and plasmid-mediated dissemination of β-lactamase genes are important clinical challenges. Until the first decade of the 21st century, the more clinically relevant β-lactamases were the ESBLs and the chromosomal and plasmid-mediated cephalosporinases (AmpCs).[3] Although carbapenem antibiotics remained active against β-lactamase-expressing bacteria, in recent years there has been an increase in the number of β-lactamases able to hydrolyse carbapenems. Of these enzymes, denoted 'carbapenemases', a growing group of OXA enzymes—the class D β-lactamases—is especially problematic.[4,5] These carbapenemases are mostly observed in *Acinetobacter baumannii*,[5,6] but the frequency of OXA-48 expression is increasing in Enterobacteriaceae,[7] largely in *Klebsiella pneumoniae*, and in *Escherichia coli*, *Enterobacter cloacae*, *Citrobacter freundii* and *Providencia rettgeri*.[8–13]

Currently, an important epidemiological change is occurring, a rapid increase in the number of isolates of carbapenemase-producing Enterobacteriaceae, mainly *K. pneumoniae*.[14] Thus, numerous hospital outbreaks of OXA-48-carrying Enterobacteriaceae have been reported worldwide[8,10,15] and the rising numbers of clinical isolates reported show OXA-48 as the most frequently detected carbapenemase in France, Belgium and Malta.[12,16] The rapid increase of such carbapenem-resistant isolates is facilitated by two main methods of dissemination: (i) horizontal transfer of plasmids encoding OXA-48; and (ii) vertical dissemination of successful clones.[17,18] The bla_{OXA-48}-like genes are encoded in transposon Tn*1999*, carried on IncL/M-type plasmids which are broad-host-range, self-conjugative and possess a high conjugation rate.[19] Along with KPC- and NDM-type carbapenemases, OXA-48 represents a major obstacle in the preservation of carbapenem efficacy against serious bacterial infections in Enterobacteriaceae.

Currently, few novel options for treatment of such MDR bacterial strains exist. One of the more promising avenues is the combination of β-lactam antibiotics with β-lactamase inhibitors, but currently commercial inhibitors are not effective against class D carbapenemases. Unlike class A enzymes, class D carbapenemases are not inhibited by β-lactamase inhibitors such as clavulanic acid, sulbactam or tazobactam.[2] Bacteria harbouring and expressing these class D β-lactamases are resistant to most antibiotics with few exceptions (e.g. tigecycline and colistin), although resistance rates to these antimicrobials are also increasing.[20–22] Considering that carbapenems are the main drug of choice to treat multiresistant hospital-acquired infections, the development of efficient inhibitors of OXA-48 enzymes is urgently needed in order to maintain the efficacy of β-lactam antibiotics.[8,23] Avibactam has generated great interest among the medical community and has very recently been approved by the FDA for treating complicated infections caused by antibiotic-resistant pathogens.[24] Avibactam demonstrates activity against OXA-48 but not against the class D carbapenemases of *A. baumannii*, such as OXA-23 or OXA-24/40, which are mainly responsible for carbapenem resistance in this MDR pathogen.[25,26] Buynak[27] has designed several β-lactamase inhibitors, of which the compound LN-1-255 represents a promising candidate in the quest for new OXA β-lactamase inhibitors. The design and synthesis of this 6-alkylidene-2′-substituted penicillin sulfone was previously reported.[28] LN-1-255 demonstrated efficacy to inhibit the class D carbapenemase OXA-24/40 of *A. baumannii* (implicating the hydrophobic barrier established through an arrangement of the Tyr-112 and Met-223 amino acids). This barrier is not present in the OXA-48 enzyme, similarly to OXA-10, another class D β-lactamase that lacks carbapenem hydrolytic activity.[29,30] LN-1-255 is also able to inhibit class A β-lactamases, such as SHV-1 and SHV-2.[31] However, the potential of LN-1-255 as an inhibitor of Enterobacteriaceae-derived class D carbapenemases has not yet been evaluated. Here, we analyse the ability of LN-1-255 to inhibit OXA-48 carbapenemase, similarly to what happens with the OXA-24/40 carbapenemase. Also, we study the synergy of this inhibitor with carbapenems against clinical isolates of *K. pneumoniae* and transformants of *E. coli* and *K. pneumoniae*.

Materials and methods

Bacterial strains, culture medium and plasmids

For microbiological studies, the bla_{OXA-48} gene was amplified from a clinical strain of *K. pneumoniae* derived from an outbreak in our hospital (A Coruña Hospital, Spain), which began in 2013 and continues until today, affecting >160 patients. Epidemiological studies using PFGE and MLST demonstrate that the outbreak resulted from the dissemination of a single clone of serotype ST-15. All carbapenem-resistant strains involved in the outbreak harbour the same conjugative plasmid, which carries the OXA-48 and CTX-M-15 genes integrated in the composite transposon Tn*1999.2*.[32] The strains utilized to transform the genetic constructs to study the MICs were obtained during previous studies and have porin deficits: *E. coli* J53 Δ*ompC/F* lacks porins OmpC and OmpF[33] and *K. pneumoniae* Δ*ompK35/36* lacks porins OmpK35 and OmpK36.[34] These strains were chosen in order to increase the genetic background of resistance upon transformation. All strains were cultured in LB medium at 37°C and stored at −80°C until analysis in LB medium containing 15% glycerol. When necessary, the LB medium was supplemented with ampicillin and/or kanamycin (Sigma-Genosys, UK).

Susceptibility testing of antibiotics and inhibitors

OXA-48 was amplified from genomic DNA using the Expand High Fidelity PCR System (Roche, Basel, Switzerland) and a primer pair containing recognition sites for the restriction enzymes BamHI (5′-AAAGGATCCATGCG TGTATTAGCCTTAT-3′) and EcoRI (5′-AAAGAATTCCTAGGGAATAATTTTTTCCT GTTT-3′). The amplified DNA fragment was then digested with BamHI and EcoRI (Fermentas, Glen Burnie, MA, USA) and ligated to a BamHI/EcoRI-digested pBGS18 plasmid.[35] This plasmid construct (pBGS18-OXA-48) was used to transform the strain *E. coli* DH5α for subcloning and then transformed into *E. coli* J53 Δ*ompC/F* and *K. pneumoniae* Δ*ompK35/36*.

Antibiotic susceptibility profiles were determined by microdilution following CLSI criteria.[36] Susceptibility to imipenem, meropenem and ertapenem (Sigma-Genosys, UK), in combination with the inhibitor LN-1-255 at fixed concentrations of 4 or 16 mg/L, was determined. For comparison, the inhibitor tazobactam was used at the same concentrations, as well as sulbactam and clavulanic acid (Sigma-Genosys, UK) at 4 mg/L. Etest of carbapenems (bioMérieux, Marcy-l'Étoile, France) in conjunction with inhibitors was performed on Mueller-Hinton II agar plates to confirm MICs. The MICs reported are the mean of three independent replicates. LN-1-255 was prepared in the laboratories of Southern Methodist University, Dallas, TX, USA, as described previously.[27] The chemical structures of LN-1-255 and tazobactam are shown in Figure 1.

Synergy studies were also performed using the chequerboard method using both *K. pneumoniae* strains. Synergy of imipenem (range 0.12-256 mg/L) in the absence and presence of LN-1-255 at 16 mg/L was combined with tigecycline, colistin and amikacin (range 0.12-256 mg/L), important treatment options against MDR pathogens. The fractional inhibitory concentration index (FICI) was calculated and interpreted as follows: FICI ≤0.5, synergy; and FICI >0.5-4, no interaction.[37]

Purification of OXA-48

For kinetic studies, bla_{OXA-48} was directionally cloned into the p-GEX-6p-1 plasmid for expression and purification (GE Healthcare, Little Chalfont, UK).

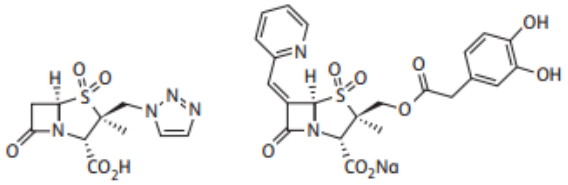

Figure 1. β-Lactamase inhibitors used in this study.

As above, this gene was amplified from genomic DNA using the Expand High Fidelity PCR System (Roche, Basel, Switzerland) with a primer pair containing recognition sites for the restriction enzymes BamHI (5′-AAA GGATCCAAGGAATGGCAAGAAAACAAA-3′) and EcoRI (5′-AAAGAATTCCTA GGGAATAATTTTTTCCTGTTT-3′). The amplified DNA fragment was then digested with BamHI and EcoRI and ligated to BamHI/EcoRI-digested p-GEX-6p-1. The recombinant plasmid was electroporated into a protease-deficient strain, *E. coli* BL21 (DE3), to generate the fusion protein glutathione *S*-transferase (GST)/OXA-48. This protein was purified to homogeneity using the GST Gene Fusion System (Amersham Pharmacia Biotech, Europe) in conjunction with the manufacturer's instructions. The purification was confirmed using SDS–PAGE gels as a band of ∼29 kDa (>95% purity) and later identification with a MALDI-TOF/TOF spectrometer (Bruker Daltonics, Billerica, MA, USA).

Kinetic experiments

Kinetic constants of OXA-48 β-lactamase were determined by continuous assays at room temperature (25°C) using a Nicolet Evolution 300 spectrophotometer (Thermo Fisher Scientific, Waltham, MA, USA). Each experiment was performed in triplicate in 50 mM sodium phosphate with 20 mM sodium bicarbonate[38] and using 0.2 and 1.0 cm pathlength cuvettes. Measurements of hydrolysis were performed with nitrocefin (Oxoid, Hampshire, UK) at 590 nM, imipenem and ertapenem, both at 299 nM. The extinction coefficients used were 15 900 M^{-1} cm^{-1} for nitrocefin, 9970 M^{-1} cm^{-1} for imipenem and 10 930 M^{-1} cm^{-1} for ertapenem. Measurements of inhibition were performed in the presence of LN-1-255 and tazobactam, using nitrocefin at 200 μM as the reporter substrate. The kinetic assays were previously described[30,39,40] and are briefly explained below. V_{max}, k_{cat} and K_m were determined by initial velocity kinetic analysis. The data were fitted to the Michaelis–Menten equation (Equation 1) using non-linear least-squares regression analysis:

$$v = \frac{V_{max}[S]}{(K_m + [S])} \quad (1)$$

The inhibitor concentration resulting in 50% reduction of nitrocefin hydrolysis after 10 min of pre-incubation of the enzyme and inhibitor at 25°C was denoted as the IC_{50}, as previously described.[30]

The apparent K_m for tazobactam and LN-1-255 was obtained as a competitive inhibition constant ($K_{i\ app}$) in the presence of nitrocefin.[40] Inverse initial velocities ($1/v_0$) were plotted against the inhibitor concentration ([I]) to obtain linear plots. Initial velocity (v_0) was determined by Equation (2):

$$v_0 = \frac{(V_{max} \times [S])}{\{(K_{m\ NCF}) \times (1 + [I]/K_{m\ NCF}) + [S]\}} \quad (2)$$

$K_{i\ app}$ was determined by dividing the value of the *y*-intercept of the linear plot by the slope and corrected for nitrocefin affinity using Equation (3):

$$K_{i\ app}(\text{corrected}) = \frac{K_{i\ app}\ (\text{observed})}{[1 + ([S]/K_{m\ NCF})]} \quad (3)$$

The inhibitor complex inactivation rate (k_{inact}) in the presence of nitrocefin was measured and K_I determined as previously described.[41] The k_{obs} values were determined using non-linear least-squares fitting of the data, employing Origin 7.5® software and Equation (4):

$$A = A_0 + v_f \times t + (v_0 - v_f) \times \frac{[1 - \exp(-k_{obs}t)]}{k_{obs}} \quad (4)$$

Here, A is absorbance, v_0 (expressed in variation of absorbance per unit time) is initial velocity, v_f is the final velocity and t is time. Each k_{obs} was plotted against [I] and fitting performed to determine k_{inact} and K_I using Equation (5). The K_I value was corrected using Equation (3).

$$k_{obs} = \frac{k_{inact}[I]}{(K_I + [I])} \quad (5)$$

The k_2/K (observed) was determined as the slope of the line obtained by plotting [I] against k_{obs}. This value was corrected for nitrocefin affinity as in Equation (6):

$$\frac{k_2}{K} = \frac{k_2}{K_{obs}} \times \left(\left(\frac{[S]}{K_{m\ NCF}}\right) + 1\right) \quad (6)$$

The k_{off} for LN-1-255 was performed using a jump dilution method followed by continuous assays as previously described.[42] Briefly, 1 μM enzyme was incubated with 10 μM LN-1-255 for 5 min at 37°C, the reaction solution was diluted 40 000-fold in assay buffer and hydrolysis of 200 μM nitrocefin was measured in 500 μL of reaction solution. Reaction solutions without OXA-48 or containing OXA-48 without LN-1-255 were used as controls.

The K_d (dissociation constant) was determined by Equation (7):

$$K_d = \frac{k_{off}}{(k_2/K)} \quad (7)$$

The partition ratio (k_{cat}/k_{inact}) or turnover number (t_n) is defined as the ratio of inhibitor/enzyme (*I*:*E*) necessary for >90% inhibition of nitrocefin hydrolysis.[30] The t_n values were determined after 5 h of incubation with increasing concentrations of inhibitor and 10 nM enzyme, varying the molar ratios of *I*:*E*. Longer incubation times could not be used due to enzyme instability and loss of activity. Incubations were done in a final reaction volume of 500 μL and 200 μM nitrocefin was added immediately before measurement, in order to determine the residual enzyme activity during 60 s.

Docking studies

The covalent binding mode of LN-1-255 with OXA-48 from *K. pneumoniae* was studied using GOLD 5.2[43] and the enzyme geometries found in the crystal structure of the OXA-48/avibactam adduct (PDB 4S2K,[44] 2.1 Å). Water molecules and ligands were removed from the crystal structure. Ligand geometry was minimized using AM1 Hamiltonian as implemented in the program Gaussian 09[45] and used as MOL2 files. The ligand was docked in 25 independent genetic algorithm (GA) runs and for each of these, a maximum number of 100 000 GA operations were performed on a single population of 50 individuals. Covalent docking was applied between the catalytic Ser-81 (oxygen atom side chain) and the carboxylate group (oxygen atom) of the indolizine obtained after covalent modification of OXA-24/40 from *A. baumannii* with LN-1-255.[26] Operator weights for crossover, mutation and migration in the entry box were used as default parameters (95, 95 and 10, respectively), as well as hydrogen bonding (4.0 Å) and van der Waals (2.5 Å) parameters. The position of avibactam in the crystal structure was used to define the active site and the radius was set to 7 Å. The 'flip ring corners' flag was switched on, while all other flags were off. The GOLD scoring function was used to rank the ligands in order of fit.

Results

Antimicrobial susceptibility assays

To determine the synergy of LN-1-255 with different carbapenems against OXA-48, *in vitro* susceptibility to imipenem/LN-1-255, meropenem/LN-1-255 and ertapenem/LN-1-255 was compared with susceptibility to these carbapenems in combination with the β-lactamase inhibitors clavulanic acid, sulbactam and tazobactam. Results are shown in Table 1. Type strains without any resistance mechanism were not presented because they showed very low carbapenem MIC values when OXA-48 was cloned into them (data not shown), thus the used transformants

Table 1. Carbapenem MIC values (mg/L) for the clinical and transformed bacterial strains used

	K. pneumoniae clinical strain (OXA-48)		*K. pneumoniae* Δ*ompK35/36*		*K. pneumoniae* Δ*ompK35/36* (OXA-48)		*E. coli* J53 Δ*ompC/F*		*E. coli* J53 Δ*ompC/F* (OXA-48)	
β-Lactam + inhibitor	4 mg/L	16 mg/L	4 mg/L	16 mg/L	4 mg/L	16 mg/L	4 mg/L	16 mg/L	4 mg/L	16 mg/L
Imipenem	64	64	0.5	0.5	128	128	0.25	0.25	1	1
Imipenem + TZB	64	32	0.5	0.25	128	128	0.25	0.125	1	0.5
Imipenem + SUL	64	NA	0.5	NA	128	NA	NA	NA	NA	NA
Imipenem + CLA	64	NA	0.5	NA	128	NA	NA	NA	NA	NA
Imipenem + LN	16	4	0.5	0.25	32	16	0.25	0.25	0.5	0.125
Meropenem	16	16	0.25	0.25	64	64	0.03	0.03	2	2
Meropenem + TZB	16	8	0.25	0.25	32	32	0.03	0.015	1	1
Meropenem + SUL	16	NA	0.25	NA	32	NA	NA	NA	NA	NA
Meropenem + CLA	16	NA	0.25	NA	32	NA	NA	NA	NA	NA
Meropenem + LN	8	4	0.25	0.25	16	8	0.03	0.03	0.25	0.06
Ertapenem	128	128	2	2	256	256	0.015	0.015	0.5	0.5
Ertapenem + TZB	128	32	2	1	256	128	0.015	0.007	0.5	0.25
Ertapenem + SUL	128	NA	2	NA	256	NA	NA	NA	NA	NA
Ertapenem + CLA	128	NA	2	NA	256	NA	NA	NA	NA	NA
Ertapenem + LN	64	16	2	1	64	64	0.015	0.015	0.015	0.007

TZB, tazobactam; SUL, sulbactam; CLA, clavulanic acid; LN, LN-1-255.
Data represent the means of three independent experiments.
The four inhibitors were tested at 4 mg/L using *K. pneumoniae* clinical and transformed strains. Tazobactam and LN-1-255 were tested up to 4 mg/L using transformed *E. coli*; and tazobactam and LN-1-255 were tested up to 16 mg/L using *K. pneumoniae* clinical and transformed strains.
NA, some combinations of carbapenems and inhibitors could not be tested due to intrinsic strain susceptibility. MICs for transformed *E. coli* were 16 mg/L sulbactam and 16–128 mg/L clavulanic acid and for *K. pneumoniae* strains were 32–256 mg/L (both inhibitors).

were porin deficient. As discussed above, carbapenem MICs were determined using 4 mg/L of all inhibitors and 16 mg/L LN-1-255 and tazobactam. Clavulanic acid and sulbactam could not be tested at 16 mg/L for *K. pneumoniae* strains or at 4 mg/L for *E. coli* strains, as the MICs of these two inhibitors for *K. pneumoniae* strains were 32–256 mg/L and for *E. coli* strains were 16 mg/L sulbactam and 16–128 mg/L clavulanic acid. This intrinsic susceptibility to sulbactam and clavulanic acid prevents clear observation of OXA-48 inhibition.

Neither sulbactam nor clavulanic acid at 4 mg/L were able to inhibit OXA-48 activity at any dilution in the performed assays. At 4 mg/L, tazobactam was able to inhibit OXA-48 activity in only one dilution and otherwise did not reduce MICs compared with carbapenems alone. At 4 mg/L, LN-1-255 was able to reduce carbapenem MICs 2–32-fold. These differences were amplified when 16 mg/L LN-1-255 or tazobactam was used.

The clinical *K. pneumoniae* isolate displayed an imipenem MIC of 64 mg/L, which was decreased 16-fold to 4 mg/L in the presence of LN-1-255 and 2-fold to 32 mg/L in the presence of tazobactam. Similarly, transformed *K. pneumoniae* Δ*ompK35/36* displayed an imipenem MIC of 128 mg/L, which was decreased 8-fold to 16 mg/L in the presence of 16 mg/L LN-1-255, but 0-fold in the presence of 16 mg/L tazobactam.

More pronounced differences were observed in transformed *E. coli* Δ*ompC/F*, with 8-, 32- and 64-fold reductions in imipenem, meropenem and ertapenem MICs in the presence of LN-1-255, compared with a 2-fold MIC decrease in the presence of tazobactam. The remaining data are shown in Table 1. Using transformed *E. coli* DH5α, the effect of 4 mg/L LN-1-255 on the carbapenem MIC was also more significant than that of 4 mg/L tazobactam. However, at inhibitor concentrations of 16 mg/L, this transformed strain was highly susceptible to the antimicrobial effect of the inhibitors, precluding quantitative analysis of effect sizes (data not shown).

By the chequerboard method, the combination of imipenem/LN-1-255 or imipenem alone was tested against tigecycline, colistin and amikacin. The presence of LN-1-255 decreased the MICs of tigecycline and amikacin by one dilution for the *K. pneumoniae* clinical strain and also the MIC of amikacin by one dilution for the Δ*ompK35/36* mutant. However, the FICI was >0.5, so no synergy was observed with these antimicrobials (data not shown).

Kinetics and inhibition studies

Kinetic properties of substrate hydrolysis by OXA-48 are shown in Table 2. The K_m for nitrocefin was 65.7 μM, which allowed us to use nitrocefin at 200 μM as a reporter substrate in the studies of inhibition kinetics. Similar K_m values were observed for both carbapenems tested (imipenem and ertapenem, 60.3 and 123.7 μM, respectively), but pronounced differences were observed in hydrolysis velocity (k_{cat}) for carbapenems. When converted to catalytic efficiency, this value was 10-fold higher for imipenem than ertapenem (0.025 and 0.002 $\mu M^{-1} s^{-1}$, respectively) while the catalytic efficiency of nitrocefin (4.8 $\mu M^{-1} s^{-1}$) hydrolysis was 192-fold higher than that of imipenem.

The OXA-48 inhibitory activities of LN-1-255 and tazobactam were determined and are summarized in Table 3. Using nitrocefin

as the indicator substrate, LN-1-255 showed inhibitory activity at much lower concentrations than tazobactam. Thus, the $K_{i\ app}$—analogous to the K_m for inhibitors—showed a higher affinity between the carbapenemase and LN-1-255 than between the carbapenemase and tazobactam ($K_{i\ app}$=0.17 and 30 μM, respectively).

In order to determine k_{inact} values and inactivation efficiencies (k_{inact}/K_I) of LN-1-255 and tazobactam, progress curves were fitted to Equation (3) to obtain k_{obs} values (Figure 2). These k_{obs} values were plotted against concentrations of both inhibitors and indicated faster acylation at lower concentrations of LN-1-255 than of tazobactam. However, in the case of LN-1-255, this determination could not be completed due to an inability to achieve the maximum rate. Instead, k_2/K was determined as an approximation of the inactivation efficiency (10×10^4 M^{-1} s^{-1}). The k_{inact}/K_I of tazobactam was 3000 M^{-1} s^{-1}, showing an OXA-48 inactivation efficiency >33-fold lower than that of LN-1-255. Similarly, the IC_{50} of LN-1-255 (0.003 μM) was much lower (~500-fold) than that of tazobactam (1.5 μM), indicating a higher relative efficacy of LN-1-255. Separate experiments (k_{off}) indicated that the off rate of LN-1-255 was 7×10^{-4} s^{-1}, representing a slow return of carbapenemase activity, with a half-life ($t_{1/2}$) of 16.5 min (Figure 3). In the case of tazobactam, an irreversible inhibitor, it was not possible to determine the off rate.[46]

Lastly, in determining the partition ratio (t_n) of LN-1-255 and tazobactam, the data showed a relative *I*:*E* significantly lower for LN-1-255 (t_n=2) than for tazobactam (t_n=1000), indicating 90% inhibition of OXA-48 at a much lower concentration (~500-fold) of LN-1-255 than of tazobactam (Figure 4).

Docking studies

Similar to a previously reported OXA-48/avibactam adduct (PDB 4S2K,[38] 2.1 Å; Figure 5a and c), our docking studies showed that the indolizine adduct obtained after covalent modification of the catalytic Ser-70 by LN-1-255 would also interact with residues Arg-250, Lys-208, Tyr-211 and Thr-209 (Figure 5b and d). Specifically, the carboxylate group of the modified ligand would be anchored in the active site by electrostatic interactions with the guanidinium group of Arg-250 and the ε-amino group of Lys-208 and hydrogen-bonding interaction with the hydroxyl group of Thr-209. In addition, the sulfinate group would establish an electrostatic interaction with the guanidinium group of Arg-250 and also the carboxylate group of the ester linkage would interact by hydrogen bonding with the main chain amide of Tyr-211. In contrast, our molecular docking studies predict that the catechol side chain would be more flexible. One of the phenol groups of the catechol moiety would interact by hydrogen bonding with the ε-amino group of Lys-208. This catechol moiety would partially occupy the large pocket close to the active site.

Table 2. Carbapenem and nitrocefin hydrolysis kinetics of OXA-48

Substrate	K_m (μM)	k_{cat} (s^{-1})	k_{cat}/K_m (μM^{-1} s^{-1})
Nitrocefin	65.7±18.9	314.7±18.9	4.79
Imipenem	60.3±12.4	1.5±0.1	0.025
Ertapenem	123.7±36.2	0.3±0.02	0.002

Data represent the means of three independent experiments.

Discussion

Carbapenem-hydrolysing class D β-lactamases can confer resistance to carbapenems, mostly in *A. baumannii* or Enterobacteriaceae with OXA-24/40 and OXA-48 as respective examples of such enzymes, limiting therapeutic options for infection with these pathogens.[20,21] The increasing number of clinical isolates and outbreaks of strains carrying class D carbapenemases underscores the need for new β-lactamase inhibitors that can restore carbapenem efficacy. The penicillin sulfone inhibitor LN-1-255 is a novel inhibitor of β-lactamases.[28] Initially, LN-1-255 was shown to be effective in inhibiting class A β-lactamases[31] and, subsequently, class D enzymes.[29,30] Similarly to OXA-24/40, carbapenem MICs in the presence of LN-1-255 were more significantly reduced when 16 mg/L rather than 4 mg/L LN-1-255 was used.[30]

We have thus observed inhibition of OXA-48 carbapenemases, both in a clinical isolate of *K. pneumoniae* and in porin-deficient transformed *K. pneumoniae* and *E. coli* strains. Depending on which carbapenem was used, we obtained 2–64-fold reductions in carbapenem MICs. However, in most cases, use of the inhibitors (clavulanic acid, sulbactam and tazobactam) did not alter carbapenem MICs. These results are consistent with those obtained in similar studies on OXA-24/40 inhibition, where carbapenem MICs decreased 8–32-fold in the presence of LN-1-255, but only up to 2-fold in the presence of tazobactam.[30] In this study, the porin deficit in *K. pneumoniae* slightly decreased the efficacy of LN-1-255 at 16 mg/L when combined with imipenem and ertapenem compared with the clinical strain (16-fold for imipenem and 8-fold for ertapenem); however, it increased the efficacy when combined with meropenem (MIC decreased 8-fold in the presence of 1-1-255 in the *ΔompK35/36* mutant and just 4-fold in the clinical strain. Thus, it seems that LN-1-255 is able to pass through the outer membrane, despite the porin deficit. In fact, this inhibitor was designed with a catecholic functionality that resembles a natural bacterial siderophore, enabling it to utilize the iron uptake system to traverse the outer membrane.[28]

Table 3. OXA-48 inhibition kinetics of LN-1-255 and tazobactam

Substrate	IC_{50} (μM)	$K_{i\ app}$ (μM)	K_I (μM)	k_{inact} (s^{-1})	k_{inact}/K_I (M^{-1} s^{-1})	k_2/K (M^{-1} s^{-1})	k_{off} (s^{-1})	$t_{1/2,off}$ (min)	K_d (nM)	t_n
LN-1-255	0.003±0.0003	0.17±0.01	NA	NA	NA	$(10\pm1)\times10^4$	$(7\pm1)\times10^{-4}$	16.5	7	2
Tazobactam	1.5±0.5	30±3	14±2	0.038±0.004	3000±500	NA	NA	NA	NA	1000

Data represent the means of three independent experiments. NA, not adequate.

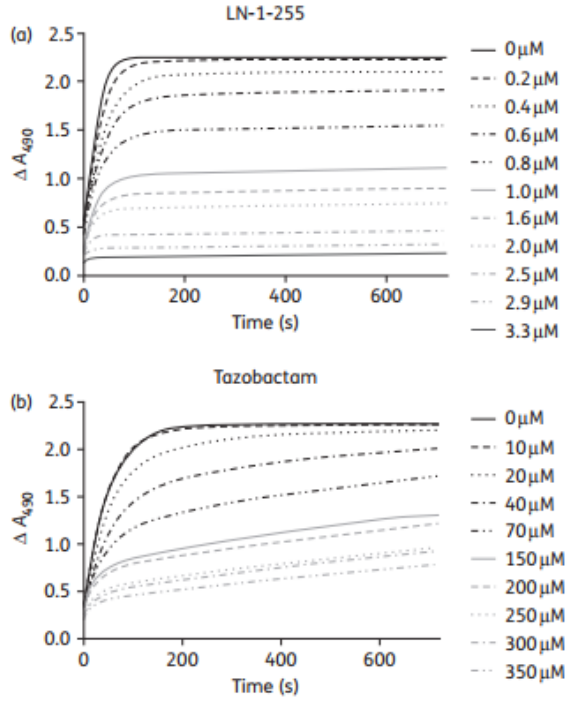

Figure 2. Progress curves of 200 μM nitrocefin hydrolysis with increasing inhibitor concentrations (0.2 μM–3.3 μM LN-1-255 and 10 μM–350 μM tazobactam) and a fixed concentration of OXA-48 (8.6 nM).

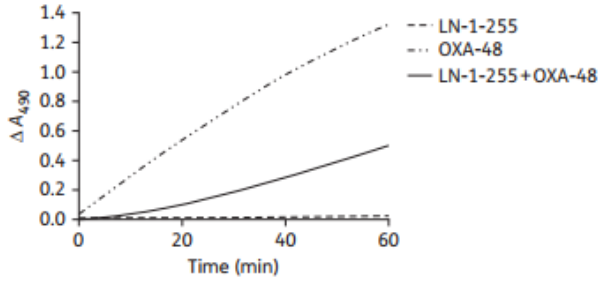

Figure 3. Progress curves for determination of off rates (k_{off}) for OXA-48/LN-1-255 and controls (OXA-48 alone and LN-1-255 alone) with 200 μM nitrocefin. OXA-48 was incubated with LN-1-255 to allow formation of the acyl-enzyme adduct and then diluted to permit enzyme reactivation.

The carbapenem hydrolysis kinetics of OXA-48 (K_m and k_{cat}) are largely concordant with those previously published by Poirel *et al.*[47,48] LN-1-255 was highly effective at inhibiting OXA-48 β-lactamase. LN-1-255 demonstrated a 33-fold higher inhibition efficiency than tazobactam, with $k_2/K = 10 \times 10^4$ M^{-1} s^{-1} and $k_{inact}/K_I = 3000$ M^{-1} s^{-1}, respectively. The inhibition due to LN-1-255 is characterized by high binding affinity, with $K_i = 0.17$ μM and $IC_{50} = 0.003$ μM, which are 180- and 500-fold lower, respectively, than those yielded using tazobactam. The off rate of LN-1-255 was moderately slow, with $k_{off} = 7 \times 10^{-4}$ s^{-1}, yielding an enzyme reactivation half-life of 16.5 min. Lastly, a partition rate (t_n) of 2

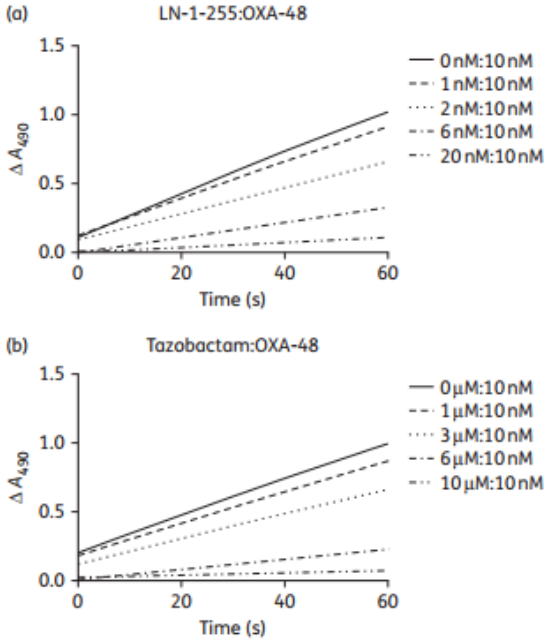

Figure 4. Progress curves for determination of t_n. OXA-48 at 10 nM was incubated with increasing concentrations of LN-1-255 (a) or tazobactam (b).

for LN-1-255 compares very favourably with that for tazobactam (>1000) required for 90% inactivation of OXA-48. These data likely indicate that LN-1-255 molecules are more slowly hydrolysed by OXA-48 than tazobactam molecules.

Regarding the *A. baumannii* OXA-24/40 carbapenemase, LN-1-255-mediated inhibition, which was previously tested by our group, proved to be similar to the binding affinity of LN-1-255 for OXA-48, with $K_{i\ app} = 0.7$ and 0.17 μM, respectively. LN-1-255 inhibition efficacies were also similar between these two enzymes, with $k_2/K = 10 \times 10^4$ M^{-1} s^{-1} for OXA-48 and $k_{inact}/K_I = 21 \times 10^4$ M^{-1} s^{-1} for OXA-24/40.[30] The crystal structure of both carbapenemases has been previously determined, OXA-48 by Docquier *et al.*[49] and OXA-24/40 by our group.[50] These two β-lactamases were the first class D carbapenemase crystal structures published and may be considered as two different carbapenemase models: although they share a common evolutionary origin, they eventually acquired their carbapenemase activity through distinct evolutionary pathways. Significant differences in the size and shape of their active sites are evident. OXA-24/40 presents a 'hydrophobic barrier' (consisting of Tyr-112 and Met-223) covering the active site, which is implicated in correct orientation of small substrates such as the carbapenems. However, this is not a conserved structure in the OXA carbapenemases and OXA-48 lacks this tunnel-like structure. By contrast, OXA-48 displays more homology with OXA-10, which is not a carbapenemase but is highly active in hydrolysing oxacillin. This ability is shared by OXA-48 but not OXA-24/40.[30,49] Despite these important differences, the compound LN-1-255 was able to inhibit both enzymes (OXA-24/40 and OXA-48) in the nM range. Later, De Luca *et al.*[51] showed that the small β5-β6 loop of

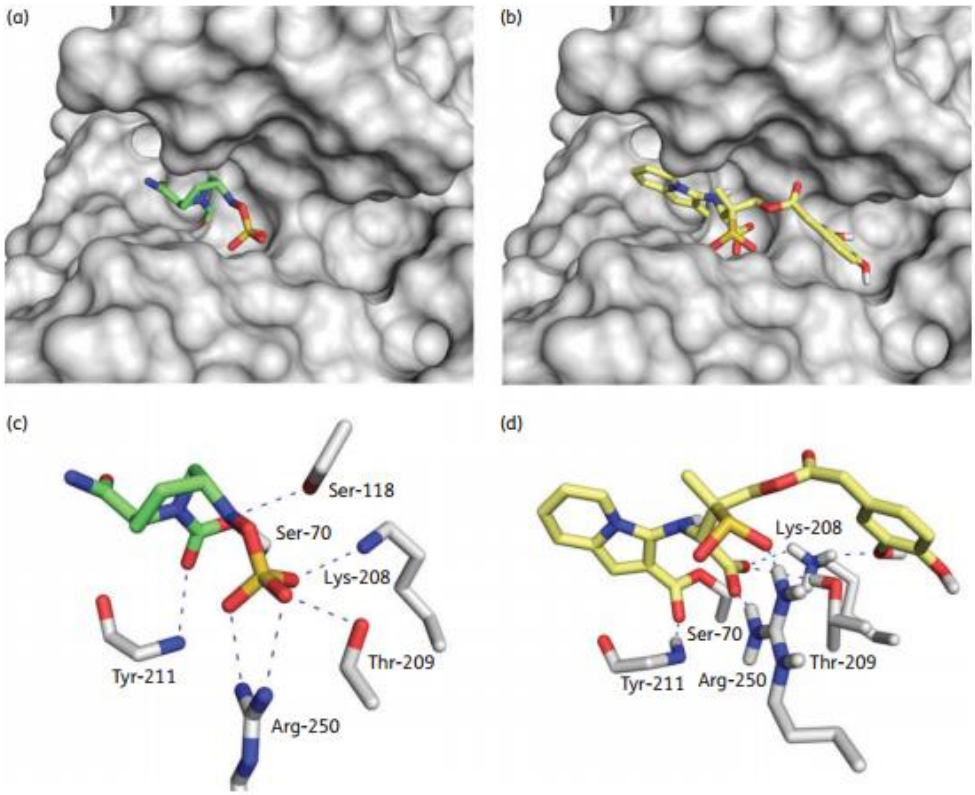

Figure 5. Docking of avibactam and LN-1-255 into the active site of OXA-48. Carbapenemase OXA-48 from *K. pneumoniae* covalently modified by avibactam and LN-1-255. (a and c) Crystal structure of OXA-48/avibactam adduct (PDB 4S2K,[44] 2.1 Å). (b and d) Inactivation of OXA-48 by LN-1-255 obtained by molecular docking studies. Hydrogen bonding and electrostatic interactions between the ligand and OXA-48 are shown as dashed blue lines. Relevant side chain residues are shown and labelled. Figure created using the PyMOL Molecular Graphics System.[53] This figure appears in colour in the online version of *JAC* and in black and white in the print version of *JAC*.

OXA-48, close to the active site, is implicated in the ability of OXA β-lactamase to hydrolyse carbapenems by facilitating movement of the deacylating water molecule towards the acylated catalytic Ser-70 residue. The relevance of this loop has been confirmed and it is present in OXA-23, OXA-24/40 and OXA-48 carbapenemases; meanwhile, it presents significant structural differences in OXA-10 β-lactamase.[49,51] This suggests that LN-1-255 interacts with this loop to prevent carbapenem access to the active site of the carbapenemases. However, further structural and biochemical work is necessary to identify the precise inhibition mechanism.

When comparing our results with those obtained by Ehmann *et al.*[52] studying avibactam and OXA-48, a new β-lactamase inhibitor, we observed a faster on rate with LN-1-255 (10×10^4 M^{-1} s^{-1} compared with 1.4×10^3 M^{-1} s^{-1} of avibactam, 71-fold lower). However, avibactam displayed a slower k_{off} (1.2×10^{-5} s^{-1}) compared with the off rate of LN-1-255 (7×10^{-4} s^{-1}), resulting in a 60-fold higher avibactam half-life.[52] Thus, the half-life of LN-1-255 of 16.5 min could be a significant drawback if used in the treatment of infections. How these kinetic data correlate to the clinical impact of these inhibitors is an issue that should be studied in experimental models of infection in the near future.

Figure 5 represents avibactam and LN-1-255 at the active binding site of OXA-48; the docking of LN-1-255 on the active site supports the inhibitory role of this compound. LN-1-255 is anchored to OXA-48, similarly to the structure of avibactam and OXA-48 published by King and Strynadka.[44] Furthermore, although avibactam is able to inhibit OXA-48, it poorly inhibits OXA-24/40 of *A. baumannii*, in contrast to LN-1-255.[26] Structurally, it has been suggested that the inhibition efficiency of LN-1-255 is mainly due to: (i) the presence of the catechol moiety that facilitates entry through the outer membrane via the cellular iron uptake pathway; and (ii) the incorporation of a (2-pyridyl)methylene group at C6 in the sulbactam core that results in the formation of an heterocyclic (indolizine) ester derivative that is resistant to hydrolysis.[26] Despite the high stability of the heterocyclic esters, LN-1-255 proved to have a higher k_{off} (7×10^{-4} s^{-1}) against OXA-48 from *K. pneumoniae* than avibactam (1.2×10^{-5} s^{-1}). It has been suggested that avibactam does not decompose via a hydrolytic mechanism of the carbamoyl linkage with the catalytic serine of the carbapenemase. Instead, it seems to occur via regeneration of the diazobicyclooctane moiety. Both acyl-enzyme intermediates are electronically

stabilized towards attack of water through resonance interactions of the acyl-enzyme carbonyl group with the lone pair of electrons on an adjacent nitrogen atom. Instead of being an ester linkage, the avibactam acyl-enzyme is a urethane, while that of LN-1-255 is a vinylogous urethane. It is likely that the more sterically bulky environment surrounding the avibactam acyl-enzyme linkage interferes with the approach of the hydrolytic water, while the more two-dimensional vinylogous urethane allows this approach to a limited extent. Also, the more bulky nature of the avibactam moiety in the site may preclude conformational movement of the inhibitor fragment to allow approach of nucleophiles to the carbonyl, thus limiting the approaching nucleophiles to the already well-positioned sulfamoyl nitrogen and regenerating the inhibitor itself. LN-1-255, by contrast, likely has more conformational freedom, potentially leading to movement that disrupts the planarity needed for resonance stabilization of the acyl-enzyme carbonyl group.

We consider that, in addition, there are some differences in the binding mode of both modified ligands that could also contribute to the lower stability of the OXA-48/LN-1-255 adduct than the corresponding OXA-48/avibactam. Comparison of the binding mode of the modified avibactam shown in the crystal structure of the OXA-48/avibactam adduct (PDB 4S2K)[44] and the predicted binding mode of the corresponding OXA-48/LN-1-255 adduct obtained by molecular docking studies revealed that both adducts interact with mainly the same active site residues, specifically, Arg-250, Lys-208, Tyr-211 and Thr-209. However, as illustrated in Figure 5, there are some differences in the binding contacts of the groups that most contribute to anchor the ligand in the active site, the sulphate of avibactam and sulfinate/carboxylate of LN-1-255 groups that might explain their different behaviour. While the sulphate group in the avibactam adduct is deeply anchored in the active site through a salt bridge with Arg-250 and hydrogen bonding with the Thr-209 side chain (Figure 5c), the sulfinate group in the modified LN-1-255 only interacts by electrostatic interaction with Arg-250 (Figure 5d). We consider that the latter is a consequence of the lack of the hydrophobic barrier present in OXA-24/40, which involves mainly residues Tyr-112 and Met-223.[30] In this case, the carboxylate group of the modified LN-1-255 interacts by hydrogen bonding with the phenol group of Tyr-112. As a consequence, the sulfinate group can be located pointing inwards. As in the crystal structure of the OXA-48/avibactam adduct, the latter group would interact by a salt bridge with the guanidinium group of Arg-261 and hydrogen bonding with the Ser-128 side chain. These binding differences might account for the overall difference in stability of the two adducts as experimentally observed (on and off rates).

Due to structural and mechanistic differences among class D carbapenemases,[49] this area of drug discovery requires further studies to identify additional inhibitors as possible therapeutic options. The results presented here provide stimulus for further *in vitro* and *in vivo* investigations to maximize the efficacy of penicillin sulfone inhibition of class D carbapenemases in Enterobacteriaceae.

Acknowledgements

We thank Dr Sebastian Albetí for the kind gift of the strain *K. pneumoniae ΔompK35/36*.

Funding

This work was supported by the Spanish National Plans for Scientific Research, Development and Technological Innovation 2013-16 and funded by the ISCIII-General Subdirection of Assessment and Promotion of the Research-European Regional Development Fund (ERDF) 'A way of making Europe': PI12/00552 to G. B. and PI14/00059 to M. P. and A. B. Also, research reported in this publication was supported in part by the National Institute of Allergy and Infectious Diseases of the National Institutes of Health (USA) under Award Numbers R01AI100560, R01AI063517 and R01AI072219 to R. A. B. This study was supported in part by funds and/or facilities provided by the Cleveland Department of Veterans Affairs (USA), Award Number 1I01BX001974 to R. A. B. from the Biomedical Laboratory Research & Development Service of the VA Office of Research and Development and the Geriatric Research Education and Clinical Center VISN 10 (USA) to R. A. B. This study was also supported by the Spanish Ministry of Economy and Competiveness (SAF2013-42899-R), Xunta de Galicia (Spain) (GRC2013-041) and the European Regional Development Fund (ERDF) to C. G.-B, and supported by National Institutes of Health (USA) to J. D. B. (1R15AI109624). J. V. A. was financially supported by the Sara Borrell Programme ISCIII-FEDER (CD13/00373). J. V. H. and A. B. were financially supported by the Miguel Servet Programme ISCIII-FEDER (CP13/00226).

Transparency declarations

None to declare.

Disclaimer

The content is solely the responsibility of the authors and does not represent the official views of the National Institutes of Health or the Department of Veterans Affairs.

References

1 The White House. *National Strategy to Combat Antibiotic-Resistant Bacteria*. 2014. http://www.cdc.gov/drugresistance/federal-engagement-in-ar/national-strategy/index.html.

2 Bush K, Jacoby GA. Updated functional classification of β-lactamases. *Antimicrob Agents Chemother* 2010; **54**: 969–76.

3 Oteo J, Perez-Vazquez M, Campos J. Extended-spectrum β-lactamase producing *Escherichia coli*: changing epidemiology and clinical impact. *Curr Opin Infect Dis* 2010; **23**: 320–6.

4 Walsh TR. Emerging carbapenemases: a global perspective. *Int J Antimicrob Agents* 2010; **36** Suppl 3: S8–14.

5 Poirel L, Naas T, Nordmann P. Diversity, epidemiology, and genetics of class D β-lactamases. *Antimicrob Agents Chemother* 2010; **54**: 24–38.

6 Bonnin RA, Nordmann P, Poirel L. Screening and deciphering antibiotic resistance in *Acinetobacter baumannii*: a state of the art. *Expert Rev Anti Infect Ther* 2013; **11**: 571–83.

7 Poirel L, Potron A, Nordmann P. OXA-48-like carbapenemases: the phantom menace. *J Antimicrob Chemother* 2012; **67**: 1597–606.

8 Nordmann P, Poirel L. The difficult-to-control spread of carbapenemase producers among Enterobacteriaceae worldwide. *Clin Microbiol Infect* 2014; **20**: 821–30.

9 Arana DM, Saez D, Garcia-Hierro P *et al*. Concurrent interspecies and clonal dissemination of OXA-48 carbapenemase. *Clin Microbiol Infect* 2015; **21**: 148.e1-4.

10 Branas P, Villa J, Viedma E *et al*. Molecular epidemiology of carbapenemase-producing *Klebsiella pneumoniae* in a hospital in Madrid: successful establishment of an OXA-48 ST11 clone. *Int J Antimicrob Agents* 2015; **46**: 111–6.

11 Grundmann H, Livermore DM, Giske CG *et al*. Carbapenem-non-susceptible Enterobacteriaceae in Europe: conclusions from a meeting of national experts. *Euro Surveill* 2010; **15**: pii=19711.

12 Dortet L, Cuzon G, Nordmann P. Dissemination of carbapenemase-producing Enterobacteriaceae in France, 2012. *J Antimicrob Chemother* 2014; **69**: 623–7.

13 Nordmann P, Naas T, Poirel L. Global spread of carbapenemase-producing Enterobacteriaceae. *Emerg Infect Dis* 2011; **17**: 1791–8.

14 Oteo J, Miró E, Pérez-Vázquez M *et al*. Evolution of carbapenemase-producing Enterobacteriaceae at the global and national level: what should be expected in the future? *Enferm Infecc Microbiol Clin* 2014; **32** Suppl 4: 17–23.

15 Canton R, Akova M, Carmeli Y *et al*. Rapid evolution and spread of carbapenemases among Enterobacteriaceae in Europe. *Clin Microbiol Infect* 2012; **18**: 413–31.

16 Glasner C, Albiger B, Buist G *et al*. Carbapenemase-producing Enterobacteriaceae in Europe: a survey among national experts from 39 countries, February 2013. *Euro Surveill* 2013; **18**: pii=20525.

17 Pitart C, Sole M, Roca I *et al*. First outbreak of a plasmid-mediated carbapenem-hydrolyzing OXA-48 β-lactamase in *Klebsiella pneumoniae* in Spain. *Antimicrob Agents Chemother* 2011; **55**: 4398–401.

18 Potron A, Kalpoe J, Poirel L *et al*. European dissemination of a single OXA-48-producing *Klebsiella pneumoniae* clone. *Clin Microbiol Infect* 2011; **17**: E24–6.

19 Poirel L, Bonnin RA, Nordmann P. Genetic features of the widespread plasmid coding for the carbapenemase OXA-48. *Antimicrob Agents Chemother* 2012; **56**: 559–62.

20 Falagas ME, Karageorgopoulos DE, Nordmann P. Therapeutic options for infections with Enterobacteriaceae producing carbapenem-hydrolyzing enzymes. *Future Microbiol* 2011; **6**: 653–66.

21 Bradford PA, Kazmierczak KM, Biedenbach DJ *et al*. Colistin-resistant Enterobacteriaceae: correlation of β-lactamase production and colistin resistance among isolates from a global surveillance program. *Antimicrob Agents Chemother* 2015; **60**: 1385–92.

22 Liu YY, Wang Y, Walsh TR *et al*. Emergence of plasmid-mediated colistin resistance mechanism MCR-1 in animals and human beings in China: a microbiological and molecular biological study. *Lancet Infect Dis* 2015; **16**: 161–8.

23 Perez-Llarena FJ, Bou G. β-Lactamase inhibitors: the story so far. *Curr Med Chem* 2009; **16**: 3740–65.

24 Zhanel GG, Lawson CD, Adam H *et al*. Ceftazidime-avibactam: a novel cephalosporin/β-lactamase inhibitor combination. *Drugs* 2013; **73**: 159–77.

25 Drawz SM, Papp-Wallace KM, Bonomo RA. New β-lactamase inhibitors: a therapeutic renaissance in an MDR world. *Antimicrob Agents Chemother* 2014; **58**: 1835–46.

26 Lahiri SD, Mangani S, Jahic H *et al*. Molecular basis of selective inhibition and slow reversibility of avibactam against class D carbapenemases: a structure-guided study of OXA-24 and OXA-48. *ACS Chem Biol* 2015; **10**: 591–600.

27 Buynak JD. The discovery and development of modified penicillin- and cephalosporin-derived β-lactamase inhibitors. *Curr Med Chem* 2004; **11**: 1951–64.

28 Buynak JD, Rao AS, Doppalapudi VR *et al*. The synthesis and evaluation of 6-alkylidene-2′β-substituted penam sulfones as β-lactamase inhibitors. *Bioorg Med Chem Lett* 1999; **9**: 1997–2002.

29 Drawz SM, Bethel CR, Doppalapudi VR *et al*. Penicillin sulfone inhibitors of class D β-lactamases. *Antimicrob Agents Chemother* 2010; **54**: 1414–24.

30 Bou G, Santillana E, Sheri A *et al*. Design, synthesis, and crystal structures of 6-alkylidene-2′-substituted penicillanic acid sulfones as potent inhibitors of *Acinetobacter baumannii* OXA-24 carbapenemase. *J Am Chem Soc* 2010; **132**: 13320–31.

31 Pattanaik P, Bethel CR, Hujer AM *et al*. Strategic design of an effective β-lactamase inhibitor: LN-1-255, a 6-alkylidene-2′-substituted penicillin sulfone. *J Biol Chem* 2009; **284**: 945–53.

32 Barba MJ, Fernandez A, Vindel A *et al*. Brotes simultáneos producidos por una cepa de *Klebsiella pneumoniae* productora de CTX-M-15 y OXA-48 y por otra cepa diferente productora de CTX-M-15 en el Complejo Hospitalario Universitario A Coruña (CHUAC). In: *Abstracts of the Eighteenth Spanish Meeting of Clinical Microbiology and Infectious Diseases, Valencia, 2014*. Abstract 51, p. 42. Spanish Society of Clinical Microbiology and Infectious Diseases, Madrid, Spain.

33 Beceiro A, Maharjan S, Gaulton T *et al*. False extended-spectrum β-lactamase phenotype in clinical isolates of *Escherichia coli* associated with increased expression of OXA-1 or TEM-1 penicillinases and loss of porins. *J Antimicrob Chemother* 2011; **66**: 2006–10.

34 Garcia-Sureda L, Juan C, Domenech-Sanchez A *et al*. Role of *Klebsiella pneumoniae* LamB porin in antimicrobial resistance. *Antimicrob Agents Chemother* 2011; **55**: 1803–5.

35 Beceiro A, Perez-Llarena FJ, Perez A *et al*. Molecular characterization of the gene encoding a new AmpC β-lactamase in *Acinetobacter baylyi*. *J Antimicrob Chemother* 2007; **59**: 996–1000.

36 Clinical and Laboratory Standards Institute. *Methods for Dilution Antimicrobial Susceptibility Tests for Bacteria that Grow Aerobically–Tenth Edition: Approved Standard M07-A10*. CLSI, Wayne, PA, USA, 2015.

37 Odds FC. Synergy, antagonism, and what the chequerboard puts between them. *J Antimicrob Chemother* 2003; **52**: 1.

38 Golemi D, Maveyraud L, Vakulenko S *et al*. Critical involvement of a carbamylated lysine in catalytic function of class D β-lactamases. *Proc Natl Acad Sci USA* 2001; **98**: 14280–5.

39 Papp-Wallace KM, Winkler ML, Taracila MA *et al*. Variants of β-lactamase KPC-2 that are resistant to inhibition by avibactam. *Antimicrob Agents Chemother* 2015; **59**: 3710–7.

40 Papp-Wallace KM, Mallo S, Bethel CR *et al*. A kinetic analysis of the inhibition of FOX-4 β-lactamase, a plasmid-mediated AmpC cephalosporinase, by monocyclic β-lactams and carbapenems. *J Antimicrob Chemother* 2014; **69**: 682–90.

41 Bethel CR, Taracila M, Shyr T *et al*. Exploring the inhibition of CTX-M-9 by β-lactamase inhibitors and carbapenems. *Antimicrob Agents Chemother* 2011; **55**: 3465–75.

42 Ehmann DE, Jahic H, Ross PL *et al*. Avibactam is a covalent, reversible, non-β-lactam β-lactamase inhibitor. *Proc Natl Acad Sci USA* 2012; **109**: 11663–8.

43 Cambridge Crystallographic Data Centre. http://www.ccdc.cam.ac.uk/products/life_sciencies/gold/.

44 King DT, Strynadka NCJ. The X-ray crystal structure is available from the Protein Data Bank (PDB: 4S2K). OXA-48 in complex with avibactam at pH 7.5. http://www.rcsb.org/pdb/explore/explore.do?structureId=4S2K.

45 Frisch GWT, Schlegel HB, Scuseria GE *et al*. *Gaussian 09, Revision A.2*. Wallingford, CT: Gaussian, 2009.

46 Bush K, Macalintal C, Rasmussen BA *et al*. Kinetic interactions of tazobactam with β-lactamases from all major structural classes. *Antimicrob Agents Chemother* 1993; **37**: 851–8.

47 Poirel L, Castanheira M, Carrer A *et al*. OXA-163, an OXA-48-related class D β-lactamase with extended activity toward expanded-spectrum cephalosporins. *Antimicrob Agents Chemother* 2011; **55**: 2546–51.

48 Poirel L, Heritier C, Tolun V *et al.* Emergence of oxacillinase-mediated resistance to imipenem in *Klebsiella pneumoniae*. *Antimicrob Agents Chemother* 2004; **48**: 15–22.

49 Docquier JD, Calderone V, De Luca F *et al.* Crystal structure of the OXA-48 β-lactamase reveals mechanistic diversity among class D carbapenemases. *Chem Biol* 2009; **16**: 540–7.

50 Santillana E, Beceiro A, Bou G *et al.* Crystal structure of the carbapenemase OXA-24 reveals insights into the mechanism of carbapenem hydrolysis. *Proc Natl Acad Sci USA* 2007; **104**: 5354–9.

51 De Luca F, Benvenuti M, Carboni F *et al.* Evolution to carbapenem-hydrolyzing activity in noncarbapenemase class D β-lactamase OXA-10 by rational protein design. *Proc Natl Acad Sci USA* 2011; **108**: 18424–9.

52 Ehmann DE, Jahic H, Ross PL *et al.* Kinetics of avibactam inhibition against class A, C, and D β-lactamases. *J Biol Chem* 2013; **288**: 27960–71.

53 DeLano WL. *The PyMOL Molecular Graphics System*. Palo Alto, CA: DeLano Scientific, 2008. http://www.pymol.org/.

VIRULENCE, 2018
VOL. 9, NO. 1, 496–509
https://doi.org/10.1080/21505594.2017.1420451

Taylor & Francis
Taylor & Francis Group

RESEARCH PAPER

OPEN ACCESS Check for updates

Pneumonia infection in mice reveals the involvement of the *feoA* gene in the pathogenesis of *Acinetobacter baumannii*

Laura Álvarez-Fraga†, Juan C. Vázquez-Ucha†, Marta Martínez-Guitián†, Juan A. Vallejo, Germán Bou, Alejandro Beceiro‡, and Margarita Poza‡

Servicio de Microbiología, Instituto de Investigación Biomédica (INIBIC), Complejo Hospitalario Universidade (CHUAC), Universidad da Coruña (UDC), A Coruña, Spain

ABSTRACT

Acinetobacter baumannii has emerged in the last decade as an important nosocomial pathogen. To identify genes involved in the course of a pneumonia infection, gene expression profiles were obtained from *A. baumannii* ATCC 17978 grown in mouse infected lungs and in culture medium. Gene expression analysis allowed us to determine a gene, the A1S_0242 gene (*feoA*), over-expressed during the pneumonia infection. In the present work, we evaluate the role of this gene, involved in iron uptake. The inactivation of the A1S_0242 gene resulted in an increase susceptibility to oxidative stress and a decrease in biofilm formation, in adherence to A549 cells and in fitness. In addition, infection of *G. mellonella* and pneumonia in mice showed that the virulence of the Δ0242 mutant was significantly attenuated. Data presented in this work indicated that the A1S_0242 gene from *A. baumannii* ATCC 17978 strain plays a role in fitness, adhesion, biofilm formation, growth, and, definitively, in virulence. Taken together, these observations show the implication of the *feoA* gene plays in the pathogenesis of *A. baumannii* and highlight its value as a potential therapeutic target.

ARTICLE HISTORY
Received 14 July 2017
Revised 14 December 2017
Accepted 19 December 2017

KEYWORDS
Acinetobacter baumannii; iron uptake; virulence; animal infection models

Introduction

Acinetobacter baumannii is a Gram negative, non-fermentative, and non-flagellated bacillus. Although it is a normal inhabitant of human skin, intestinal tract and respiratory system, it is currently considered one of the most dangerous opportunistic pathogens. Recently, the World Health Organization included *A. baumannii* in a list of the most important antibiotic resistant pathogens [1]. This bacterium exhibits an excellent ability to develop antibiotic resistance which often results in strains resistant to several antimicrobial families [2,3]. Carbapenems are broadly used to treat *A. baumannii* multiresistant strains; however, resistance to these antimicrobials increased dangerously in the last decade [4]. Similarly, an increment of resistance rates is emerging in the case of last resort antimicrobials such as colistin [5] or tigecycline [6]. Resistance to these antimicrobials has also appeared which lead us to the urgent need to design and evaluate new antimicrobial therapies. In the last decades, the number of hospital outbreaks caused by *A. baumannii* has increased noticeably, partly due to its multidrug resistance profile [2,7–10]. Although the clinical importance of *A. baumannii* infections has increased, the pathogenicity of this microorganism is sparsely understood. Clinical *A. baumannii* strains exhibit remarkably variations in virulence-associated phenotypes such as motility, adherence, biofilm formation, invasion, iron uptake or cell capsule development among others [11,12]. Some studies have shown that *Acinetobacter* species may reach the human skin and mucosal membranes and then colonize and persist on the host several weeks [13]. Bacterial adherence constitutes an essential step in the colonization process. The ability of the AbH12O-A2 strain, which caused the largest outbreak of *A. baumannii* known worldwide [14–19], to adhere to human cells was one of the main factors involved in its persistence [14]. After adhesion, bacteria may form biofilms that are involved in the persistence of this pathogen in the hospital environment. Some components, such as the staphylococcal biofilm-associated protein (Bap), the CsuA/BABCDE usher-chaperone system or the poly-beta-1–6-*N*-acetylglucosamine have been

CONTACT Margarita Poza margarita.poza.dominguez@sergas.es; Alejandro Beceiro alejandro.beceiro.casas@sergas.es Servicio de Microbiología, 3ª planta Hospital Universitario, As Xubias S/N, 15006 A Coruña, Spain.
†Authors contributed equally to this work.
‡Both authors contributed equally to this work (being Alejandro Beceiro and Margarita Poza the both authors).
Supplemental data for this article can be accessed on the publisher's website at www.tandfonline.com/kvir.

described as involved in the *A. baumannii* biofilm formation and adherence phenotypes [20–24]. The outer membrane protein OmpA plays a role in biofilm formation on abiotic surfaces and has been shown to promote the adherence to eukaryotic host and invasion [25].

Iron is essential for growth in most bacteria due to its redox activity and its role in many vital metabolic reactions, being a cofactor for many bacterial enzymes. Therefore, iron is necessary for bacteria to infect and multiply in tissues and body fluids of the host, playing a relevant role in pathogenesis [26]. Under *in vivo* conditions, iron is not readily available due to cells uptake or sequestration by proteins such as transferrin or lactoferrin, which are components of the innate immunity system that provide defense against pathogens [27,28]. Bacteria encode multiple iron uptake pathways, which provide specificities and affinities for various forms of environmental or host iron. Under iron-limited conditions many invading bacteria respond by producing specific iron chelators, such as siderophores, that remove the iron from the host sources [29-31]. In addition, many bacteria, such as *Escherichia coli, Shigella flexneri, Helicobacter pylori, Campylobacter jejuni* or *Legionella pneumophila*, take up soluble ferrous iron *via* the Feo system [32–40], which is proposed to be the major ferrous iron transport system known in prokaryotes [41]. The Feo system was first identified in *E. coli* [42,43] and it is encoded by the *feoABC* operon. FeoB, a bacterial ferrous iron transporter, is composed of a hydrophilic cytoplasmic domain and an integral membrane domain [44,45]. The C-terminal membrane domain of FeoB is responsible for the formation of a pore in the membrane and the N-terminal contains a GTP-binding domain that regulates the transport activity. The roles of *feoA* and *feoC* remain unknown although *feoC* is predicted to encode for a transcriptional repressor of *feoAB* [32,43,45]. In pathogenic bacteria such as *E. coli*, *H. pylori* or *L. pneumophila*, mutations in the *feoB* gene have been shown to cause deficiency in ferrous iron uptake and virulence [26,33,37–39], including assays emulating conditions encountered during infection of a mammalian host [46]. High-throughput sequencing technologies demonstrated the presence of the Feo system in 50 clinical strains of *A. baumannii* [47].

In the present work, we identified a gene over-expressed during the course of the lung infection of *A. baumannii* in mice, the A1S_0242 gene (*feoA*). We evaluated the role of this gene in fitness, biofilm production, attachment to biotic surfaces, resistance to oxidative stress, and, finally, in the pathogenesis of *A. baumannii* using *Galleria mellonella* and murine pneumonia models.

Results

Genetic context of the feoA *gene*

Transcriptomic analysis revealed a collection of genes differentially expressed in the *A. baumannii* lung infection model. Raw data have been deposited in the GEO database under the accession code GSE100552. Between them, the A1S_0242 (*feoA*) gene was over-expressed in bacteria over the course of the lung infection compared to bacteria grown in LB media, as shown by Illumina (2.67-fold more +/− 0.75) and qRT-PCR (6.34-fold more +/− 2.03) analysis.

The genetic context of this gene was studied. The *feoA* gene, previously annotated in the ATCC 17978 genome (CP018664.1) as a putative ferrous iron transporter protein A containing a *feoA* domain, was found as part of a single operon comprising genes A1S_0242, A1S_0243 and A1S_0244, as assessed by RNA reverse transcription (Figure 1). The A1S_0243 gene was annotated in the ATCC 17978 genome (CP018664.1) as a ferrous transport protein B harboring a *feoB* domain. The A1S_0244 gene was found as a hypothetical protein, with no conserved domains. Real time RT-PCR assays confirmed that both A1S_0243 and A1S_0244 surrounding genes were over-expressed during the lung infection (1.95-fold more +/− 0.36 and 2.78-fold more +/− 0.96, respectively) compared with genes from bacteria grown in LB-flasks.

Moreover, two homologues to the A1S_0242 gene were found in the *A. baumannii* ATCC 17978 genome (CP018664.1). These genes were A1S_3850 and A1S_0652 that showed 53% and 54% of identity with the *feoA* gene, respectively. The A1S_3850 gene, previously annotated in the ATCC 17978 genome as a hypothetical

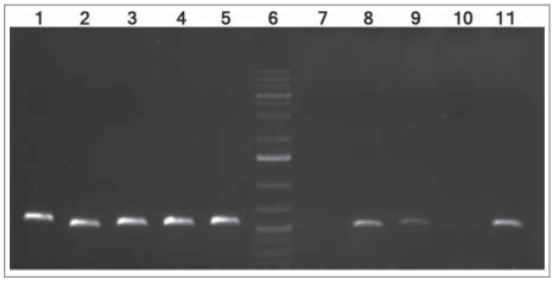

Figure 1. cDNA amplification of genes from the A1S_0242–0244 operon of *A. baumannii* ATCC 17978 strain. The intergenic regions from genes A1S_0242–0243 and A1S_0243–0244 are shown in lanes 8 and 9, respectively. The intergenic regions from genes A1S_0241–0242 and A1S_0244–0245 are shown in lanes 7 and 10, respectively (negative controls). Genomic DNA was used as template for positive control (lanes 1 to 5, respectively). Lanes 5 and 11 show the *gyrB* amplification from DNA and cDNA, respectively (positive controls). Lane 6 shows GeneRuler 1 Kb Plus DNA Ladder (Thermo Fisher Scientific).

protein, is part of a single operon comprising genes A1S_2929, A1S_3850 and A1S_2930 (data not shown). The A1S_2929 and the A1S_2930 genes were annotated as a putative cation efflux system protein and a putative ferrous iron transport protein B containing a *feoB* domain, respectively. The A1S_0652 gene was annotated as a putative ferrous iron transport protein A containing a *feoA* domain followed by the A1S_0653 gene encoding a putative ferrous iron transport protein B. Deeper bioinformatic analysis revealed that the A1S_0652 gene was located in the plasmid pAB3 (GenBank accession number CP012005) of the *A. baumannii* ATCC 17978-mff strain (CP012004.1) while the A1S_3850 was found in the chromosome.

All the publicly available complete genomes of *A. baumannii* were analyzed in order to find the A1S_0242 and the A1S_3850 genes. The A1S_0242 gene was found in the 100% of the 76 *A. baumannii* complete genomes analyzed, while the A1S_3850 gene was located in the 14.5% of them. Similarly, in species such as *A. pittii*, *A. nosocomialis*, *A. soli* or *A. calcoaceticus*, the A1S_3850 gene was occasionally found while the A1S_0242 gene was present in all the analyzed genomes.

The discovery of these two A1S_0242 homologues induced us to investigate possible interactions between those three genes, being the A1S_0242 gene the main objective of our work. Gene knockout mutants of the ATCC 17978 strain lacking the A1S_0242 and A1S_3850 genes were constructed in order to analyze their interaction. Therefore, the isogenic mutant derivatives Δ0242 and Δ3850 strains as well as the double mutant Δ0242/Δ3850 strain were obtained. Due to the plasmid location of the A1S_0652 gene, it was not possible to perform a knockout mutant lacking this gene.

The complementation of the A1S_0242 gene with the parental allele (Δ0242 complemented) was performed through the over-expression of the gene cloned into the pWH1266-Km vector. Data from qRT-PCR analysis revealed that indeed the A1S_0242 was highly over-expressed under the control of the tetracycline promoter compared to its expression in the wild type gene (Table S1). As expected, the Δ0242 strain, as well as the Δ0242 strain harboring the empty pWH1266-Km vector (Δ0242 + pWH1266-Km), revealed no expression of the A1S_0242 gene. Table S1 also shows that there is no expression of the A1S_3850 gene in the Δ3850 strain and the over-expression of the A1S_3850 gene from the plasmid was confirmed.

Also qRT-PCR analyses were performed in order to investigate the effects of the lack of the A1S_0242 gene on the expression of its homologue genes. Data revealed that when the A1S_0242 gene was absent, the A1S_3850 and the A1S_0652 genes maintained their expression levels (Table 1). Also, the deletion of the A1S_3850 did not vary the expression of the A1S_0242 gene whereas the expression of the A1S_0652 gene increased. In addition, the deletion of both A1S_0242 and A1S_3850 genes revealed a minimal increase in the A1S_0652 expression level, due to the effect of the A1S_3850 gene.

Next, the abilities of the Δ0242 strain and its isogenic derivative mutants were tested under *in vitro* and *in vivo* conditions to confirm the role of this gene in fitness and virulence. The A1S_3850 mutants were also included in some assays in order to discard its relevance in the pathogenesis of the ATCC 17978 strain.

Effects of the feoA gene deletion and vector loading on fitness

To determine whether the deletion of genes A1S_0242 and A1S_Δ3850 affect the bacterial growth rate, growth curve rates were measured in iron-sufficient and iron-restricted media. Determination of the growth rate constant (μ) gives a measure of fitness or replication ability [48]. The growth rates of the Δ0242 mutant did not show significant differences compared to the wild type strain in presence of iron (Figure 2). However, when the metal chelator 2,2′-bipyridil (BIP) was added to the medium, the mean generation of the Δ0242 mutant was higher (65 min, $\mu = 0.0105 +/- 0.0003$) with respect to the ATCC 17978 strain (45 min, $\mu = 0.015 +/- 0.0012$), showing significant differences in fitness ($p > 0.05$). In contrast, the deletion of A1S_Δ3850 did not show inhibition of growth compared with the ATCC 17978 parental strain. In agreement with these results, the double mutant Δ0242/Δ3850 showed a growth rate similar to the single mutant Δ0242 in BIP presence (Figure 2).

Studies of bacterial growth performed with the ATCC 17978 derivative strains carrying the pWH1266-Km vector showed that this plasmid load represents a very relevant biological cost, as shown in Figure S1. These means that all the strains carrying the pWH1266-Km vector showed a significantly lower fitness than the wild type strain. For this reason, complemented strains were not included in assays where the growth rate was limiting.

Table 1. Interaction of genes A1S_0242, A1S_3850 and A1S_0652 measured by qRT-PCR.

	ATCC 17978	Δ0242*	Δ3850*	Δ0242/Δ3850*
A1S_0242	1	0	1.02 +/− 0.32	0
A1S_0652	1	0.97 +/− 0.21	2.73 +/− 1.09	1.11 +/− 0.48
A1S_3850	1	0.97 +/− 0.04	0	0

*Data were obtained as a fold-change relative to the ATCC 17978 sample (value 1), using the *rpoB* gene as housekeeping for normalization.

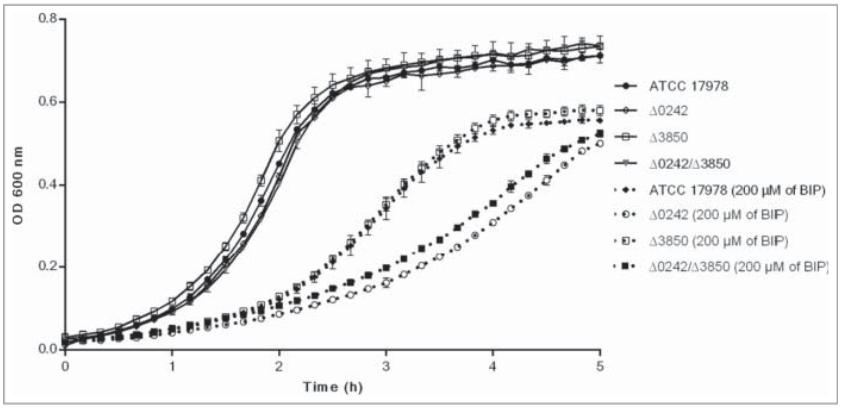

Figure 2. Growth curves of the ATCC 17978 strain and the isogenic mutant derivative strains Δ0242, Δ3850 and Δ0242/Δ3850 in presence and absence of the iron chelator 2,2′-bipyridyl (BIP). Data correspond to the mean of three replicates and bars represent the standard deviations.

The feoA *gene deletion reduces biofilm formation and attachment to eukaryotic cells abilities*

The biofilm formation ability was evaluated and the Δ0242 mutant derivative strain showed a significant decrease (*ca.* 2,15-fold less, $p = 0.0034$) with respect to the ATCC 17978 parental strain (Figure 3). Complementation of the strain with the parental allele partially restored the biofilm formation phenotype. Deletion of the A1S_3850 revealed no significant differences in biofilm formation with respect to the wild type strain. Biofilm formation was similar for the single Δ0242 and the double mutant Δ0242/Δ3850 strains.

As shown in Figure 4, the inactivation of the A1S_0242 gene led to a reduction in the ability of the *A. baumannii* strain ATCC 17978 to adhere to human alveolar epithelial cells A549 (*ca.* 4-fold, p value < 0.0001). In this case, the fitness of the strains was a limiting factor as can be seen in Figure S2, the wild type strain harboring the plasmid (ATCC 17978 + pWH1266-Km) showed an important decrease in biofilm formation ability, compared with the wild type strain (ATCC 17978). The complemented strain (Δ0242 complemented) partially restored the wild type phenotype loading plasmid (ATCC 17978 + pWH1266-Km), as reflected in Figure S2. As shown in Figure S1, all strains harboring the pWH1266-Km vector resulted in an increase in the lag time and in a lower optical density at the end of growth curve analysis, which indicates a fitness decrease caused by the plasmid metabolic load. Besides, the Δ3850 strain showed no significant differences with respect to the wild type and the double mutant strain showed similar attachment abilities as the Δ0242 strain (Figure 4). No invasiveness was detected at 24 h in all cases (data not shown).

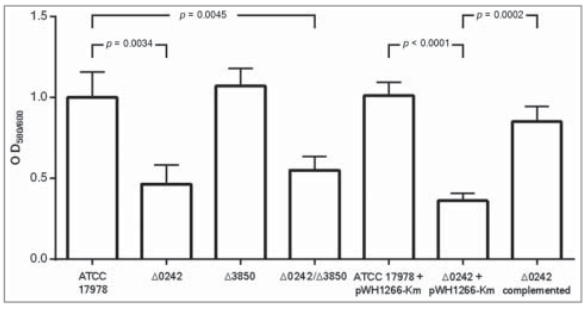

Figure 3. Quantification of biofilm formation by the *A. baumannii* ATCC 17978 strain, the mutant derivative strain Δ0242, the mutant derivative strain Δ3850, the double mutant derivative strain Δ0242/Δ3850, the ATCC 17978 harboring the empty vector pWH1266-Km (ATCC 17978 + pWH1266-Km), the mutant derivative strain harboring the empty vector pWH1266-Km (Δ0242 + pWH1266-Km) and the mutant derivative Δ0242 over-expressing the A1S_0242 gene from the pWH1266-Km plasmid (Δ0242 complemented).

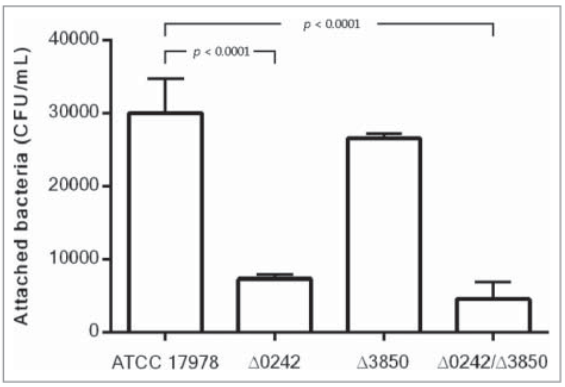

Figure 4. Quantification of bacterial adhesion to A549 cells by the *A. baumannii* ATCC 17978 strain, the mutant derivative strain Δ0242, the mutant derivative strain Δ3850 and the double mutant strain Δ0242/Δ3850.

Effects of the feoA gene inactivation on susceptibility to oxidative stress

When strains were subjected to reaction oxygen species (ROS) by the addition of paraquat in the presence of 100 μM of the iron chelator 2,2′-bypiridyl (BIP), the Δ0242 mutant strain showed a MIC to paraquat of 8 mg/L, while the wild type strain ATCC 17978 showed a value of 32 mg/L, which indicates a significant increase in susceptibility to oxidative stress of the mutant strain with respect to the wild type strain (Table 3). No differences were found in the susceptibility to paraquat between the Δ0242 mutant and the Δ0242/Δ3850 double mutant (MIC of 8 mg/L). In concordance, the Δ3850 mutant neither showed significant differences with respect to the wild type strain (MIC of 32 mg/L). A slightly higher susceptibility to paraquat in the Δ0242 mutant was also observed in the medium without limitation of metal availability. Besides, when the strains carried the plasmid pHW1266-Km, the susceptibility to paraquat increased in all cases, due to the fitness loss as explained above (Figure S1). In Table 3 it can be observed that, even taking into account this global increased of susceptibility to paraquat in strains carrying the plasmid, the phenotype of higher susceptibility to oxidative stress in the presence of BIP of the Δ0242 mutant strain carrying the plasmid (Δ0242+pWH1266-Km, MIC of 1 mg/L) was restored in the complemented strain, this showing the same MIC to paraquat as the wild type strain carrying the pWH1266-Km vector (MIC of 4 mg/L).

The feoA gene is involved in virulence

In order to explore the role of the *feoA* gene during the course of the *in vivo* infection, experimental animal models were performed in *G. mellonella* and mice.

The *A. baumannii* ATCC 17978 and the Δ0242, Δ3850 and Δ0242/Δ3850 derivative mutant strains were tested in the *G. mellonella* infection model. The survival assays (Figure 5) showed that the Δ0242 and Δ0242/Δ3850 mutant strains were significantly affected in their ability to infect and kill the caterpillars compared with the wild type strain ($p < 0.05$).

These results were in agreement with the mortality rates of *G. mellonella* infected with different inocula of the *A. baumannii* strains (Table 4). Briefly, lethal doses (LD) of the ATCC 17978 strain were similar to those showed by the mutant Δ3850. Besides, the lethal doses of the mutant Δ0242 were similar to those found in the Δ0242/Δ3850 mutant strain. The inactivation of the gene A1S_3850 did not affected the virulence ability of the ATCC 17978 strain using this *G. mellonella* infection model. The LD_{50} of the ATCC 17978 strain and the Δ3850 mutant was approximately 5-fold lower

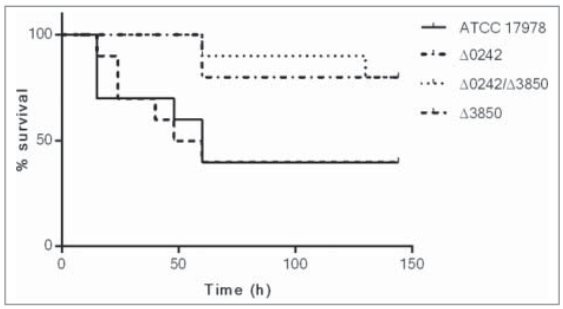

Figure 5. Survival of *Galleria mellonella* larvae (n = 10 *per* group) after infection with *A. baumannii* ATCC 17978, Δ0242, Δ3850 and Δ0242/Δ3850 strains. Survival was significantly higher in caterpillars infected with the Δ0242 mutant than those infected with the wild type strain ($p < 0.05$). No deaths were observed in any of the two control groups (not injected and injected with sterile PBS).

than that of the Δ0242 and Δ0242/Δ3850 mutant strains at 24 h, and 3.5-fold lower at 144 h. The LD_{100} of the ATCC 17978 strain and the Δ3850 mutant was approximately 4-fold lower than that of the Δ0242 and Δ0242/Δ3850 mutant strains at 24 h, and 3-fold lower at 144 h.

The virulence of the ATCC 17978 and Δ0242 strains was also assessed using a murine pneumonia model by measuring survival time of infected mice. Two groups of 10 mice were intratracheally infected with 5.5×10^7 CFUs/mouse, which means a LD_{90} of the wild type strain. However, the same dose of the Δ0242 mutant derivative strain produced only 30% of mortality (Figure 6A). Thus, a significant decrease in virulence using a mouse pneumonia model was observed when the gene A1S_0242 was deleted ($p < 0.01$).

A second model was also performed using an experimental pneumonia model in mice in order to determine the bacterial load in lungs and the frequency of sterile blood cultures (Table 5 and Figure 6B). Data revealed that, in groups inoculated with the ATCC 17978 strain, the bacterial load was approximately 1 log higher than in mice inoculated with the Δ0242 mutant strain ($p < 0.01$). Besides, the frequency of sterile blood cultures increased up to 75% in the group inoculated with the Δ0242 mutant strain compared with the mice inoculated with the ATCC 17978 strain (8.4%), ($p < 0.01$). Similarly, the survival time was significantly higher in the group of mice inoculated with the Δ0242 mutant strain than in the mice harboring the wild type strain ($p < 0.01$).

Discussion

The success of lung infection partly depends on the ability of bacteria to acquire iron, a cofactor needed for

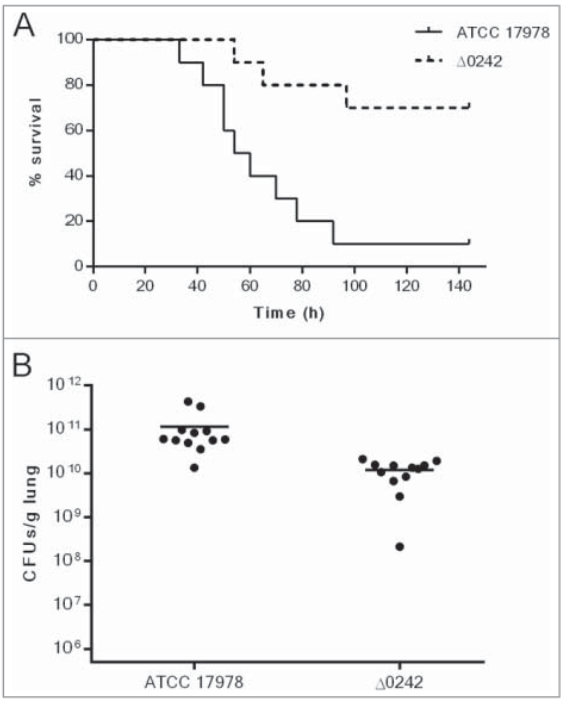

Figure 6. Pneumonia infection in mice. A) Survival of BALB/c (n = 10 *per* group) mice after pneumonia infection with *A. baumannii* ATCC 17978 and Δ0242 strains. Survival was significantly higher in mice infected with the Δ0242 mutant ($p < 0.01$). B) Bacterial load determination in lungs of mice infected with the ATCC 17978 strain and the Δ0242 mutant. Bacterial load ($p < 0.01$) was significantly lower in mice infected with the Δ0242 mutant.

many enzymatic reactions. Iron is essential for vital functions of bacteria and its presence in the host environment is restricted. This iron restriction constitutes an immune defense mechanism. *A. baumannii* is able to grow under iron-limiting conditions such as those occurred during human infection, however there is scarce information about the iron uptake of this microorganism during the course of the infection. Different studies showed that *A. baumannii* produces siderophores [49] such as the iron chelating agent acinetobactin [18,31,47], the fimsbactin A-F [29] or the baumanoferrin A and B [30] which are required for virulence. In addition, some outer membrane proteins such as OprD and OmpW have been related to iron uptake in *A. baumannii* [50,51]. Recently, a study concerning the gene expression profile of *A. baumannii* revealed that most of the genes hyper-expressed during bacteremia were those involved in iron transport and uptake [52].

At neutral pH and aerobic conditions, the ferric iron Fe^{3+} is insoluble. At this point, bacteria depend on siderophores for the iron uptake, such as acinetobactin, pyoverdin or enterobactin, previously described in *A. baumannii*, *P. aeruginosa* and *E. coli*, respectively [53,54], as well as additional molecules with Fe-chelating ability, such as citrate in *P. aeruginosa* [55]. In contrast, in anaerobic conditions, ferrous iron Fe^{2+} is abundant and is captured through uptake systems [56], such as the Feo system. However, a relevant link exists between the Feo system and the citrate-mediated Fe^{3+} acquisition of *P. aeruginosa*. The ferric iron Fe^{3+} chelated by citrate must be reduced to Fe^{2+} prior to its transport into the cytosol by the membrane transporter FeoB. A ferric citrate-specific cytoplasmic membrane transport component is absent in *P. aeruginosa* [57,58]. Similar cooperation between the FeoB transporter and the citrate-promoted Fe acquisition has been suggested in other species, such as *H. pylori* [37] and *Leptospira biflexa* [59]. Genes encoding for the baumanoferrin biosynthetic gene cluster found in *A. baumannii* [30] showed to be homologous to components of the acinetoferrin system, a citrate-based siderophore described in *A. haemolyticus* [60]. However, similar relationships between these siderophores and the Feo system are yet unknown.

Transcriptome analysis of *A. baumannii* ATCC 17978 strain, using RNA isolated from BAL of the infected lungs as starting material, revealed that the A1S_0242 gene (a ferrous iron transporter protein A) was over-expressed during the course of the pneumonia infection. Further analysis of the genome revealed the presence of other two genes (A1S_3850 and A1S_0652) homologues to A1S_0242, both harboring a *feoA* domain. This motivated us to study the genetic context of those genes. Informatic analyses revealed the presence of the A1S_0242 gene in all the complete *A. baumannii* genomes while the A1S_3850 and the A1S_0652 genes were rarely found.

The Feo systems found in *A. baumannii* ATCC 17978 contain in all cases genes similar to the previously described *feoA* and *feoB* genes but lacks the *feoC* gene found in other species. More functional studies related to the A1S_0244 could explain if this gene could act as a *feoAB* repressor in *A. baumannii*. The presence of these three genes containing a *feoA* domain in the strain ATCC 17978 triggered us to study the function of the A1S_0242 (*feoA*) and its interaction with the other two homologue genes (A1S_3850 y A1S_0652). Real time procedures revealed that the lack of A1S_0242 does not vary A1S_0652 and A1S_3850 expression while deletion of A1S_3850 increased the A1S_0652 expression.

In a previous work [61], transcriptional profiles indicated that the A1S_0242 and the A1S_3850 genes expression remained unaltered in biofilm-associated cells when compared to the planktonic cells, while the A1S_0652

gene increased. However, when the transcriptional profile of *A. baumannii* was determined during bacteremia [52], it was recovered that the expression of A1S_0650 and A1S_3850 genes remained unaltered whereas the expression of the A1S_0242 gene increased. Moreover, Eijkelkamp *et al.* [62] studied the transcriptional profiles of the genes of *A. baumannii* under iron limiting conditions. In this case, it was found that the A1S_0242 and A1S_0652 genes were up-regulated under iron limiting conditions while the A1S_3850 gene did not showed any different expression profile.

In this study we report many evidences of the implication of the A1S_0242 gene (*feoA*) in fitness and virulence of *A. baumannii* ATCC 17978. The importance of the *feoA* gene was first evidenced in fitness. The Δ0242 mutant showed a lower growth rate than the wild-type strain in iron-limited conditions. In contrast the mutants Δ3850 and Δ0242/Δ3850 did not decreased in growth rates compared with the parental and Δ0242 strains, respectively, thus minimizing the relevance of the A1S_3850 gene present in the ATCC 17978 strain.

Significant differences were also found in biofilm production or cellular attachment. The deletion of *feoA* demonstrated that this gene was involved is those mechanisms used by *A. baumannii* to colonize and infect the host organs while deletion of the homologue gene A1S_3850 did not show any changes. In agreement with previous results, the mutant Δ0242 showed a higher susceptibility to oxidative stress than the wild-type strain. Superoxide dismutase plays a key role in metabolizing O_2^-, avoiding reactions that can cause damage and the formation of reactive oxygen species. This enzyme frequently uses Fe as metal cofactor to catalyze the detoxification of superoxide [63]. Therefore, the Δ0242 mutant strain was more susceptible to the oxidative stress induced by paraquat probably due to decreased superoxide dismutase activity. The Δ3850 and the double mutant Δ0242/Δ3850 did not showed any effect on biofilm production, cellular attachment or oxidative stress, which once more highlights the important role of the A1S_0242 gene in pathogenesis and indicates the irrelevant role of the A1S_3850 gene in these processes.

Fitness is usually defined as the capacity for survival and reproduction in a particular environment [64], and virulence is defined as the degree of pathogenicity (ability of an agent to cause disease). Most pathogens use of a combination of two properties to cause disease: (i) toxicity, the degree to which a substance causes harm, and (ii) invasiveness, the ability to penetrate into the host and spread [48,65]. In the present study we have proved that fitness is reduced when the *feoA* gene (A1S_0242) is inactivated under iron-limited conditions. Additionally, virulence decreased as judged by the reduced ability of the mutant Δ0242 strain to attach to alveolar cells and the increased susceptibility to oxidative stress, which is one of the main antibacterial mechanisms during phagocytosis [66], being all these processes implicated in the pathogenicity of *A. baumannii*. Data indicated that the increase of survival and lethal doses obtained in the *in vivo* models with the Δ0242 mutant strain is probably due to a double effect or synergy between the fitness lost and the decrease of virulence, caused by a reduced ability to arrest iron from the environment.

Moreover, complementation experiments were performed in order to better demonstrate the role of *feoA* in virulence. Since the load of the pWH1266-Km vector decreases fitness (see Figure S1) not all assays could be performed with the complemented mutants. Accordingly, those assays in which fitness does not play a relevant role, such as biofilm production, were performed including the complemented strains. These assays clearly demonstrated that the complementation is possible and indeed restored the original phenotype. However, those assays where fitness is a limiting factor, such as the *in vivo* assays in animal models, were carried out without the complemented strains.

In a recent screening of genes involved in bacterial survival of *A. baumannii* using a mouse model of bloodstream infection, from a transposon mutant library comprising more than 100,000 mutants, 89 were selected for further studies [46]. Between them, two genes belonged to iron uptake systems, the *fepA* and the *feoB* genes, supporting the role of these systems in the *A. baumannii* pathogenesis [46]. However, no *in vivo* assays were performed on the study to confirm the results. In the present study, the implication of FeoA in the pathogenesis of *A. baumannii* was also evidenced using experimental *in vivo* infections that imply the host response. In the first model, previously validated to study *A. baumannii* infections in iron-defective conditions [18,67], caterpillars of *G. mellonella* were infected with the wild-type and mutant strains. Data indicated an impaired in virulence showing a lower capacity to persists and kill the caterpillars in the case of the Δ0242 strain but not in the case of the Δ3850 strain, which shows again the lack of implication of the A1S_3850 in pathogenesis. Similarly, in the pneumonia models of infection in mice, the mutant Δ2042 strain with reduced iron transport functions was less virulent than the wild-type strain. Both assays with invertebrate and vertebrate hosts reflected similar effects. Taken together these observations indicate that the *feoA* gene of *A. baumannii* is essential for the full virulence of this microorganism. However, virulence of *A. baumannii*, using the animal models here presented, was not entirely inhibited, suggesting that other iron transport systems previously described such as *fepA*, acinetobactin, baumanoferrin or fimsbactin [29,30,46,47] are present in the ATCC 17978

strain and should be active when the Feo system is abolished.

In summary, data indicated that the A1S_0242 gene (*feoA*) from *A. baumannii* ATCC 17978 strain, which is involved in iron uptake and that was found as over-expressed during the course of a pneumonia infection, plays a role in adhesion, biofilm formation and resistance to oxidative stress. Definitively, in the present study we demonstrated that the FeoA protein is needed for the full virulence phenotype of the strain ATCC 17978 of *A. baumannii* and that the FeoA-mediated acquisition of iron is essential for the *A. baumannii* pathogenesis.

Material and methods

Bacterial strains

A. baumannii ATCC 17978 and its derivative strains and *E. coli* listed in Table 2 were routinely grown or maintained in Luria-Bertani (LB) or Mueller-Hinton (MH) media with 20% agar added for plates for general purposes. All strains were grown at 37 °C and stored at -80 °C in LB broth containing 10% glycerol. When appropriate, cultures were supplemented with kanamycin (Km) at a final concentration of 50 mg/L (Sigma-Aldrich, #K1377).

Bacterial RNA extraction from murine pneumonia infection

An experimental pneumonia model was used to describe the transcriptome of the ATCC 17978 strain during the course of the infection. BALB/c 9- to 11-week old male mice weighing 25 to 30 g were intratracheally inoculated with approximately 5.5×10^7 CFUs/mouse of exponentially grown cells of the ATCC 17978 strain into mice. The number of bacteria present in the inoculum was checked by plate counting in LB agar plates. Briefly, mice anesthetized with an oral suspension of sevoflurane (Zoetis, #NADA 141–103) were suspended by their incisors on a board in a semi-vertical position. The efficacy of the intratracheal inoculation was confirmed by using an endoscope on the oral cavity. The trachea was accessed using a blunt-tipped needle for the inoculation of a 40-μL bacterial suspension made in sterile saline solution and 10% porcine mucin (wt/vol) (Sigma) mixed at a 1:1 ratio. A solution of ketamine (500 μg/mouse) (Pfizer, #47639/24/15) and medetomidine (15 μg/mouse) (Domtor, #933ESP) was immediately intraperitoneally injected after inoculation in order to keep the mice at least 20 min in a 30° inclined position. Dead mice in the first 4 h after inoculation were not included in the final analyses. Mice were euthanized with an overdose of thiopental sodium (Sandoz, NDC0781–6160-43) 20 h after inoculation. Then, a bronchoalveolar lavage (BAL) was performed to obtained bacteria suitable for RNA extraction (*in vivo* samples). All mice were maintained in the specific pathogen-free facility at the Technology Training Center of the Hospital of A Coruña (CHUAC, Spain). All experiments were done with the approval of and in accordance with regulatory guidelines and standards set by the Animal Ethics Committee (CHUAC, Spain, project code P82), in accordance with the Helsinki Declaration of 1975. RNA extracted from bacteria grown in LB-flasks (OD_{600} = 1.0) at 37°C and 180 rpm was used as experimental control (*in vitro* samples). Total RNA was immediately extracted from both samples using the RNeasy Mini Kit (Qiagen #74104), treated with DNAse I (Invitrogen, # 18068015) and purified with RNeasy MinElute Cleanup Kit (Qiagen, #74204). Final concentrations and purity grades of the samples were determined using a BioDrop μLITE

Table 2. Bacterial strains and plasmids used in this work.

Strain or plasmid	Relevant characteristics	Sources or references
STRAINS		
A. baumannii		
ATCC 17978	Clinical isolate	ATCC
Δ0242	A1S_0242 gene deletion mutant obtained from the ATCC 17978 strain	This study
ATCC 17978 + pWH1266-Km	ATCC 17978 harboring the empty pWH1266-Km plasmid; Km^R, Tet^R	This study
Δ0242 + pWH1266-Km	Δ0242 harboring the empty pWH1266-Km plasmid; Km^R, Tet^R	This study
Δ0242 complemented	Δ0242 harboring the pWH1266-Km-0242 plasmid; Km^R	This study
Δ3850	A1S_3850 gene deletion mutant obtained from the ATCC 17978 strain	This study
Δ3850 + pWH1266-Km	Δ3850 harboring the empty pWH1266-Km plasmid; Km^R, Tet^R	This study
Δ3850 complemented	Δ3850 harboring the pWH1266-Km-3850 plasmid; Km^R	This study
Δ0242/Δ3850	A1S_0242 and A1S_3850 genes deletion double mutant obtained from the ATCC 17978 strain	This study
E. coli		
TG1	Used for DNA recombinant methods	Lucigen
PLASMIDS		
pWH1266-Km	*A. baumannii* shuttle vector; Km^R, Tet^R	Álvarez-Fraga *et al.* 2016 [68]
pWH1266-Km-0242	pWH1266-Km harboring the A1S_0242 gene; Km^R	This study
pWH1266-Km-3850	pWH1266-Km harboring the A1S_3850 gene; Km^R	This study
pMo130	Suicide vector for the construction of *A. baumannii* isogenic derivative; Km^R, SacB, XylE	Hamad *et al.* 2009 [69]

Km^R: kanamycin resistance. Tet^R: tetracycline resistance.

Table 3. Susceptibility to oxidative stress generated by paraquat.

	MICs to paraquat (mg/L)	
	MH broth	MH broth + 100 μM BIP
ATCC 17978	64	32
Δ0242	32	8
Δ3850	64	32
Δ0242/Δ3850	32	8
MICs to paraquat (mg/L) with strains carrying the pWH1266-Km vector		
ATCC 17978 + pWH1266-Km	8	4
Δ0242 + pWH1266-Km	4	1
Δ0242 complemented	4	4

(Isogen Life Science) and a Bioanalyzer 2100 (Agilent Technologies Inc.).

Deep sequencing procedures

To characterize the complete transcriptomes of the studied samples, mRNA libraries from *in vivo* and *in vitro* samples obtained as explained above were prepared following the Truseq RNA sample preparation protocols from Illumina Inc. at CIC bioGUNE's genome analysis platform (Derio, Spain). Three biological replicates were studied for each sample.

Read processing and comparisons of gene expression profiles

Fifty nucleotide reads from each mRNA library were obtained using HiScanSQ (Illumina Inc., CIC bioGUNE, Bilbao, Spain). Short reads were aligned against the complete genome of *A. baumannii* ATCC 17978 and plasmids pAB1 and pAB2 (GenBank accession codes: NC_009085.1, NC_009083.1 and NC_009084.1, respectively). The genetic profiles comparison was done at CIC bioGUNE's genome analysis platform (Derio, Spain). Raw data were deposited in the GEO database under the accession code GSE100552.

Bioinformatic analysis

Genome analyses were done using the basic local Alignment Search Tool of the NCBI (BLAST,https://blast.ncbi.nlm.nih.gov/Blast.cgi).

Construction of isogenic deletion derivatives

In the present work, we focused on the study of the A1S_0242 gene. The Δ0242 isogenic deletion mutant derivative of the ATCC 17978 strain was constructed by deleting a region of the A1S_0242 gene. The suicide vector pMo130 (Genbank: EU862243), was used as described before [68] where upstream and downstream regions flanking the A1S_0242 gene were PCR-amplified and cloned into the pMo130 vector using primers listed in Table S2. The plasmid construction obtained was used to transform ATCC 17978 cells by electroporation [61]. Recombinant colonies representing the first crossover event were selected as previously described [69]. The second crossover event leading to gene knockout was confirmed by PCR using primers listed in Table S2 as described before [68]. The A1S_3850 was found in the genome of the 17978 strain as an A1S_0242 homologue. In order to study its interference with the A1S_0242 gene as well as discard its relevance in pathogenesis, a Δ3850 isogenic deletion mutant of the ATCC 17978 strain was constructed following the protocol described above and using the primers listed in Table S2. In addition, a double isogenic mutant strain, Δ0242/Δ3850, was performed following the same protocol where the second

Table 4. Mortality of *G. mellonella* infected with the *A. baumannii* ATCC 17978 and its derivative strains using lethal dose 50 (LD_{50}) and lethal dose 100 (LD_{100}).

	Bacterial inoculum (CFUs/larva)							
	$8*10^5$	$2*10^5$	$8*10^4$	$2.6*10^4$	$8*10^3$	$2.6*10^3$		
Strains	Mortality of larvae (%)at 24 h						LD_{50} 24 h	LD_{100} 24 h
ATCC 17978	100	100	85.7	57.1	42.8	0	$1.9*10^4$	$17*10^4$
Δ0242	100	71.4	57.1	0	0	0	$10.5*10^4$	$63*10^4$
Δ3850	100	100	100	42.8	28.5	0	$1.95*10^4$	$11.7*10^4$
Δ0242/Δ3850	100	85.7	57.1	0	0	0	$9.3*10^4$	$53.2*10^4$
Strains	Mortality of larvae (%) at 144 h						LD_{50} 144 h	LD_{100} 144 h
ATCC 17978	100	100	100	85.7	42.8	0	$1*10^4$	$6*10^4$
Δ0242	100	100	85.7	14.2	0	0	$4.35*10^4$	$18.1*10^4$
Δ3850	100	100	100	100	28.5	0	$1.15*10^4$	$3.05*10^4$
Δ0242/Δ3850	100	100	85.7	42.8	0	0	$3.4*10^4$	$16.4*10^4$

Table 5. Effect of *feoA* gene (A1S_0242) inactivation over bacterial load in lungs, blood and mice survival.

Treatment group (*n*)	Bacterial load in lung (mean log_{10}CFU/g of lung +/− SD)	% Sterile blood cultures	Mean of survival time (h) of mice
ATCC 17978 (*12*)	11.04 (+/− 0.35)	8.4%	43.4
Δ0242 (*12*)	10.04 (+/− 0.29)	75%	64.1[a]

[a]: Two mice survived at 72 h.

deletion (Δ3850) was constructed over the Δ0242 mutant.

Complementation of the mutant strains

The pWH1266-Km plasmid was constructed as previously described [68]. Then, in order to complement the Δ0242 strain, the A1S_0242 gene was amplified from the genome of the ATCC 17978 strain using primers listed in Table S2 and then cloned into the *Eco*RV and *Bam*HI restriction sites of the pWH1266-Km plasmid under the control of the tetracycline resistance gene promoter using the primers listed in Table S2. The resulting construction was used to transform Δ0242 mutant cells by electroporation. Transformants were selected on kanamycin-containing plates and checked by PCR using primers listed in Table S2. Moreover, ATCC 17978 and Δ0242 strains harboring the empty pWH1266-Km vector were used as experimental controls. Finally, the Δ3850 derivative strain was also complemented following the same procedure described above.

Retrotranscription and real-time RT-PCR assays

Total RNA from ATCC 17978 strain and the isogenic mutants (OD_{600} = 1.0) was isolated using the High Pure RNA Isolation Kit (Roche, #11828665001). RNA samples were treated with DNAse I (Invitrogen, #18068015) and purified with GeneJET RNA Cleanup and Concentration Micro Kit (Thermo Fisher Scientific, #K0841).

In order to analyze the polycistronic nature of the A1S_0242–0244 operon, the cDNA was obtained from RNA samples using the iScript cDNA Synthesis Kit (Bio-Rad, #170–8890) following the manufacturer's recommendations. The cDNA from ATCC 17978 was amplified with the GoTaq G2 Flexi DNA Polymerase (Promega, #M7808) using pairs of primers designed to anneal to the 3′-end of every gene and the 5′-end of the next one (Table S2). Genomic DNA and total RNA without reverse transcription were used as templates for positive and negative controls, respectively, and the amplicons were detected by standard 1% agarose gel electrophoresis. The *gyrB* gene was used as a positive control. All the assays were performed in triplicate.

Real-time reverse transcription-PCR (qRT-PCR) was carried out to determine the expression level of the genes of interest using UPL (Roche) and TaqMan (Applied Biosystems) probes and primers listed in Table S2. The LightCycler 480 RNA Master hydrolysis probes kit (Roche, #04991885001) and the LightCycler 480 RNA instrument (Roche) were used together and the following protocol was used: initial incubation of 65 °C, 3 min, followed by a denaturation step at 95 °C for 30 s, 45 cycles at 95 °C, 15 s and 60 °C, 45 s, and a final elongation step at 40 °C, 30 s. The expression level was standardized relative to the transcription level of the housekeeping gene *rpoB*. All the assays were performed in triplicate.

Growth curve analysis

Fitness was assessed by measuring the growth rates of the ATCC 17978 strain and the mutant derivatives strains. Briefly, 1.5 ml of LB medium were inoculated with approximately 5×10^7 CFU of each strain, previously grown until the stationary phase, and incubated at 37°C with constant shaking at 180 rpm. Assays were performed in MH medium (*normal conditions*) and in MH supplemented with 200 μM of 2,2′-bipyridyl (BIP, Sigma-Aldrich, #D216305) (*iron deficit conditions*). Growth was monitored using 24-well plates in an Epoch 2 Microplate Spectrophotometer (BioTek Instruments, Inc.) and OD_{600} values were recorded every 10 min. At least three independent experiments were performed for each strain. The growth rate constant (μ) was calculated on the basis of the exponential segment of the growth curve and defined as $\ln_2/g$, where g is the doubling time or mean generation time. The results were compared using Student's t test.

Quantitative biofilm assay

Biofilm formation was determined following the protocol previously described by Tomaras *et al.* [23] and modified by Alvarez-Fraga *et al.* [68]. Briefly, colonies of *A. baumannii* were grown on LB plates and used to inoculate LB broth. Overnight cultures were centrifuged and the pellet washed and resuspended in 5 mL of SB medium (0.5% NaCl and 1% tryptone). A 1:100 dilution of each sample was stagnant incubated at 37°C for 48 h. In order to evaluate the total cell biomass the growth was measured at OD_{600}. Biofilm formation ability was analyzed by crystal violet staining followed by solubilisation with ethanol-acetone. In order to avoid variations due to differences in bacterial growth under different experimental conditions, the OD_{580}/OD_{600} ratio was used to normalize the amount of biofilm formed to the total cell content of each sample. Eight independent replicates were performed. Student's t-test was performed to evaluate the statistical significance of observed differences.

Adhesion to A549 human alveolar epithelial cells

The ability of the isogenic *A. baumannii* strains (Δ0242, Δ3850 and the double mutant Δ0242/Δ3850) to adhere to A549 human epithelial cells was evaluated and compared to the wild type strain. Invasion and adhesion

abilities were analyzed as previously described by Gaddy *et al.* [25] with some modifications [68]. Briefly, A549 human alveolar epithelial cells were grown at 37°C and 5% CO_2 in DMEM medium (Sigma-Aldrich, #D5671) containing 10% of fetal bovine serum (FBS) and 1% of penicillin-streptomycin (Gibco, #15070063). Monolayers were washed with saline solution and HBSS (Hank's balanced salt solution, Gibco, #11520476) without glucose (mHBSS). After that, A549 cells were infected with 10^7 bacteria *per* well and incubated, 3 h for the adherence determination, in mHBSS at 37 °C. To analyze the attachment ability of bacteria, A549 cells were washed with saline solution and lysed in 500 μL of 0.5% sodium deoxycholate. Dilutions of the lysates were plated onto LB agar and incubated at 37 °C for 24 h. Colony forming units were counted to determine bacteria that had attached to or invaded A549 cells. Four independent replicates were done. Student's t-tests were performed to evaluate the statistical significance of the observed differences.

Determination of susceptibility to oxidative stress

The susceptibility to oxidative stress of the ATCC 17978 strain type and the isogenic mutant derivative strains was determined by microdilution using paraquat (Sigma-Aldrich, #856177) to achieve oxidative stress conditions in order to obtain the Minimal Inhibitory Concentration (MIC), following the CLSI criteria [70]. Briefly, strains were grown in MH plates for 24 h at 37°C. Then, 150 μL of serial dilutions of MH medium containing paraquat were performed in 96-well plates in the presence (100 μM) or absence of the metal chelator 2,2- bipyridyl (BIP). Plates were then inoculated with 7.5 μL of a 0.5 McFarland cellular suspension containing approximately 1×10^7 CFU/mL of bacteria. Bacterial growth on plates was studied after incubation al 37°C for 24 h.

Galleria mellonella virulence assay

The virulence of the wild type strain and its derivative mutant strains was evaluated using a *G. mellonella* survival assay and a determination of the lethal doses (LD_{50} and LD_{100}). Caterpillars were obtained from Bio Systems Technology (Exeter, UK) and stored at 15 °C prior to use. *A. baumannii* cells previously grown for 24 h in LB broth were collected by centrifugation and resuspended in sterile phosphate-buffered saline (PBS). Appropriate bacterial inocula were determined spectrophotometrically at OD_{600} and confirmed by plate counting using LB agar plates. Thus, *G. mellonella* survival assays were performed by injecting 10 μL-suspension containing approximately 2×10^4 CFU/larva in groups of 10 larvae as previously described [71]. Two control groups were included; not injected larvae (intact) and larvae injected with an equivalent volume of sterile PBS. The tested groups included larvae infected with ATCC 17978, Δ0242, Δ3850 and Δ0242/Δ3850 strains. After injection, the larvae were incubated at 37°C in darkness, and death was assessed at 8 h intervals over 6 days. Caterpillars were considered dead and removed if they displayed no response to probing. The resulting survival curves were plotted using the Kaplan-Meier method [72] and analyzed using the log-rank (Mantel-Cox) test.

LD_{50} and LD_{100} were calculated using groups of 7 larvae of *G. mellonella* infected as described above. Larvae were infected with each strain with an inoculum of 10 μL starting at 8×10^5 CFUs/larvae, and then the inocula serially diluted at 2×10^5, 8×10^4, 2.6×10^4, 8×10^3 and 2.6×10^3 CFUs/larvae. Control groups were also included. Lethal doses were obtained for 24 and 144 h post-infection [73].

Murine pneumonia virulence assay

The pneumonia model was used to evaluate the virulence ability of the ATCC 17978 and the isogenic mutant Δ0242 strain using BALB/c male mice. The procedure followed was the above described for bacterial RNA extraction from the infection, with the exception of the euthanasia that occurred using an overdose of thiopental sodium 144 h after inoculation. Death was assessed at 8 h intervals. The survival curves were plotted using the Kaplan-Meier method [72] and analyzed using the log-rank (Mantel-Cox) test.

To ascertain the relevance of the *feoA* gene in virulence in mice pneumonia a second series of assays was performed to determine the effect of the inactivation of *feoA* on the bacterial load in lungs and presence of bacteria in blood. Groups of 12 mice were intratracheally inoculated as previously described with the ATCC 17978 and the mutant Δ0242 strains. Mice were inoculated with approximately 2 x LD_{100} of the ATCC 17978 (12×10^7 CFUs/mouse) and observed for mortality over 72 h. All the animals were analyzed immediately after death. Blood and lung samples were obtained and processed as previously described previously [74]. Student's t-test was performed to evaluate the statistical significance of differences.

Disclosure of potential conflicts of interest

No potential conflicts of interest were disclosed.

Acknowledgements

This work has been funded by Projects PI15/00860 to GB, CP13/00226 to AB, PI11/01034 to MP and P14/00059 and

PI17/01482 to MP and AB, all integrated in the National Plan for Scientific Research, Development and Technological Innovation 2013–2016 and funded by the ISCIII – General Subdirection of Assessment and Promotion of the Research-European Regional Development Fund (FEDER) "A way of making Europe". The study was also funded by the project IN607A 2016/22 (Consellería de Cultura, Educación e Ordenación Universitaria) to G.B. Also supported by Planes Nacionales de I+D+i 2008–2011 / 2013–2016 and Instituto de Salud Carlos III, Subdirección General de Redes y Centros de Investigación Cooperativa, Ministerio de Economía y Competitividad, Spanish Network for Research in Infectious Diseases (REIPI RD12/0015/0014 and REIPI RD16/0016/006) co-financed by European Development Regional Fund "A way to achieve Europe" and operative program Intelligent Growth 2014–2020. J. A. Vallejo was financially supported by the Sara Borrell Programme (ISCIII, Spain CD13/00373), J.C. Vázquez-Ucha was financially supported by the Miguel Servet Programme (ISCIII, Spain CP13/00226) and M. Martínez-Guitián was financially supported by the grant Clara Roy (Spanish Society of Clinical Microbiology and Infectious Diseases). We thank M. I. Voskuil (Dept. of Immunology and Microbiology, University of Colorado Medical School, CO, USA) for providing pMo130.

Funding

Consellería de Cultura, Educación y Ordenación Universitaria Xunta de Galicia-Spain, Miguel Servet program-ISCIII-Spain, Sara Borrell Program-ISCIIII-Spain, REIPI-Spain, SEIMC-Spain, ISCIIII-Spain.

References

[1] Global priority list of antibiotic-resistant bacteria to guide research, discovery and development of new antibiotics. Geneva (Switzerland): World Health Organization. 2017.

[2] Peleg AY, Seifert H, Paterson DL. *Acinetobacter baumannii*: emergence of a successful pathogen. Clin Microbiol Rev. 2008;21:538–82. doi:10.1128/CMR.00058-07.

[3] Maragakis LL, Perl TM. *Acinetobacter baumannii*: epidemiology, antimicrobial resistance, and treatment options. Clin Infect Dis. 2008;46:1254–63. doi:10.1086/529198.

[4] Gales AC, Jones RN, Sader HS. Contemporary activity of colistin and polymyxin B against a worldwide collection of Gram-negative pathogens: results from the SENTRY Antimicrobial Surveillance Program (2006–09). J Antimicrob Chemother. 2011;66:2070–4. doi:10.1093/jac/dkr239.

[5] Karaiskos I, Souli M, Galani I, et al. Colistin: still a lifesaver for the 21st century? Expert Opin Drug Metab Toxicol. 2017;13:59–71. doi:10.1080/17425255.2017.1230200.

[6] Pournaras S, Koumaki V, Gennimata V, et al. In Vitro Activity of Tigecycline Against *Acinetobacter baumannii*: Global Epidemiology and Resistance Mechanisms. Adv Exp Med Biol. 2016;897:1–14.

[7] Bou G, Cerveró G, Domínguez MA, et al. PCR-based DNA fingerprinting (REP-PCR, AP-PCR) and pulsed-field gel electrophoresis characterization of a nosocomial outbreak caused by imipenem- and meropenem-resistant *Acinetobacter baumannii*. Clin Microbiol Infect. 2000;6:635–43. doi:10.1046/j.1469-0691.2000.00181.x.

[8] Higgins PG, Dammhayn C, Hackel M, et al. Global spread of carbapenem-resistant Acinetobacter baumannii. J Antimicrob Chemother. 2010;65:233–8. doi:10.1093/jac/dkp428.

[9] Valencia R, Arroyo LA, Conde M, et al. Nosocomial outbreak of infection with pan-drug-resistant *Acinetobacter baumannii* in a tertiary care university hospital. Infect Control Hosp Epidemiol. 2009;30:257–63. doi:10.1086/595977.

[10] Corbella X, Montero A, Pujol M, et al. Emergence and rapid spread of carbapenem resistance during a large and sustained hospital outbreak of multiresistant *Acinetobacter baumannii*. J Clin Microbiol. 2000;38:4086–95.

[11] McConnell MJ, Actis L, Pachón J. *Acinetobacter baumannii*: human infections, factors contributing to pathogenesis and animal models. FEMS Microbiol Rev. 2013;37:130–55. doi:10.1111/j.1574-6976.2012.00344.x.

[12] Smani Y, Dominguez-Herrera J, Pachón J. Association of the outer membrane protein Omp33 with fitness and virulence of *Acinetobacter baumannii*. J Infect Dis. 2013;208:1561–70. doi:10.1093/infdis/jit386.

[13] Lee JC, Koerten H, van den Broek P, et al. Adherence of *Acinetobacter baumannii* strains to human bronchial epithelial cells. Res Microbiol. 2006;157:360–6. doi:10.1016/j.resmic.2005.09.011.

[14] Pérez A, Merino M, Rumbo-Feal S, et al. The FhaB/FhaC two-partner secretion system is involved in adhesion of *Acinetobacter baumannii* AbH12O-A2 strain. Virulence. 2017;8(6):959–974. doi:10.1080/21505594.

[15] Méndez JA, Mateos J, Beceiro A, et al. Quantitative proteomic analysis of host–pathogen interactions: a study of *Acinetobacter baumannii* responses to host airways. BMC Genomics. 2015;16:422. doi:10.1186/s12864-015-1608-z.

[16] Merino M, Alvarez-Fraga L, Gomez MJ, et al. Complete Genome Sequence of the Multiresistant *Acinetobacter baumannii* Strain AbH12O-A2, Isolated during a Large Outbreak in Spain. Genome Announc. 2014;2: doi:10.1128/genomeA.01182-14.

[17] Acosta J, Merino M, Viedma E, et al. Multidrug-resistant *Acinetobacter baumannii* Harboring OXA-24 carbapenemase, Spain. Emerg Infect Dis. 2011;17:1064–7. doi:10.3201/eid/1706.091866.

[18] Gaddy JA, Arivett BA, McConnell MJ, et al. Role of acinetobactin-mediated iron acquisition functions in the interaction of *Acinetobacter baumannii* strain ATCC 19606T with human lung epithelial cells, *Galleria mellonella* caterpillars, and mice. Infect Immun. 2012;80:1015–24. doi:10.1128/IAI.06279-11.

[19] Mendez JA, Soares NC, Mateos J, et al. Extracellular proteome of a highly invasive multidrug-resistant clinical strain of *Acinetobacter baumannii*. J Proteome Res. 2012;11:5678–94. doi:10.1021/pr300496c.

[20] Loehfelm TW, Luke NR, Campagnari AA. Identification and characterization of an *Acinetobacter baumannii* biofilm-associated protein. J Bacteriol. 2008;190:1036–44. doi:10.1128/JB.01416-07.

[21] Choi AH, Slamti L, Avci FY, et al. The pgaABCD locus of *Acinetobacter baumannii* encodes the production of poly-beta-1–6-N-acetylglucosamine, which is critical for

biofilm formation. J Bacteriol. 2009;191:5953–63. doi:10.1128/JB.00647-09.
[22] Tomaras AP, Flagler MJ, Dorsey CW, et al. Characterization of a two-component regulatory system from *Acinetobacter baumannii* that controls biofilm formation and cellular morphology. Microbiology. 2008;154:3398–409. doi:10.1099/mic.0.2008/019471-0.
[23] Tomaras AP, Dorsey CW, Edelmann RE, et al. Attachment to and biofilm formation on abiotic surfaces by *Acinetobacter baumannii*: involvement of a novel chaperone-usher pili assembly system. Microbiology. 2003;149:3473–84. doi:10.1099/mic.0.26541-0.
[24] de Breij A, Gaddy J, van der Meer J, et al. CsuA/BABCDE-dependent pili are not involved in the adherence of *Acinetobacter baumannii* ATCC19606(T) to human airway epithelial cells and their inflammatory response. Res Microbiol. 2009;160:213–8. doi:10.1016/j.resmic.2009.01.002.
[25] Gaddy JA, Tomaras AP, Actis LA. The *Acinetobacter baumannii* 19606 OmpA protein plays a role in biofilm formation on abiotic surfaces and in the interaction of this pathogen with eukaryotic cells. Infect Immun. 2009;77:3150–60. doi:10.1128/IAI.00096-09.
[26] Dashper SG, Butler CA, Lissel JP, et al. A novel *Porphyromonas gingivalis* FeoB plays a role in manganese accumulation. J Biol Chem. 2005;280:28095–102. doi:10.1074/jbc.M503896200.
[27] Nairz M, Schroll A, Sonnweber T, et al. The struggle for iron – a metal at the host-pathogen interface. Cell Microbiol. 2010;12:1691–702. doi:10.1111/j.1462-5822.2010.01529.x.
[28] Chu BC, Garcia-Herrero A, Johanson TH, et al. Siderophore uptake in bacteria and the battle for iron with the host; a bird's eye view. Biometals. 2010;23:601–11. doi:10.1007/s10534-010-9361-x.
[29] Proschak A, Lubuta P, Grun P, et al. Structure and biosynthesis of fimsbactins A-F, siderophores from *Acinetobacter baumannii* and Acinetobacter baylyi. Chembiochem. 2013;14:633–8. doi:10.1002/cbic.201200764.
[30] Penwell WF, DeGrace N, Tentarelli S, et al. Discovery and Characterization of New Hydroxamate Siderophores, Baumannoferrin A and B, produced by *Acinetobacter baumannii*. Chembiochem. 2015;16:1896–1904. doi:10.1002/cbic.201500147.
[31] Shapiro JA, Wencewicz TA. Acinetobactin Isomerization Enables Adaptive Iron Acquisition in *Acinetobacter baumannii* through pH-Triggered Siderophore Swapping. ACS Infect Dis. 2016;2:157–68. doi:10.1021/acsinfecdis.5b00145.
[32] Weaver EA, Wyckoff EE, Mey AR, et al. FeoA and FeoC are essential components of the *Vibrio cholerae* ferrous iron uptake system, and FeoC interacts with FeoB. J Bacteriol. 2013;195:4826–35. doi:10.1128/JB.00738-13.
[33] Naikare H, Palyada K, Panciera R, et al. Major role for FeoB in *Campylobacter jejuni* ferrous iron acquisition, gut colonization, and intracellular survival. Infect Immun. 2006;74:5433–44. doi:10.1128/IAI.00052-06.
[34] Mortensen BL, Skaar EP. The contribution of nutrient metal acquisition and metabolism to *Acinetobacter baumannii* survival within the host. Front Cell Infect Microbiol. 2013;3:95. doi:10.3389/fcimb.2013.00095.
[35] Runyen-Janecky LJ, Reeves SA, Gonzales EG, et al. Contribution of the Shigella flexneri Sit, Iuc, and Feo iron acquisition systems to iron acquisition *in vitro* and in cultured cells. Infect Immun. 2003;71:1919–28. doi:10.1128/IAI.71.4.1919-1928.2003.
[36] Robey M, Cianciotto NP. Legionella pneumophila *feoAB* promotes ferrous iron uptake and intracellular infection. Infect Immun. 2002;70:5659–69. doi:10.1128/IAI.70.10.5659-5669.2002.
[37] Velayudhan J, Hughes NJ, McColm AA, et al. Iron acquisition and virulence in *Helicobacter pylori*: a major role for FeoB, a high-affinity ferrous iron transporter. Mol Microbiol. 2000;37:274–86. doi:10.1046/j.1365-2958.2000.01987.x.
[38] Stojiljkovic I, Cobeljic M, Hantke K. Escherichia coli K-12 ferrous iron uptake mutants are impaired in their ability to colonize the mouse intestine. FEMS Microbiol Lett. 1993;108:111–5. doi:10.1111/j.1574-6968.1993.tb06082.x.
[39] Boyer E, Bergevin I, Malo D, et al. Acquisition of Mn(II) in addition to Fe(II) is required for full virulence of *Salmonella enterica* serovar Typhimurium. Infect Immun. 2002;70:6032–42. doi:10.1128/IAI.70.11.6032-6042.2002.
[40] Kammler M, Schön C, Hantke K. Characterization of the ferrous iron uptake system of *Escherichia coli*. J Bacteriol. 1993;175:6212–9. doi:10.1128/jb.175.19.6212-6219.1993.
[41] Stevenson B, Wyckoff EE, Payne SM. *Vibrio cholerae* FeoA, FeoB, and FeoC Interact To Form a Complex. J Bacteriol. 2016;198:1160–70. doi:10.1128/JB.00930-15.
[42] Hantke K. Regulation of ferric iron transport in *Escherichia coli* K12: isolation of a constitutive mutant. Mol Gen Genet. 1981;182:288–92. doi:10.1007/BF00269672.
[43] Hantke K. Ferrous Iron Transport, p 178–184. In: Crosa J, Mey A, Payne S, editors. Iron Transport in Bacteria. Washington, DC: ASM Press; 2004. doi:10.1128/9781555816544.ch12.
[44] Hantke K. Selection procedure for deregulated iron transport mutants (fur) in *Escherichia coli* K 12: fur not only affects iron metabolism. Mol Gen Genet. 1987;210:135–9. doi:10.1007/BF00337769.
[45] Cartron ML, Maddocks S, Gillingham P, et al. Feo-transport of ferrous iron into bacteria. Biometals. 2006;19:143–57. doi:10.1007/s10534-006-0003-2.
[46] Subashchandrabose S, Smith S, DeOrnellas V, et al. Acinetobacter baumannii Genes Required for Bacterial Survival during Bloodstream Infection. mSphere. 2015;1:doi:10.1128/mSphere.00013-15.
[47] Antunes LC, Imperi F, Towner KJ, et al. Genome-assisted identification of putative iron-utilization genes in *Acinetobacter baumannii* and their distribution among a genotypically diverse collection of clinical isolates. Res Microbiol. 2011;162:279–84. doi:10.1016/j.resmic.2010.10.010.
[48] Beceiro A, Tomas M, Bou G. Antimicrobial resistance and virulence: a successful or deleterious association in the bacterial world? Clin Microbiol Rev. 2013;26:185–230. doi:10.1128/CMR.00059-12.
[49] Dorsey CW, Beglin MS, Actis LA. Detection and analysis of iron uptake components expressed by *Acinetobacter baumannii* clinical isolates. J Clin Microbiol. 2003;41:4188–93. doi:10.1128/JCM.41.9.4188-4193.2003.
[50] Catel-Ferreira M, Marti S, Guillon L, et al. The outer membrane porin OmpW of *Acinetobacter baumannii* is

involved in iron uptake and colistin binding. FEBS Lett. 2016;590:224–31. doi:10.1002/1873-3468.12050.
[51] Catel-Ferreira M, Nehme R, Molle V, et al. Deciphering the function of the outer membrane protein OprD homologue of *Acinetobacter baumannii*. Antimicrob Agents Chemother. 2012;56:3826–32. doi:10.1128/AAC.06022-11.
[52] Murray GL, Tsyganov K, Kostoulias XP, et al. Global gene expression profile of *Acinetobacter baumannii* during bacteremia. J Infect Dis. 2017;215:S52–7. doi:10.1093/infdis/jiw529.
[53] Miethke M, Marahiel MA. Siderophore-based iron acquisition and pathogen control. Microbiol Mol Biol Rev. 2007;71:413–51. doi:10.1128/MMBR.00012-07.
[54] Zimbler DL, Penwell WF, Gaddy JA, et al. Iron acquisition functions expressed by the human pathogen *Acinetobacter baumannii*. Biometals. 2009;22:23–32. doi:10.1007/s10534-008-9202-3.
[55] Harding RA, Royt PW. Acquisition of iron from citrate by *Pseudomonas aeruginosa*. J Gen Microbiol. 1990;136:1859–67. doi:10.1099/00221287-136-9-1859.
[56] Ratledge C, Dover LG. Iron metabolism in pathogenic bacteria. Annu Rev Microbiol. 2000;54:881–941. doi:10.1146/annurev.micro.54.1.881.
[57] Marshall B, Stintzi A, Gilmour C, et al. Citrate-mediated iron uptake in *Pseudomonas aeruginosa*: involvement of the citrate-inducible FecA receptor and the FeoB ferrous iron transporter. Microbiology. 2009;155:305–15. doi:10.1099/mic.0.023531-0.
[58] Ganne G, Brillet K, Basta B, et al. Iron Release from the Siderophore Pyoverdine in *Pseudomonas aeruginosa* Involves Three New Actors: FpvC, FpvG, and FpvH. ACS Chem Biol. 2017;12:1056–65. doi:10.1021/acschembio.6b01077.
[59] Louvel H, Saint Girons I, Picardeau M. Isolation and characterization of FecA- and FeoB-mediated iron acquisition systems of the spirochete *Leptospira biflexa* by random insertional mutagenesis. J Bacteriol. 2005;187:3249–54. doi:10.1128/JB.187.9.3249-3254.2005.
[60] Sahl JW, Gillece JD, Schupp JM, et al. Evolution of a pathogen: a comparative genomics analysis identifies a genetic pathway to pathogenesis in *Acinetobacter*. PLoS One. 2013;8:e54287. doi:10.1371/journal.pone.0054287.
[61] Rumbo-Feal S, Gomez MJ, Gayoso C, et al. Whole transcriptome analysis of *Acinetobacter baumannii* assessed by RNA-sequencing reveals different mRNA expression profiles in biofilm compared to planktonic cells. PLoS One. 2013;8:e72968. doi:10.1371/journal.pone.0072968.
[62] Eijkelkamp BA, Hassan KA, Paulsen IT, et al. Investigation of the human pathogen *Acinetobacter baumannii* under iron limiting conditions. BMC genomics. 2011;12:126. doi:10.1186/1471-2164-12-126.
[63] Miller AF. Superoxide dismutases: ancient enzymes and new insights. FEBS Lett. 2012;586:585–95. doi:10.1016/j.febslet.2011.10.048.
[64] Lenski RE. Quantifying fitness and gene stability in microorganisms. Biotechnology. 1991;15:173–92.
[65] Madigan MT MJ, Dunlap PV, Clark DP. Brock biology of microorganisms. 12th ed. Texas, USA: Pearson Education Inc. 2009.
[66] Hassett DJ, Cohen MS. Bacterial adaptation to oxidative stress: implications for pathogenesis and interaction with phagocytic cells. FASEB J. 1989;3:2574–82.
[67] Rumbo-Feal S, Perez A, Ramelot TA, et al. Contribution of the *A. baumannii* A1S_0114 Gene to the Interaction with Eukaryotic Cells and Virulence. Front Cell Infect Microbiol. 2017;7:108. doi:10.3389/fcimb.2017.00108.
[68] Álvarez-Fraga L, Pérez A, Rumbo-Feal S, et al. Analysis of the role of the LH92_11085 gene of a biofilm hyperproducing *Acinetobacter baumannii* strain on biofilm formation and attachment to eukaryotic cells. Virulence. 2016;7:443–55. doi:10.1080/21505594.2016.1145335.
[69] Hamad MA, Zajdowicz SL, Holmes RK, et al. An allelic exchange system for compliant genetic manipulation of the select agents *Burkholderia pseudomallei* and Burkholderia mallei. Gene. 2009;430:123–31. doi:10.1016/j.gene.2008.10.011.
[70] CLSI W, PA, USA. Methods for Dilution Antimicrobial Susceptibility Tests for Bacteria that Grow Aerobically–Tenth Edition: Approved Standard M07-A10, 2015.
[71] Hornsey M, Longshaw C, Phee L, et al. *In vitro* activity of telavancin in combination with colistin versus Gram-negative bacterial pathogens. Antimicrob Agents Chemother. 2012;56:3080–5. doi:10.1128/AAC.05870-11.
[72] Kaplan EL, Meier P. Nonparametric Estimation from Incomplete Observations. J Am Statist Assoc. 1958;53:457–81. doi:10.1080/01621459.1958.10501452.
[73] Lopez-Rojas R, Dominguez-Herrera J, McConnell MJ, et al. Impaired virulence and *in vivo* fitness of colistin-resistant *Acinetobacter baumannii*. J Infect Dis. 2011;203:545–8. doi:10.1093/infdis/jiq086.
[74] Rodriguez-Hernandez MJ, Pachon J, Pichardo C, et al. Imipenem, doxycycline and amikacin in monotherapy and in combination in *Acinetobacter baumannii* experimental pneumonia. J Antimicrob Chemother. 2000;45:493–501. doi:10.1093/jac/45.4.493.

AMERICAN SOCIETY FOR MICROBIOLOGY | Antimicrobial Agents and Chemotherapy®

EXPERIMENTAL THERAPEUTICS

Therapeutic Efficacy of LN-1-255 in Combination with Imipenem in Severe Infection Caused by Carbapenem-Resistant *Acinetobacter baumannii*

Juan Carlos Vázquez-Ucha,[a] Marta Martínez-Guitián,[a] María Maneiro,[b] Kelly Conde-Pérez,[a] Laura Álvarez-Fraga,[a] Gabriel Torrens,[c] Antonio Oliver,[c] John D. Buynak,[d] Robert A. Bonomo,[e,f,g,h,i,j,k] Germán Bou,[a] Concepción González-Bello,[b] Margarita Poza,[a] Alejandro Beceiro[a]

[a]Servicio de Microbiología do Complexo Hospitalario Universitario da Coruña (CHUAC), Instituto de Investigación Biomédica da Coruña (INIBIC)–Centro de Investigacións Científicas Avanzadas (CICA), A Coruña, Spain

[b]Centro Singular de Investigación en Química Biolóxica e Materiais Moleculares (CIQUS), Departamento de Química Orgánica, Universidade de Santiago de Compostela, Santiago de Compostela, Spain

[c]Servicio de Microbiología y Unidad de Investigación, Hospital Universitari Son Espases, Institut d'Investigació Sanitaria Illes Balears, Palma de Mallorca, Spain

[d]Department of Chemistry, Southern Methodist University, Dallas, Texas, USA

[e]Medical Service, Louis Stokes Cleveland Department of Veterans Affairs Medical Center, Cleveland, Ohio, USA

[f]Department of Medicine, Case Western Reserve University School of Medicine, Cleveland, Ohio, USA

[g]Department of Pharmacology, Case Western Reserve University School of Medicine, Cleveland, Ohio, USA

[h]Department of Molecular Biology and Microbiology, Case Western Reserve University School of Medicine, Cleveland, Ohio, USA

[i]Department of Biochemistry, Case Western Reserve University School of Medicine, Cleveland, Ohio, USA

[j]Department of Proteomics and Bioinformatics, Case Western Reserve University School of Medicine, Cleveland, Ohio, USA

[k]CWRU-Cleveland VAMC Center for Antimicrobial Resistance and Epidemiology (Case VA CARES), Cleveland, Ohio, USA

ABSTRACT The carbapenem-hydrolyzing class D β-lactamases (CHDLs) are the main mechanism of carbapenem resistance in *Acinetobacter baumannii*. CHDLs are not effectively inactivated by clinically available β-lactam-type inhibitors. We have previously described the *in vitro* efficacy of the inhibitor LN-1-255 in combination with carbapenems. The aim of this study was to compare the efficacy of LN-1-255 with that of imipenem in murine pneumonia using *A. baumannii* strains carrying their most extended carbapenemases, OXA-23 and OXA-24/40. The $bla_{OXA\text{-}23}$ and $bla_{OXA\text{-}24/40}$ genes were cloned into the carbapenem-susceptible *A. baumannii* ATCC 17978 strain. Clinical isolates Ab1 and JC12/04, producing the enzymes OXA-23 and OXA-24/40, respectively, were used in the study. Pharmacokinetic (PK) parameters were determined. An experimental pneumonia model was used to evaluate the efficacy of the combined imipenem–LN-1-255 therapy. MICs of imipenem decreased between 32- and 128-fold in the presence of LN-1-255. Intramuscular treatment with imipenem–LN-1-255 (30/50 mg/kg) decreased the bacterial burden by (i) 4 and 1.7 $\log_{10}$ CFU/g lung in the infection with the ATCC 17978-OXA-23 and Ab1 strains, respectively, and by (ii) 2.5 and 4.5 $\log_{10}$ CFU/g lung in the infection produced by the ATCC 17978-OXA-24/40 and the JC12/04 strains, respectively. In all assays, combined therapy offered higher protection against pneumonia than that provided by monotherapy. No toxicity was observed in treated mice. Imipenem treatment combined with LN-1-255 treatment significantly reduced the severity of infection by carbapenem-resistant *A. baumannii* strains carrying CHDLs. Preclinical assays demonstrated the potential of LN-1-255 and imipenem therapy as a new antibacterial treatment.

KEYWORDS *Acinetobacter baumannii*, animal models, antimicrobial agents, beta-lactamase inhibitor, class D carbapenemases, preclinical drug studies

Citation Vázquez-Ucha JC, Martínez-Guitián M, Maneiro M, Conde-Pérez K, Álvarez-Fraga L, Torrens G, Oliver A, Buynak JD, Bonomo RA, Bou G, González-Bello C, Poza M, Beceiro A. 2019. Therapeutic efficacy of LN-1-255 in combination with imipenem in severe infection caused by carbapenem-resistant *Acinetobacter baumannii*. Antimicrob Agents Chemother 63:e01092-19. https://doi.org/10.1128/AAC.01092-19.

Address correspondence to Alejandro Beceiro, Alejandro.Beceiro.Casas@sergas.es.

J.C.V.-U., M.M.-G., and M.M. contributed equally to this work. C.G.-B., M.P., and A.B. contributed equally to this work.

Received 29 May 2019
Returned for modification 14 July 2019
Accepted 23 July 2019
Accepted manuscript posted online 5 August 2019
Published 23 September 2019

Acinetobacter baumannii is a nosocomial pathogen that frequently acquires and easily develops mechanisms of resistance to multiple antibiotics, which are associated with an increased risk of clinical failure, prolonging the lengths of hospital stays and therefore increasing health care costs (1). Drug-resistant infections are currently responsible for more than half a million deaths worldwide each year. It is expected that, by 2050, antimicrobial resistance will have caused the death of more than ten million people, and it is projected that related health care costs worldwide will be greater than $300 million per year (2). *A. baumannii* is considered one of the most threatening opportunistic pathogens for global health, and it has been included in a "critical priority" category by the World Health Organization (3).

The β-lactams are the most relevant family of antibiotics. In particular, carbapenems are extensively used for multidrug-resistant (MDR) pathogens such as species in the genus *Acinetobacter*, particularly *A. baumannii* (4, 5). Consequently, the production of β-lactamase enzymes is the most relevant mechanism of antibiotic inactivation through the cleavage of the β-lactam ring. The carbapenem-hydrolyzing class D β-lactamases (CHDLs), such as OXA-23 or OXA-24/40, are the most important carbapenemases produced by *A. baumannii* (6–10). The spread of OXA carbapenemases in the last decade is seriously compromising the use of these antibiotics, threatening the sustainability of carbapenem efficacy against *A. baumannii*. Few real alternatives against this pathogen have been commercialized in the last two decades.

Drug discovery has led to the development of β-lactamase inhibitors and to the rescue of failing β-lactams, combating the clinical challenge given by antimicrobial resistance. Over the last years, an increasing number of inhibitors have been developed, including avibactam, relebactam, and several boronic acid β-lactamase inhibitors (11). These new inhibitors present excellent activity against class A and class C β-lactamases and against many carbapenemases. It has been demonstrated that OXA-48 from *Enterobacteriaceae* can be inactivated by avibactam, which, in combination with ceftazidime, ceftaroline or aztreonam, is a very interesting option to treat infections caused by bacteria carrying this enzyme (12). However, the CHDLs of *A. baumannii* are not effectively inactivated by the clinically available β-lactam-type inhibitors and remain nonsusceptible to the new inhibitor combinations (11, 13). There is a shortage of relevant literature that describes candidates for new inhibitors of the OXA carbapenemases of *A. baumannii*. Thus, the treatment of *Acinetobacter* sp. isolates expressing CHDLs is an increasingly relevant clinical problem (1, 14), and the development of efficient inhibitors is needed to preserve the efficacy of carbapenems (15).

Our group has previously demonstrated that a series of β-lactam derivatives, substituted penicillin sulfones, present an exceptional potency against the *Acinetobacter* sp. CHDL OXA-24/40. Within a series of developed compounds, the compound LN-1-255 presented affinity in the nM range for all of the *A. baumannii* CHDLs tested, including the relevant OXA-23, OXA-24/40, OXA-58, and OXA-143 CHDLs (10, 16–18). The combination of carbapenems with LN-1-255 led to an important decrease in the MICs of these antibiotics (10). Similarly, this inhibitor also demonstrated good inhibitory activity against the CHDL OXA-48, as assessed by both kinetic and microbiological studies (10, 17). Other OXA or class A noncarbapenemase β-lactamases are also inhibited by this compound (19).

Since the inhibition potency of LN-1-255 against the major representative enzymes of all CHDL families described to date in *A. baumannii* has been previously demostrated by our group (10), in the present study we propose a new antimicrobial strategy. Therefore, the objective of this study is the evaluation of a new therapy combining imipenem and LN-1-255 for the treatment of an experimental murine pneumonia model caused by carbapenem-resistant *A. baumannii* transformants and clinical isolates carrying CHDLs.

RESULTS

Antimicrobial susceptibility assays. *In vitro* susceptibility to a combined therapy of imipenem and LN-1-255 was compared to susceptibility to imipenem alone. All trans-

TABLE 1 Imipenem susceptibility profile

Laboratory strain or clinical isolate	MIC (mg/liter) for[a]: Imipenem	Imipenem + LN-1-255 (4 mg/liter)	Imipenem + LN-1-255 (16 mg/liter)
A. baumannii ATCC 17978	0.5	0.5	0.5
A. baumannii ATCC 17978 + pET-RA/OXA-23	16	2	0.5
A. baumannii Ab1(OXA-23)	32	4	1
A. baumannii ATCC 17978 + pET-RA/OXA-24/40	64	2	0.5
A. baumannii JC12/04 (OXA-24/40)	32	2	0.5

[a]MICs for LN-1-255 were >512 mg/liter for all tested *A. baumannii* strains.

formants studied were imipenem resistant. As previously described, the inhibitor was able to reduce imipenem MICs by between 8- and 32-fold at 4 mg/liter and between 32- and 128-fold at 16 mg/liter (Table 1). Data indicated that a clear synergy occurred when imipenem was combined with LN-1-255. No antimicrobial activity was observed with LN-1-255 alone (MIC > 512 mg/liter).

***bla*$_{OXA-51-like}$ expression analysis.** Reverse transcription-quantitative PCR (qRT-PCR) analyses were performed in order to investigate the effect of a possible overexpression of the chromosomal OXA-51-like β-lactamase of the *A. baumannii* strains, which could sequester the inhibitor during treatments. Data revealed that *bla*$_{OXA-51-like}$ was not overexpressed in any of the tested strains. Taking the relative expression of the *bla*$_{OXA-51-like}$ gene in the ATCC 17978 strain as 1, the expression of this gene in ATCC 17978+pET-RA/OXA-23, ATCC 17978+pET-RA/OXA-24/40, Ab1, and JC12/04 strains was 0.86, 0.91, 0.41, and 0.57, respectively. Therefore, a similar expression pattern of the *bla*$_{OXA-51-like}$ gene was observed in the studied strains, and no overexpression was detected in any case.

Efficacy of the treatment. The 100% lethal dose (LD_{100}) used in the pneumonia models was 2.1×10^7 CFU/mouse for ATCC 17978 carrying pET-RA/OXA-24/40, 0.7×10^7 CFU/mouse for JC12/04, 2.9×10^7 CFU/mouse for ATCC 17978 carrying pET-RA/OXA-23, and 3.2×10^7 CFU/mouse for Ab1. After treatment, bacterial concentration in the lungs was consistently reduced when the inhibitor LN-1-255 was used intramuscularly at 50 mg/kg (Fig. 1, Table 2). Although all strains used that harbored CHDLs were imipenem resistant, the treatment with imipenem led to a slight decrease of the bacterial load in the infected lungs compared to that in the untreated control groups (0.5 to 1.5 $\log_{10}$ CFU/g lung). However, more interestingly, the treatment with imipenem and LN-1-255 decreased the bacterial load by 4 $\log_{10}$ CFU/g lung and 1.7 $\log_{10}$ CFU/g lung in the infections caused by the ATCC 17978 strain carrying pET-RA/OXA-23 and by the clinical isolate Ab1, respectively, showing statistical differences from the results obtained in imipenem monotherapy ($P < 0.02$). Conversely, the combined treatment with imipenem and LN-1-255 decreased the bacterial load by 2.5 $\log_{10}$ CFU/g lung and 4.5 $\log_{10}$ CFU/g lung in the infections caused by the ATCC 17978 strain carrying pET-RA/OXA-24/40 and by the clinical isolate JC12/04, respectively, and it also showed statistical differences from the imipenem treatment ($P < 0.01$).

Other intramuscular dosages of LN-1-255 (20 and 150 mg/kg) in combination with imipenem also reduced the bacterial load of lungs infected by clinical isolates and transformants carrying OXA-23 and OXA-24/40 compared to that when treated with imipenem alone. However, none of these dosages presented a higher bacterial clearance than the dosage of 50 mg/kg. Similarly, neither the intraperitoneal nor subcutaneous routes improved on the results obtained using the intramuscular route (data not shown).

No antimicrobial activity was observed when LN-1-255 was used alone; this inhibitor in treatments by itself did not decrease the bacterial load compared to that of the untreated groups. When imipenem combined with LN-1-255 was used to treat the infection caused by the imipenem-susceptible parental strain ATCC 17978 *A. baumannii*, no increment of efficacy was observed; the use of imipenem–LN-1-255 did not

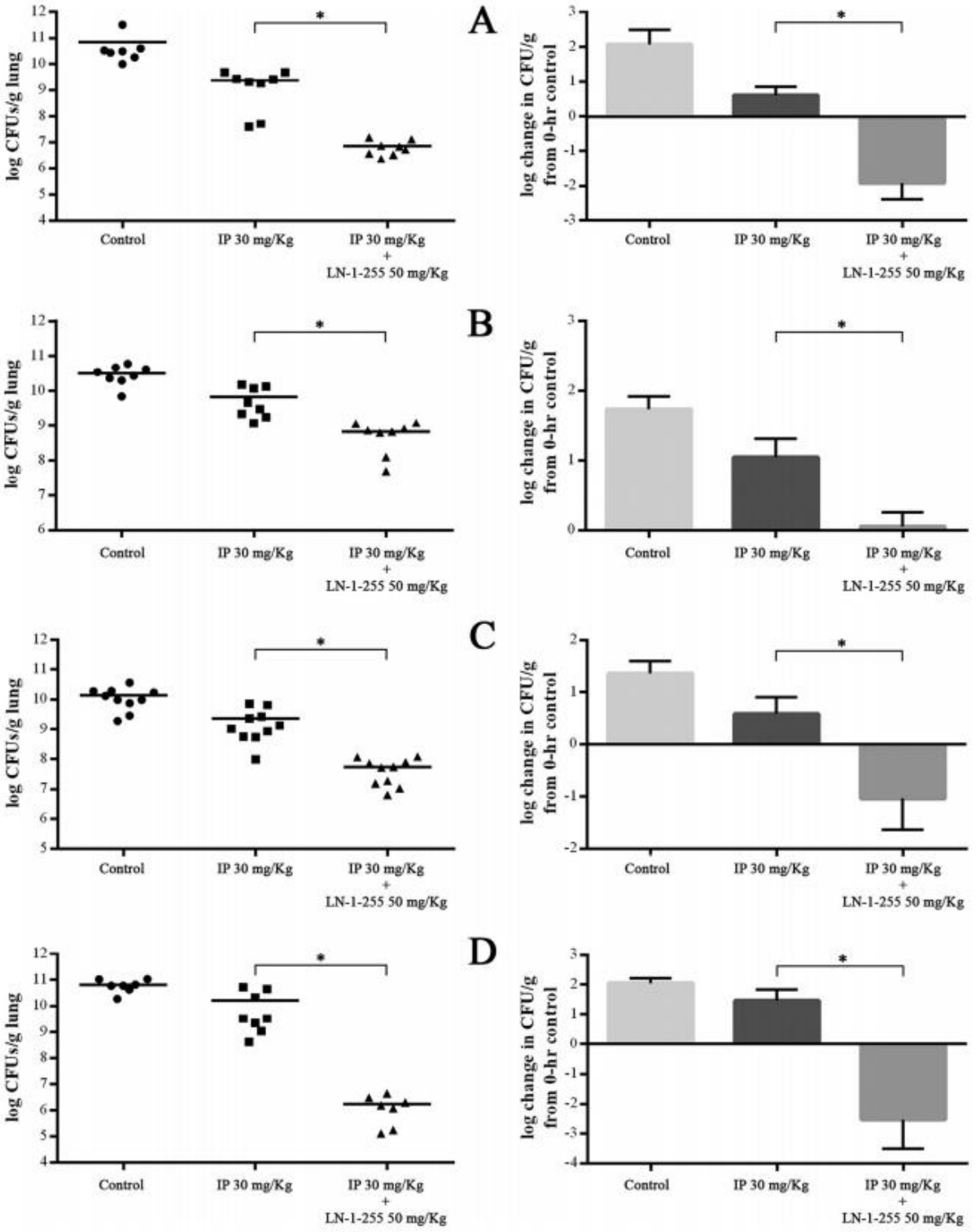

FIG 1 Effect of the combined therapy with imipenem and LN-1-255 on the clearance of *A. baumannii* strains in mouse lung. Left, each value and means of total counts in lungs are reflected. Right, values are means, and bars indicate standard deviation of total counts related to the bacterial load of the infected control mice at 0 h. (A) *A. baumannii* ATCC 17978 + pET-RA/OXA-23. (B) *A. baumannii* Ab1. (C) *A. baumannii* ATCC 17978 + pET-RA/OXA-24/40. (D) *A. baumannii* JC12/04. Student's *t* test was used to validate the experimental data (*, $P < 0.05$).

TABLE 2 Effects of monotherapy and combined therapy on the clearance of strains from mouse lungs

A. baumannii strain	Bacterial load (mean $\log_{10}$CFU/g lung ± SEM)			Decrease in bacterial load compared with that of nontreated mice ($\log_{10}$CFU/g lung)	
	Nontreated	Imipenem	Imipenem + LN-1-255	Imipenem	Imipenem + LN-1-255
ATCC 17978 + pET-RA/OXA-23	10.6 ± 4.5	9.1 ± 2.4	6.6 ± 1.4	1.5	4.0
Ab1 (OXA-23)	10.3 ± 1.8	9.6 ± 2.6	8.6 ± 2.1	0.7	1.7
ATCC 17978 + pET-RA/OXA-24/40	10.0 ± 2.3	9.2 ± 3.1	7.5 ± 1.8	0.8	2.5
JC12/04 (OXA-24/40)	10.7 ± 1.9	10.2 ± 3.6	6.2 ± 1.7	0.5	4.5

decrease the bacterial load compared with that in the control treatment (imipenem alone; data not shown).

Pharmacokinetic parameters in mice. Dosages of 20, 50, and 150 mg/kg of LN-1-255 inoculated intramuscularly were tested for pharmacokinetic activity. Pharmacokinetic curves of the inhibitor serum and epithelial lining fluid (ELF) concentration are shown in Fig. 2 and Table 3. The inhibitor maximum concentration of drug in serum (C_{max}) obtained in serum and ELF at 50 mg/kg were 5.4 and 5.6 mg/liter, showing a half-life ($t_{1/2}$) of 22 and 98 min, respectively. For this dosage, the area under the concentration-time curve (AUC) was also better in ELF (4.1 mg · h/liter) than in blood (2.8 mg · h/liter). Pharmacokinetic (PK) parameters were lower at 20 mg/kg than at 50 mg/kg. However, PK results were slightly more favorable at 150 mg/kg, showing a C_{max} value 20% higher in ELF than that for 50 mg/kg.

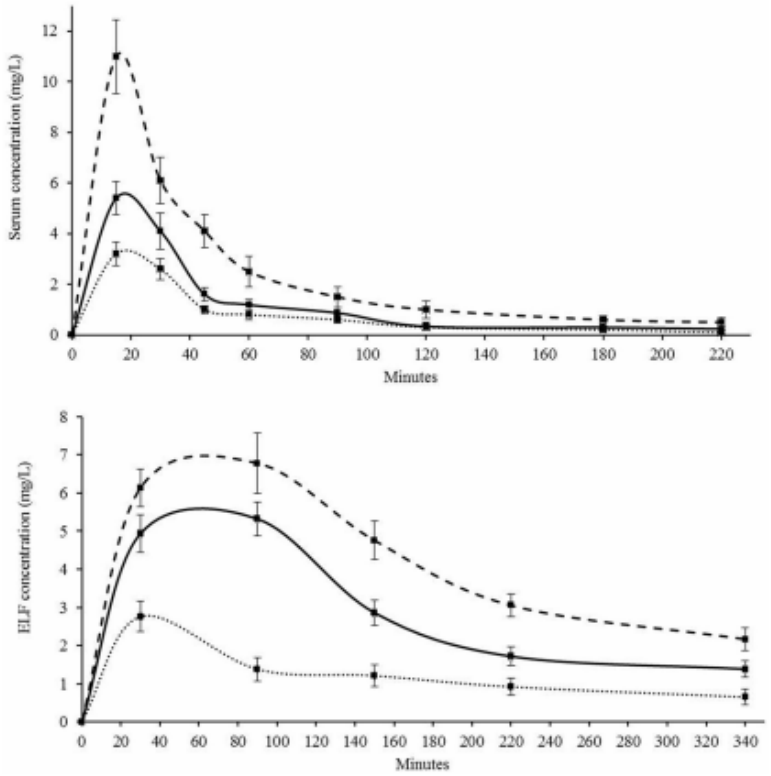

FIG 2 Pharmacokinetics of LN-1-255 in mice after intramuscular administration measured in (a) serum and (b) ELF. Dotted line, 20 mg/kg; solid line, 50 mg/kg; dashed line, 150 mg/kg. Three replicates were carried out for each time point.

TABLE 3 Pharmacokinetic parameters of LN-1-255 in blood and epithelial lining fluid

Dosage (mg/kg)	Pharmacokinetic parameters for[a]:					
	Serum			Lung		
	C_{max}	$t_{1/2\ (min)}$	AUC (mg · h/liter)	C_{max}	$t_{1/2\ (min)}$	AUC (mg · h/liter)
20	3.3 ± 0.45	21 ± 2	1.8	2.8 ± 0.43	58 ± 7	1.8
50	5.4 ± 0.65	22 ± 2	2.8	5.6 ± 0.48	98 ± 12	4.1
150	11.3 ± 1.45	16 ± 1	5.4	7.0 ± 0.81	135 ± 13	5.1

[a]C_{max}, maximum concentration of drug in serum; $t_{1/2}$, half-life.

Using as reference an imipenem-susceptible strain of *A. baumannii* such as ATCC 17978 (MIC for imipenem, 0.12 mg/liter), the literature shows that the time above the MIC (T>MIC) parameter of imipenem in murine plasma using 30 mg/kg is ca. 2 h. Thus, if dosages were administered every 3 h in our study, about 66% of time during the treatment imipenem concentration in plasma would be over the MIC. For therapeutic success with carbapenems, it is necessary to reach a concentration over the MIC at least 40% of the time (20, 21). The T>MIC parameter for imipenem against the imipenem-resistant strains used in this study was minimal or nonexistent (MICs of 16 to 64 mg/liter). Thus, based on the pharmacokinetic/pharmacodynamic (PK/PD) data of LN-1-255, it was necessary to establish a pattern between doses that would allow reaching a compound concentration during the infection capable of inhibiting the carbapenemases and to decrease the MICs to imipenem as long as possible to obtain an appropriate T>MIC parameter. Using the intramuscular dosage for LN-1-55 of 50 mg/kg every 3 h and taking as reference an effective inhibitor concentration of 4 mg/liter (minimal effective concentration [MEC]), we can see in Fig. 2 that the time above the MEC (T>MEC) parameter of LN-1-255 is 1.81 h, ca. 60% of the treatment duration. This allowed us to match the T>MIC parameter of imipenem, previously described, with the T>MEC of LN-1-255 during the treatments, in order to maximize the synergy between both compounds.

Toxicity. LN-1-255 was well tolerated in mice. No mortality was observed in the groups of uninfected mice treated with a single intramuscular dose of 350 mg/kg of LN-1-255 or in those groups which received six doses of 150 mg/kg every 3 h. Adverse effects such as muscle spasms, weight loss, or transitory movement disorders were not observed at the administered doses over 7 days.

DISCUSSION

The carbapenems remain the most-used antibiotics to treat *A. baumannii* infections (22). However, the isolation of carbapenem-resistant strains is increasing globally (23). Relevant efforts have been made to develop new β-lactamase inhibitors to recover the activity of β-lactams in species such as *Pseudomonas aeruginosa* or *A. baumannii*. The greatest advances have taken place in the development of non-β-lactam inhibitors, especially the diazabicyclooctanones (DBOs), such as avibactam (approved for clinical use) or relebactam (in the late stage of development), which are able to inhibit class A and class C β-lactamases (24). Avibactam also presents activity against the relevant carbapenemase OXA-48 but does not present any activity against CHDLs of *A. baumannii* (17, 25).

A quality leap forward was made on the development of DBOs when compounds with activity against class A, C, and D β-lactamases (including carbapenemases) were described. Recently, the new combination of sulbactam and ETX2514 has been able to restore the activity of sulbactam. The authors demonstrated its activity in a collection of *A. baumannii* clinical isolates and in a murine thigh model and a pneumonia model similar to the one presented in this work (26, 27). Other β-lactamases inhibitors include the boronates, such as vaborbactam (RPX7009), in combination with meropenem (phase IV). However, this inhibitor lacks activity against *A. baumannii* or *P. aeruginosa* (28, 29).

LN-1-255, a new β-lactamase inhibitor, is being developed to address growing

carbapenemase resistance due to CHDLs. It has been previously shown to preserve imipenem activity against OXA-48-producing strains (17) and against the most relevant CHDLs of *A. baumannii* (10). Porin loss seems not to affect this inhibitor, probably due to its structural similarity with siderophores (17). The significant activity of LN-1-255 against CHDLs is mainly due to its excellent kinetics; it shows a very high affinity for these β-lactamases (inhibits the OXA carbapenemases with low K_i values in the nM range), and the turnover number (the time-dependent partitioning of the initial enzyme/inhibitor complex between hydrolysis and enzyme inactivation) was remarkable and similar for all of the CHDLs tested, 2-6 (10). The LN-1-255 inhibitor also demonstrated an excellent microbiological synergy and a significantly higher activity than tazobactam and avibactam against all tested CHDLs (OXA-23, OXA-24/40, OXA-58, OXA-143, OXA-235, and the chromosomally encoded OXA-51) (10). Analyzing the good results obtained *in vitro* and these new *in vivo* results, it is possible to hypothesize that this inhibitor could be used to treat the lung infections caused by all of the CHDL-carrying *A. baumannii* strains. Moreover, *in vitro* synergy was also observed between meropenem and LN-1-255, which could be another alternative to treat infections caused by carbapenem-resistant *A. baumannii* strains.

The pneumonia model was chosen in this study because the majority of *A. baumannii* strains are isolated from the respiratory tract of hospitalized patients, this type of nosocomial infection being the most predominant caused by this pathogen (1). Usually the dose regimen for treatment is calculated to obtain serum concentrations of imipenem above the MIC (T>MIC) during 35 to 40% of the interval between doses (30, 31), which means approximately 3 h against imipenem-susceptible strains. In this study, we have used imipenem-resistant strains, which do not meet the criteria when a "standard" imipenem dosage is used, and thus the regimen of imipenem 30 mg/kg in monotherapy will result in a therapeutic failure. Imipenem dosage at 30 mg/kg reaches a C_{max} in serum of 16.9 to 26.7 mg/liter (20, 21), minimally decreasing the bacterial load in lungs of the imipenem-resistant strains used in this study (MICs, 16 to 64 mg/liter). Previous literature has defined the C_{max} value in plasma only, so there is no information for murine lungs. The plasma C_{max} of imipenem is similar or slightly lower than the MICs of used strains (1 to 2 dilutions), which may produce the slight observed decrease in bacterial load (0.5 to 1.5 $\log_{10}$ CFU/g lung), along with the immune response of nonimmunosuppressed mice. With LN-1-255 in combined therapy with imipenem, we have tried to recover the effectiveness of the standard regimen, and thus, finally, the interval between drug doses was 3 h and an intraperitoneal dosage of 50 mg/kg of LN-1-255 was used to avoid therapeutic failure. The other concentrations and routes tested were less effectiveness at decreasing the bacterial load of infected lungs. The C_{max} of LN-1-255 at 50 mg/kg obtained in mice lungs was 5.6 mg/liter, which was enough to decrease by 1.7 to 4.5 $\log_{10}$ the bacterial load in pneumonia when the inhibitor was used in combination with imipenem. *In vitro* assays showed a clear synergy when the inhibitor was used at 4 mg/liter against class D carbapenemase-producing *A. baumannii* strains in this and previously published studies (10), a concentration that was maintained for 60% of the time between doses in this study.

The intramuscular administration of 50 mg/kg of LN-1-255 reached in ELF a C_{max} and T>MEC about 20% and 30% lower, respectively, than those obtained using 150 mg/kg. However, these apparently better PK/PD parameters obtained with the dosage of 150 mg/kg did not increase the clearance in lungs during the infection. We hypothesized that, although LN-1-255 is not toxic at these doses in healthy mice, very high doses used repeatedly may have some deleterious effect in unhealthy (infected) mice. Last, β-lactam dosages used in treatments are usually lower than 50 to 100 mg/kg, and thus 50 mg/kg of the compound LN-1-255 (a penicillin sulfone) was the selected dosage to study in combination with imipenem for experimental treatments. It is also necessary to highlight the important role of the immune system (neutrophils) in combating bacterial infections. The depletion of neutrophils results in deficiency in bacterial clearance, and severe neutropenia or immunosuppression has been associated with higher mortality (32). In this study, immunocompetent mice were used, and the

TABLE 4 Strains and plasmids used in this work[a]

Strain or plasmid	bla_{OXA} gene	Features	Reference or source
Strains			
A. baumannii ATCC 17978	NA	*A. baumannii* type strain	ATCC
A. baumannii ATCC 17978 + pET-RA/OXA-23	OXA-23	*A. baumannii* ATCC 17978 harboring pET-TRA-KM plasmid overexpressing OXA-23	10
A. baumannii Ab1	OXA-23	*A. baumannii* clinical isolate from A Coruña (Spain)	42
A. baumannii ATCC 17978 + pET-RA/OXA-24/40	OXA-24/40	*A. baumannii* ATCC 17978 harboring pET-TRA-KM plasmid overexpressing OXA-24/40	10
A. baumannii JC12/04	OXA-24/40	*A. baumannii* clinical isolate from A Coruña (Spain)	This study
Escherichia coli BL21	OXA-24/40	*E. coli* type strain	GE Healthcare (Chicago, IL, USA)
Plasmids			
pET-RA-KM		Cloning vector harboring kanamycin and rifampicin resistance markers	10
pGEX-6P-1		Cloning vector for expressing GST fusion proteins with a PreScission protease site	GE Healthcare (Chicago, IL, USA)

[a]NA, not applicable; ATTC, American Type Culture Collection; GST, glutathione *S*-transferase.

immune system certainly has a relevant role in decreasing the infection by carbapenem-resistant *A. baumannii* strains treated with the studied imipenem–LN-1-255 combination.

To our knowledge to date, no inhibitors have presented efficacy in preclinical studies against CHDL-produced *A. baumannii* strains except for the recently published DBO ETX2514 and the β-lactam-based inhibitor LN-1-255. The ETX2514 inhibitor was tested in thigh and pneumonia murine infection models (26). Using different sulbactam-ETX2514 concentrations, the authors observed a 1- to 5-$\log_{10}$ decrease of bacterial load in pneumonia caused by a multidrug-resistant strain expressing an OXA-24/40 variant. Also, when sulbactam-EXT2514 was used at 15/50 mg/kg (similar to our dosage) in a thigh murine model, the bacterial load decreased by approximately 3.5 log. In the present study, the combination imipenem–LN-1-255 at 30/50 mg/kg in a pneumonia model infection caused by the clinical isolate with OXA-24/40 decreased the bacterial load by 3.8 log. Thus, the results obtained here showed similar *in vivo* efficacy of both inhibitors against CHDL-producing carbapenem-resistant *A. baumannii* strains.

Infections caused by antibiotic-resistant bacteria have increased rapidly in the last decades, and new therapeutic targets and antimicrobial agents are urgently needed. In antimicrobial development, PK/PD evaluation in experimental infection models are essential to design optimal dosing regimens and planning clinical trials, which are extremely costly. In this work, we have probed the *in vivo* efficacy of the LN-1-255 inhibitor, using a murine model of infection caused by CHDL-carrying *A. baumannii* transformant strains and clinical isolates. We have also described the pharmacokinetic parameters and demonstrated the lack of toxicity of this compound. The scarce arsenal against multidrug-resistant (MDR) *A. baumannii* infection supports the potential clinical use of the LN-1-255 inhibitor in combination with β-lactams.

MATERIALS AND METHODS

Bacterial strains, culture media, cloning, and susceptibility testing. The recipient strain for the expression of OXA-23 and OXA-24/40 enzymes was the antibiotic-susceptible *A. baumannii* ATCC 17978 strain. The *A. baumannii* clinical isolates used were Ab1 (carrying OXA-23) and JC12/04 (carrying OXA-24/40), both previously isolated in our hospital (Table 4). All strains were grown in Luria-Bertani (LB) broth or agar at 37°C. MICs and checkerboard assays were performed by microdilution in Mueller-Hinton II broth (Becton, Dickinson and Company, Sparks, MD, USA) (33, 34). Bacterial strains were frozen in LB broth with 15% glycerol and were maintained at −80°C until analysis. All chemicals were purchased from Sigma-Aldrich (Madrid, Spain) unless otherwise mentioned. LN-1-255 was synthetized by our group, as previously reported (Fig. 3) (35).

The cloning procedures for bla_{OXA} genes using the pET-RA-Km vector and the susceptibility testing of imipenem and LN-1-255 have been previously described by Vázquez-Ucha et al. (10).

RNA extraction and qRT-PCR analysis. RNA extraction from strains grown at an optical density at 600 nm (OD_{600}) of 1.0 was performed using the High Pure RNA isolation kit (Roche, Basel, Switzerland). Real-time PCR was done using *rpoB* as the housekeeping gene (36), the LightCycler 480 RNA Master

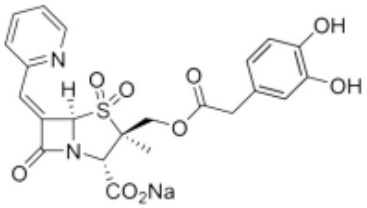

LN-1-255

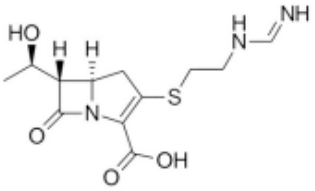

IMIPENEM

FIG 3 β-Lactam compounds used in this study.

hydrolysis probe kit (Roche), and the LightCycler 480 RNA instrument (Roche). The following primers were used: OXA51.FW-3′-GTCGATAATTTTTGGCTGGTG-5′ and OXA51.REV-3′-TTAGCCTAGCTTGTAAGCAA ACTGTG-5′. The relative expression of $bla_{\text{OXA-51-like}}$ from the different *A. baumannii* strains was compared. All assays were done in triplicate.

Animal infection. Immunocompetent BALB/c male mice from 9 to 11 weeks old and weighing 20 to 25 g were housed in regulation cages with food and water *ad libitum*. Mice were bred in our colony and used for all experiments. All mice were maintained in the specific-pathogen-free facility at the Centro Tecnológico de Formación de la Xerencia de Xestión Integrada A Coruña (CTF-XXIAC). The study was approved by the Ethics and Clinical Research Committee (CHUAC, project code P2015/82; Spain), in accordance with the Helsinki Declaration of 1975. This committee follows the recommendations of the National Committee for the Replacement, Refinement and Reduction of Animal Research (NC3Rs).

An experimental pneumonia model was used to evaluate the efficacy of LN-1-255 and imipenem against carbapenem-resistant *A. baumannii* during the course of the infection caused by transformant and clinical strains.

For bacterial inoculation, the strains were cultured at 37°C until they reached an OD_{600} of 0.7. The cultures were centrifuged, and pellets were washed and adjusted in sterile NaCl 0.9% to the required cellular suspension. The CFU of bacterial inoculums were quantified by colony counting in LB plates.

Briefly, mice anesthetized by inhalation of Sevoflurane (Zoetis, Madrid, Spain) were suspended by their incisors on a board in a semivertical position. An endoscope was used on the oral cavity to confirm the intratracheal inoculation. The trachea was accessed using a blunt-tipped needle and a 100-μl Hamilton syringe for the inoculation of a 40-μl bacterial suspension made in sterile saline solution and 10% porcine mucin (wt/vol) mixed at a 1:1 ratio. Immediately after the inoculation, a solution of ketamine (500 μg/mouse; Pfizer, Madrid, Spain) and medetomidine (15 μg/mouse; Ecuphar, Barcelona, Spain) was intraperitoneally injected in order to keep the mice over 10 min in a vertical position and then 20 min in a 30° inclined position. Antisedan (15 μg/mouse; Ecuphar, Barcelona, Spain) was injected, also intraperitoneally, for restoring the state of consciousness and normalizing the physiological variables of mice. Mice were finally euthanized with an overdose of thiopental sodium (Sandoz, Holzkirchen, Germany) after 22 h of treatment.

Infections were performed using the LD_{100} of each strain. In order to calculate the exact LD_{100}, previous to the treatment, lung inoculations in groups of 4 mice infected with each strain were performed, using the following inocula: 0.1×10^7, 0.4×10^7, 1×10^7, 4×10^7, and 20×10^7 CFU/mouse.

Treatments. In order to obtain the best results by decreasing the bacterial load in synergy with imipenem, a screening was performed using different concentrations of LN-1-255 (20, 50, and 150 mg/kg) and three inoculation routes (intraperitoneal, intramuscular, and subcutaneous). The screening of the best LN-1-255 dosage was performed using reduced (n = 4 to 6) groups of mice in assays by duplicate. The optimum imipenem dose was 30 mg/kg, intramuscularly, a dosage previously described as effective against *A. baumannii* in experimental pneumonia models (20, 21, 37).

For establishing the best treatment model, groups of 9 to 11 mice were infected following the optimum dosage and inoculation route. Mice were randomly located in each group, and treatments were begun 90 min after bacterial inoculation in lungs, where the initial infection took place. For each assay, the first group (control) did not receive antimicrobial treatment (only sterile phosphate-buffered saline [PBS]), the second group was treated only with imipenem (30 mg/kg intramuscularly), and the third group was treated with imipenem (30 mg/kg, intramuscularly) and LN-1-255 at the best dosage and

inoculation route observed (50 mg/kg, intramuscularly). For final established treatments, the interval between drug doses was 3 h. Mice were monitored for 22 h, euthanized with an overdose of thiopental sodium, and analyzed immediately after death. After the treatments, lungs were extracted in aseptic conditions, homogenized in sterile PBS, and CFU were enumerated by plating 10^{-2}-fold serial dilutions in LB plates. Results were expressed as means ± standard deviations of the $\log_{10}$ CFU per gram of lung.

Two series of assays were used as control to discard the possible specific antimicrobial activity of the inhibitor, as follows: (i) similarly to that described above, pneumonia infections caused by both carbapenem-resistant derivatives of ATCC 17978 carrying OXA-23 or OXA-24/40 CHDLs were treated with only LN-1-255 (50 mg/kg, intramuscularly) and compared with untreated infections, and (ii) pneumonia infections caused by the susceptible parental strain ATCC 17978 were treated intramuscularly with imipenem (30 mg/kg) and compared with those treated by the combination of imipenem (30 mg/kg) and LN-1-255 (50 mg/kg).

LN-1-255 pharmacokinetics. Pharmacokinetics of LN-1-255 were determined after intramuscular administration of a single dose of 20, 50, or 150 mg/kg of body weight. To obtain pharmacokinetic parameters in serum, blood samples were collected from submandibular vein of anesthetized mice, or the animals were euthanized and blood was extracted from the periorbital plexuses. Three mice per time point (0, 30, 45, 60, 90, 120, and 180 min) were used. Sera were separated from the blood cells by centrifugation (2,000 × *g*, 20 min) and stored at −80°C until subsequent analysis. To obtain the pharmacokinetic parameters in lung, the concentrations of LN-1-255 in epithelial lining fluid (ELF) were measured following the protocol described by Gotfried et al. (38). Bronchoalveolar lavage was performed with 2 ml of 0.9% NaCl in three anesthetized mice per time point (0, 30, 90, 150, 220, and 340 min). The supernatant and cells were separated by centrifugation (400 × *g*, 5 min) and frozen at −80°C. To calculate the ELF obtained, curves of urea concentration in plasma and bronchoalveolar lavage (BAL) fluid were determined using the urea nitrogen colorimetric detection kit (Thermo Fisher, Waltham, MA, USA) and an Epoch 2.0 spectrophotometer (BioTek, Winooski, VT, USA).

The serum and ELF drug concentrations were calculated using a kinetic assay, which detected the inhibition of hydrolysis of the reporter substrate nitrocefin (Oxoid, Hampshire, UK) by the purified β-lactamase OXA-24/40. The enzyme OXA-24/40 was expressed in *Escherichia coli* BL21 and purified using the previously described procedures. All assays were performed at 25°C using the proteins under steady-state conditions on an Epoch 2 spectrophotometer (39). Briefly, 40 ng/ml of carbapenemase was added to the reaction mixture, which included 200 μM nitrocefin and mice serum diluted to 10% vol/vol. Final concentrations of inhibitor in serum were estimated by extrapolation from the regression line of known LN-1-255 concentrations (0.01 to 25 mg/liter). The lower limits of detection were 0.007 mg/liter.

***In vivo* toxicity.** Once the optimum therapeutic dose of LN-1-255 was established, toxicity studies were performed. The *in vivo* toxicity was evaluated using the previously described methods (40, 41). Groups of 4 mice received a single intramuscular dose of LN-1-255 at 350 mg/kg (7-fold normal treatment). Also, two groups of 4 mice received 6 intramuscular or intraperitoneal doses of 150 mg/kg (3-fold normal treatment), respectively. Over 7 days, survival and signs of toxicity in mice were monitored.

Statistics. Differences between groups in the presence of imipenem and the inhibitor LN-1-255 were established using the Student's *t* test, carried out using Prism (GraphPad Software, San Diego, CA, USA). Differences were considered significant at $P \leq 0.05$.

ACKNOWLEDGMENTS

This work has been funded by projects PI15/00860 to G.B., CP13/00226 to A.B., and P14/00059 and PI17/01482 to M.P. and A.B., all of which were integrated into the National Plan for Scientific Research, Development and Technological Innovation 2013–2016 and funded by the ISCIII–General Subdirection of Assessment and Promotion of the Research-European Regional Development Fund (FEDER) "A way of making Europe," The study was also funded by project IN607A 2016/22 (Consellería de Cultura, Educación e Ordenación Universitaria) to G.B. This study was also funded by the Spanish Ministry of Economy and Competiveness (SAF2016-75638-R), Xunta de Galicia (Centro Singular de Investigación de Galicia accreditation 2016 to 2019, ED431G/09), and by the European Regional Development Fund (ERDF) to C.G.-B. This work was also supported by Planes Nacionales de I+D+i 2008-2011/2013-2016 and by Instituto de Salud Carlos III, Subdirección General de Redes y Centros de Investigación Cooperativa, Ministerio de Economía y Competitividad, Spanish Network for Research in Infectious Diseases (REIPI RD16/0016/006), cofinanced by the European Development Regional Fund "A way to achieve Europe" and operative program Intelligent Growth 2014–2020. Also, this study was supported in part by funds from the National Institute of Allergy and Infectious Diseases of the National Institutes of Health (USA) under award numbers R01AI063517, R01AI072219, and R01AI100560, by funds and/or facilities provided by the Cleveland Department of Veterans Affairs, the Veterans Affairs Merit Review Program award 1I01BX001974, and by the Geriatric Research Education and Clinical Center VISN 10 to R.A.B. J.D.B. acknowledges support from the National Institutes of Allergy and Infectious Diseases under award number R15AI142699. J.C.V.-U. was financially

supported by the Miguel Servet Programme (CP13/00226; ISCIII, Spain) and by Consellería de Cultura, Educación e Ordenación Universitaria (IN607A 2016/22), and M.M.-G. was financially supported by a Clara Roy grant (Spanish Society of Clinical Microbiology and Infectious Diseases [SEIMC]).

The content is solely the responsibility of the authors and does not represent the official views of the National Institutes of Health or the Department of Veterans Affairs.

We have no conflicts of interest to declare.

REFERENCES

1. Peleg AY, Seifert H, Paterson DL. 2008. *Acinetobacter baumannii*: emergence of a successful pathogen. Clin Microbiol Rev 21:538–582. https://doi.org/10.1128/CMR.00058-07.
2. Review on Antimicrobial Resistance. 2014. Antimicrobial resistance: tackling a crisis for the health and wealth of nations. Review on Antimicrobial Resistance, United Kingdom.
3. World Health Organization. 2017. Global priority list of antibiotic-resistant bacteria to guide research, discovery and development of new antibiotics. World Health Organization, Geneva, Switzerland.
4. Toth M, Antunes NT, Stewart NK, Frase H, Bhattacharya M, Smith CA, Vakulenko SB. 2016. Class D β-lactamases do exist in Gram-positive bacteria. Nat Chem Biol 12:9–14. https://doi.org/10.1038/nchembio.1950.
5. Poole K. 2004. Resistance to beta-lactam antibiotics. Cell Mol Life Sci 61:2200–2223. https://doi.org/10.1007/s00018-004-4060-9.
6. Kaitany KC, Klinger NV, June CM, Ramey ME, Bonomo RA, Powers RA, Leonard DA. 2013. Structures of the class D carbapenemases OXA-23 and OXA-146: mechanistic basis of activity against carbapenems, extended-spectrum cephalosporins, and aztreonam. Antimicrob Agents Chemother 57:4848–4855. https://doi.org/10.1128/AAC.00762-13.
7. Queenan AM, Bush K. 2007. Carbapenemases: the versatile beta-lactamases. Clin Microbiol Rev 20:440–458. https://doi.org/10.1128/CMR.00001-07.
8. Walther-Rasmussen J, Høiby N. 2006. OXA-type carbapenemases. J Antimicrob Chemother 57:373–383. https://doi.org/10.1093/jac/dki482.
9. Smith CA, Antunes NT, Stewart NK, Toth M, Kumarasiri M, Chang M, Mobashery S, Vakulenko SB. 2013. Structural basis for carbapenemase activity of the OXA-23 β-lactamase from *Acinetobacter baumannii*. Chem Biol 20:1107–1115. https://doi.org/10.1016/j.chembiol.2013.07.015.
10. Vázquez-Ucha JC, Maneiro M, Martínez-Guitián M, Buynak J, Bethel CR, Bonomo RA, Bou G, Poza M, González-Bello C, Beceiro A. 2017. Activity of the β-lactamase inhibitor LN-1-255 against carbapenem-hydrolyzing class D β-lactamases from *Acinetobacter baumannii*. Antimicrob Agents Chemother 61:e01172-17. https://doi.org/10.1128/AAC.01172-17.
11. Drawz SM, Papp-Wallace KM, Bonomo RA. 2014. New beta-lactamase inhibitors: a therapeutic renaissance in an MDR world. Antimicrob Agents Chemother 58:1835–1846. https://doi.org/10.1128/AAC.00826-13.
12. Livermore DM, Mushtaq S, Warner M, Zhang J, Maharjan S, Doumith M, Woodford N. 2011. Activities of NXL104 combinations with ceftazidime and aztreonam against carbapenemase-producing *Enterobacteriaceae*. Antimicrob Agents Chemother 55:390–394. https://doi.org/10.1128/AAC.00756-10.
13. Naas T, Nordmann P. 1999. OXA-type beta-lactamases. Curr Pharm Des 5:865–879.
14. Shlaes DM. 2013. New β-lactam-β-lactamase inhibitor combinations in clinical development. Ann N Y Acad Sci 1277:105–114. https://doi.org/10.1111/nyas.12010.
15. Perez-Llarena FJ, Bou G. 2009. Beta-lactamase inhibitors: the story so far. Curr Med Chem 16:3740–3765. https://doi.org/10.2174/092986709789104957.
16. Bou G, Santillana E, Sheri A, Beceiro A, Sampson JM, Kalp M, Bethel CR, Distler AM, Drawz SM, Pagadala SR, van den Akker F, Bonomo RA, Romero A, Buynak JD. 2010. Design, synthesis, and crystal structures of 6-alkylidene-2′-substituted penicillanic acid sulfones as potent inhibitors of *Acinetobacter baumannii* OXA-24 carbapenemase. J Am Chem Soc 132:13320–13331. https://doi.org/10.1021/ja104092z.
17. Vallejo JA, Martínez-Guitián M, Vázquez-Ucha JC, González-Bello C, Poza M, Buynak JD, Bethel CR, Bonomo RA, Bou G, Beceiro A. 2016. LN-1-255, a penicillanic acid sulfone able to inhibit the class D carbapenemase OXA-48. J Antimicrob Chemother 71:2171–2180. https://doi.org/10.1093/jac/dkw105.
18. Pattanaik P, Bethel CR, Hujer AM, Hujer KM, Distler AM, Taracila M, Anderson VE, Fritsche TR, Jones RN, Pagadala SR, van den Akker F, Buynak JD, Bonomo RA. 2009. Strategic design of an effective beta-lactamase inhibitor: LN-1-255, a 6-alkylidene-2′-substituted penicillin sulfone. J Biol Chem 284:945–953. https://doi.org/10.1074/jbc.M806833200.
19. Drawz SM, Bethel CR, Doppalapudi VR, Sheri A, Pagadala SR, Hujer AM, Skalweit MJ, Anderson VE, Chen SG, Buynak JD, Bonomo RA. 2010. Penicillin sulfone inhibitors of class D beta-lactamases. Antimicrob Agents Chemother 54:1414–1424. https://doi.org/10.1128/AAC.00743-09.
20. Beceiro A, López-Rojas R, Domínguez-Herrera J, Docobo-Pérez F, Bou G, Pachón J, Spanish Network for Research in Infectious Diseases (REIPI). 2009. *In vitro* activity and *in vivo* efficacy of clavulanic acid against *Acinetobacter baumannii*. Antimicrob Agents Chemother 53:4298–4304. https://doi.org/10.1128/AAC.00320-09.
21. Rodríguez-Hernández MJ, Pachón J, Pichardo C, Cuberos L, Ibáñez-Martínez J, García-Curiel A, Caballero FJ, Moreno I, Jiménez-Mejías ME. 2000. Imipenem, doxycycline and amikacin in monotherapy and in combination in *Acinetobacter baumannii* experimental pneumonia. J Antimicrob Chemother 45:493–501. https://doi.org/10.1093/jac/45.4.493.
22. Ruiz J, Núñez ML, Pérez J, Simarro E, Martínez-Campos L, Gómez J. 1999. Evolution of resistance among clinical isolates of *Acinetobacter* over a 6-year period. Eur J Clin Microbiol Infect Dis 18:292–295. https://doi.org/10.1007/s100960050280.
23. Poirel L, Nordmann P. 2002. Acquired carbapenem-hydrolyzing beta-lactamases and their genetic support. Curr Pharm Biotechnol 3:117–127. https://doi.org/10.2174/1389201023378427.
24. Coleman K. 2011. Diazabicyclooctanes (DBOs): a potent new class of non-β-lactam β-lactamase inhibitors. Curr Opin Microbiol 14:550–555. https://doi.org/10.1016/j.mib.2011.07.026.
25. Lahiri SD, Mangani S, Jahic H, Benvenuti M, Durand-Reville TF, De Luca F, Ehmann DE, Rossolini GM, Alm RA, Docquier JD. 2015. Molecular basis of selective inhibition and slow reversibility of avibactam against class D carbapenemases: a structure-guided study of OXA-24 and OXA-48. ACS Chem Biol 10:591–600. https://doi.org/10.1021/cb500703p.
26. Durand-Réville TF, Guler S, Comita-Prevoir J, Chen B, Bifulco N, Huynh H, Lahiri S, Shapiro AB, McLeod SM, Carter NM, Moussa SH, Velez-Vega C, Olivier NB, McLaughlin R, Gao N, Thresher J, Palmer T, Andrews B, Giacobbe RA, Newman JV, Ehmann DE, de Jonge B, O'Donnell J, Mueller JP, Tommasi RA, Miller AA. 2017. ETX2514 is a broad-spectrum β-lactamase inhibitor for the treatment of drug-resistant Gram-negative bacteria including *Acinetobacter baumannii*. Nat Microbiol 2:17104. https://doi.org/10.1038/nmicrobiol.2017.104.
27. Barnes MD, Bethel CR, Rutter JD, Akker FVD, Papp-Wallace KM, Bonomo RA. 2017. The novel β-lactamase inhibitor, ETX-2514, in combination with sulbactam effectively inhibits *Acinetobacter baumannii*. Open Forum Infect Dis 4:S368. https://doi.org/10.1093/ofid/ofx163.900.
28. Cho JC, Zmarlicka MT, Shaeer KM, Pardo J. 2018. Meropenem/vaborbactam, the first carbapenem/β-lactamase inhibitor combination. Ann Pharmacother 52:769–779. https://doi.org/10.1177/1060028018763288.
29. Lapuebla A, Abdallah M, Olafisoye O, Cortes C, Urban C, Quale J, Landman D. 2015. Activity of meropenem combined with RPX7009, a novel β-lactamase inhibitor, against Gram-negative clinical isolates in New York City. Antimicrob Agents Chemother 59:4856–4860. https://doi.org/10.1128/AAC.00843-15.
30. Nielsen EI, Cars O, Friberg LE. 2011. Pharmacokinetic/pharmacodynamic (PK/PD) indices of antibiotics predicted by a semimechanistic PKPD model: a step toward model-based dose optimization. Antimicrob Agents Chemother 55:4619–4630. https://doi.org/10.1128/AAC.00182-11.
31. Craig WA. 1998. Pharmacokinetic/pharmacodynamic parameters: rationale for antibacterial dosing of mice and men. Clin Infect Dis 26:1–10. https://doi.org/10.1086/516284.

32. Guo B, Abdelraouf K, Ledesma KR, Chang KT, Nikolaou M, Tam VH. 2011. Quantitative impact of neutrophils on bacterial clearance in a murine pneumonia model. Antimicrob Agents Chemother 55:4601–4605. https://doi.org/10.1128/AAC.00508-11.
33. Hsieh MH, Yu CM, Yu VL, Chow JW. 1993. Synergy assessed by checkerboard. A critical analysis. Diagn Microbiol Infect Dis 16:343–349. https://doi.org/10.1016/0732-8893(93)90087-N.
34. Clinical and Laboratory Standards Institute. 2012. Performance standards for antimicrobial susceptibility testing. 17th informational supplement, M07-A9. Clinical and Laboratory Standards Institute, Wayne, PA.
35. Buynak JD, Rao AS, Doppalapudi VR, Adam G, Petersen PJ, Nidamarthy SD. 1999. The synthesis and evaluation of 6-alkylidene-2′beta-substituted penam sulfones as beta-lactamase inhibitors. Bioorg Med Chem Lett 9:1997–2002. https://doi.org/10.1016/S0960-894X(99)00325-X.
36. Álvarez-Fraga L, Vázquez-Ucha JC, Martínez-Guitián M, Vallejo JA, Bou G, Beceiro A, Poza M. 2018. Pneumonia infection in mice reveals the involvement of the *feoA* gene in the pathogenesis of *Acinetobacter baumannii*. Virulence 9:496–509. https://doi.org/10.1080/21505594.2017.1420451.
37. Parra Millán R, Jiménez Mejías ME, Sánchez Encinales V, Ayerbe Algaba R, Gutiérrez Valencia A, Pachón Ibáñez ME, Díaz C, Pérez Del Palacio J, López Cortés LF, Pachón J, Smani Y. 2016. Efficacy of lysophosphatidylcholine in combination with antimicrobial agents against *Acinetobacter baumannii* in experimental murine peritoneal sepsis and pneumonia models. Antimicrob Agents Chemother 60:4464–4470. https://doi.org/10.1128/AAC.02708-15.
38. Gotfried MH, Danziger LH, Rodvold KA. 2001. Steady-state plasma and intrapulmonary concentrations of levofloxacin and ciprofloxacin in healthy adult subjects. Chest 119:1114–1122. https://doi.org/10.1378/chest.119.4.1114.
39. Santillana E, Beceiro A, Bou G, Romero A. 2007. Crystal structure of the carbapenemase OXA-24 reveals insights into the mechanism of carbapenem hydrolysis. Proc Natl Acad Sci U S A 104:5354–5359. https://doi.org/10.1073/pnas.0607557104.
40. López-Rojas R, Sánchez-Céspedes J, Docobo-Pérez F, Domínguez-Herrera J, Vila J, Pachón J. 2011. Pre-clinical studies of a new quinolone (UB-8902) against *Acinetobacter baumannii* resistant to ciprofloxacin. Int J Antimicrob Agents 38:355–359. https://doi.org/10.1016/j.ijantimicag.2011.06.006.
41. O'Reilly T, Andes DA, Ostergaard C, Frimodt-Moller N. 2005. Evaluation of antimicrobials in experimental animal infections. *In* Lorian V (ed), Antibiotics in laboratory medicine, 5th ed. Lippincott Williams and Wilkins, Philadelphia, PA.
42. Higgins PG, Pérez-Llarena FJ, Zander E, Fernández A, Bou G, Seifert H. 2013. OXA-235, a novel class D β-lactamase involved in resistance to carbapenems in *Acinetobacter baumannii*. Antimicrob Agents Chemother 57:2121–2126. https://doi.org/10.1128/AAC.02413-12.

VIII. *CURRÍCULUM VITAE*.

CVA.

Fecha del CVA	30/01/2020

Parte A. DATOS PERSONALES

Nombre y Apellidos	Marta Martínez Guitián		
DNI	47364298-F	Edad	31
Núm. identificación del investigador	Researcher ID		
	Scopus Author ID		
	Código ORCID	0000-0002-3457-0613	

A.1. Situación profesional actual

Organismo				
Dpto. / Centro				
Dirección	Armuño-Lubre, 20, 15166, Bergondo			
Teléfono	(+34) 646117258	Correo electrónico	Marta.Martinez.Guitian@sergas.es	
Categoría profesional			Fecha inicio	
Espec. cód. UNESCO				
Palabras clave				

A.2. Formación académica (titulo, institución, fecha)

Licenciatura/Grado/Doctorado	Universidad	Año
Máster Universitario en Farmacología	Universitat Autònoma de Barcelona	2014
Licenciatura en Farmacia	Universidad de Santiago de Compostela	2011

A.3. Indicadores generales de calidad de la producción científica

Número total de citas: 62.
Promedio anual de citas en el periodo 2015-2019: 12,40 por año.
Índice h: 5.
índice i10: 4.
Publicaciones totales (en Q1/en D1): 11 (9/8).
Comunicaciones a congresos (internacionales): 35 (25).

Parte B. RESUMEN LIBRE DEL CURRÍCULUM

Año 2010: Realización de prácticas en el Departamento de Proteómica en el Instituto de Investigación Biomédica de A Coruña, dirigidas por el Dr. Jesús Mateos y el Dr. Francisco J. Blanco. Experiencia en identificación y caracterización de proteínas mediante espectrometría de masas.

Año 2011: Beca de Colaboración de la Xunta de Galicia en el grupo de investigación Farmacología de las Enfermedades Crónicas (CD Pharma) de la Universidad de Santiago de Compostela. Evaluación de moléculas con actividad antagónica de la endotelina-I como posible tratamiento para enfermedades cardiovasculares, como la hipertensión arterial, dirigido por el Dr. Manuel Campos Toimil.

Año 2014: Incorporación al Servicio de Microbiología del Complexo Hospitalario Universitario de A Coruña para la realización de la Tesis Doctoral, bajo la supervisión del Dr. Alejandro Beceiro y el Dr. Germán Bou. Descripción de genes implicados en virulencia y resistencia de patógenos multirresistentes, así como búsqueda de nuevas moléculas y estrategias eficaces para su tratamiento. Experiencia en técnicas de microbiología básica, en biología molecular y celular, microscopía de fluorescencia, técnicas en inmunoanálisis, modelos animales y proteómica. Participación en 35 comunicaciones a congresos (25 internacionales), en un proyecto de investigación financiado por el ISCIII, 11 artículos científicos en D1 y Q1, 6 de primera autora. Índice h de 5 y 62 citaciones. Obtención de la beca Clara Roy de la SEIMC

de 2 años de duración y de distintas becas de viaje de los Congresos ECCMID y SEIMC. Realización del curso de experimentación animal categoría C y 2 cursos de microscopía de fluorescencia.

Parte C. MÉRITOS MÁS RELEVANTES (ordenados por tipología)

C.1. Publicaciones

1 **Artículo científico**. Martínez-Guitián M.; et al. 2019. Antisense inhibition of lpxB gene expression in Acinetobacter baumannii by peptide-PNA conjugates and synergy with colistin.Journal of Antimicrobial Chemotherapy.

2 **Artículo científico**. Arca-Suárez J.; et al. 2019. Challenging Antimicrobial Susceptibility and Evolution of Resistance (OXA-681) during Treatment of a Long-Term Nosocomial Infection Caused by a Pseudomonas aeruginosa ST175 Clone Antimicrobial Agents and Chemotherapy. ASM. 63-10.

3 **Artículo científico**. Vázquez-Ucha JC.; et al. 2019. Therapeutic Efficacy of LN-1-255 in Combination with Imipenem in Severe Infection Caused by Carbapenem-Resistant Acinetobacter baumannii.Antimicrobial Agents and Chemotherapy. 63-10.

4 **Artículo científico**. Martínez-Guitián M.; et al. 2018. Involvement of HisF in the Persistence of Acinetobacter baumannii During a Pneumonia Infection.Frontiers in Cellular and Infection Microbiology. 9-310.

5 **Artículo científico**. Gato E.; et al. 2018. Draft Genome Sequences of Two Epidemic OXA-48-Producing Klebsiella pneumoniae Clinical Strains Isolated during a Large Outbreak in Spain.Genome Announcements. 6-13.

6 **Artículo científico**. Álvarez-Fraga L.; et al. 2018. Pneumonia infection in mice reveals the involvement of the feoA gene in the pathogenesis of Acinetobacter baumannii.Virulence. 9-1, pp.496-509.

7 **Artículo científico**. Vázquez-Ucha JC.; et al. 2017. Activity of the β-Lactamase Inhibitor LN-1-255 against Carbapenem-Hydrolyzing Class D β-Lactamases from Acinetobacter baumannii.Antimicrobial Agents and Chemotherapy. ASM. 64-11.

8 **Artículo científico**. Rumbo, C.; et al. 2016. Assessment of antivirulence activity of several d-amino acids against Acinetobacter baumannii and Pseudomonas aeruginosa.The Journal of Antimicrobial Chemotherapy. 71-12, pp.3473-3481. ISSN 1460-2091.

9 **Artículo científico**. Martínez Guitián, M.; et al. 2016. LN-1-255, a penicillanic acid sulfone able to inhibit the class D carbapenemase OXA-48.The Journal of Antimicrobial Chemotherapy. 71-8, pp.2171-2180. ISSN 1460-2091.

10 **Artículo científico**. Martínez Guitián, M.; et al. 2016. Synergy between Colistin and the Signal Peptidase Inhibitor MD3 Is Dependent on the Mechanism of Colistin Resistance in Acinetobacter baumannii.Antimicrobial Agents and Chemotherapy. 60-7, pp.4375-4379. ISSN 1098-6596.

11 **Artículo científico**. González Bello, C.; et al. 2015. Chemical Modification of a Dehydratase Enzyme Involved in Bacterial Virulence by an Ammonium Derivative: Evidence of its Active Site Covalent Adduct.Journal of the American Chemical Society. 137-29, pp.9333-9343. ISSN 1520-5126.

C.2. Proyectos

Nuevas estrategias frente al patógeno multirresistente Acinetobacter baumannii: silenciamiento (siRNA) bacteriano y desarrollo de nuevos inhibidores. Evaluación en estudios preclínicos. Alejandro Beceiro Casas. (Complejo Hospitalario Universitario Juan Canalejo). 2018-2021. 127.000 €.

C.3. Contratos

Beca Clara Roy Sociedad Española de Enfermedades Infecciosas y Microbiología Clínica. Marta Martínez Guitián. 01/12/2017-01/12/2019. 36.000 €.

C.4. Patentes